Università degli Studi di Ferrara

DOTTORATO DI RICERCA IN

Terapie Avanzate e Farmacologia Sperimentale

"Advanced Therapies and Experimental Pharmacology"

CICLO XXXVII

COORDINATRICE (Coordinator)
Prof.ssa Varani Katia

IMMUNOMETABOLIC DETERMINANTS OF AGING AND THEIR EFFECTS ON VACCINE RESPONSES IN OLDER ADULTS

Settore Scientifico Disciplinare: Bios-07

Dottorando
Dott. Proietto Davide

_____
(firma)

Tutore
Prof. Gavioli Riccardo

_____
(firma)

Co-Tutore
Prof. Nicoli Francesco

_____
(firma)

Co-Tutore
Dott.ssa Torreggiani Elena

_____
(firma)

Anni 2021/2024

Index

1. ABSTRACT **4**

2. GENERAL INTRODUCTION **7**

2.1 Immune system 7

2.1.1 Humoral immunity 7

2.1.2 Cellular Immunity 8

2.1.2.1 Phases of the cellular response – Priming of naïve T cells and memory response 9

2.2 Immunometabolism 15

2.2.1 Glycolysis and oxidative phosphorylation 16

2.2.2 Synthesis (FAS) and oxidation (FAO) of Fatty Acids 17

2.2.3 Glutamine metabolism 18

2.2.4 Metabolism of naïve T lymphocytes 19

2.2.5 Metabolism of effector T lymphocytes 19

2.2.6 Metabolism of memory T lymphocytes 20

2.2.6.1 Mitochondrial properties and morphology in effector and memory T lymphocytes 21

2.3 Immunosenescence 23

2.3.1 Immunosenescence and immunometabolism 26

2.3.2 Immunosenescence and responses to vaccination 27

2.4 COVID-19 and pneumococcal disease 28

3. OBJECTIVES **31**

CHAPTER 1: The effect of aging on the immunophenotype and the role of myocardial infarction **33**

1.1 Introduction 33

1.2 Material and Methods 35

1.2.1 Study Cohorts 35

1.2.2 Flow cytometry 37

1.2.3 Statistical analysis 37

1.3 Results 39

1.3.1 The impact of Immunosenescence and Myocardial Infarction on the remodelling of immunotypes 39

1.3.2 Monitoring of homeostasis and immunological profile after Myocardial Infarction 43

1.4 Discussion 49

CHAPTER 2: Aging Curtails the Diversity and Functionality of Nascent $CD8^+$ T Cell Responses against SARS-CoV-2 **51**

2.1 Introduction 51

2.2 Material and Methods 51

2.2.1 Main Cohort 51

2.2.2 Peptides and Tetramers 52

2.2.3 In Vitro Priming of Human Antigen-Specific $CD8^+$ T Cells 52
2.2.4 ELIspot Assay 53
2.2.5 Flow Cytometry 53
2.2.6 HLA-Peptide Binding Assay 54
2.2.7 Statistical Analysis 54
2.3 Results 55
2.3.1 Cohort Description 55
2.3.2 Peptides Characterization 56
2.3.3 Aging Impairs the Induction of Effector $CD8^+$ T Cells Defined by the Expression of T-bet 56
2.3.4 Aging Impairs the Induction of Effector $CD8^+$ T Cells Defined by the Expression of IFNγ 58
2.4 Discussion 60
CHAPTER 3: Age differentially impacts adaptive immune responses induced by adenoviral versus mRNA vaccines against COVID-19 62
3.1 Introduction 62
3.2 Materials and methods 63
3.2.1 Main Cohort 63
3.2.2 Validation cohort 66
3.2.2 Samples 67
3.2.3 Peptides and tetramers 67
3.2.4 ELISpot assays 68
3.2.5 Flow cytometry 68
3.2.6 *In vitro* expansion of antigen-specific T cells 69
3.2.7 Cytotoxicity assay 69
3.2.8 Statistical analysis 69
3.3 Results 71
3.3.1 ChAdOx1-S is less reactogenic than BNT162b2 71
3.3.2 Immunization regimen impacts the diversity of $CD8^+$ T cell responses 74
3.3.3 Age impacts cellular and humoral immune responses elicited by primary vaccination with BNT162b2 78
3.3.4 Cellular immune responses are optimally maintained in older individuals vaccinated with ChAdOx1-S 80
3.3.5 Impact of naïve decrease on cellular responses 81
3.4 Discussion 83
CHAPTER 4: Study of T lymphocyte metabolism as a function of the degree of response to antipneumococcal vaccination 85
4.1 Introduction 85
4.2 Materials and Methods 87
4.2.1 Main Cohort 87
4.2.2 Basal metabolic profiling by Flow Cytometry 87
4.2.3 SCENITH assay 88
4.2.4 Flow cytometry 89

4.2.5 Statistical analysis 90
4.3 Results 91
4.3.1 Characterization of basal metabolism and expression of nutrient markers in T cells from subjects of different age groups 91
4.3.2 Young and old adults vaccinated with PCV13 vaccine show similar cellular responses 93
4.3.3 Basal metabolic properties of naïve T cells from responder and non-responder groups 95
4.3.4 Increased protein synthesis and metabolic shift characterizes naïve T cells from responders 97
4.3.5 The expression of nutrient receptors confers metabolic advantages to naïve T cells of responder donors 102
4.3.6 Naïve T cell metabolic properties are associated with systemic immune system, age-related, features 103
4.3.7 LDL-r expression can predict the responsiveness to PCV13 vaccination 107
4.4 Discussion 110
4. CONCLUSIONS 113
5. BIBLIOGRAPHY 117

1. ABSTRACT

As of 1 January 2023, the population of the European Union (EU) was estimated at 448.8 million; children aged 0 to 14 years made up 14.9% of the total population, while 63.8% were of working age (15 to 64 years). Older adults, aged 65 and over, accounted for 21.3%, representing an increase of 3.0 percentage points over the past decade (data from Eurostat, an official website of the European Union; https://ec.europa.eu/eurostat/statistics-explained/index.php?title=Population_structure_and_ageing).
The European Union is experiencing a demographic shift towards an aging population, leading to increased healthcare costs and rising vulnerability to infections. Immunosenescence is considered a key driver of this decline in the quality of life of older subjects. Aging is associated with qualitative and quantitative declines in immune cell function, resulting in reduced vaccine efficacy and heightened susceptibility to pathogens such as SARS-CoV-2 and *Streptococcus pneumoniae*. However, the intrinsic mechanisms that explain this functional decline, are not fully known and clear, and especially it is not well understood how the response to a given vaccine varies within the elderly population.
This study investigated age-related changes in the immune system and their impact on vaccine responses, focusing on SARS-CoV-2 and PCV13 (anti-pneumococcal vaccine) vaccines.
The research primarily focused on quantitative analyses of lymphocyte subsets, followed by qualitative assessments of immune responses to novel viral antigens, including *in vitro* priming against SARS-CoV-2 antigens and responses to SARS-CoV-2 vaccinations. Additionally, the study examined immunometabolism mechanisms to understand immune responses to the PCV13 vaccine, which contains 13 *S. pneumoniae* polysaccharides conjugated to the mutated diphtheria toxin: CRM197 protein.
This study first examined how T and B lymphocyte subsets change with aging; in particular, two cohorts (RIV and PIpELINe cohort) were used to analyse the immunophenotype changes. The RIV cohort consisted in healthy individuals stratified by age: young adults aged 18 to 40 years (92 participants), middle-aged adults aged 41 to 65 years (121 participants), and older adults over 65 years (36 participants), without heart attack history. The PIpELINe cohort comprised 53 individuals over 65 years old with a history of myocardial infarction (MI), as part of a longitudinal study monitoring both the quantitative and functional characteristics of the immune system after MI. Indeed, aging is associated with the cumulative burden of comorbidities, and we sought to assess how these could impact immunosenescence trajectories.
Comparison between these cohorts revealed significant age-related remodelling of lymphocyte subsets, with older adults exhibiting a decrease in naïve lymphocytes and an increase in terminally differentiated effector memory cells re-expressing CD45RA (T_{EMRA}) cells. These T_{EMRA} cells increase

with chronic infections (e.g., CMV) and are characterized by an exhausted profile. Myocardial infarction substantially remodels both innate and adaptive immunity subsets. During this stressful event, indeed, there is a decrease in naïve subsets ($CD4^+$ and $CD8^+$ T cells) and an increase in T_{EMRA}, along with changes in the expression of activation markers, such as HLA-DR. While this response is crucial for managing acute stress, such as during a MI, it also led to an increase in exhausted lymphocyte populations and altered immune functionality. Therefore, age profoundly remodels the immune system and acute event accelerate this pattern.

As the naïve T cells compartment is the most affected by senescence, we sought to understand how this impacted the response to novel viral antigens using an *in vitro* approach to prime SARS-CoV-2-specific naïve $CD8^+$ T cells from healthy, unexposed donors of different age groups. SARS-CoV-2, as an emerging pathogen, served as an ideal model for studying primary immune responses in unexposed individuals. Compared to younger adults, older individuals showed a weaker ability to prime SARS-CoV-2-specific T cells, both in magnitude and quality of the response, and recognized fewer viral epitopes.

To confirm these results, we measured immune responses to new vaccination assessing the impact of aging on immunity to COVID-19 vaccines, particularly focusing on adenoviral (ChAdOx1-S) and mRNA (BNT162b2) vaccines. A functional and observational study was conducted to compare Spike (S) protein-specific immune responses in age-stratified participants with no prior SARS-CoV-2 infection. The participants received two doses of either BNT162b2 (mRNA vaccine) or ChAdOx1-S (adenoviral vaccine), followed by a booster dose of either BNT162b2 or mRNA-1273. For each vaccine, the donors were stratified by age: young (18-40 years), middle-aged (41-65 years) and older (>65 years) adults. Aging significantly reduced S protein-specific $CD8^+$ T cell responses, particularly in individuals initially vaccinated with BNT162b2. This decrease was linked to a progressive loss of naïve lymphocytes in older adults. Instead, initial vaccination with ChAdOx1-S followed by an mRNA booster (BNT162b2 or mRNA-1273) elicited more sustained immunological memory in older adults and provided robust and durable immune protection. This suggests that older individuals respond differently as a function of the vaccine platform received, providing a proof of concept that optimal strategy might mitigate age-related vaccine response limitations.

Indeed, elderly individuals do not always exhibit a “poor” response to vaccination, as we demonstrated in the VITAL cohort, composed of subjects of different age groups vaccinated with the PCV13 vaccine. In this context, despite immunometabolic differences at naïve T cells level between young and elderly individuals in naïve $CD4^+$ and $CD8^+$ T cells, the cellular response to the PCV13 vaccine was comparable between the two groups. This finding suggests that immunosenescence should not be viewed as the sole determinant of a negative response to vaccination. Instead, it

highlights the potential to evaluate vaccine responsiveness based on baseline biological factors that could explain and predict how individual will react to the vaccination. Within this context, we observed that individuals that developed good cellular responses to PCV13 were characterized by a specific metabolic pattern at the level of naïve T cells prior to vaccination. Indeed, their naïve T cells were characterized by increased expression of nutrient markers, including LDL-r and amino acid receptors and exhibit stronger metabolic shift upon activation.

These findings underscore the importance of understanding immunosenescence beyond traditional markers and suggest strategies to optimize vaccine efficacy in older adults, such as tailored vaccine platforms and evaluations of metabolic markers.

2. GENERAL INTRODUCTION

2.1 Immune system

The immune system protects the body against viruses, bacteria, and other microorganisms at a rapid, precise, and powerful level. It is composed of two subsystems: the innate immunity and the adaptive immunity.

The innate immune response, which is non-specific and immediate, acts as the first line of defence to block pathogen invasion and initiate the inflammatory process. Additionally, innate immune cells support the activation of adaptive immunity, primarily through two mechanisms: activation of pro-inflammatory signalling pathways and phagocytosis of the pathogen by macrophages and dendritic cells (DCs); this is followed by antigen processing and presentation to T lymphocytes via Major Histocompatibility Complex (MHC) molecules.

The adaptative or acquired immune response, which is specific and delayed, is activated by the innate component; it provides a stronger and more specialized defence against infection through sophisticated mechanisms in which T and B lymphocytes recognize antigens with highly variable receptors. Antigen-specific adaptive resistance develops slower than innate responses and maintains an immunological memory when compared to previously encountered antigens.

Immune responses are systemic, starting in a specific tissue and later extending to more distant sites. This characteristic is essential for the effectiveness of vaccines, which induce a specific immunity that might extend to several tissues while being activated at a specific subcutaneous or muscular site [1].

2.1.1 Humoral immunity

Humoral immunity is the main defence mechanism against extracellular microbes and their toxins, and it is mediated by B lymphocytes. After their proliferation and differentiation, they become plasma cells, which secrete various classes of antigen-specific molecules, namely antibodies (Abs) or immunoglobulin (Igs), which are a family of glycoproteins, produced by B lymphocytes following exposure to antigens. They are divided into:

- antibodies expressed on the surface of B lymphocytes, which serve as receptors (BCRs) for the microbial antigen and are involved in B lymphocyte activation;
- secreted Abs, which act as mediators of specific humoral immunity and trigger molecular and cellular effector mechanisms to eliminate the antigen to which they are bound.

Igs are characterized by the variable and constant regions. The variable region determines the antigen specificity, while the constant region is important for the creation of the antigen binding domain and

for the effector function, including the Igs capacity of being secreted or remaining on the surface of cell. Furthermore, the constant regions determine the classification of Abs into five different types: IgA, IgD, IgE, IgG, and IgM, each possessing distinct properties and specialized functions. IgM are the main Igs involved in the primary immune response, being produced early in the course of an infection. They provide the first line of humoral immunity defence, after which high-affinity IgG responses are initiated and play a key role in long-term immune memory.

Antibodies perform different effector functions to contrast infections caused by pathogens (e.g. bacteria and virus). These include the *neutralisation of pathogens or toxins* by binding to pathogen proteins, thus preventing their adhesion to target cells and blocking interaction with cell receptors. Abs also activate *the complement system*, mediate *antibody-dependent cellular cytotoxicity* (ADCC) and facilitate the *opsonisation* of antigens. During opsonization, Abs bind to the surface of the microorganism and promote its phagocytosis by macrophages, neutrophils, or natural killer (NK) cells. This process is mediated by the Fc receptor, which, once triggered, sends signals to activate the cell' microbicidal activity or phagocytic capacity [2,3].

Antibody responses can be T-dependent or T-independent, based the involvement of T helper lymphocytes, which stimulate antibody production by B lymphocytes and enable Ig class switching. Notably, the nature of the antigen may dictate this aspect. After the protein antigens interacts with BCRs, it is endocytosed and presented; indeed, antigens are internalised in B lymphocytes and processed to peptide fragments, complexed to MHC class II molecules, and presented to $CD4^+$ helper T lymphocytes. In this way, antigen-specific T cells, bind to and recognize the peptide-MHC complex, sending costimulatory signals, through cytokine secretion, necessary for B-cell activation. The cytokine secretion of $CD4^+$ helper T lymphocytes is important for controlling the isotype of IgG secreted; in particular, interleukin-4 (IL-4) induces IgG1 production, while IFNγ (secreted by both $CD4^+$ and $CD8^+$ T cells) and interleukin-6 (IL-6) induce IgG2a production. Class switching to IgG2a and survival of memory B cells secreting IgG2a require the expression of the transcription factor T-bet [4,5]. Polysaccharide and lipid antigens instead induce T-independent antibody responses, stimulating the proliferation and differentiation of B cells without the help of T lymphocytes.

2.1.2 Cellular Immunity

Cellular or cell-mediated immunity is a component of the adaptive immune system that relies on specialized cells (T lymphocytes) instead of antibodies to mount immune responses. While humoral immunity is dedicated to the elimination of microorganisms at the level of extracellular compartments, cellular immunity is also able to eliminate intracellular microorganisms, that live and replicate inside infected cells, thus being inaccessible to circulating antibodies.

T lymphocytes initiate specific responses against antigens (Ags) presented by Major Histocompatibility Complex (MHC) molecules. Indeed, intracellular or internalized antigens are processed by cellular proteolytic systems ('antigen processing') to generate small peptides or epitopes. The complexes epitope-MHC are then transported to the cell surface, where they are recognized by specific T cell receptors (TCRs). There are two distinct classes of MHC molecules, which bind different types of antigens and are recognised by different functional classes of T lymphocytes: *i*) *MHC class I* which presents intracellular antigens (e.g. endogenous peptides derived from intracellular sources such as replicating virus) that activate $CD8^+$ T cells, and *ii*) *MHC class II* which presents extracellular antigens (e.g. exogenous peptides derived from extracellular sources) [6], that are internalized by antigen-presenting cells (APCs), such as macrophages, B cells, and dendritic cells through phagocytosis or endocytosis. These antigens are then processed in lysosomes and presented as peptides. They are important for the $CD4^+$ T cell activation

2.1.2.1 Phases of the cellular response – Priming of naïve T cells and memory response

Antigen recognition, co-stimulation and the presence of cytokines are necessary steps to induce the proliferation of T lymphocytes and their differentiation into effector and memory cells.

Intracellular or internalized Ags are processed and presented by APCs, in the form of a peptide-MHC complex. Dendritic cells (DCs) are the most efficient APCs for initiating primary responses as they activate naïve T lymphocytes; after recognizing Ags in the infected peripheral tissues, APCs transport them to secondary lymphoid organs, where naïve T lymphocytes gather and interact with thousands of MHC-peptide complexes exposed on the cell surface.

The antigens recognised by APCs are internalised and processed to peptide fragments, which are then complexed to MHC molecules and exposed on the cell surface. Many other membrane proteins take part in the activation process, such as:

- adhesion molecules, which stabilise the interaction between the lymphocyte and the APCs;
- co-receptors, which send biochemical signals;
- signals from the TCR complex and co-stimulatory molecules.

The TCR and CD3 are essential and specific for recognizing and interacting with the MHC-peptide complex on APCs [Figure 2.1.2.1.1 (A)]. The TCR directly binds the MHC-peptide complex and consists of a protein dimer made of two subunits: α and β, or in some specific cases γ and δ. CD3 is responsible for signal transduction, activating pathways like the mammalian target of rapamycin

(mTOR) and activating transcription factors (TFs) such as NFAT, AP-1, and NFκB into the nucleus to drive the expression of key T cell genes [7–9].

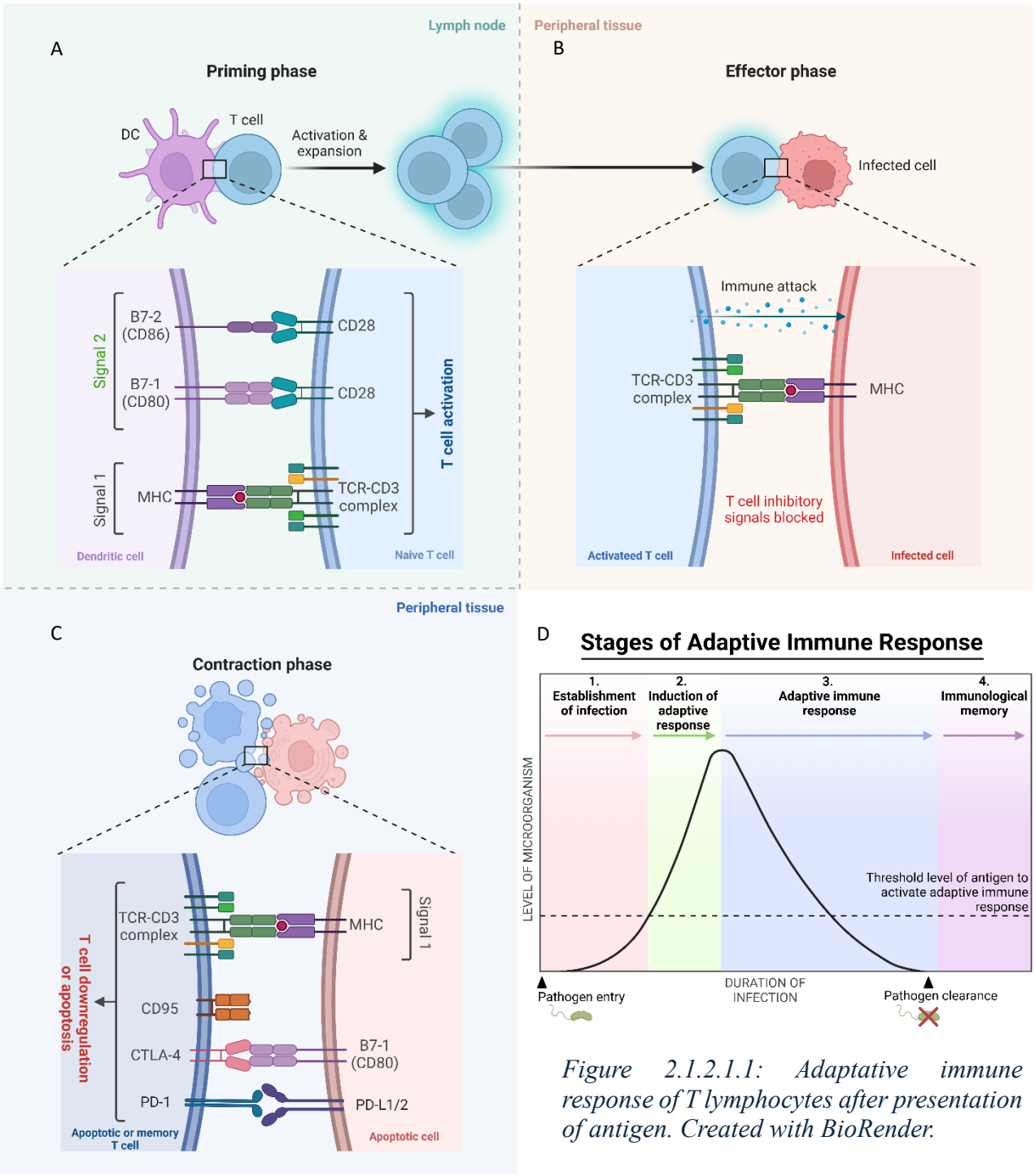


Figure 2.1.2.1.1: Adaptative immune response of T lymphocytes after presentation of antigen. Created with BioRender.

In addition to the TCR-mediated signal, T lymphocyte activation, expansion and differentiation can be induced by costimulatory molecules and cytokines produced by cells of innate immunity in response to the activation of Pattern Recognition Receptors (PRRs). In the absence of co-stimulation, antigen-recognising T lymphocytes are either not activated or enter a prolonged state of inability to respond to the antigen.

B7-1 (CD80) and B7-2 (CD86), proteins expressed on the membrane of APCs, bind the CD28 receptor expressed on T lymphocytes, triggering a series of second messengers involved in cell activation. These signals induce the expression of anti-apoptotic molecules, the stimulation of metabolic activity and the production of pro-inflammatory cytokines by APCs or neighbouring cells. These cytokines, including IFNα and γ, interleukin-2 (IL-2), interleukin-12 (IL-12), interleukin-23 (IL-23) or other pro-inflammatory cytokines, enhance clonal expansion, effector functions and memory development. Upon receiving appropriate antigenic and costimulatory signals, naïve T cells are committed to clonal expansion [9–11] and differentiate into effector cells, which counteract ongoing infections, and into memory cells, which ensure a faster and more specific lymphocyte response to a second possible infection by the same pathogen [Figure 2.1.2.1.1 (B)]. Effector T lymphocytes migrate from the lymph nodes to the site of infection or vaccination, where they exert their functions that may differ depending on their subset.

Effector $CD4^+$ T cells coordinate the immune response. They either remain in lymph nodes to provide help to B lymphocytes, or they migrate to the infection site to support the innate immunity and cytotoxic T lymphocytes (CTLs, $CD8^+$ T cells). Indeed, the activation of naïve $CD4^+$ T cells by MHC class II- bound epitope on APCs, generates different subsets of effector cells: Th1, Th2, Th17, or Treg. These subsets support antibody production by B lymphocytes and enhance the recognition of innate immune cells (e.g. neutrophils, macrophages, eosinophils). Moreover, T helper cells recognizing the MHC class II-bound epitope on the same DC presenting to $CD8^+$ T cells can facilitate CTL activation through cytokine secretion (promoting CTL expansion) or by enhancing the expression of co-stimulatory molecules on DCs to support $CD8^+$ T cells cytotoxicity [12].

Effector $CD8^+$ T cells target and destroy virus-infected or cancer cells by releasing cytotoxic molecules, such as perforin and granzymes. In addition, they produce pro-inflammatory cytokines (e.g. IFNγ) to regulate and coordinate the function of other cells. For instance, IFNγ and IL-12 regulate signalling pathways, driving the expression of effector genes, including the transcription factor T-bet, important for the function of effector $CD4^+$ and $CD8^+$ T cells [13,14].

Antigen elimination leads to the decline of T-response, characterized by the exhaustion and death of most effector cells (~90%) [Figure 2.1.2.1.1 (C-D)]. This occurs through different steps of deactivation, such as PD1-PDL1/2and CTLA4-CD80/86 interactions, apoptosis mediated by the upregulation of CD95 (Fas) [15,16] and Activation-Induced Cell Death (AICD). After antigen elimination, a small proportion of lymphocytes survive in a quiescent state, forming the memory T cell pool, responsible for the immune memory [17]. Memory T cells indeed are capable of mounting a faster and more robust and effective response upon re-exposure to the same antigen.

The memory T cell compartment consists of both $CD4^+$ and $CD8^+$ T cells that can rapidly reacquire effector functions, such as killing infected cells and/or secreting inflammatory cytokines that inhibit pathogens [10]. These cells present a distinct phenotype, such as the expression of CD45RO (in contrast to CD45RA, typical of naïve T cells) [18] and a different metabolism compared to effector cells [19,20].

The maintenance of memory cells relies on cytokines such as IL-7 and IL-15, which promote homeostasis and survival by inducing the expression of anti-apoptotic proteins (e.g. Bcl-2 and Bcl-X_L) and keep these cells in a mild and continuous proliferative state [21,22]. Memory $CD4^+$ and $CD8^+$ T cells can migrate to various tissues and are less dependent on co-stimulation compared to naïve cells. This allows the antigen presentation by APCs or other infected cells to occur also in peripheral tissues and not only in lymph node.

The migration and activation of memory T cells depend on their different phenotypes and the expression of regulatory molecules.

Memory T cells, either $CD4^+$ and $CD8^+$, can be divided in two large subpopulations: "Central Memory T cells" (T_{CM} cells, $CCR7^+CD27^+CD45RA^-$) and "Effector Memory T cells" (T_{EM} cells, $CCR7^-CD27^{-/+}CD45RA^{-/+}$). T_{CM} cells are a long-lived and self-renewing population that continuously recirculates through lymphoid tissues. They have a high capacity for clonal expansion following antigen exposure. The expression of lymphoid tissue-homing molecules, such as CD62L and C-C chemokine receptor type 7 (CCR7), guides their constant recirculation through lymphoid tissues via the blood.

T_{EM} cells have high capacity of replication and secretion of pro-inflammatory cytokines, but they have a lower longevity and developmental plasticity compared to T_{CM}; they are disseminated in peripheral tissues where they exert immediate effector functions. Compare with T_{CM} cells, the T_{EM} cells largely lack CD62L and CCR7 expression but express chemokine and adhesion molecules that allow them to rapidly infiltrate inflamed tissues [23,24].

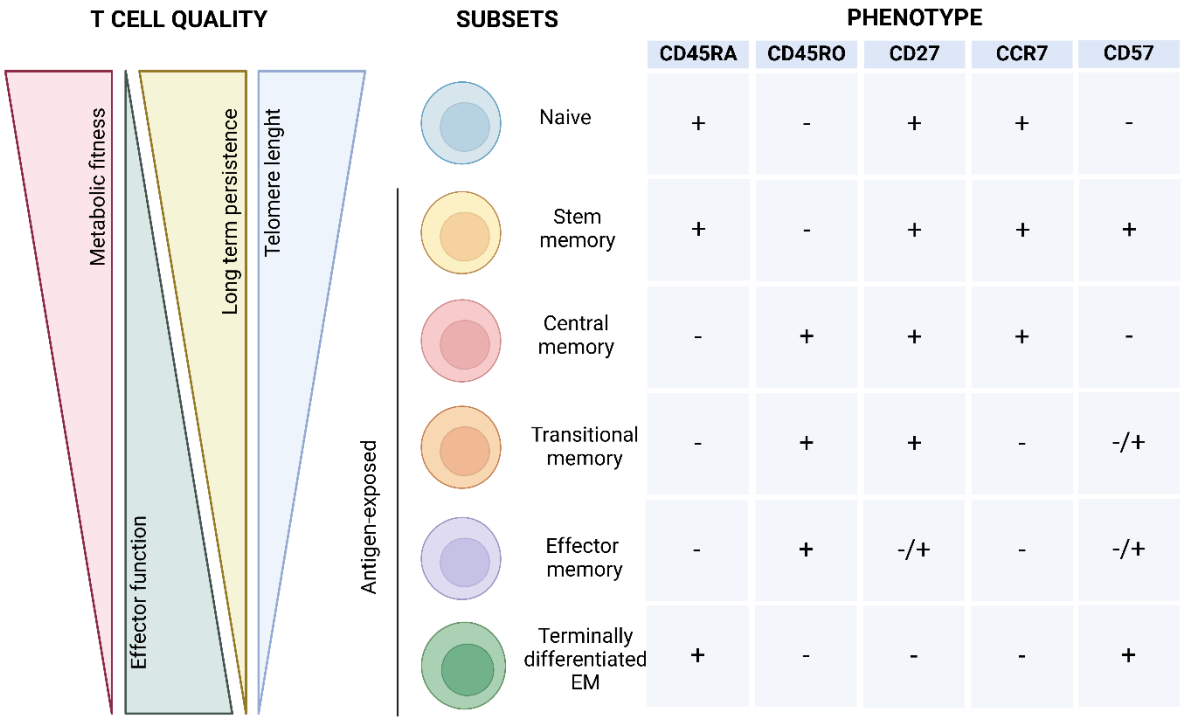
T "memory stem" (T_{SCM}) cells represent a rare subset of memory lymphocytes with stem cell–like properties, including self-renewal and the ability to differentiate into the full spectrum of memory and effector T cell subsets; they are $CCR7^+CD27^+CD45RA^+$ but they express also positive for CD57, a marker for understanding immune cell differentiation, function, and its implications in health and disease. Research in mice, nonhuman primates, and humans suggests that T_{SCM} cells are minimally differentiated and sit at the top of the hierarchical organization of memory T lymphocytes.

Their long lifespan and capacity to regenerate the diverse memory T cell compartment give them a dual role (both protective and potentially pathogenic) in human diseases; increasing evidence highlights their beneficial function in acute and chronic infections, positioning them as promising

candidates for therapeutic applications, such as vaccination and adoptive T cell therapy for infectious diseases and cancer [25].

In human, there is a subpopulation of T_{EM} cell, known as terminally differentiated effector memory cells re-expressing CD45RA (T_{EMRA}) cells, which represents a terminally differentiated subset with robust effector activity, such as high expression of pro-inflammatory markers and reduced proliferation capacity. These cells are characterized by the expression of the CD45RA isoform (instead of CD45RO) and are more prone to exhaustion under conditions of chronic stimulation (such as cytomegalovirus (CMV), Epstein-Barr virus (EBV), Human Immunodeficiency Virus (HIV), etc…) or immune dysfunction; their exhaustion status depends on the microenvironment and the duration of antigen exposure [26].

Another cell subpopulation, named Transitional Memory T cells (T_{TM}), can be identified by the markers $CCR7^{-}CD27^{+}CD45RA^{-}$. These cells show an intermediate differentiation status between T_{CM} and T_{EM} cells, characterized by intermediate telomere length, proliferative potential, and cytotoxic function, reflecting their transitional status in the memory T cell hierarchy [Figure 2.1.2.1.2] [26,27]



	CD45RA	CD45RO	CD27	CCR7	CD57
Naive	+	-	+	+	-
Stem memory	+	-	+	+	+
Central memory	-	+	+	+	-
Transitional memory	-	+	+	-	-/+
Effector memory	-	+	-/+	-	-/+
Terminally differentiated EM	+	-	-	-	+

Figure 2.1.2.1.2: Quality and phenotype of different subsets of T cells.

In older adults, the percentage of memory T cells is higher compared to naïve T cells, and this trend increases with age. There is, indeed, an inverse relationship between the proportion of naïve T cells and age. The decline in naïve T cell numbers and impaired lymphopoiesis with aging is caused by multiple factors, including thymic involution, defects in lymphopoietic progenitors, and persistent exposure to pathogens (both chronic and new infections). In addition, naïve T cells in older adults

exhibit reduced intrinsic and extrinsic activity due to metabolic alterations, which negatively impact their function and overall metabolism [28–30].

2.2 Immunometabolism

Metabolic reprogramming precedes and drives immune cell differentiation, activation and death [31], providing a rationale for manipulating certain components of cell metabolism as a therapeutic strategy against many common diseases.

At the cellular level, emerging evidence demonstrates a complex interplay between metabolism and inflammation, which must be precisely regulated to support biological functions. In addition, macrophages, dendritic cells and T lymphocytes can undergo metabolic reprogramming to support different types of cellular functions and activities. This reprogramming is controlled by key receptors, growth factors, cytokines (such as IL-7), and the availability of certain nutrients.

T lymphocytes show a great metabolic flexibility [32]; indeed, after TCR stimulation, they undergo a metabolic shift from a quiescent (low energy demand) to an activated state (high energy demand), evidenced by a change from catabolic to anabolic metabolism [33,34], which is necessary to support proliferation, increased cell mass and differentiation. This metabolic switch is reversible [35] and T cells sense the availability of nutrients in their microenvironment and adapt accordingly. Mitochondria are essential in driving this adaptation, optimizing their function to meet the dynamic metabolic demands of the cell [19]. The dynamic properties of mitochondria, including fusion, are crucial for their optimal function in energy generation [36].

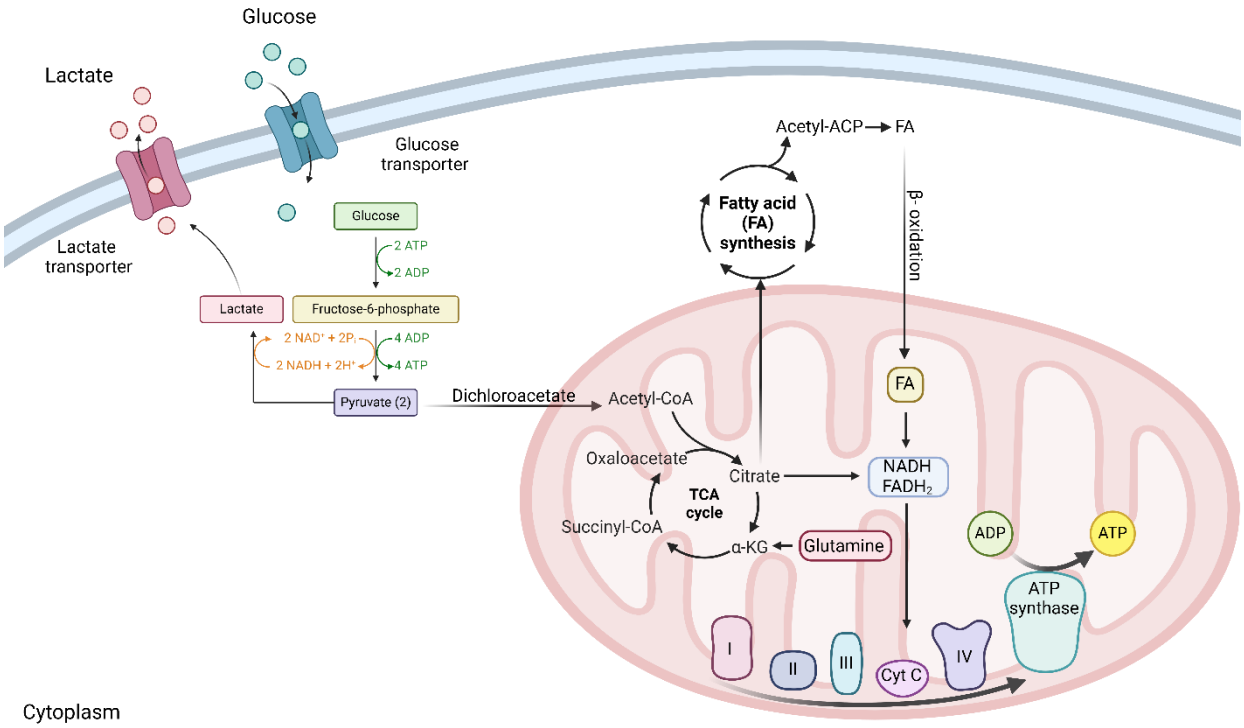


Figure 2.2.1: Schematic overview of basic cell metabolic pathways. Created with BioRender.

Six main metabolic pathways delineate T cells metabolic reprogramming: glycolysis, the tricarboxylic acid (TCA) cycle, the pentose phosphate pathway, fatty acid oxidation, fatty acid synthesis and glutamine metabolism [37] [Figure 2.2.1].

2.2.1 Glycolysis and oxidative phosphorylation

Under conditions of cellular homeostasis glucose serves as the main source of energy. After being imported from the extracellular space by specialised transporters (e.g. GLUT-1), glucose is irreversibly converted into glucose-6-phosphate (G6P) by the hexokinase and further metabolized in the cytoplasm into pyruvate, via glycolysis. This process, which is NAD^+ dependent, ensures the net production of 2 ATP molecules/glucose molecule and does not require oxygen. Pyruvate is transported into the mitochondria where it is converted to acetyl-CoA, which then enters the tricarboxylic acid (TCA) cycle to produce reduced cofactors NADH and $FADH_2$. These molecules serve as electron carriers, donating electrons to the electron transport chain in the inner mitochondrial membrane.
The electron transport chain consists of a series of transmembrane embedded proteins and organic molecules organized into four large complexes labelled I to IV. The first two complexes (I and II) oxidize NADH and $FADH_2$, respectively, transferring their electrons sequentially to complex III and complex IV. Lastly electrons are transferred to molecular oxygen, leading to the production of H_2O. During this process, complexes I, III, and IV pump protons across the inner mitochondrial membrane into the intermembrane space, creating an electrochemical proton gradient across the membrane. The return of protons to the mitochondrial matrix through ATP synthase drives the phosphorylation of ADP into ATP. This process, called oxidative phosphorylation (OXPHOS), can guarantee the production of 36 molecules of ATP per glucose molecule.

The activated lymphocytes need high quantity of energy [38–40]. To meet their demand, most pyruvate is converted to lactate in the cytosol by the lactate dehydrogenase (LDH) and only a small percentage (~5%) enters the mitochondria for oxidative phosphorylation. This strategy yields less energy production compared to cellular respiration (2 ATP *vs* 36 ATP per glucose molecule, respectively) but generates energy 10-100 times faster. This phenomenon, named ‘aerobic glycolysis’ or “Warburg’s Effect”, enables rapid ATP production and sustains glycolysis by regenerating NAD^+. High lactate production, even in the presence of oxygen, is characteristic of both activated immune responses and neoplastic conditions, reflecting high aerobic glycolytic activity.

2.2.2 Synthesis (FAS) and oxidation (FAO) of Fatty Acids

Fatty acid synthesis (FAS) [Figure 2.2.2.1] is an anabolic process that enables cells to generate lipids, necessary for their growth and proliferation, starting from precursors derived from other metabolic pathways, in particular glycolysis, the TCA cycle and the pentose phosphate pathway. When fatty acid synthesis is blocked, the maturation of $CD4^+$ and $CD8^+$ T lymphocytes is impaired [17].
During the TCA cycle, acetyl-CoA is condensed with oxaloacetate, generating citrate, which is transported from the mitochondria into the cytosol, where it is converted back into the two starting molecules.

The acetyl-CoA derived from this process can be carboxylated by the acetyl-CoA carboxylase (ACC) to produce malonyl-CoA. The fatty acid synthase (FASN) catalyses the condensation of acetyl-CoA with malonin-CoA, in an NADPH-dependent manner, elongating the fatty acid chain to generate palmitic acid and, for this, linear fatty acids of different length and degrees of unsaturation. Subsequently, fatty acid molecules can be condensed on glycerol to produce triacylglycerols and phospholipids, essential components of cell membrane [41,42]. Fatty acid synthesis also plays a key role in inflammatory responses in both innate and adaptive immune systems [43].

Fatty acid oxidation (FAO) [Figure 2.2.2.1] is a catabolic process in which fatty acids are broken down to generate energy. This pathway allows the production of large amounts of ATP; for instance, the oxidation of a single palmitate molecule yields more than 100 ATP molecules. The first step of FAO takes place in the cytosol where fatty acids are activated to acyl-CoA, through a reaction catalysed by the enzyme acyl-CoA synthetase in an ATP-dependent manner.

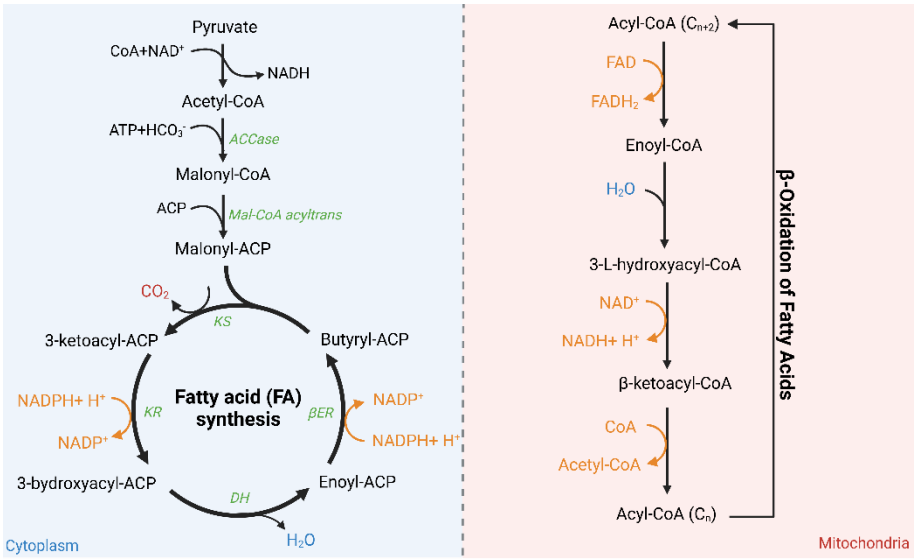


Figure 2.2.2.1: Fatty acid synthesis (FAS) and β-oxidation of Fatty acids (FAO).

The subsequent oxidation mechanism depends on the length of the aliphatic tail:

- *short-chain fatty acids* (SCFAs), with fewer than 6 carbon atoms, passively diffuse into the mitochondria;
- *medium-chain* (MCFAs) (between 6-12 carbon atoms) and *long-chain* fatty acids (LCFAs) (greater than 12 carbon atoms) required to be transported into the mitochondria via the carnitine shuttle. These fatty acid molecules are first conjugated to the carnitine by the carnitine-palmitoyltransferase I (CPT1). The resulting acyl-carnitine complex is then transported across the inner mitochondrial membrane, where carnitine palmitoyltransferase II (CPT2) regenerates acyl-CoA, which enters the β-oxidation pathway[44]

  The carnitine shuttle system ensures that cytosolic CoA, which is mainly used for fatty acid biosynthesis, is kept separate from mitochondrial CoA, which is used for fatty acid oxidative degradation.

After the fatty acids enter the mitochondria, β-oxidation takes place. During this process, acyl-CoA molecules are sequentially broken to produce acetyl-CoAs, NADH and $FADH_2$, which are further utilised in the TCA cycle and in the electron transport chain to generate ATP.

2.2.3 Glutamine metabolism

Glutamine is transported into cytoplasm through glutamine transporters, such as SLC1A5, SLC38A1, and SLC38A217. It plays a pivotal role in protein synthesis, energy demand, biosynthesis of nucleotides, and in epigenetic change regulation as reported by recent studies [45].

From the cytosol, the glutamine is transported in the mitochondria for the glutaminolysis. Here, glutamine is converted into glutamate by amidohydrolase enzymes (GLSs), that catalyse the reaction releasing ammonium ions. Mitochondrial glutamate can then be employed for various functions: it can participate in the biosynthesis of glutathione (an endogenous antioxidant tripeptide molecule, composed of glutamate, cysteine and glycine) and of non-essential amino acids (NEAAs). In addition, it can serve as an exchange factor for importing extracellular cystine[46].

Within the mitochondria, glutamate is converted into alpha-ketoglutarate (α-KG) by glutamate dehydrogenase 1 (GLUD1 or GDH1) or by several mitochondrial aminotransferases, including glutamic-pyruvic transaminase 2 (GPT2) and glutamic-oxaloacetic transaminase 2 (GOT2).

α-KG can then enter in the TCA cycle, supporting the oxidative phosphorylation (OXPHOS) pathway or the reductive carboxylation pathway [47]. In the oxidative phosphorylation pathway, glutamine metabolites contribute to the generation of electron donors, such as NADH or FADH2, following the synthesis of guanosine triphosphate (GTP) and adenosine triphosphate (ATP).

2.2.4 Metabolism of naïve T lymphocytes

Naïve T lymphocytes are “resting cells” characterised by an intense catabolic activity to the detriment of a limited anabolic capacity marked by a low energy state, reduced nutrient uptake, lack of cytokine secretion and cell division [37].

Glucose and fatty acid uptake are minimal in naïve T cells which also exhibit low levels of neutral lipid (NL) [48]. These characteristics reflect the cells' reliance on available nutrients. In absence of TCR stimulation, the most active metabolic pathways in naïve cells are oxidative phosphorylation (OXPHOS) and β-oxidation of fatty acids (FAO). Although these cells possess a very low mitochondrial membrane potential, they preferably use the oxidative phosphorylation for glucose degradation (a mitochondria-dependent process). In addition, leveraging catabolic-type metabolism such as fatty acid oxidation, glucose and amino acid degradation, naïve T cells ensure the generation of intermediates that support their energy requirements.

To maintain metabolic and energetic homeostasis, naïve T cells need specific signalling molecules, such as IL-7 and IL-15, which support their catabolic survival functions [34]. In contrast to this maintenance phase, the differentiation of naïve T cells into effector T cells upon antigen encounter requires an increased demand of nutrients such as glucose, glutamine, L-arginine, and other amino acids [49,50]

2.2.5 Metabolism of effector T lymphocytes

Upon TCR stimulation, to become fully activated and proliferative, naïve T cells shift from oxidative metabolism to a reliance on aerobic glycolysis (Warburg’s metabolism) and glutamine metabolism. Although this metabolic pathway, as explained above, is less efficient in terms of energy production, lactate secretion guarantees availability of glycolytic precursors for anabolic reactions, such as protein synthesis, nucleotide synthesis and fatty acid synthesis (*de novo* FAS). Lactate generation is also crucial as it regenerates NAD^+, which is essential for maintaining redox homeostasis and support glucose degradation into pyruvate.

Erika L. Pearce and colleagues claim that oxidative phosphorylation occurs simultaneously with aerobic glycolysis in activated T cells, although the latter is more upregulated, while mitochondrial respiration plays a relatively minimal role [51–53]. In addition to glucose, amino acids are critical for T cell proliferation and function. Specifically, glutamine metabolism is important for T cell proliferation but not for their cytokine production. Indeed, in the absence of glutamine, T cells are unable to proliferate but can still secrete cytokines. These findings suggest a synergistic contribution of glucose and amino acid (e.g. glutamine) metabolism to sustain T cell proliferation and effector functions.

When T cells assume their effector role, they shift their metabolism from fatty acid oxidation (FAO) to fatty acid synthesis (FAS), in order to meet the increasing requirements for cell division and for supporting processes involved in protein post-translational modifications.
The main modulators of metabolic regulation during activation are AMP-activated protein kinase (AMPK) and mammalian target of rapamycin (mTOR). AMPK is an AMP-activated protein kinase, which acts as an inhibitor of anabolic pathways by interfering with mTOR, thereby inhibiting T cell differentiation. AMPK is activated in response to energy and cellular stress, particularly when ATP consumption increases (e.g., during exercise, cell growth, or anabolic processes) or ATP production decreases (e.g., due to low glucose availability, oxidative stress, or hypoxia). These conditions are detected as a drop in the ATP-to-AMP/ADP ratio [54,55]. In contrast, mTOR is a serine/threonine kinase that induces the transcription of important glycolytic enzymes and enhances the translation of hypoxia-inducible factor 1-alpha (HIF-1α) mRNA [56,57]. HIF-1α, an isoform of the transcription factor HIF-1, plays a pivotal role in promoting the Warburg effect in activated T, even in the presence of sufficient oxygen [44,58,59].
Usually, T cell activation leads to a downregulation of AMPK activity in favours of mTOR.

2.2.6 Metabolism of memory T lymphocytes

Antigen elimination leads to the contraction of the cellular response, with the elimination of a large proportion of the effector population (~90%), while a small fraction of lymphocytes survives forming the memory T cell pool, responsible for immunological memory.
Memory T lymphocytes are quiescent cells, characterized by a catabolic metabolism marked by an increased respiratory reserve capacity, which correlates with the ability to oxidise substrates in the mitochondria [44,60]. This capacity is a hallmark of memory T cells, enabling faster cell reactivation as it provides rapid energy production upon antigen re-encounter. A crucial role in the metabolism of memory T cells is also played by the extensive oxidation of fatty acids. Specifically, the increased expression of lysosomal hydrolases, like lysosomal acid lipase (LALs), allows, through hydrolysis, the mobilization of fatty acids for β-oxidation [61,62].

The metabolic switch to an oxidative state in memory T cells is confirmed by the inhibition of the two mTOR complexes: mTORC1 and mTORC2. Inhibition of mTORC1 (mammalian target of rapamycin complex) by AMPK (AMP-activated protein kinase) promotes the survival of memory T cells and the oxidation of long-chain fatty acids by acting on TRAF6 (TNF Receptor Associated Factor 6). Conversely, mTORC2 inhibition promotes memory T cell development by reducing the

phosphorylation of Forkhead box protein O1 (FOXO1), allowing its translocation to the nucleus where it promotes memory-related gene expression [44,63,64].
Similar to naïve T cells, memory T cells require IL-7 and IL-15 for catabolic survival. In addition, interleukin-10 (IL-10) signalling plays a crucial role in suppressing the proliferation of activated T cells [65,66].

2.2.6.1 Mitochondrial properties and morphology in effector and memory T lymphocytes

Effector and memory T cells present differences in effector functions and cell marker expression as well as in mitochondria functionality and morphology. Indeed, both T cells subtypes exhibit a different mitochondrial networking and morphology, that reflect their distinct metabolic requirements. In effector cells, mitochondria are recruited to the immune synapse after an antigen encounter, following cleavage from mitochondrial-endoplasmic reticulum (ER) contact sites, to favour calcium influx and T cell activation. Conversely, memory T cells reorganize their mitochondria to closely associate with the ER, a characteristic lacking in naïve and effector T cells, thus providing a pool of mitochondria which support the aerobic glucose metabolism. Another feature that impacts on metabolism and distinguishes mitochondria of effector and memory T cells is the remodelling of their morphology, including changes in mass, volume and cristae structure. Effector cells exhibit mitochondrial fission, which leads to cristae loosing and reduced electron transport efficiency, causing reactive oxygen species (ROS) production and upregulation of anaerobic glycolysis. In contrast to effectors, memory T cells undergo mitochondrial fusion, which ensures protection against ROS-induces DNA damage and sustains survival under stress conditions. These capacities rely on the presence of mitochondria characterized by an increased volume, mass and cristae density, which leads to reduced ROS production and efficient mitochondrial respiration [19,61,67,68] [Figure 2.2.6.1].

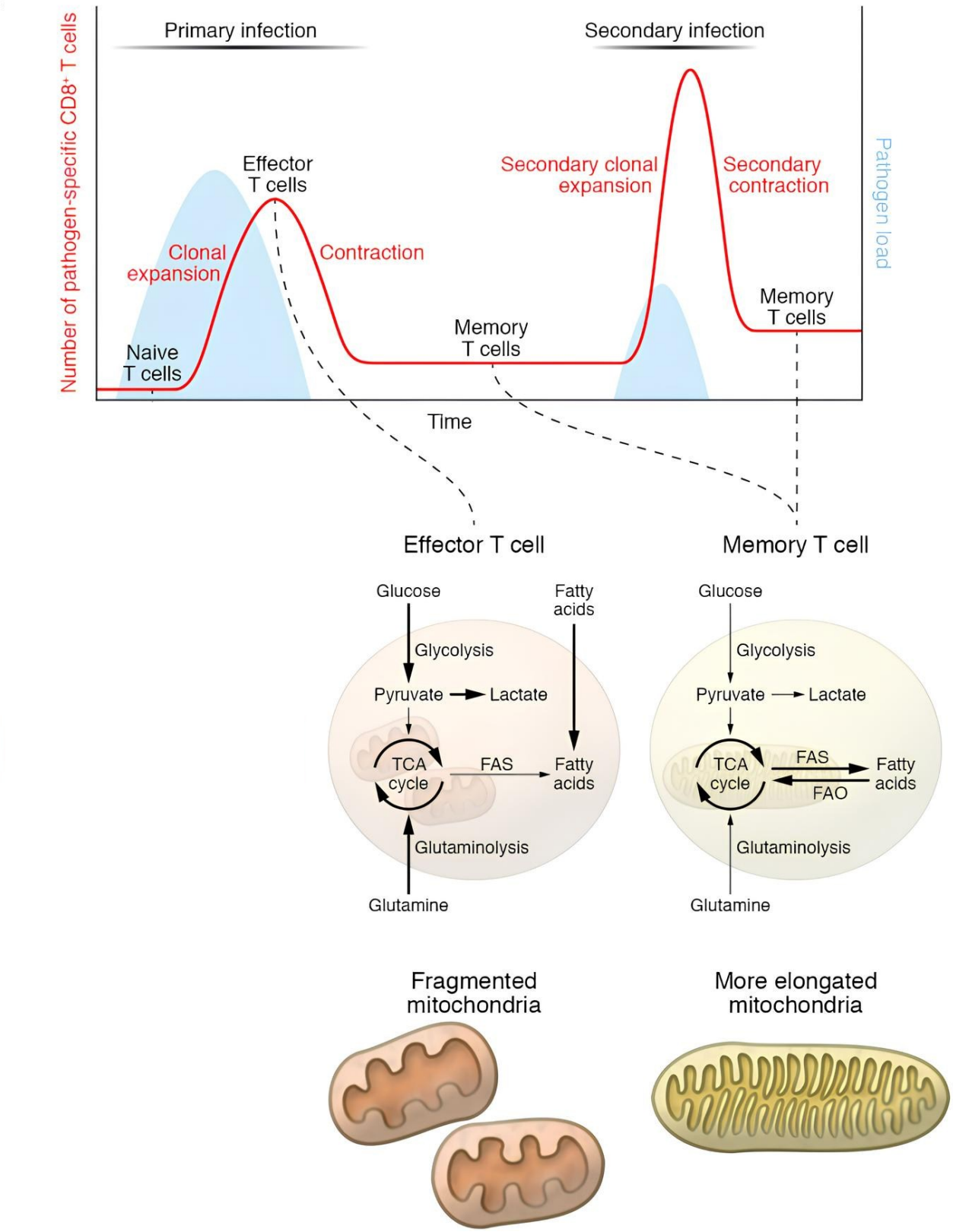


Figure 2.2.6.1: The different metabolic pathways of T lymphocytes (effector and memory T cells), from "Targeting memory T cell metabolism to improve immunity" of Mauro Corrado, Erika L. Pearce.

2.3 Immunosenescence

Immunosenescence is an irreversible and progressive deterioration of the immune system, caused by the natural aging process [Table 2.3.1].

Table2.3.1: The effects of aging on immune system (by "The Complex Role of Regulatory T Cells in Immunity and Aging" of Lourdes Rocamora-Reverte, 2021)

Immune organ/cell	Changes in aging
Thymus	↓ bone marrow progenitors ↓ sex hormones ↓ thymic ephitelial cells ↑ adipose tissue
APC	↓ antigen processing capacity ↓ antigen presenting capacity ↑/ ↓ chemotaxis, cytokine production and signal transduction
Neutrophils	↓ chemotaxis, cytokine production and signal transduction
B cells	↓ somatic hypermutation ↓ Ig class switch ↓ number of plasma cells
T cells	↓ TCR repertoire ↑ effector-memory cells ↑ DNA damage accumulation

The severity of many infections increases with age, making the elderly population more susceptible to infections, cancer, autoimmunity, and inflammation disorders. Additionally, older adults have a reduced capability to respond to pathogen challenges and exhibit a diminished responsiveness to preventive vaccinations [69–72].

Several factors contribute to immunosenescence, such as: mitochondrial dysfunction, oxidative stress, genomic instability, epigenetic alterations, telomere shortening, expression of senescence-associated markers (e.g. CD57, KLRG1, p38, and γH2AX) and of specific NK inhibitors (KLRG1 and NKG2A) and activators (NKG2C and NKG2D) markers impair the adaptative responses [73–76]. In the elderly population the capacity of APCs to process and present antigens to T cells declines and other processes as chemotaxis, cytokine production and signal transduction are impaired upon antigen recognition [77]. These alterations lead to the establishment of a chronic, low-grade inflammatory state, commonly referred to as *inflammaging,* characterised by dysregulation and increased release of various pro-inflammatory mediators, including tumour necrosis factor-α (TNFα), interleukin-1β (IL-1β) and IL-6 [78–80] .

Although these cytokines are involved in normal immune function, their persistent high levels can damage tissues, contributing to an increased incidence of chronic diseases [79].
Reduced immune defence in older individuals results in the accumulation of damage-associated molecular patterns (DAMPs) and pathogen-associated molecular patterns (PAMPs) in the body, thus contributing to chronic immune system activation and, consequently exacerbating inflammation [81].

As described by Rodriguez and colleagues, one of the major age-associated changes during immunosenescence is thymic involution, characterized by the reduction both in size and functions. This process leads to a significant alteration of naïve T cell number, with a most pronounced, to decrease in $CD8^+$ cells compared to $CD4^+$ T cells population [82]. This decrease is accompanied by a decline in T cell receptor clonal diversity and increase in memory subpopulation, with accumulation of terminally differentiated T cells (T_{EMRA}) that are either dysfunctional or exhausted [83]Furthermore, these highly differentiated memory cells possess several markers of cellular senescence, such as a reduced mitochondria number, impaired glycolysis upregulation after antigen presentation, shortened telomeres and markers of DNA damage associated with compromised repair mechanisms [74].
Thymic involution is likely driven by multiple factors, such as a decrease in sex hormone levels, loss of thymic epithelial cells (TEC) and increase of adipose tissue. The accumulation of adipose tissue exacerbates inflammation through the production of pro-inflammatory cytokines, such as IL-6 [84], which then suppresses TEC functions, reducing thymopoiesis and cellularity, together with a reduction of trophic cytokines, such as IL-7, which are important for the maintenance of resting cells.
Following reduced thymic production, the organism preserves the naïve T pool through homeostatic proliferation, a TCR-independent signal. Homeostatic proliferation occurs when T lymphocytes react to IL-7, via the IL-7 receptor (CD127), and IL-2, which transmit signals to the nucleus though the phosphorylation of Signal transducer and activator of transcription 5 (STAT-5) [85].
Although the expression level of CD127 and STAT5 is quantitatively similar in young and old individuals, however, the proliferation of peripheral naïve T cells in the elderly is not sufficient to keep their number constant [86,87].
Senescent naïve T cells are characterized by the loss of the co-stimulatory molecules CD27 and CD28, a decrease in growth factor IL-2 and an increase in the production of pro-inflammatory cytokines [88,89]. These changes contribute to tissue damage and to the pathogenesis of aging.
The loss of co-stimulatory molecules affects the efficacy of activation, clonal expansion and differentiation of T cells. In the elderly, TCRs, which enable a broad response to pathogens, undergo a considerable reduction in repertoire, limiting the diversity of immune response.

Furthermore, homeostatic proliferation accelerates telomere shortening contributing to a persistent DNA damage response during replicative senescence. Consequently, homeostatic proliferation leads to deflection and narrowing of the repertoire and efficient amplification of self-responsive clones, which may contribute to decreased acquired immune response capacity and increased predisposition to self-response [90].
Despite these changes, the total immune cell pool remains stable between young and old adults, largely due to the compensatory role of NK cells. In the elderly, the persistent activation of mitogen-activated protein kinase (MAPK) p38 drives the increase in memory T cells [91], which results in the presence of many terminally differentiated memory cells, as T_{EMRA}, which are non-proliferating T cells.

Recent studies have identified several hallmarks of senescence $CD8^+$ naïve T lymphocytes: *i*) a quantitative decrease [92], *ii*) increased apoptosis susceptibility [93], *iii*) low intrinsic and extrinsic activity due to metabolic alterations [48,94], *iv*) suboptimal proliferation and differentiation in response to TCR-mediated activation [78,95]. The presence of few and dysfunctional naïve T cells leads to a decline in primary immune responses in the elderly, making them less responsive and more vulnerable to new infections [96,97]. Thus, in addition to the decline of the naïve lymphocyte repertoire in favour of the memory repertoire (switch of subsets), it has been observed a decrease of T cell cytotoxicity, thus reducing their functionality [98].
Humoral immunity too results compromised in older subjects: the percentage of peripheral B lymphocytes decreases, but the number and frequency of pro-inflammatory B cells rises. These changes are largely due to the increase in the pro-inflammatory signals CD40L, IFNγ and interleukin-21 (IL-21). The decline in naïve B cells leads to a reduction in the production of high-affinity antibodies, which explains the decrease of antibody maintenance [98,99].

Finally, the innate immunity compartment is not spared by aging: it has been found that myeloid-derived suppressor cells accumulate in the marrow, through an NF-κB-dependent mechanism. They produce IL-1β and have enhanced suppressive activity on T cell proliferation and B cells lymphopoiesis [100]. Furthermore, aged macrophages exhibit an intensification of inflammatory pathways, including the NLRP3 inflammasome activation, while phagocytic capacity is reduced.

2.3.1 Immunosenescence and immunometabolism

Despite the study of immune cell metabolism in older age is a relatively new area of study, some evidence highlights that bioenergetic features of adaptive and innate immune cells are compromised in the elderly. The following observation have been collected in older subjects:

i) A dysregulation of nicotinamide adenine dinucleotide (NAD^+) metabolism, negatively affecting the metabolism of key nutrients such as glucose, lipids and amino acids in immune cells. This impairment leads to a decrease in glycolytic and mitochondria metabolism, resulting in alterations of T and B cell activation [98,101]. The reduction of NAD^+, due to chronic inflammation, leads to an increase in oxidative stress and pro-inflammatory cytokine production.

ii) The accumulation of senescent cells in the adipose tissue and liver, making people's health status precarious. Senescent cells are characterised by impaired proliferation and a high-level production of phenotype factors (SASPs) [94,102]. In turn, SASPs, stimulate the expression of CD38, a NAD degrading enzyme, on immune cell surface, leading to a depletion of NAD^+ [103]. During aging, also the proteostasis, is impaired, causing an accumulation of misfolded proteins in tissues, which contributes to the occurrence of diseases.

iii) Senescent B-cells, which impairs the effectiveness of humoral responses, are accompanied by a shift in cell metabolism. B-cells, reliant on glycolytic metabolism for activation and differentiation, show with aging a decrease in glycolysis further to relevant defects in mitochondrial energy production [104].

iv) Senescent T lymphocytes in the thymus, increasing the risk of autoimmunity, infection [94] and leading to altered tissue homing and functionality. These senescent cells present dysfunctional mitochondria induce inflammaging.

v) Several metabolic changes at level of T cells. While β-oxidation of fatty acids is more active in adults compared to the elderly, aged naïve T cells have higher lipid uptake and increased storage of neutral lipid [105]. This is likely driven by up-regulation of Diglyceride Acyltransferase (DGAT-1), which encodes for the key enzyme involved in the triglyceride storage. In addition to DGAT-1, increased mRNA expression of Inhibitor DNA-binding 2 protein HLH (ID2), a metabolic regulatory factor promoting a high mitochondrial membrane potential and neutral lipid accumulation, is observed. ID2 exerts its effects by inhibiting fatty acid oxidation promoters in naïve elderly cells. Despite aging, naïve T cells in elderly individuals exhibit no significant alterations in the expression of genes regulating metabolic exchange, as glycolytic enzymes are over-regulated after activation like adults. However,

differences emerge in the expression of HIF-1 and RPS6KB1 (ribosomal protein S6 kinase B1) which are increased in adult cells compared to elderly ones [105].

2.3.2 Immunosenescence and responses to vaccination

Currently, more than 11% of the world's population is 60 years of age or older and this percentage is expected to increase to 33% by 2050 [106]. Specifically, in the European Union, the population over 65 increased from 17.6% to 20.6% between 2010 and 2020 and is predicted to exceed 31% by 2100 [107]. With a globally aging population and rising susceptibility to epidemics, developing effective vaccines and adjuvants for elderly individuals is essential to pose significant societal, economic, and healthcare challenges.

Despite the elderly are encouraged to get vaccinated against influenza, herpes zoster, pneumococcal disease, respiratory syncytial virus, tetanus, and diphtheria, immunosenescence diminishes vaccine efficacy. For instance, the effectiveness of influenza vaccines drops from 70-90% in younger individuals to 30-50% in those over 65 [108,109]. This can be explained by the quantitative and qualitative reductions of naïve B and T cells that hampers the immune response to new antigens in the elderly.

Dendritic cells are critical APCs that initiate naïve T cells and play a crucial role in mounting strong and long-lasting vaccine-specific responses. Aging results in a reduction of DCs subset numbers and in a decline of their phagocytic, antigen-presenting, and cytokine-secreting capabilities. These decreases hinder T cell activation and weaken immune responses [110].

The hematopoietic function of bone marrow diminishes with age leading to a decrease in B cell numbers: However, age-associated B cells (ABCs) increase, impairing young B cell generation and vaccine efficacy [111]. Despite an increase in antibody quantity in the elderly, their functionality decreases, as demonstrated by the decline of their neutralising power. This phenomenon was particularly evident during the SARS-CoV-2 pandemic [112].

As mentioned above, T lymphocytes play a crucial role in counteracting new pathogens and, especially during vaccination, in ensuring a memory pool of immune cells. This memory pool is critical for reducing the severity of bacterial and viral infections if the pathogen is encountered again. However, thymic involution in aging leads to a loss of naïve T cells. This is accompanied by a decline in TCR expression and costimulatory molecules like CD27 and CD28, resulting in impaired T cell activation and proliferation following vaccination. In some cases, T cells have been shown to express an exhausted phenotype, which is characterised by a high production and expression of depletion markers such as Tim-3, PD1, CD38 and HLA-DR. These markers are expressed in chronic infection (e.g. CMV or Herpes Simplex Virus 1 and 2 (HSV1/2)) and tumours, where effector functions, such

as cytotoxic activity of $CD8^+$ T lymphocytes and cytokine production, are reduced [113,114]. With aging, a high proportion of the T cell population adopt this exhausted phenotype, expressing high level of Tim-3 and PD-1, even in the absence of infection or tumours. This phenotype leads to a decline in T lymphocyte function, contributing to a reduced response to pathogens or vaccination [115].

Given these challenges, it is crucial to design vaccines that consider the impact of aging on immune system. This involves targeting of specific immune pathways and cells affected by immunosenescence, including the enhancement of dendritic cell function, reduction of senescent macrophages and boosting T and B cell responses. Understanding and addressing these age-related changes may lead to more effective vaccines or possible new adjuvants, providing better protection for the elderly and contributing to healthier aging worldwide.

2.4 COVID-19 and pneumococcal disease

Age-related changes in the immune system are thought to underlie the vulnerability of elderly individuals to emerging viral diseases, such as coronavirus disease 2019 (COVID-19). During the SARS-CoV-2 pandemic elderly subjects with pre-existing and precarious health conditions (e.g. CVD, pulmonary disease or metabolic disorders) were particularly at risk of mortality and illness due to COVID-19. This heightened vulnerability underscores the urgent need for targeted interventions, particularly vaccination [107,116,117].

While older adults faced the highest fatality rates, younger populations were also susceptible to SARS-CoV-2 infection. Although young individuals generally experienced less severe outcomes compared to the elderly, they showed a higher prevalence of long COVID syndrome [118]. As mentioned earlier, the global population is getting older, prompting many nations to prioritise mass vaccination campaigns, starting with the elderly. This strategy has proven highly effective in decreasing new cases, hospitalisations, deaths and access to intensive care units, underscoring the effectiveness of herd vaccination starting with this more fragile population group [Figure 2.4.1].

This has led to the development of specific vaccines against the SARS-CoV-2 virus, giving rise to new vaccine technologies or the use of new adjuvants, which enhance the vaccine response. The most widely used vaccines in the European Union are vaccines based on mRNA (Comirnaty and Spikevax) and vaccines with an adenoviral vector (Vaxzevria and Janssen), marketed by BioNTech/Pfizer, Moderna, AstraZeneca and Johnson & Johnson. Despite the varying efficacy and safety of these vaccines, which are all based on the same vaccine antigen (Spike protein of SARS-CoV-2), they all represent a very good success for the outcome against the pandemic, demonstrating excellent immunogenicity and vaccine coverage.

Thanks to the availability of these vaccines, the effects of the SARS-CoV-2 pandemic has been significantly mitigated. Moreover, it has also made possible the long-term control of the pandemic and spurred the development to new vaccine techniques, laying the groundwork for new vaccine therapies. In conclusion, the development of new effective vaccines, and the prioritisation of older adults in vaccination strategies, has been crucial against SARS-CoV-2.

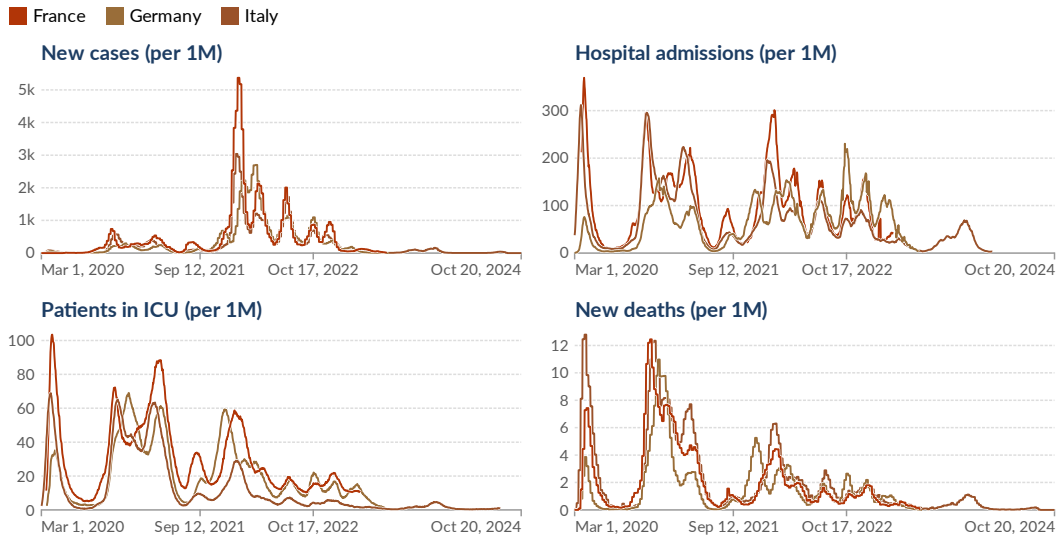


Figure 2.4.1: Confirmed COVID-19 cases, deaths, hospital admissions, and patients in intensive care unit (ICU) per million people. Data from "Our world in Data" (https://ourworldindata.org/covid-deaths).

Streptococcus pneumoniae (pneumococcus), a gram-positive bacterium and major causative agent of pneumonia in both adults and children, is an important and complex public health challenge, as it is difficult to treat due to antibiotic resistance, wide serotype diversity (90 serotypes but only a part are responsible for pneumococcal disease) and complexity in conjunction with other pulmonary and cardiac comorbidities [119]. These factors complicate both treatment and prevention strategies, highlighting critical issues in current guidelines for managing pneumococcal infections. The vaccination strategy remains a good 'weapon' capable of combating and preventing this pathogen. Indeed, vaccines play an important and fundamental role not only for individual protection, but also contribute to important socio-economic benefits, by reducing public healthcare costs and limiting the spread of antibiotic-resistant strains.

Age has a critical role on the severity of pneumococcal infections. The elderly experience a greater invasiveness of pneumococcal disease and pneumonia. In particular, the over-50s are subjected to considerable mortality and morbidity, which underlines the fact that therapeutic interventions (e.g. antibiotics) are not effective against the resolution of the disease, and vaccination remains a preventive but also a therapeutic tool. Another significant challenge posed by *Streptococcus pneumoniae* infection, is its interaction with other bacteria or virus, particularly influenza viruses.

Indeed, this co-infection significantly increase the percentage of poor clinical outcomes, further complicating the clinical management [120]. This underlines the importance of concomitant vaccination with both influenza and pneumococcal vaccine to mitigate and decrease the risk of severe bacterial infections.

As mentioned before, the vaccination strategy remains an excellent option to prevent and treat infections and possible side effects caused by this bacterium. There are two types of anti-pneumococcal vaccine: polysaccharide vaccine (PPV) and glycoconjugate vaccine (PCV), with different characteristics, indications, immunological mechanisms and immunogenicity. Both are based on the induction of immune responses against polysaccharides, constituents of the bacterial capsule, which differ between the different pneumococcal serotypes. Each vaccine is characterised by the number of polysaccharide antigens it is composed of and thus the number of serotypes against which it is expected to be active.

The PPV-23 vaccine, a polysaccharide vaccine, has a broad serotype response, as it consists of 23 polysaccharides covering the different bacterial strains. This ensures a good vaccine coverage, but elicits a T-independent response, resulting in lower immunogenicity (especially in infants) and less disease resolution. In contrast, PCV vaccines, usually conjugated to diphtheria toxin (CRM_{197} vector protein, a non-toxic mutant of diphtheria toxin (derived from Corynebacterium diphtheriae C7) expressed in recombinant form in Pseudomonas fluorescens), induce a T-dependent response, which allows for a larger immunological memory in all age groups [107,121].

The introduction of PCV vaccines, such as PCV-7 and after PCV-13 in the paediatric population and PCV-21 (available since middle 2021) in adult population, have radically reduced the incidence of pneumococcal disease, but has also indirectly benefited the elderly, because transmission between these two age groups has been reduced, underlining the importance of mass and widespread vaccination [122]. Despite these advantages, emerging infectious serotypes pose an ongoing challenge in the design of new anti-pneumococcal vaccines. The development of new vaccines with broader immunogenic coverage is essential. These vaccines must effectively coordinate humoral (B cells) and cellular (T cells) immune response to counteract serotype substitution and enhance long-term protection.

The achievement of this goal requires constant research and policy attention, leading to a multidisciplinary approach that ensures individual health and advancing the collective good.

3. OBJECTIVES

Today, most people can anticipate living into their sixties and beyond, with every nation experiencing an increase in both the number and proportion of older individuals in the population. According to the World Health Organisation (WHO), by 2030, one in six people globally will be aged 60 or older, with the number of individuals in this age group rising from 1 billion in 2020 to 1.4 billion. By 2050, the population of those aged 60 and above will double to 2.1 billion, and the number of people aged 80 and older is projected to triple, reaching 426 million. In addition, advanced age is often associated with a rise in both acute and chronic illnesses, leading to a significant decline in quality of life. Consequently, this increases the need to provide care for older individuals in poor health.

Notably, elderly people are more frequently and severely affected by infections compared to younger individuals [123,124]. For instance, co-infections caused by *Streptococcus pneumoniae* are particularly relevant in the context of viral respiratory infections, such as influenza or COVID-19, and disproportionally impact older individuals [125–127].

Vaccination has been proven to be the most cost-effective strategy to fight pathogens. In recent years, new vaccine technologies have been developed, such as those deployed for anti-SARS-CoV-2 vaccines (e.g. mRNA vaccines), ensuring good efficacy and safety, but the response of older people to vaccination is considered generally suboptimal [128]. For instance, studies show that the immunogenicity to the SARS-CoV-2 vaccine BNT162b2 [129,130], Human Papillomavirus (HPV) vaccines [131], and Hepatitis B vaccines [132] is indeed reduced in the elderly.

The need to learn more about immune reactivity to infections and vaccinations in the elderly has never been greater and this work aims to unravel how the immune system ages and how it responds to new pathogens or vaccines. Older adults are characterised by immunosenescence, a physiological decline of the immune system, which affects the quality and quantity of immune cells.

In the first part of this thesis, we focused on the remodelling of the immune system with advancing age; in particular, the phenotype of T and B lymphocyte subsets and the expression of activation markers has been investigated. Consecutively, we looked longitudinally at the remodelling of the immune system in elderly infarcted adults, as under acute stress conditions (as in the case of myocardial infarction) the immune system adapts to cope with the emergency condition. This is of particular relevance as several comorbidities accumulate with age and impact immunosenescence trajectories.

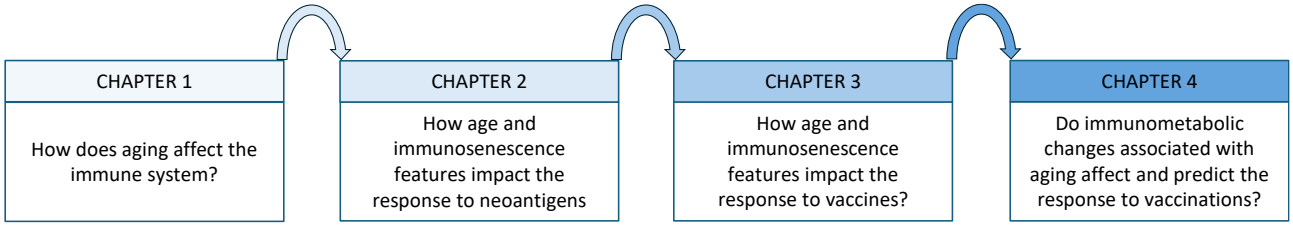
The second part of the thesis was focused on examining age-related alterations in epitope-specific naïve $CD8^+$ T cells. This investigation was conducted within the context of COVID-19, analysing the capacity of older adults to generate primary immune responses to SARS-CoV-2, a model well-suited for studying primary responses in previously unexposed individuals.

To confirm results obtained through *in vitro* models, we next wanted to assess, *ex vivo*, the extent of potentially diminished vaccine response in the elderly. Therefore, in the third part, we examined the immune response to the BNT162b2 (mRNA) and ChAdOx1-S (viral vector) COVID-19 vaccines, six months after primary vaccination and approximately six months following the booster dose. Donors were categorized into age groups: young (18–40 years), middle-aged (40–65 years), and older (>65 years). We thus measured the durability of the cellular memory responses as a function of age of the recipient and of the type of vaccine administered.

Immunosenescence impacts T cell metabolism by altering metabolic pathways in both resting and activated states. With this in mind, we investigated the immunometabolism of naïve $CD4^+$ and $CD8^+$ T lymphocytes in participants vaccinated with PCV13, an anti-pneumococcal vaccine. Specifically, we conducted metabolic analyses before vaccination (Day 0) to identify differences between young and older individuals and assess how these might affect vaccine responsiveness. We purposefully focused on naïve T cells because the initial results highlighted a strong quantitative remodelling of this subset with age. Sections 2 and 3 demonstrated, both *in vitro* and *ex vivo*, that immune responses induced by neoantigens (arising from naïve T cells) were significantly altered in the elderly. Therefore, we aimed to explore whether these age-related declines in immunity could be attributed not only to quantitative but also to qualitative defects at the level of naïve T cells.

However, the magnitude of the cellular response to PCV13 seemed barely influenced by age; although specific metabolic differences were observed between naïve T cells from younger and older participants, these did not affect the immunity to this specific vaccine. As within both age groups (younger and older subjects) we had similar proportion of individuals with poor and high cellular responses to PCV13, we next shifted our focus to variations in responsiveness and individual differences among participants, with the aim of identifying metabolic determinants of naïve T cells that, before vaccination, can predict and explain poor responsiveness.

As the global population ages, understanding the impact of immunosenescence on vaccine responses becomes increasingly important. By identifying key markers of immune function and tailoring vaccination strategies, we can improve health outcomes and strengthen the ability of older adults to fight infections, ensuring a healthier future for aging populations.



CHAPTER 1:

The effect of aging on the immunophenotype and the role of myocardial infarction

1.1 Introduction

Aging is complex biological process with outcomes that span form individual's health to social/psychological conditions [133], with negative impacts on the immune system. Indeed, growing older a gradual qualitative and quantitative deterioration of immune functions occur (immunosenescence), with reduction of adaptive immunity mechanisms and non-specific production of pro-inflammatory cytokines, which cause chronic inflammation (inflammaging); this contributes to increased susceptibility to infections and decreased response to vaccines [134].

Thymic involution is the cornerstone of immune system senescence, as the reduction of thymic cells and increase in adipocytes, fails to ensure the maturation of naïve T lymphocytes, resulting in a decrease in naïve cells, thus decreasing the diversity of the T lymphocyte repertoire, leading to a decline response to new antigens. This especially appeared evident during the COVID-19 pandemic and seasonal influenza virus infections [135].

The reduction of the naïve pool in some cases results in an increase of memory T/ B cells, which tend to become more senescent or exhausted with age, producing high amounts of cytokines and pro-inflammatory mediators with a downregulation of co-stimulatory markers such as CD27 and CD28. These soluble factors stimulate other cells to become metabolically active, but immunologically non-functional, altering T cell functions such as proliferation, migration, and pathogen elimination. Inflammaging, caused by a dysregulated production of cytokines and senescence-associated secretory phenotype (SASP), which accumulate in the body, does not guarantee T cell homeostasis, leading to basal and chronic inflammation, which has various negative effects on systems and apparatuses, generating chronic age-associated diseases, such as cardiovascular diseases (CVD), endocrine and metabolic diseases, cancer, Alzheimer's disease, and autoimmune diseases.

Another important point, associated with CVD, is the presence of high visceral adipose tissue (VAT), which contributes to the formation of chronic low-grade inflammation, which involves a complicated network of responses of the immune system, including adaptative (T and B cells) and innate immunity, such as macrophages. Obesity accelerates T cell immunosenescence, independent of chronological aging, and ensures the appearance of exhausted immunophenotypes.

Immunosenescence and cardiovascular system are intricately intertwined, significantly impacting the progression of dysmetabolism and cardiac diseases. The risk of myocardial infarction (MI) increases significantly with age and epidemiological data show that the incidence of MI is relatively low in individuals under 45 years of age, and approximately 80% of deaths due to acute MI are in individuals aged over 65 years, with 60% occurring in those aged 75 or older. The elderly individuals face a 4.9 to 6.3 times higher risk of death compared to those aged 45-64 [136,137]. Additionally, older patients are more prone to severe complications, including cardiogenic shock and significant bleeding, during hospitalization. These outcomes reflect the combined effects of advanced comorbidities and age-related physiological changes, which complicates the recovery [136,138].

The immune homeostasis caused by the proliferation and senescence of $CD4^+$ T cells is involved in age-related cardiac dysfunction [139,140]; in fact, excessive accumulation of memory T cells and T_{EMRA} correlates with an elevated risk of cardiovascular disease, heart failure progression, and increased cardiac-specific mortality rates.

The dysregulation of lipid metabolism is, together with the chronic low-grade inflammation that characterizes older age, the major causes of myocardial infarction (MI), which determinates the formation of atherosclerotic plaques, with high percentage of $CD4^+$ T_{EMRA}, can secrete significant amounts of CCR5, CCR7, and CXCR1, promoting inflammation at the site of atherosclerotic plaques [141].

During MI, the blockage of coronary arteries leads to ischaemic damage and the death of cardiomyocytes, with the formation of necrotic tissue and then scar tissue; this damage triggers an immediate inflammatory response, with T cells contributing to both the extent of the injury and the initiation of repair.

The first cells to respond to damage are $CD4^+$ T lymphocytes (associated with atherosclerotic plaque formation and chronic inflammation), which infiltrate the myocardium and start to release large amounts of IL-6, increasing local inflammation [142]. $CD8^+$ T lymphocytes increase ischaemic phenomena, as they kill damaged cardiomyocytes, but at the same time they are also involved in exacerbating tissue damage, as many senescent cytotoxic cells (CD28null) are concentrated in the damaged tissue, producing high levels of IFNγ [143,144]. This has been seen in patients with acute coronary syndromes and emphasises the direct damage by $CD8^+$ T lymphocytes.

After heart attack (HA) there is remodelling of myocardial tissue, with re-establishment of homeostasis and a decrease of inflammation, caused by this stress condition.

Post-MI, there is a loss of cardiomyocytes with the replacement of a collagen-based scar, which reduce the functionality of heart. This necrotic tissue releases danger signals that activate innate immune responses, leading to an intense inflammatory reaction, such as the proinflammatory

cytokines like TNF-α and interleukins, which further recruit immune cells like neutrophils and monocytes to the infarct area. This process is important to help clear cells but also release mediators that suppress inflammation and activate the reparative cells, including fibroblasts, important for preserving the structural integrity of heart. The mature fibroblasts form a cross-linked collagen matrix that stabilizes the infarct.

Regulatory T cells (Tregs) play a crucial role in maintaining immune homeostasis, and their functionality is significantly impacted by the aging process or during MI. Research indicates that as individuals age, there are notable changes in Treg frequencies, with an increase in lymphoid organs [145,146], and decline in functional capabilities, which can have profound implications for immune responses and overall health [146].

During the healing phase of MI, Tregs cells secrete high levels of anti-inflammatory cytokines, such as IL-10, and their presence correlates with favourable outcomes of improvement, with reduced cardiac fibrosis. Conversely, an increase of T_{EM} cells in the damaged tissue contributes to chronic inflammation and this prolonged immune activation can compromise the repair process, leading to negative remodelling and an increased risk of heart failure.

To provide a comprehensive overview of immune cell subset redistribution with aging, we first aimed to characterize quantitative alterations in different $CD4^+$ and $CD8^+$ T cell subsets across various age groups. Additionally, recognizing that aging is a complex condition influenced not only by chronological age but also by the onset of comorbidities, we included a subgroup of older individuals with myocardial infarction (MI) in our analysis. This subgroup was compared with age-matched subjects without acute cardiac events.

1.2 Material and Methods

1.2.1 Study Cohorts

Healthy donors without recent history of acute cardiac events (n= 249) were recruited at Ferrara Blood Bank and Geriatric Department of Ferrara Hospital, Italy. Donors were stratified according to age as young (YA, 18-40 years, n= 92), middle-aged (MA, 41-65 years, n= 121) or old (OA w/o HA, >65 years, n= 36); this cohort (or RIV cohort) is discussed in the Chapter 3 of this thesis and their information reported in Table 3.2.1.1. The study was approved by the Ethical Committee of the Istituto Nazionale per le Malattie Infettive Lazzaro Spallanzani (protocol number 488). This RIV study was cross-sectional (longitudinal sampling occurred only for a portion of individuals) 53 elderly patients hospitalized for MI (≥ 65 years old, OA with heart attack (HA)) have been enrolled and samples collected at 1 month, 6 months and 1 year after inclusion visit (PIpELINe cohort). Inclusion criteria are as follow: patients over 65 years, myocardial infarction (MI) (with (STE) or without

superelevation of the tract ST (NSTE-MI)) with indication to invasive management, Short Physical Performance Battery (SPPB) value between 4-9 one month after hospital discharge. The exclusion criteria are as follow: multivessel coronary artery disease or left main coronary artery disease candidate to surgical revascularization, non-cardiovascular co-morbidity reducing life expectancy to <1 year, any factor precluding 1-year follow-up, severe aortic or mitral disease, ejection fraction <30%, severe cognitive impairment (SPMSQ <4), disease of hematopoietic system, and malignancies.

Available information regarding these patients includes demographics (age and sex), medical history, details of cardiovascular anatomy and revascularization, ECG, laboratory test results, weight, height, smoking and drugs therapy, immune cell absolute. All information is reported in Table 1.2.3.1.

The current study was an observational analysis of immunotypes from the "*Effectiveness of an early, tailored, Physical activity Intervention in ELderly patients with myocardial INfarction (PIpELINe)*" randomized clinical trial (NCT03021044), which evaluate the effectiveness of an early, tailored, physical activity intervention in older patients with myocardial infarction. The study protocol was approved by the institutional ethics committee (376/2019/AOUFe) and was conducted in accordance with the principles of the Declaration of Helsinki. Patients were informed that their participation was voluntary, and all of them gave written informed consent. All data collected were treated confidentially and anonymized.

Venous blood samples were collected into acid citrate dextrose tubes. From blood samples we obtained peripheral blood mononuclear cells (PBMCs) and plasma. PBMCs were isolated from venous blood samples via Ficoll-Paque (GE-Healthcare) density gradient centrifugation according to standard protocols and cryopreserved in dimethyl sulfoxide (DMSO; 10% v/v; Sigma-Aldrich) and Fetal Calf Serum (FCS; 90% v/v; Sigma-Aldrich) in liquid nitrogen.

Data were acquired using a FACSCanto II (BD Biosciences), compensated using CompBeads (BD Biosciences), and analyzed using FlowJo software version 10.8 (FlowJo LLC, Ashland, OR USA).

1.2.2 Flow cytometry

Immunophenotypic analyses were performed at each time point using whole fresh blood stained with anti-CD3 peridinin-chlorophyll-protein (PerCP)-Cyanine5.5 (Cy5.5) (clone OKT3, 1:50 dilution, catalog no. 45-0037-42, anti-CD4 phycoerythrin (PE)-Cyanine7 (Cy7) (clone RM4-5, 1:50 dilution, catalog no. 25-0049-42 Thermo Fisher Scientific), anti-CD4 fluorescein isothiocyanate (FITC) (clone RPA-T4, 2:50 diution, catalog no. 555346, BD Biosciences), anti-CD8 FITC (clone MEM-31, 3:50 dilution, catalog no. 21270083, ImmunoTools), anti-CD8 APC/Fire750 (clone SK1, 1:50 dilution, catalog no. 300932, BioLegend), anti-CD11b VioGreen (clone REA713, 1.5:50 dilution, catalog no 130-110-559, Miltenyi Biotec), anti-CD14 phycoerythrin (PE)-Cyanine7 (Cy7) (clone 61D3, 4:50 dilution, catalog no. 25014942, ThermoFisher Scientific), anti-CD15 V450 (clone H198, 4:50 dilution, catalog no. 48015942, ThermoFisher Scientific), anti-CD16 FITC (clone LNK16, 5:50 dilution, catalog no. 21279163, ImmunoTools), anti-CD19 VioGreen (clone REA675, 1.5:50 dilution, catalog no. 130-113-649, Miltenyi Biotec), anti-CD27 allophycocyanin (APC) (clone REA499, 1.5:50 dilution, catalog no. 130-113-626, Miltenyi Biotec), anti-CD38 phycoerythrin (PE) (clone HIT2, 5:50 dilution, catalog no. 21270384, ImmunoTools), anti-CD45RA PerCP-Cy5.5 (clone HI100, 3:50 dilution, catalog no. 45-0458-42, Thermo Fisher Scientific), anti-CD45RO VioBlue (clone UCHL1, 1.5:50 dilution, catalog no. 130-113-554, Myltenyi Biotec), anti-HLA-A2 PE (clone BB7.2, 1:50 dilution, catalog no.343306, BioLegend), anti-HLA-DR APC (clone LN3, 4:50 dilution, catalog no. 17995642, Thermo Fisher Scientific), and anti-HLA-DR PECy7 (clone G46-6, 1:50 dilution, catalog no. 560651, BD Biosciences).

Red blood cells were lysed using FACS LysisSolution (catalog no. 349202, BD Biosciences). Absolute cell numbers were calculated using Precision Count Beads (1:2 dilution, catalog no. 424902, BioLegend):

$$Absolute\ Cell\ Count\ (Cell{:}\ \mu L) = Precision\ Count\ Beads^{TM}\ Concentration\ (Beads{:}\ \mu L) \times \frac{Cell\ count}{Precision\ Count\ Beads^{TM}\ Count}$$

1.2.3 Statistical analysis

Univariate statistical analyses were performed using GraphPad Prism 10. Groups were compared using the one-way ANOVA followed by Kruskal-Wallis's multiple comparisons test (for comparisons between two or more than two groups, respectively), Spearman's rank test (to assess correlations) or a Wilcoxon matched-pairs signed-rank test (to compare average values with a given threshold or to compare the same donor at different timepoints). P values below 0.05 were considered statistically significant.

Table 1.2.3.1: Longitudinal distribution of demographic charatheristics.

	ELDERLY WITH MYOCARDIAL INFARCTION		
Timepoints	**T1** (1 month)	**T2** (6 months)	**T3** (1 year)
No. of donors	(53)	(46)	(42)
Sex			
Male (%)	66	67	69
Female (%)	34	33	31
Age			
Median (range)	78 (65- 92)	78.5 (65- 91)	77.5 (65- 91)
BMI			
Median (range)	26.7* (19.4- 44.3)	26.4 (18.6- 44.3)	26.4 (18.9- 45.6)
Smoke			
Active Smoker	15.4*	13	9.5
Ex-smoker	38.5*	39	43
No-smoker	45.3*	50	48
Comorbidities			
Hypertension (%)	94*	96	93
Coagulation diseases (%)	90*	96	98
Anaemia (%)	9.6*	9	9.5
DM II (%)	33	33	31
Hypercholesterolemia (%)	8*	9	0
Dyslipidaemias (%)	98*	83	69
Gastrointestinal diseases (%)	21*	22	19
Chronic renal failure (%)	17*	15	14
Benign prostatic hyperplasia (%)	21*	20	17
Asthma (%)	2*	2	2
BPCO (%)	8*	7	7
Depression/ Anxiety/ Mood disorders (%)	17*	22	19
Hypothyroidism (%)	6*	7	5
Rheumatoid arthritis (%)	0*	0	0
Cancer	0*	0	0
Number of comorbidities			
Median (range)	6* (3- 12)	6 (3- 13)	6 (3- 12)
Number of drugs			
Median (range)	7* (5- 8)	7 (5- 10)	6 (3- 12)

*Data from 52 donors

1.3 Results

1.3.1 The impact of Immunosenescence and Myocardial Infarction on the remodelling of immunotypes

To understand how the immune system changes with age, we studied the remodelling of the immune system in a cohort ("RIV cohort", described in Chapter 3), stratified by age: young (YA, n= 92), middle-aged (MA, n= 121) and old (OA w/o HA, n= 36); in this cohort, infarcted subjects were excluded for this analysis. To assess the impact of acute cardiac events, we compared the RIV cohort with 53 elderly infarcted subjects ("PIpELINe cohort", OA with HA), monitoring the different trends of the immune subpopulations, post infarction. The comparison was performed between RIV cohort and the first time point (T1) of PIpELINe cohort.

Using weight and height data, the 'Body Max Index' (BMI) was calculated for RIV and PIpELINe cohorts. We observed that elderly infarcted subjects, at time T1, have the highest BMI among the analysed cohorts. Notably most donors fall within the overweight, obese or severely obese categories, in contrast to non-infarcted elderly subjects and especially to younger age groups [Figure 1.3.1.1 (A)].

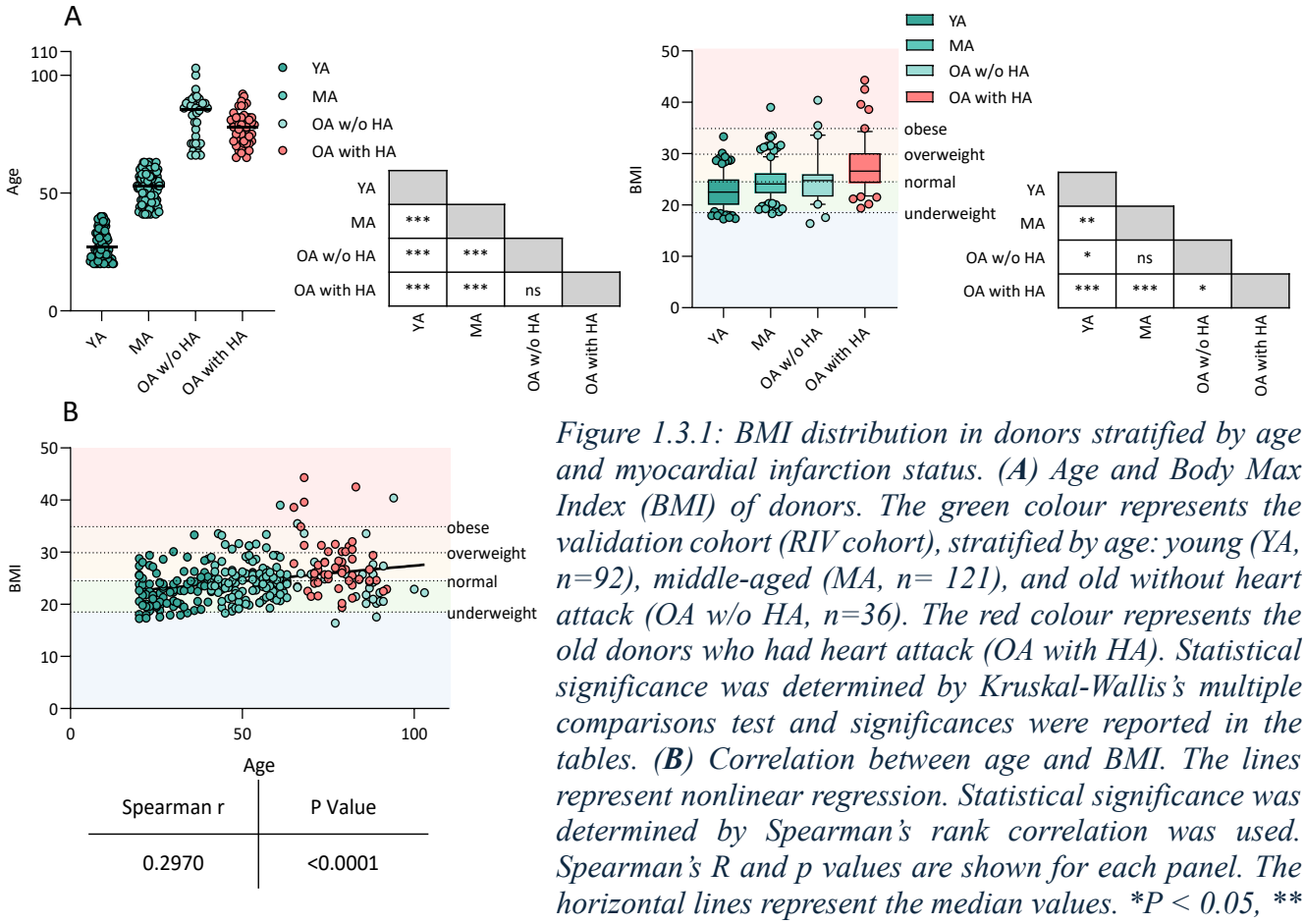


*Figure 1.3.1: BMI distribution in donors stratified by age and myocardial infarction status. (**A**) Age and Body Max Index (BMI) of donors. The green colour represents the validation cohort (RIV cohort), stratified by age: young (YA, n=92), middle-aged (MA, n= 121), and old without heart attack (OA w/o HA, n=36). The red colour represents the old donors who had heart attack (OA with HA). Statistical significance was determined by Kruskal-Wallis's multiple comparisons test and significances were reported in the tables. (**B**) Correlation between age and BMI. The lines represent nonlinear regression. Statistical significance was determined by Spearman's rank correlation was used. Spearman's R and p values are shown for each panel. The horizontal lines represent the median values. *P < 0.05, ** < 0.01, ***P < 0.001.*

A positive correlation was observed between these age and BMI [Figure 1.3.1.1 (B)], most likely justified by an increase in sedentariness, due to less walking and especially an increase in visceral adipose tissue (VAT) [147–149].

For each donor, the immunophenotype was analysed on whole blood and the absolute number of $CD4^+$ T, $CD8^+$ T and B subpopulations was quantified using precision beads. Analysis of total lymphocyte populations revealed a significant age-related decrease of each subpopulation, with a higher number of total $CD4^+$, $CD8^+$ and B lymphocytes in YA and MA subjects (YA>MA) compared to elderly subjects (OA w/o HA> OA with HA) [Figure 1.3.1.2 (A)].

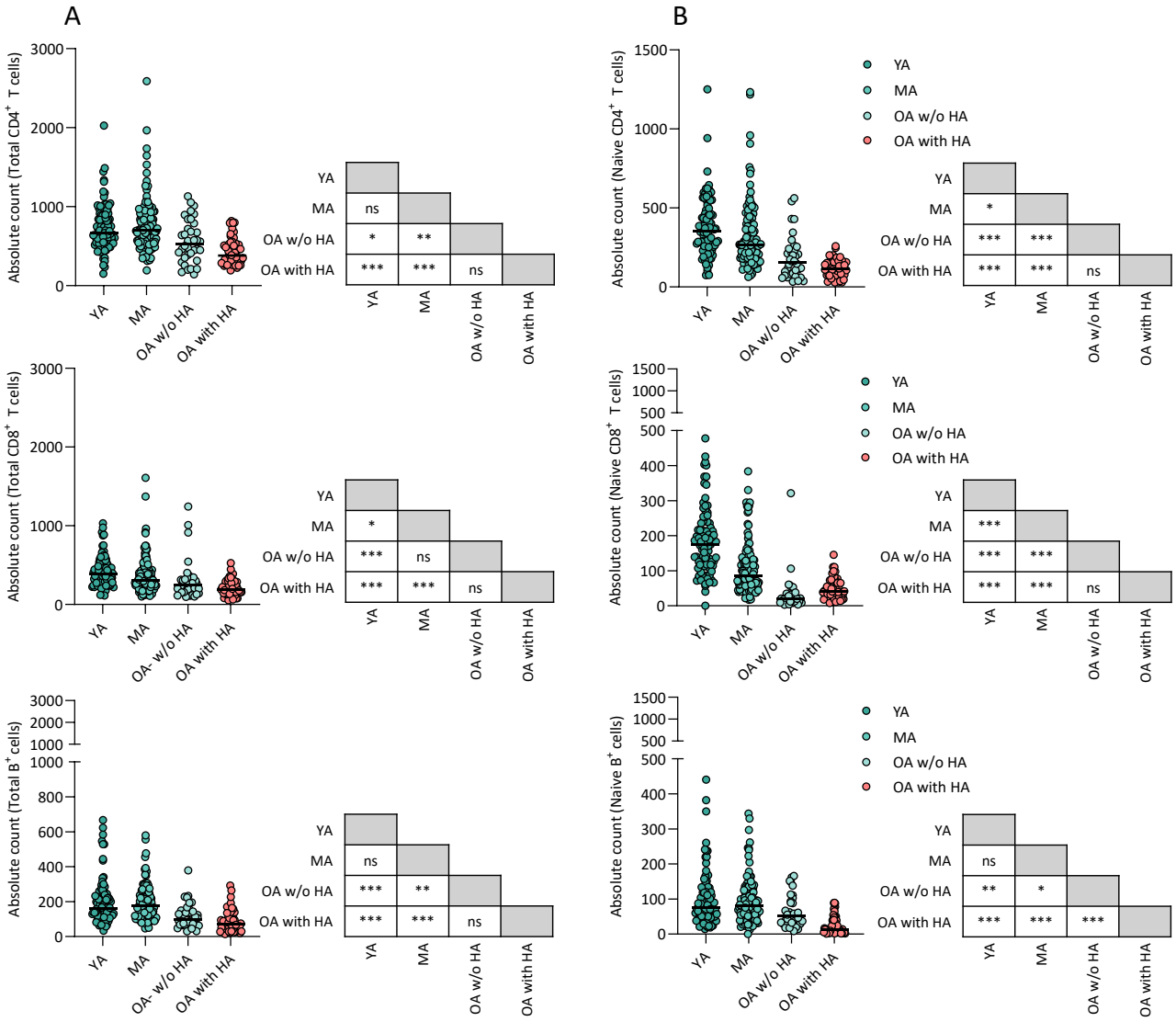


*Figure 1.3.1.2: Distribution of total and naïve $CD4^+$ T, $CD8^+$ T, and B cells in relation with age and myocardial infarction status. Absolute count of (**A**) total and (**B**) naïve lymphocytes: the green colour represents the validation/ healthy control cohort (RIV cohort), stratified by age: young (YA, n=92), middle-aged (MA, n= 121), and old without heart attack (OA w/o HA, n=36). The red colour represents the old donors who had heart attack (OA with HA). Statistical significance was determined by Kruskal-Wallis's multiple comparisons test and reported in the tables. The horizontal lines represent the median values. *P < 0.05, **P < 0.01, ***P < 0.001.*

This progressive decline is also observed considering the absolute number of naïve ($CD27^-$ $CD45RA^+CD45RO$) T and naïve ($CD27^-CD38^+$) B cells. [Figure 1.3.1.2 (B)].

Specifically, within the older age groups, OA with HA subjects exhibit a significantly lower number of total $CD4^+$, $CD8^+$ and B cells compared to the control group (OA w/o). A similar trend is observed for naïve $CD4^+$ T and B cells [Figure 1.3.1.2 (B)], underlining the impact of a stressful event, such as myocardial infarction, on immune system remodelling [150].

As mentioned above, age plays a key role in negatively modifying the immune system. Indeed, as reported in previous studies, the decline of naïve cells, due to intrinsic and extrinsic factors of the individual, such as thymic involution and chronic exposure to pathogens, strongly correlates with aging. As shown in Figure 1.3.1.3 (A), the absolute number of naïve $CD4^+$ T, $CD8^+$ T and B cells fall with advancing age. Furthermore, the correlation between the absolute number of naïve cells with BMI shows that subjects with a higher BMI have fewer naïve cells [Figure 1.3.1.3 (B)].

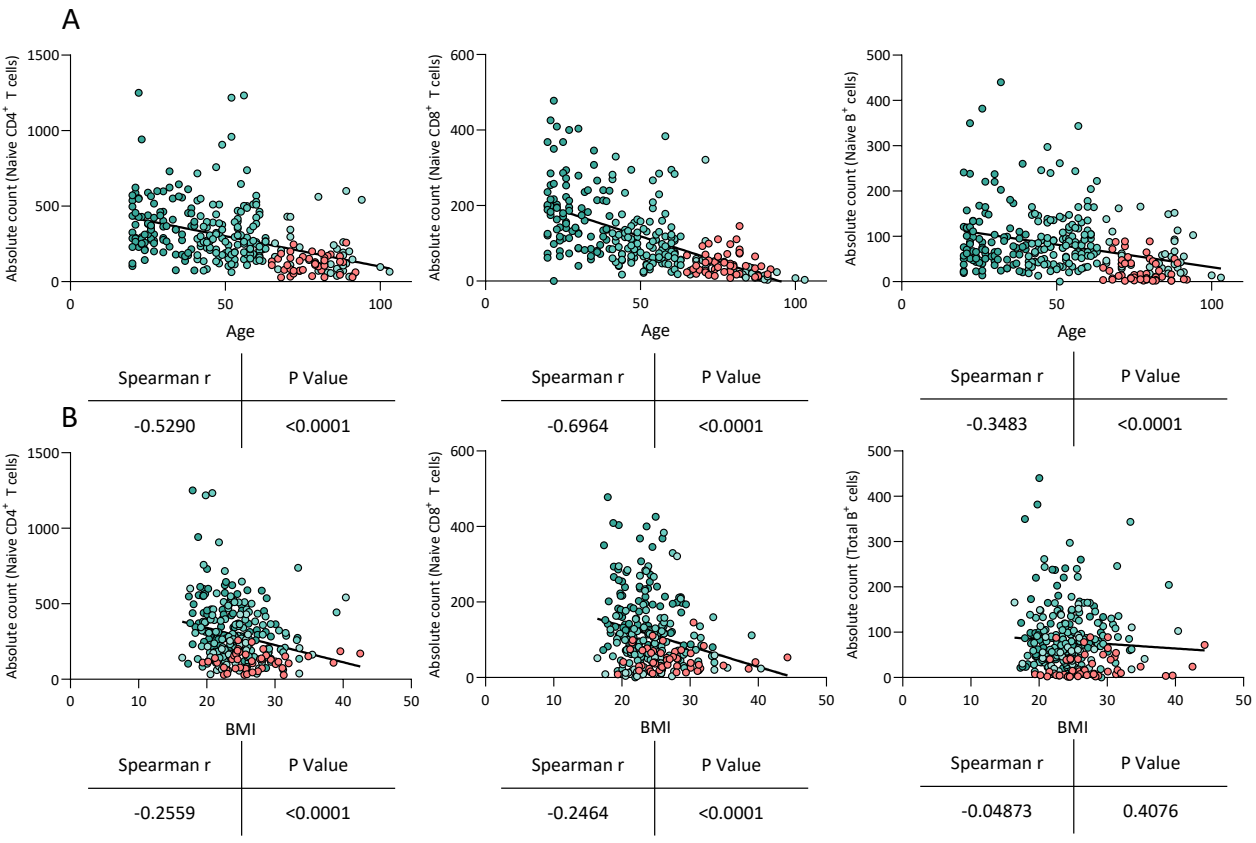
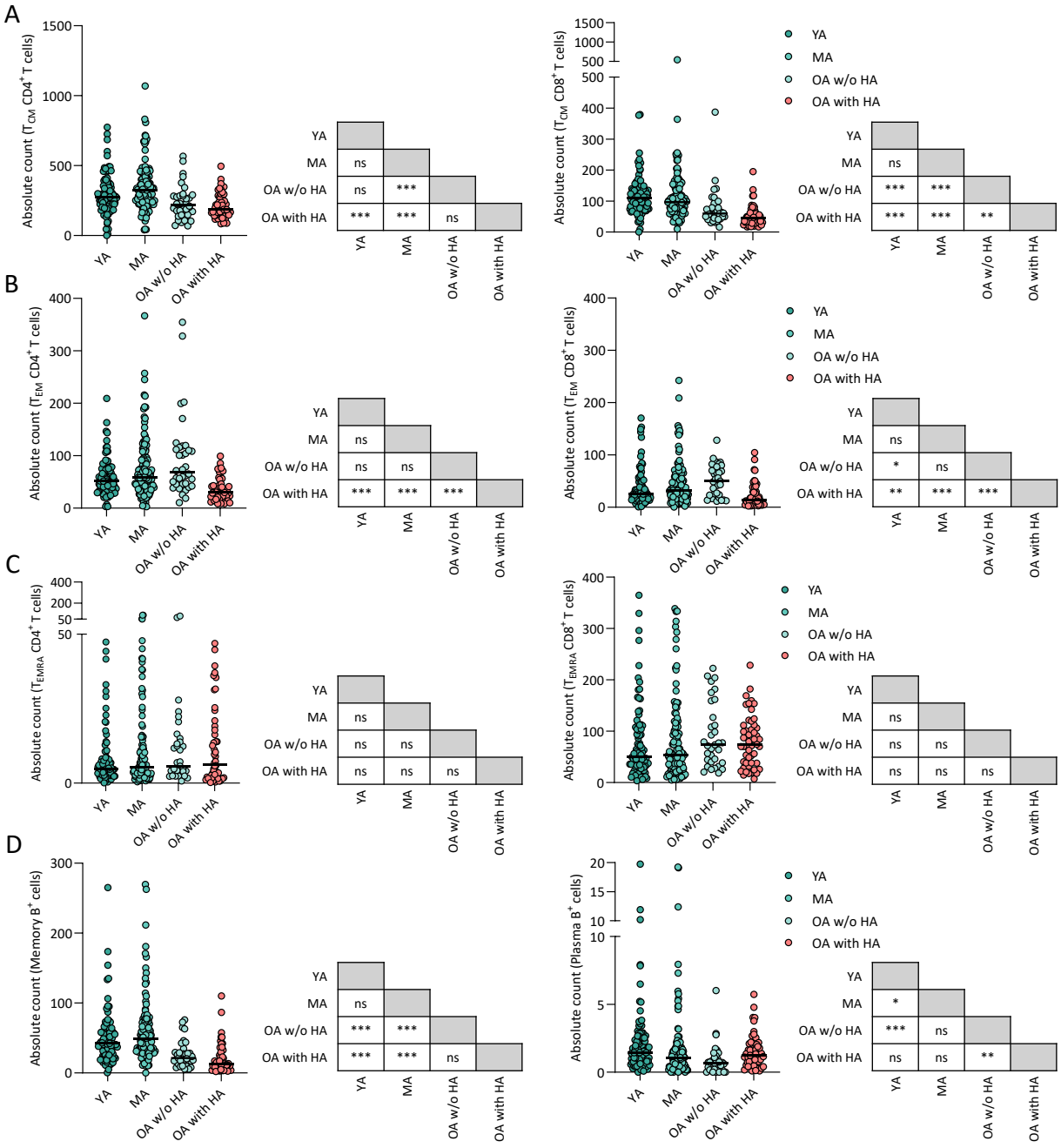


*Figure 1.3.1.3: Correlation between absolute count of naïve $CD4^+$, $CD8^+$ and B cells with age and BMI. Correlations between the absolute count of naïve lymphocytes and (**A**) age and (**B**) BMI. The green colour represents the validation/ healthy control cohort (RIV cohort), stratified by age: young (YA, n=92), middle-aged (MA, n= 121), and old without heart attack (OA w/o HA, n=36). The red colour represents the old donors who had heart attack (OA with HA). Statistical significance was calculated using Spearman's rank correlation, and Spearman's r and p values are shown for each panel. The lines represent nonlinear regression.*

In summary, older age, loss of naïve cells and higher BMI are mutually associated, highlighting the systemic impact of aging on the whole organism [151].

Evaluating central memory (T_{CM}, $CD27^+$ $CD45RA^+CD45RO^-$) $CD4^+$ and $CD8^+$ T lymphocytes and memory B cells ($CD27^+$ $CD38^-$), a decrease with age is observed [Figure 1.3.1.4 (A, B, D- left)]. This trend aligns with the reductions seen in total and naïve cell populations. Interestingly, comparing the two groups of elderly subjects, the infarcted donors (OA with HA) have fewer memory cells than the control (OA w/o HA), although not always reaching the threshold for statistical significance.



The caption follows in the other page

*Figure 1.3.1.4: Distribution of $CD4^+$ T, $CD8^+$ T and B cell subsets. Absolute count of central memory (**A**) (T_{CM}, top), (**B**) effector memory (T_{EM}, central), and terminally differentiated effector memory (**C**) (T_{EMRA}, bottom) of T cells, as well as (**D**) memory (bottom left) and plasmablast (Plasma, bottom right) of B cells. The green colour represents the validation/ healthy control cohort (RIV cohort), stratified by age: young (YA, n=92), middle-aged (MA, n= 121), and old without heart attack (OA w/o HA, n=36). The red colour represents the old donors who had heart attack (OA with HA). Statistical significance was determined by Kruskal-Wallis's multiple comparisons test and the significances were reported in the tables. The horizontal lines represent the median values. *P < 0.05, **P < 0.01, ***P < 0.001.*

In contrast, effector memory (T_{EM}, $CD27^-CD45RA^-CD45RO^+$) and terminally differentiated effector memory T cells (T_{EMRA}, $CD27^-CD45RA^+CD45RO^-$) $CD4^+$ and $CD8^+$ T cells as well as and plasmablasts ($CD27^+CD38^+$), do not exhibit a decline with age but a slight increase, especially in $CD8^+$ T lymphocytes [Figure 1.3.1.4 (C, D- right)]. Both groups of elderly subjects show comparable number of T_{EMRA} cells.

The increase in these cell populations, as reported in other studies [152,153], reflects a senescent immunological profile characterized by a dysregulation of the memory response and production of inflammatory cytokines. Evidence also reported that these populations are closely linked to myocardial infarction [154–156].

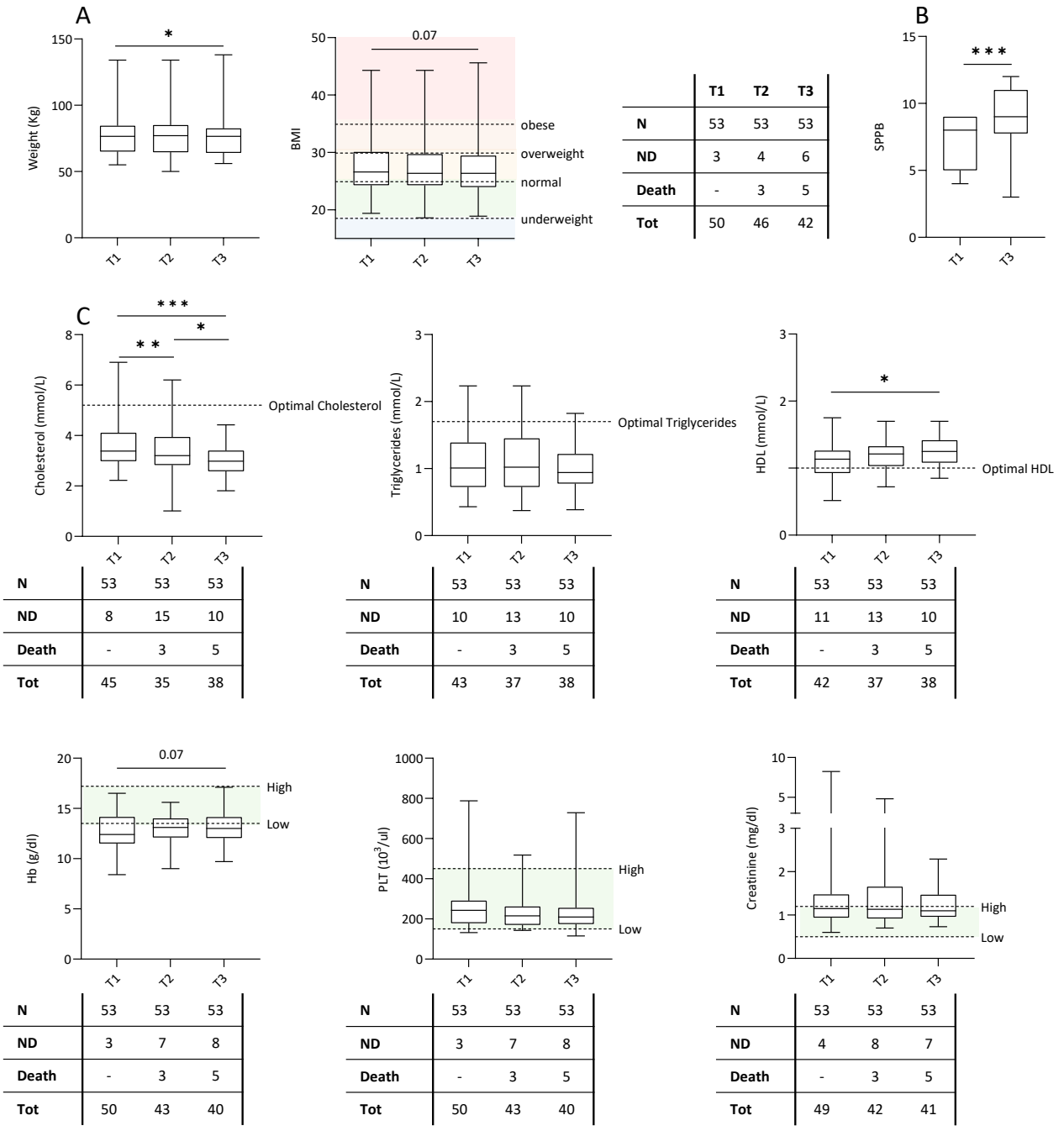
1.3.2 Monitoring of homeostasis and immunological profile after Myocardial Infarction

The PIpELINe is a prospective, randomized, multicentre trial, including patients ≥ 65 years old (OA), admitted to hospital for myocardial infarction (MI) and with a low physical performance one month after discharge, as defined as short physical performance battery (SPPB) value between 4 and 9 [157,158]. It is a longitudinal study, which evaluates the effectiveness of a multidisciplinary intervention (dietary counselling, strict management of cardiovascular and metabolic risk factors, and exercise training) in favouring recovery and avoiding possible relapses following a heart attack.

The clinical parameters (weight, height, BMI, cholesterol, triglycerides, High Density Lipoprotein (HDL), haemoglobin (Hb), platelets (PLT) and creatinine), were collected during the visits, carried out at the Cardiology Unit of the Ferrara University Hospital, at the different timepoints (1-month post-MI- T1, 6 months post-MI- T2, and 12 months post-MI- T3). On the other hand, SPPB values, an essential metric for assessing a person's mobility, strength and balance, especially in elderly subjects or frail subjects [159], were evaluated at the Centre for Sports and Exercise Science, Department of Neuroscience and Rehabilitation, University of Ferrara at time points T1 and T3.

To understand whether the recovery period after MI impacted the T cell subset redistribution and monitor possible biological and immune changes, immunophenotypic analysis of a subgroup of patients with MI (n=53) was conducted. Specifically, monitoring occurred at baseline (T1), 6- (T2),

and 12-months (T3) post-infarction. The 53 subjects displayed a slight but significant decrease in weight between T1 versus T3, which contributed to a non-significant decrease in BMI over the same period (p= 0.07) [Figure 1.3.2.1 (A)]. Following the MI event, donors showed improvements in physical performance, going from a median SPPB value at T1 of 8 (range 4- 9) to 10 at T3 (range 5-



	T1	T2	T3
N	53	53	53
ND	3	4	6
Death	-	3	5
Tot	50	46	42

	T1	T2	T3
N	53	53	53
ND	8	15	10
Death	-	3	5
Tot	45	35	38

	T1	T2	T3
N	53	53	53
ND	10	13	10
Death	-	3	5
Tot	43	37	38

	T1	T2	T3
N	53	53	53
ND	11	13	10
Death	-	3	5
Tot	42	37	38

	T1	T2	T3
N	53	53	53
ND	3	7	8
Death	-	3	5
Tot	50	43	40

	T1	T2	T3
N	53	53	53
ND	3	7	8
Death	-	3	5
Tot	50	43	40

	T1	T2	T3
N	53	53	53
ND	4	8	7
Death	-	3	5
Tot	49	42	41

*Figure 1.3.2.1: Longitudinal monitoring of physical and biological parameters of the Pipeline cohort. Physical parameters such as (**A,B**) weight, BMI and SPPB values at the different time points are shown above: T1 (baseline, 1-month post-MI), T2 (6 months post-MI) and T3 (12 months post MI). (**C**) The middle panels show lipid profile values (cholesterol, triglycerides, and HDL), while the panels below show haemoglobin (Hb), platelet (PLT) and creatinine values. Below each panel is a table with the number of donors for each timepoints (N), number of undetermined (ND), deaths and the number of total donors (Tot) on which the statistical analysis was performed. The dotted lines represent the thresholds of the optimal values according to the guidelines. Statistical significance was determined by Wilcoxon matched-pairs signed-rank. *P < 0.05, **P < 0.01, ***P < 0.001.*

12); this underlines the effectiveness of the multidisciplinary approach implemented by the department of Cardiology Unit and Centre for Sports and Exercise Science of University of Ferrara [Figure 1.3.2.1 (B)]. There is also an important improvement in biological parameters, especially in the lipid profile. Indeed, a significant decrease in total blood cholesterol was observed over the period T1-T3 along with a slight decrease in triglycerides. Notably, a substantial increase in HDL values was reported between T1 and T3. In addition, a decreasing and an increasing trend in creatinine and haemoglobin (Hb), respectively, can be noted comparing T1 with T3, while no differences were observed for platelet (PLT) count [Figure 1.3.2.1 (C)]. These improvements in the physical performance and lipid profile are most likely attributable to both a post-MI recovery and a study's multidisciplinary approach, which included healthier dietary habits, exercise, and optimization of medication regimens. Concerning the immunophenotypic profile, differences were observed in total $CD4^+$, $CD8^+$, and B cells, along with their subpopulations, monitored across all three timepoints.

As shown in Figure 1.3.2.2 both total $CD4^+$ and $CD8^+$ T lymphocytes and B lymphocytes exhibit a progressive increase over time. This suggests a remodelling of adaptive immunity, towards an initial state of homeostasis, though not yet indicative of full health.

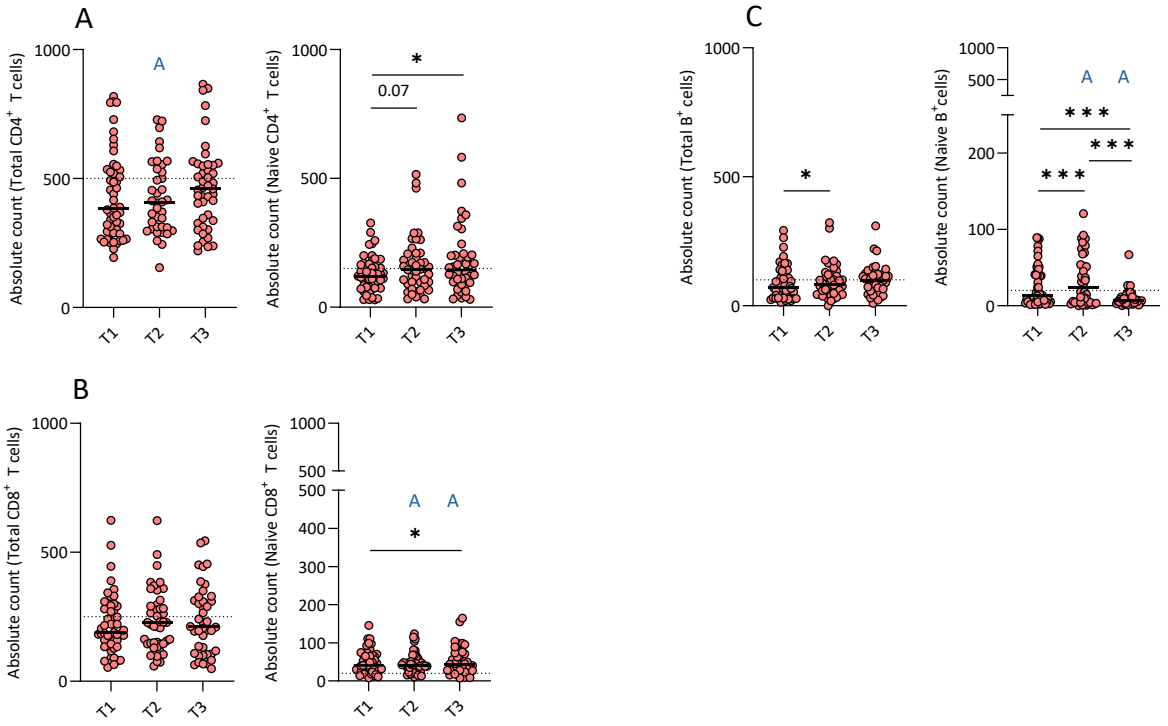


*Figure 1.3.2.2: Longitudinal monitoring of total and naïve $CD4^+$, $CD8^+$ and B cells. The absolute count of (**A,B**) total and naïve T and (**C**) B cells was reported for the three different timepoint: T1 (n=53), T2 (n=46), and T3 (n=42). Dotted lines represent the absolute count of the corresponding cell population (total or subsets) for the OA group without HA, providing a reference for tracking trends in the OA group with HA over time. Statistical significance was determined by Wilcoxon matched-pairs signed-rank. The horizontal lines represent the median values. *P < 0.05, **P < 0.01, ***P < 0.001. ^{A}P < 0.05. (Mann-Whitney test showing the significance differences with OA w/o HA group).*

Interestingly, a similar trend is also observed in naïve T and B-lymphocytes. Indeed, a significant increase in these subpopulations is reported from T1 and T3, reflecting a re-establishment of the absolute number of naïve cells over time. Post-MI remodelling is also evident in other subpopulations of adaptive immunity [Figure 1.3.2.3]. One-year post-HA, a significant increase in T_{EMRA} $CD4^+$ T cells and memory B cells is observed, accompanied by a decrease of T_{EMRA} $CD8^+$ T cells plasmablasts [Figure 1.3.2.3 (C,D)]. This shift in subset balance is important as it evinces the resolution of acute inflammation triggered by the infarction. At T1, a higher amount of plasmablasts was detected, likely attributable to post-infarction autoimmune syndrome (Dressler's syndrome), a type of pericarditis that can occur weeks after the infarction, characterised by an increased antibody response and elevated plasmablast number [156,160].

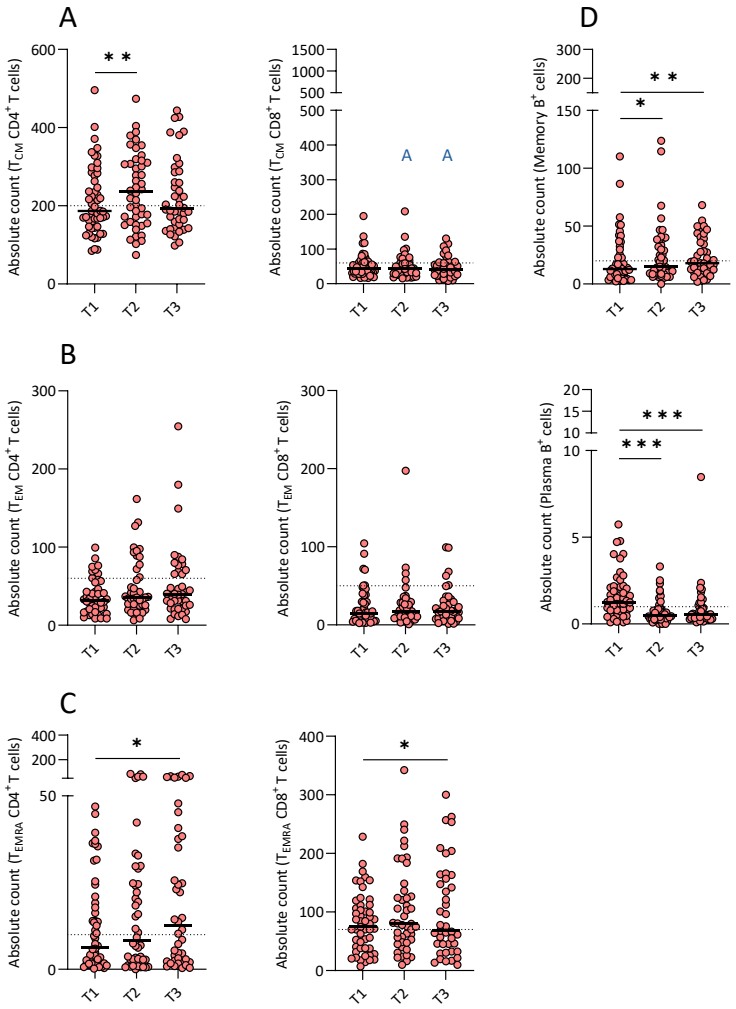


*Figure 1.3.2.3: Longitudinal monitoring of memory subsets of $CD4^+$, $CD8^+$ and B cells. The absolute count of $CD4^+$ (left column) and $CD8^+$ (right column) memory subsets (T_{CM} (**A**), T_{EM} (**B**) and T_{EMRA} (**C**)), and (memory and plasmablasts (**D**)) of B (right column) cells was reported for the three different timepoint: T1 (n=53), T2 (n=46), and T3 (n=42). The dotted lines were the median OA w/o HA's absolute count T and B cells, which was reported to have a comparison of restoration of adaptative populations after MI. Statistical significance was determined by Wilcoxon matched-pairs signed-rank. The horizontal lines represent the median values *P < 0.05, **P < 0.01, ***P < 0.001. ^{A}P < 0.05 (Mann-Whitney test showing the significance differences with OA w/o HA group).*

To further support the hypothesis of the decrease in acute inflammation and to confirm the restoration of homeostasis, we measured the expression of activation markers in total (including naïve) and memory (excluding naïve) subsets of $CD4^+$ an $CD8^+$ T cells [Figure 1.3.2.4 (A,B)]. It is well known that MI triggers a strong inflammatory and immune response due to ischaemic damage and subsequent necrosis of cardiac tissue. During an infarction, the expression of HLA-DR and CD38 may increase as a response to this injury, as markers of immune activation. High HLA-DR expression rates were observed at T1, which declined dramatically at 6- and 12-months post-MI. Instead, no significant differences were observed for CD38 expression.

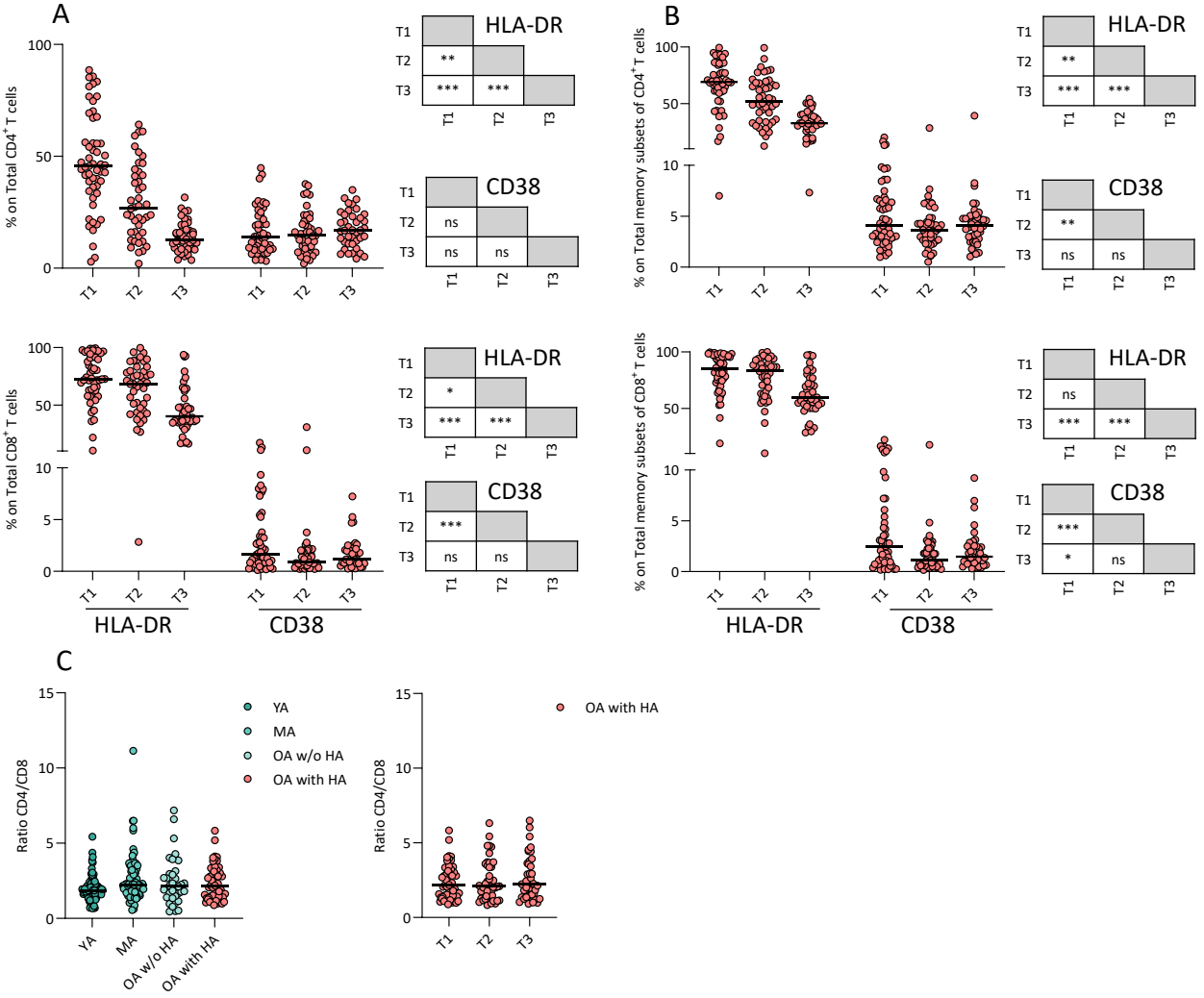


*Figure 1.3.2.4: Expression of activation markers in total and memory subset of $CD4^+$ and $CD8^+$ T cells. The frequency of expression of HLA-DR and CD38 expression was evaluated in total (including naïve) and memory (excluding naïve) subsets of (**A**) $CD4^+$ and (**B**) $CD8^+$ T cells. (**C**) The ratio CD4/CD8 was reported to monitor the acute inflammation, activation of adaptative immunity. The green colour was the RIV cohort (control) and the red colour the Pipeline cohort, which was compared with the control (left, only T1) or longitudinally (T1, T2, and T3). Statistical significance was determined by Wilcoxon matched-pairs signed-rank (A-B) and Kruskal-Wallis's multiple comparisons test (B) and the significances were reported in the tables. The horizontal lines represent the median values. *P < 0.05, **P < 0.01, ***P < 0.001.*

This decrease was evident both in total $CD4^+$ and $CD8^+$ T cells as well as in the memory subset. Despite these changes in activation marker expression and the observed shift in specific cell populations, the CD4/CD8 ratio remained stable [Figure 1.3.2.4 (C)], throughout the study. This was consistent both when comparing T1 with the RIV cohort and when comparing T1 with T2 and T3, suggesting a good balance among the T cell populations.

In parallel with the study of adaptive immunity, we also focused on monitoring specific innate immune subpopulations within the PIpELINe cohort. These included total monocytes (HLA-DR^+CD11b^+), classical monocytes ((HLA-$DR^+CD11b^+CD14^+CD16^-$), intermediate monocytes (HLA-$DR^+CD11b^+CD14^+CD16^+$), non-classical monocytes (HLA-$DR^+CD11b^+CD14^{low}CD16^+$) and myeloid-derived suppressor cells or MDSC (HLA-$DR^-CD11b^+CD15^+$).

Data collected from the immunophenotype PIpELINe cohort, revealed a significant increase in total monocytes [Figure 1.3.2.5 (A)], presumably driven by the non-classical monocyte subpopulation, which play a late-stage role in the pathogenesis of myocardial infarction. A study by Tsujioka et al. [161] showed that a higher level of non-classical monocytes in peripheral blood was associated with a better post-MI prognosis, as these cells contribute to endothelial stabilisation and the prevention of further ischaemic damage.

The beneficial action of this class of monocytes is supported by MDSCs, which showed a significant decrease between T1 and T2, suggesting a reduced cell clearance and oxidative stress, processes that are typically heightened during MI, but subside with infarct resolution [162] [Figure 1.3.2.5 (B)].

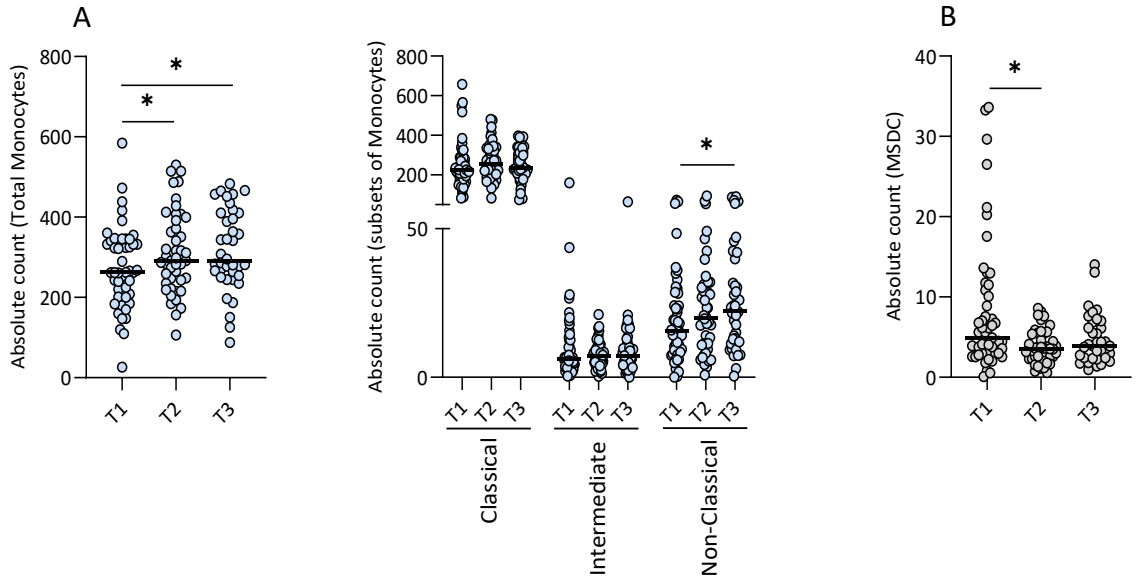


*Figure 1.3.2.5: Longitudinal monitoring of innate immunity. In the panels were reported the absolute number of total monocytes, its subpopulations (Classical, Intermediate, and Non-classical) (A), and myeloid-derived suppressor cells (MDS,C)(B) for the three different timepoints: T1 (n= 49), T2 (n= 45), and T3 (n= 38). Statistical significance was determined by Wilcoxon matched-pairs signed-rank. The horizontal lines represent the median values *P < 0.05.*

1.4 Discussion

Aging has a significant impact on the immune system, influencing the quantity and quality of lymphocytes and innate subpopulations. This process, called immunosenescence, is characterised by a reduction in naïve T and B cells and an increase in memory subsets, in particular terminally differentiated memory cells (T_{EMRA}), caused by chronic infection, such as recurrent CMV infections [134,151,163,164]. In the context of myocardial infarction, immunosenescence appears to be exacerbated, accelerating the typical immune decline with aging. Indeed, infarcted elderly subjects (OA with HA) have significant lower numbers of total $CD4^+$, $CD8^+$ T and B cells compared to non-infarcted elderly controls (OA without HA), suggesting that infarct-related physiological stress accelerates the immunesenescence process [165]. The decrease in naïve cells, already substantial in the elderly, is even more pronounced in infarcted subjects. and this reduction impairs the immune system's ability to respond to emerging infections, new viral exposures and vaccines [166]. The reduced number of naïve cells can be attributed to intrinsic (e.g. thymic involution) and extrinsic (e.g. chronic inflammation and prolonged exposure to pathogens, like CMV) factors, phenomena that are exacerbated following infarction, which is known to trigger an acute inflammatory response at both tissue and systemic level [89,167,168]. In fact, as reported in the results, there is an increase in plasmablates and in MDSCs one month after the infarction (T1), followed by a decrease at T2 and T3. This dynamic promotes an increase in memory cell populations, such as the $CD4^+$ T lymphocyte EMRA and non-classical monocytes, leading to a state of inflammaging [154,167,169]. Inflammaging is further aggravated by the accumulation of visceral adipose tissue (VAT), which promotes the production of pro-inflammatory cytokines, correlating positively with BMI and age.

The observed decrease in specific memory subpopulations, such as central memory (T_{CM}) cells, emphasises an advanced state of immunosenescence in both elderly groups (OA w/o HA from RIV cohort and OA with HA from PIpELINe cohort). However, the increase in T_{EMRA} cells suggests an accelerated terminal differentiation process, probably driven by CMV infections. This is associated with a senescent phenotype, characterised by the secretion of inflammatory cytokines (SASP, senescence-associated secretory phenotype), which sustain a condition of chronic low-grade inflammation [170].

The MI-driven stress condition, as evidenced by T1 data, triggers a status of acute inflammation that gradually resolves over time with adjustments in drug therapy and employing a multidisciplinary approach. Indeed, longitudinal data indicate improvements in physical performance and lipid profile in infarcted subjects between T1 and T3. These improvements are accompanied by a partial remodelling of adaptive immunity, including an increase in naïve cells and a decrease in plasmablasts, suggesting a resolution of the acute post-infarct inflammatory state. Despite these positive changes,

myocardial infarct accelerates the immunosenescence process [171]. Persistent high number of T_{EMRAs} indicates that, although there is an initial recovery, subjects remain in a state of inflammaging, with a potential risk of developing secondary cardiovascular complications and an inefficient immune response to new infections or vaccines [154,172].

CHAPTER 2:

Aging Curtails the Diversity and Functionality of Nascent CD8$^+$ T Cell Responses against SARS-CoV-2

2.1 Introduction

In December 2019, a novel coronavirus, severe acute respiratory syndrome coronavirus-2 (SARS-CoV-2), was discovered as the causative agent of an outbreak of lower respiratory tract infections in Wuhan, China. As the virus spread globally, it became clear that elderly individuals responded suboptimally to vaccination and were particularly susceptible to severe disease, with high attendant rates of mortality [173–176]. These observations suggested an age-related link between antiviral immunity and disease outcome, but a precise understanding of the determinative biological processes has been lacking to date. Physiological aging has been linked with a progressive decline in immune functionality, known as immunosenescence, which could account for the increased vulnerability of elderly individuals to emerging infectious agents, such as SARS-CoV-2 [80,177]. In line with this notion, a relative scarcity of naïve T cells has been associated with severe coronavirus disease 2019 (COVID-19) [178]. Naïve T cells are known to become less frequent and more dysfunctional with age [92,105,179,180]. It is therefore plausible that functional and numerical alterations in the naïve pool could impair the induction of de novo SARS-CoV-2-specific effector/memory T cells in the elderly, consistent with previously described age-related immune deficits in the context of acute COVID-19 [180]. To address this potential mechanistic link, we used an in vitro priming approach to quantify the induction of epitope-specific effector/memory CD8$^+$ T cells from naïve precursors as a function of age. Importantly, all donors were unvaccinated and previously unexposed to SARS-CoV-2, enabling a robust assessment of priming efficacy in the absence of immunological memory.

2.2 Material and Methods

2.2.1 Main Cohort

Peripheral blood samples were obtained from anonymized donors (age, 20–69 years; female, n = 2; male, n = 14) via the Blood Bank at Azienda Ospedaliera-Universitaria di Ferrara, Italy. The protocol was approved by the Azienda Unità Sanitaria Locale di Ferrara. All donors expressed human leukocyte antigen (HLA)-A2. Peripheral blood mononuclear cells (PBMCs) were isolated from buffy coats via density gradient centrifugation using Ficoll-Paque (GE Healthcare, Milan, Italy) and

cryopreserved in fetal bovine serum (FBS; Euroclone, Milan, Italy) containing 10% dimethyl sulfoxide (DMSO; Sigma-Aldrich, Milan, Italy). Samples were obtained either before or during 2020. Donors in the latter group were only included after testing seronegative for SARS-CoV-2. Serostatus was assessed using a SARS-CoV-2 RBD Total Antibody ELISA Kit (Mabtech, Stockholm, Sweden).

2.2.2 Peptides and Tetramers

HLA-A2-restricted peptides were synthesized in solid phase and purified via high- performance liquid chromatography (>97%). The melanoma-derived EV10 peptide (ELAGIGILTV) was used as a model antigen, given constitutively high cognate precursor frequencies among individuals expressing HLA-A2 [181]. SARS-CoV-2 peptides were selected from different viral proteins on the basis of immunodominance/immunoprevalence [97] and matched to the wildtype strain HKU-001a [Table 2.2.2.1]. Peptides were dissolved initially in DMSO and used at a final concentration of 1 μM. Fluorescent peptide/HLA-A2 tetramers were generated as described previously [182]. All tetramers were used at an identical titer immediately after conjugation to ExtrAvidin-PE (Sigma-Aldrich).

Table 2.2.2.1: SARS-CoV-2 peptides and tetramers restricted by HLA-A2.

Protein	Peptide ID	Sequence	Residues	Length	Tetramer
E	SLV	SLVKPSFYV	50–58	9	A*02:01 SV9
M	KLL	KLLEQWNLV	15–23	9	A*02:01 KV9
N	LLL	LLLDRLNQL	222–230	9	A*02:01 LL9
RdRpol	MLD	MLDMYSVML	5291–5299	9	-
S	YLQ	YLQPRTFLL	269–277	9	A*02:01 YL9
S	KIA	KIADYNYKL	417–425	9	-
S	TLD	TLDSKTQSL	109–117	9	-
ORF3a	LLY	LLYDANYFL	139–147	9	-
ORF6	HLV	HLVDFQVTI	3–11	9	A*02:01 HI9

2.2.3 In Vitro Priming of Human Antigen-Specific $CD8^+$ T Cells

PBMCs were thawed and resuspended in 75-cm^2 tissue culture flasks (7×10^7 cells/flask to prime SARS-CoV-2-specific naïve T cells) or 48-well tissue culture plates (2.5×10^5 cells/well to prime EV10-specific naïve T cells) containing AIM-V medium (Thermo Fisher Scientific, Monza, Italy) supplemented with FLT3L (50 ng/mL; Miltenyi Biotec, Bologna, Italy) to mobilize resident dendritic cells (DCs) [97]. After 24 h (day 1), the corresponding peptides were added to the cultures at a final concentration of 1 μM, and DC maturation was induced with TNF-α (1000 U/mL; Miltenyi Biotec), IL-1β (10 ng/mL; Miltenyi Biotec), IL-7 (0.5 ng/mL; R&D Systems, Minneapolis, MN, USA), and prostaglandin E2 (1 μM; Calbiochem, Milan, Italy). On day 2, complement-inactivated FBS (Euroclone) was added at a final v/v ratio of 10%. Medium was replaced on days 4 and 7 with fresh RPMI 1640 (Euroclone) enriched with 10% FBS (Euroclone), non-essential amino acids (1X;

Euroclone), and sodium pyruvate (1 mM; Sigma-Aldrich). Antigen-specific $CD8^+$ T cells were characterized on day 10.

2.2.4 ELIspot Assay

Functional responses were quantified using a human interferon (IFN)-γ ELISpot PLUS (HRP) Kit (Mabtech). PBMCs were primed as described above and seeded in duplicate at 1×10^5 cells/well in 100 µL of fresh RPMI 1640 (Euroclone) enriched with 10% FBS (Euroclone), non-essential amino acids (1X; Euroclone), and sodium pyruvate (1 mM; Sigma-Aldrich). Experimental wells contained peptides at a final concentration of 1 µM. Negative control wells lacked peptide, and positive control wells contained anti-CD3 (clone CD3-2; Mabtech). Plates were incubated for 24h and developed according to the manufacturer's instructions (Mabtech). IFNγ -secreting cells were quantified as spot-forming units (SFUs) per 10^6 cells using an automated ELISpot Reader (AELVIS, Hannover, Germany). Positive responses were assigned after background subtraction at 50 SFUs per 10^6 cells (mean). Data were excluded in the absence of a response to anti-CD3.

2.2.5 Flow Cytometry

Ex vivo analyses were performed using thawed PBMCs. Cells were stained first with LIVE/DEAD Fixable Aqua (Thermo Fisher Scientific) for 10 min at room temperature and then with the following directly conjugated monoclonal antibodies for 15 min at room temperature: anti-CCR7–PE-Cy7 (clone 3D12; BD Biosciences, Milan, Italy), anti-CD8– APC-Cy7 (clone SK1; BD Biosciences), anti-CD27–FITC (clone M-T271; Miltenyi Biotec), anti-CD45RA–PerCP-Cy5.5 (clone HI100; Thermo Fisher Scientific), anti-HLA-DR–APC (clone LN3; Thermo Fisher Scientific), and anti-PD1–PE (clone REA1165; Miltenyi Biotec). Naïve T cells were defined as $CCR7^+CD27^+CD45RA^+$ Tetramer staining was performed using $2–3 \times 10^6$ primed cells on day 10. Cells were stained serially with LIVE/DEAD Fixable Aqua (Thermo Fisher Scientific) for 10 min at room temperature, individual or pooled tetramers for 15 min at 37 ◦C, and the following directly conjugated monoclonal antibodies for 15 min at room temperature: anti-CD3–PerCP- Cy5.5 (clone SK7; Thermo Fisher Scientific), anti-CD4–FITC (clone RPA-T4; BD Biosciences), anti-CD8–APC/Fire 750 (clone RPA-T8; BioLegend, Amsterdam, Netherlands), anti-CD14–FITC (clone 18D11; ImmunoTools, Friesoythe, Germany), and anti-CD19–FITC (clone HI19a; ImmunoTools). After fixation/permeabilization using a Transcription Factor Buffer Set (BD Biosciences), cells were stained with anti-Tbet–eFluor 660 (clone 4B10; Thermo Fisher Scientific) for 40 min at 4 ◦C. Tetramer-labeled $CD3^+CD8^+$ T cells were identified among viable cells after exclusion of FITC+ events (dump channel). A positivity threshold was calculated after performing identical experiments in donors lacking expression of HLA-A2. Data

were acquired using a FACSCanto II (BD Biosciences), compensated using Comp-Beads (BD Biosciences), and analysed using FlowJo software version 10.8 (FlowJo LLC, Ashland, OR, USA).

2.2.6 HLA-Peptide Binding Assay

Aliquots of 1×10^6 T2 cells, a lymphoma-derived line expressing low amounts of HLA-A2, were incubated overnight at 26°C in 1 mL of AIM-V medium containing individual peptides at concentrations ranging from 10^{-5} M to 10^{-8} M. Cells were then incubated for a further 4 h at 37°C, washed extensively in phosphate-buffered saline, and stained with anti-HLA-A2–PE (clone BB7.2; BioLegend). Mean fluorescence intensity was determined via flow cytometry and used to calculate peptide-induced stabilization as the percent increase over baseline expression of HLA-A2 [183,184].

2.2.7 Statistical Analysis

Statistical significance was assessed using the Mann–Whitney U test or the Pearson correlation coefficient in Prism software version 8 (GraphPad, San Diego, CA, USA).

2.3 Results

2.3.1 Cohort Description

PBMCs were collected from anonymized adult donors before (2018–2019) or during [Figure 2.3.1.1 (A)]. Donors in the latter group were only included after testing seronegative for SARS-CoV-2. Samples were stratified according to age as "young" (range, 20–52 years; median, 25 years; female, n = 2; male, n = 6) or "old" (range, 65–69 years; median, 68 years; female, n = 0; male, n = 8). Basal levels of activation and differentiation in the peripheral $CD8^+$ T cell compartment was characterized using flow cytometry. A proportionate reduction in the size of the naïve pool was observed with age [Figure 2.3.1.1 (B)]. Moreover, higher fractions of total (including naïve) and memory (excluding naïve) $CD8^+$ T cells displayed an activated phenotype in old versus young individuals, as defined by the expression frequencies of HLA-DR and PD-1 [Figure 2.3.1.1 (C)].

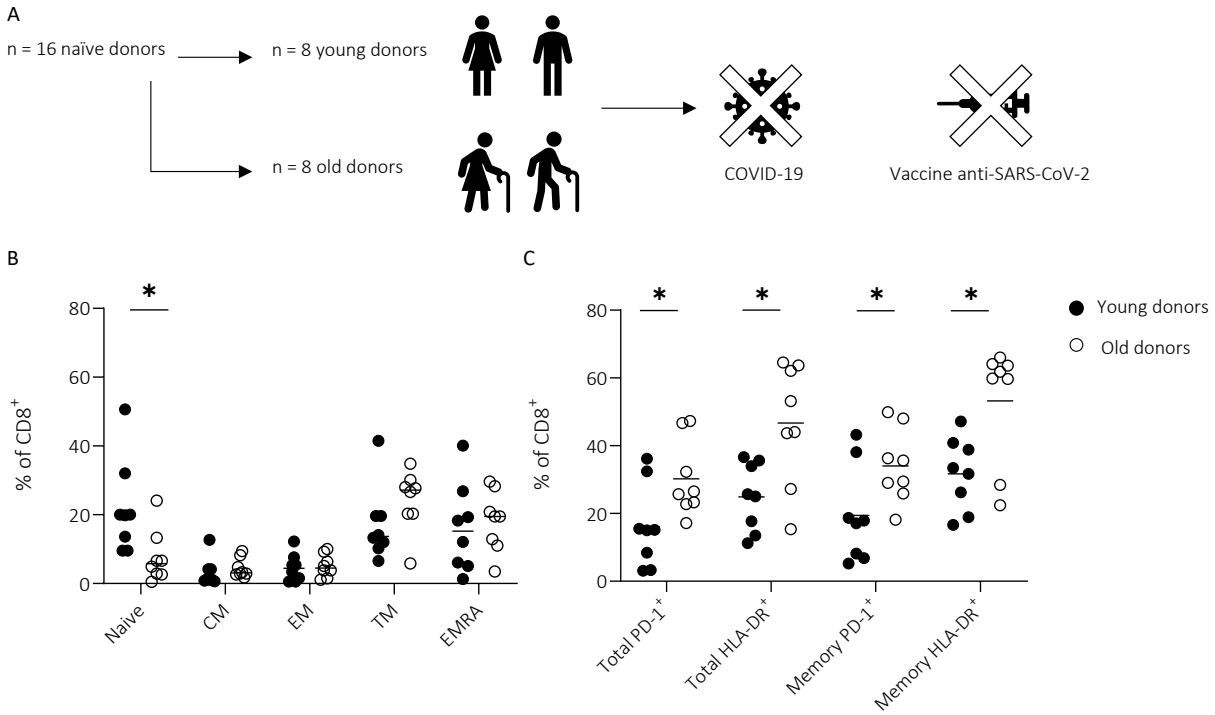


*Figure 2.3.1.1: Activation and differentiation in the peripheral $CD8^+$ T cell compartment as a function of age. (**A**) Donors were stratified according to age. (**B**) Frequencies of naïve ($CCR7^+CD27^+CD45RA^+$), central memory (CM; $CCR7^+CD27^+CD45RA^-$), transitional memory (TM; $CCR7^-CD27^+CD45RA^-$), effector memory (EM; $CCR7^-CD27^-CD45RA^-$), and terminally differentiated EM (EMRA; $CCR7^-CD27^-CD45RA^+$) CD8+ T cells. (**C**) Expression frequencies of HLA-DR and PD-1 among total (including naïve) and memory (excluding naïve) $CD8^+$ T cells. (B,C) Horizontal lines represent median values. * $P < 0.05$ (Mann–Whitney U test).*

2.3.2 Peptides Characterization

HLA-A2-restricted peptide epitopes derived from different viral proteins were used to measure primary $CD8^+$ T cell responses against SARS-CoV-2 [Table 2.2.2.1]. The affinity of each peptide for this restriction element was determined using a surface stabilization assay.

All peptides bound strongly to HLA-A2. In most cases, stabilization was detected at low peptide concentrations (10^{-7} M and 10^{-8} M), although some differences were apparent, especially at high peptide concentrations (10^{-5} M and 10^{-6} M), consistent with a binding hierarchy [Figure 2.3.2.1]. The lowest relative affinities were observed for the spike-derived peptides YLQ and TLD.

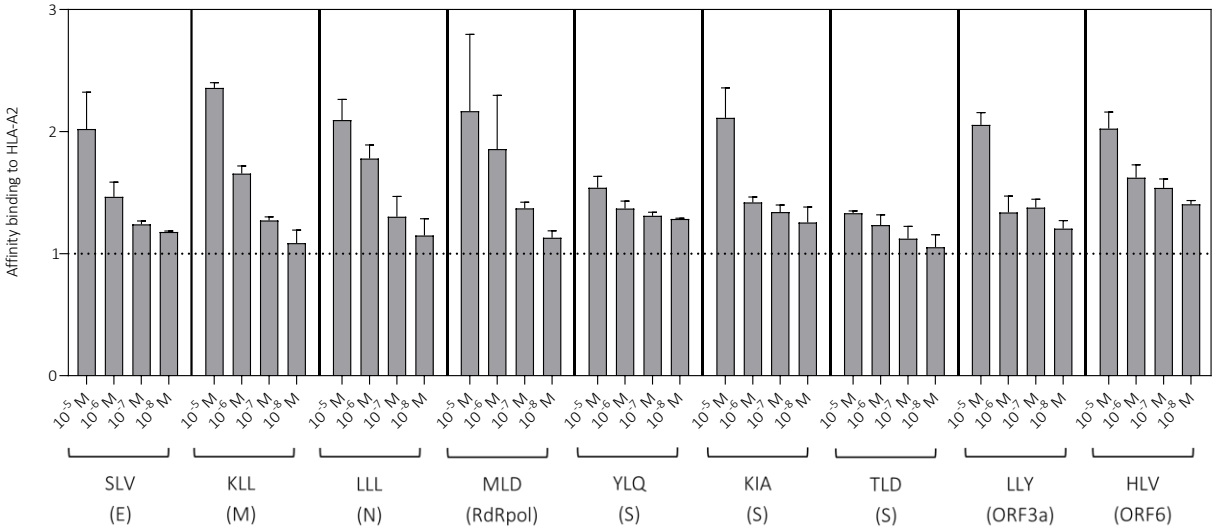


Figure 2.3.2.1: Peptide binding to HLA-A2. Peptide binding affinity was measured across a range of concentrations using a surface stabilization assay. Data are shown as median + SEM. The dotted line indicates no binding (1). E, envelope; M, membrane; ORF, open reading frame; RdRpol, RNA-dependent RNA polymerase; S, spike.

2.3.3 Aging Impairs the Induction of Effector $CD8^+$ T Cells Defined by the Expression of T-bet

PBMCs were stimulated *in vitro* with the model peptide EV10 and a panel of peptides derived from SARS-CoV-2 [Table 2.2.2.1], all restricted by HLA-A2 [Figure 2.3.3.1 (A)]. Epitope-specific $CD8^+$ T cells were quantified via tetramer staining on day 10. This experimental approach to the measurement of priming efficacy has been fully validated in humans and mice [92,185] . EV10-specific $CD8^+$ T cells from young donors expanded to a substantially greater extent than EV10-specific $CD8^+$ T cells from old donors, resulting in a median frequency difference that exceeded one order of magnitude [Figure 2.3.3.1 (B)]. In contrast, only very low frequencies of SARS-CoV-2-specific $CD8^+$ T cells (often <0.1%) were detected using a pool of tetramers (n = 5), irrespective of age [Figure 2.3.3.1 (B)]. Similar results were obtained using each tetramer individually [Figure

2.3.3.1 (C)]. To extend these findings, we measured the expression of T-bet, a transcription factor that plays a key role in effector differentiation, among primed $CD8^+$ T cells specific for EV10 or SARS-CoV-2. T-bet was expressed at lower frequencies among primed $CD8^+$ T cells from old versus young donors, irrespective of specificity [Figure 2.3.3.1 (D)]. Moreover, a direct correlation was observed between T-bet expression frequencies among EV10-specific $CD8^+$ T cells and T-bet expression frequencies among SARS-CoV-2-specific $CD8^+$ T cells [Figure 2.3.3.1 (E)]. Collectively, these data suggested that age rather than specificity was a key determinant of effector $CD8^+$ T cell differentiation, as defined by the expression of T-bet.

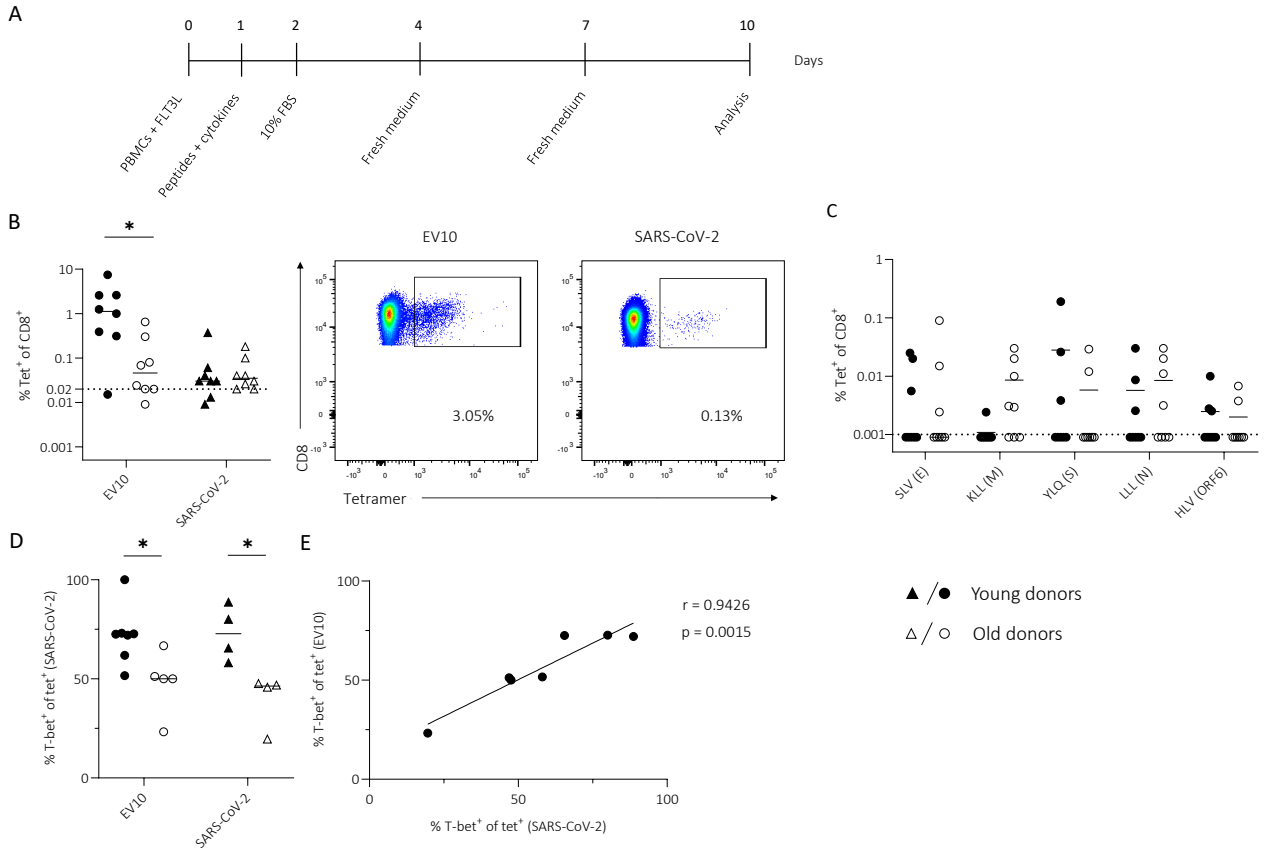


*Figure 2.3.3.1: T-bet expression among primed $CD8^+$ T cells specific for EV10 or SARS-CoV-2. **(A)** Schematic representation of the in vitro priming approach. **(B,C)** Epitope-specific $CD8^+$ T cell frequencies quantified using the EV10 tetramer or SARS-CoV-2 tetramers in a single pool (n = 5) **(B)** or individually **(C)**. Dotted lines indicate the limit of detection. **(D)** T-bet expression frequencies among tetramer-labeled $CD8^+$ T cells quantified as in **(B)**. **(E)** Pearson correlation showing T-bet expression frequencies among EV10-specific $CD8^+$ T cells versus T-bet expression frequencies among SARS-CoV-2-specific $CD8^+$ T cells. **(B-D)** Horizontal lines represent median values. * P < 0.05 (Mann–Whitney U test).*

2.3.4 Aging Impairs the Induction of Effector CD8$^+$ T Cells Defined by the Expression of IFNγ

To assess the functional correlates of differential T-bet expression patterns among epitope-specific CD8$^+$ T cells primed via our *in vitro* approach, we used ELISpot assays to quantify the secretion of IFNγ. IFNγ response frequencies were consistently higher among young versus old donors after stimulation with peptides derived from SARS-CoV-2 (n = 9) [Figure 2.3.4.1 (A)]. In the latter group, no responses were observed against the spike-derived peptides KIA and TLD, and responses against the non-spike-derived peptides SLV, MLD, LLY, and HLV were limited to a single donor in each case [Figure 2.3.4.1 (B)]. To assess the presence of cross-reactive responses due to memory T cells specific for common cold coronaviruses (HCoV), in the previous study [97] we stimulated PBMCs directly ex vivo with the HLA-A2-presented epitopes; IFNγ secretion was measured 24 h after stimulation. No positive responses toward the SARS-CoV-2 epitopes were observed. Accordingly, there was an age-related difference in the frequency of epitope recognition, albeit just below the threshold required for significance [Figure 2.3.4.1 (C)].

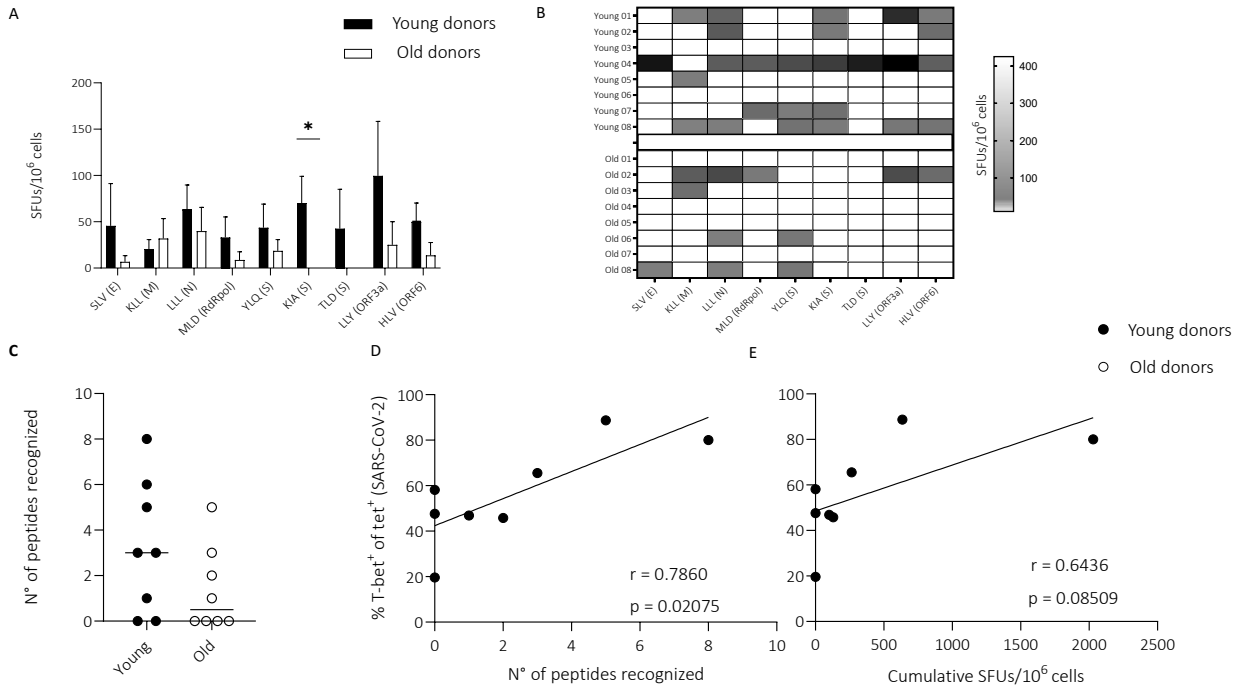


*Figure 2.3.4.1: IFNγ expression among primed CD8$^+$ T cells specific for SARS-CoV-2. (**A**) Epitope-specific response frequencies quantified using ELISpot assays to capture IFN-γ after stimulation with peptides derived from SARS-CoV-2. Responses above 50 SFUs per 106 cells were considered positive. Data are shown as median + SEM. (**B**) Data from (**A**) shown as a heatmap. (**C**) The total number of peptides recognized by each donor. Horizontal lines represent median values. (**D,E**) Pearson correlations showing T-bet expression frequencies among SARS-CoV-2-specific CD8$^+$ T cells versus epitope recognition frequencies, measured as a binary outcome for each peptide (**D**), and overall response frequencies, measured as cumulative SFUs (**E**). Dots correspond with the data shown in Figure 2.3.3.1(D) (young, n = 4; old, n = 4). (a) * p < 0.05 (Mann–Whitney U test).*

Of note, T-bet expression frequencies among SARS-CoV-2-specific $CD8^+$ T cells correlated directly with epitope recognition frequencies (immunoprevalence), measured as a binary outcome for each peptide [Figure 2.3.4.1 (D)], and overall response frequencies (immunodominance), measured as cumulative SFUs [Figure 2.3.4.1 (E)]. No correlation was detected between epitope recognition frequencies and peptide binding affinities for HLA-A2 [Figure 2.3.4.2].

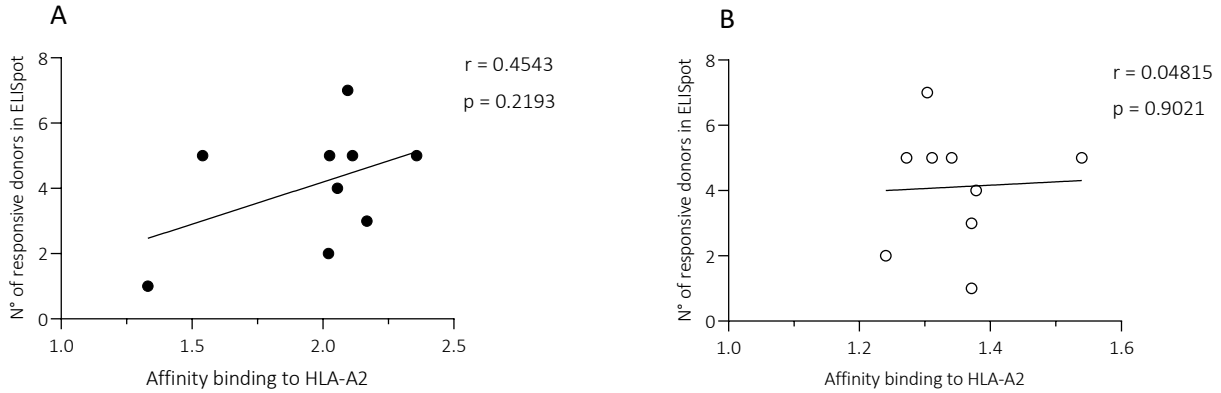


*Figure 2.3.4.2: Correlation between peptide binding affinity and immunoprevalence. Affinity binding to HLA-A2 was calculated for each peptide at 10^{-5} M (**A**) or 10^{-7} M (**B**) and correlated with the number of responsive donors as determined using ELISpot assays to capture IFN-γ. Significance was determined using the Pearson correlation coefficient.*

Collectively, these data suggested that age rather than specificity was a key determinant of effector $CD8^+$ T cell differentiation, as defined by the induction of IFNγ

2.4 Discussion

Aging is known to alter the composition and functionality of the immune system [92,105,186]. These changes limit the ability of elderly individuals to mount de novo cellular immune responses against previously unencountered pathogens in the context of natural infection and/or vaccination [179,187]. T cells are particularly susceptible to the ravages of age, potentially explaining the vulnerability of elderly individuals to emerging viral infections, such as SARS-CoV-2 [173]. This notion has gained traction following descriptions of an inverse correlation between the size of the naïve pool and the severity of COVID-19 [[178,188,189].

In this study, we used an *in vitro* approach to prime epitope-specific $CD8^+$ T cells from healthy donors stratified by age, ensuring a complete absence of prior exposure to antigens derived from SARS-CoV-2. We found that age was associated with reductions in the diversity and magnitude of functional $CD8^+$ T cell responses elicited against SARS-CoV-2, measured via the recall induction of IFNγ. Of note, we also found that epitope recognition frequencies were not associated with peptide binding affinities for HLA-A2, consistent with previous work [190–192].

In young donors, EV10 elicited substantially more robust CD8+ T cell responses than any of the peptides derived from SARS-CoV-2, most likely reflecting preservation of the naïve pool and the constitutively high precursor frequencies associated with the expression of HLA-A2 [97]. In contrast, viral specificities were barely detectable via tetramer staining on day 10, irrespective of age. Similar findings have been reported previously [193,194]. SARS-CoV-2-specific responses were nonetheless detected functionally. This discrepancy could reflect lower thresholds for activation versus tetramer binding and/or differences in the respective limits of detection [195]. Moreover, the functional data revealed an age-related deficit in the mobilization of effector $CD8^+$ T cells against various epitopes derived from SARS-CoV-2, consistent with the lower T-bet expression frequencies observed among tetramer-labeled $CD8^+$ T cells from old versus young donors at the same time point, an observation that extended to the model antigen EV10.

These collective observations confirmed and extended previous findings based on the use of peptide matrices to assess priming efficacy [97]. In particular, we used a cleaner approach focused on single epitopes to identify functional responses and further incorporated phenotypic assessments to provide additional mechanistic information, namely the expression of HLA-DR, PD-1, and T-bet. Accordingly, we generated a comprehensive dataset showing that age-related changes in the basal activation status and overall size of the naïve T cell pool were linked with an impaired ability to mount de novo $CD8^+$ T cell responses against previously unencountered pathogens, exemplified in this study by SARS-CoV-2.

Immunosenescence is thought to underlie the vulnerability of elderly individuals to COVID-19 [196]. The data presented here revealed a global decline in priming efficacy with age, which led to a reduction in the diversity of functional $CD8^+$ T cell responses elicited in vitro against a panel of typically immunodominant epitopes derived from SARS-CoV-2. Although further studies will be required to link these findings with immune control of viral replication and vaccine efficacy, our work has established a testable mechanistic paradigm that could expedite the development of new interventions designed to enhance and/or preserve the operational integrity of the naïve T cell pool as a means of protecting the elderly against potentially fatal episodes of COVID-19.

CHAPTER 3:

Age differentially impacts adaptive immune responses induced by adenoviral versus mRNA vaccines against COVID-19

3.1 Introduction

Immunization against severe acute respiratory syndrome coronavirus 2 (SARS-CoV-2) began at the end of 2020, preventing millions of deaths worldwide. The first approved vaccines were based on mRNA technology, namely BNT162b2 (Pfizer/BioNTech) and mRNA-1273 (Moderna), or adenoviral vectors, namely ChAdOx1-S (AstraZeneca) and Ad26.COV2.S (Janssen), encoding the spike (S) protein of SARS-CoV-2. However, it subsequently became clear that vaccine efficacy waned quickly [197,198], especially against newly emerging viral variants that diverged rapidly from the wild-type strain [199]. The global spread of variants of concern that could escape existing immunity [199] led to the introduction of further booster immunizations beyond the third dose to maintain vaccine efficacy, which had already exceeded 90% [200,201]. National regulations dictated which vaccine formulation was used for boosting after the second dose [202]. As the virus spread globally, it became clear that older individuals were particularly susceptible to severe disease, with high attendant rates of mortality [173,175].

Vaccine efficacy was also found to be suboptimal in older individuals [203,204], facilitating breakthrough infections with SARS-CoV-2 [205,206]. These observations suggested an age-related link between antiviral immunity and disease outcome. Physiological aging has been linked with a progressive decline in immune functionality, known as immunosenescence, which could account for the increased vulnerability of older individuals to coronavirus disease 2019 (COVID-19) [177,207]. Accordingly, we recently demonstrated that aging is associated with a reduction in the diversity and magnitude of functional $CD8^+$ T cell responses elicited against SARS-CoV-2 [97,208], consistent with the typical features of immunosenescence [48,209], which collectively limit the ability of older individuals to mount de novo adaptive immune responses against previously unencountered pathogens in the context of natural infection or vaccination [179,187].

This phenomenon impacts both cellular and humoral immunity [128]. In line with these observations, recent studies have shown that the BNT162b2 vaccine becomes less effective with age [197,210,211] as reported previously for vaccines against other viral infections, such as yellow fever and hepatitis B [212,213]. To circumvent this issue, booster doses of some vaccines are recommended throughout

life [214], but this solution is only partially effective in an aging population [213]. SARS-CoV-2 vaccine efficacy correlates with antibody-mediated neutralization, which is generally directed against the receptor-binding domain (RBD) of the S protein [215,216]. Studies to date have indicated that neutralizing antibody titers decline rapidly within a few months after vaccination [215,216] whereas S protein-specific $CD4^+$ and $CD8^+$ T cell-mediated immunity is somewhat more stable [217,218]. However, the extent to which the process of aging and the type of vaccine affect cellular and humoral immune responses has not been addressed directly. Therefore, we sought to characterize cellular and humoral immunity as continuous and discrete functions of age at memory time points after primary vaccination with two doses of BNT162b2 or two doses of ChAdOx1-S and after booster vaccination with a subsequent dose of BNT162b2 or mRNA-1273.

3.2 Materials and methods

3.2.1 Main Cohort

Healthy donors with no known history of SARS-CoV-2 infection (n = 230) were enrolled at a median of 6 months after a second homologous immunization against COVID-19, comprising either two doses of BNT162b2 (n = 128) or two doses of ChAdOx1-S (n = 92) [Table 3.2.1.1]. A subset of these participants (n = 99) and newly enrolled volunteers (n = 43) also provided samples at a median of 5 months after boosting with BNT162b2 or mRNA-1273 [Table 3.2.1.2]. Donors in all groups were stratified by age as young (Y, 18–40 years), middle-aged (M, 41–65 years), or old (O, >65 years). The study was approved by the Ethical Committee of the Istituto Nazionale per le Malattie Infettive Lazzaro Spallanzani (protocol number 488). All participants provided written informed consent in accordance with the principles of the Declaration of Helsinki. Venous blood samples were collected into acid citrate dextrose tubes from donors recruited at long-term care facilities, the Ferrara Blood Bank, or the Geriatric Department of Ferrara Hospital, Italy. Evidence of prior infection sufficient for exclusion was based on a self-reported positive test for COVID-19 or serum reactivity against the viral nucleocapsid protein detected using a chemiluminescent microparticle SARS-CoV-2 IgG Immunoassay (Abbott).

Table 3.2.1.1: Characteristics of participants recruited after primary

	Donors enrolled after two doses of ChAdOx1-S (*AstraZeneca*)			Donors enrolled after two doses of BNT162b2 (*Pfizer/BioNTech*)		
	Y (24)	M (61)	O (7)	Y (62)	M (49)	O (17)
Sex						
Male (%)	29	38	57	39	39	41
Female (%)	71	62	43	61	61	59
Age (years)	31	53	72	27	51 [1]	84
Mean (range)	(20–40)	(41–63)	(66–67)	(20–40)	(41–61)	(66–100)
BMI						
Mean (range)	22.8 (17.9–30.1)	24.8 [2] (18.7–39.0)	24.4 [3] (16.4–28.1)	22.7 [4] (17.3–33.3)	24.8 (18.3–33.6)	26.1 (17.6–40.4)
Smokers (%)	21	15	0 [3]	28 [4]	12	19 [5]
Comorbidities[8]						
Hypertension (%)	0	7	71	3	20	65
Cardiac insufficiency (%)	0	2	0	0	0	29
Arrhythmia (%)	0	0	0	0	0	18
COPD (%)	0	0	0	0	0	18
Asthma (%)	0	2	0	3	2	0
Allergies (%)	0	0	0	2	6	12
Hyperlipidemia (%)	0	3	0	0	6	24
Dyslipidemia (%)	0	2		0	0	12
Diabetes (%)	0	0	0	0	0	6
Hypothyroidism (%)	0	10	14	3	10	0
Osteoporosis (%)	0	0	0	0	0	18
Neuropathy (%)	0	2	0	2	0	18
Epilepsy (%)	0	0	0	0	0	6
Celiac disease (%)	0	2	14	0	0	0
Endometriosis (%)	4	0	0	0	0	0
Gastrointestinal disease (%)	0	3	0	0	2	29
Kidney failure (%)	0	0	0	0	0	6
Hyperplasia/hypertrophy (%)	0	2	43	0	0	24
Anemia (%)	0	0	0	0	0	12
Viral infection (%)	0	2	0	0	0	0
Polycystic ovary (%)	0	0	0	2	0	0
Rheumatoid arthritis (%)	0	0	0	0	2	0
Depression/anxiety (%)	0	0	0	0	4	6
Number of comorbidities	0	0	1	0	1	3
Mean (range)	(0–1)	(0–2)	(1–2)	(0–1)	(0–3)	(0–8)
Number of medications						
Mean (range)	0 (0–1)	1 (0–4)	2 (1–3)	0 (0–2)	1 (0–4)	5 (1–10)
Physical activity						
None (%)	46	34 [6]	80 [7]	38 [4]	48 [1]	94
Mild (%)	12	19 [6]	20 [7]	13 [4]	15 [1]	0
Moderate (%)	21	42 [6]	0 [7]	29 [4]	22 [1]	6
Intense (%)	21	5 [6]	0 [7]	20 [4]	15 [1]	0
Months after vaccination	6	6	5	5	6	7
Mean (range)	(4–7)	(5–7)	(5–6)	(3–10)	(4–11)	(5–9)

Donor numbers are indicated in parentheses: Y, young (18–40 years); M, middle-aged (41–65 years); O, old (>65 years). [1]Data from 48 donors. [2]Data from 60 donors. [3]Data from 6 donors. [4]Data from 61 donors. [5]Data from 16 donors. [6]Data from 57 donors. [7]Data from 5 donors. [8]Comorbidities not detected were Alzheimer's disease, arthrosis, autoimmune disease, cancer, hyperthyroidism, hypoglycemia, and Parkinson's disease. COPD, chronic obstructive pulmonary disease.

Table 3.2.1.1: Characteristics of participants recruited after booster vaccination

	Donors enrolled after two doses of ChAdOx1-S (AstraZeneca) and one booster dose of BNT162b2 (Pfizer/BioNTech) or mRNA-1273 (*Moderna*)			**Donors enrolled after two doses of BNT162b2 (*Pfizer/BioNTech*) and one booster dose of BNT162b2 (*Pfizer/BioNTech*) or mRNA-1273 (*Moderna*)**		
	Y (11)	M (38)	O (7)	Y (15)	M (33)	O (28)
Sex						
Male (%)	55	39	29	40	33	29
Female (%)	45	61	71	60	67	71
Age (years)	33	56	71	28	52 [1]	85
Mean (range)	(25–40)	(41–63)	(61–80)	(20–40)	(41–63)	(66–103)
BMI						
Mean (range)	22.9 (17.9–30.1)	24.5 (18.7–39.0)	25.2 [2] (22.5–28.1)	22.5 (17.4–28.8)	24.6 (19.4–33.2)	24.7 [3] (17.6–40.4)
Smokers (%)	18	13	14	20	9	7 [3]
Comorbidities[6]						
Hypertension (%)	0	8	71	0	30	50
Cardiac insufficiency (%)	0	3	29	0	0	21
Arrhythmia (%)	0	0	0	0	0	11
Asthma (%)	0	3	0	0	3	0
Allergies (%)	0	0	0	0	6	7
Hyperlipidemia (%)	0	3	14	0	9	18
Dyslipidemia (%)	0	3	14	0	0	11
Diabetes (%)	0	0	0	0	0	7
Hypothyroidism (%)	0	11	14	6	9	7
Osteoporosis (%)	0	0	14	0	3	11
Alzheimer's (%)	0	0	0	0	0	11
Neuropathy (%)	0	0	14	0	0	14
Autoimmune disease (%)	0	0	0	0	3	4
Epilepsy (%)	0	0	0	0	0	4
Celiac disease (%)	0	3	0	0	0	0
Endometriosis (%)	9	0	0	0	0	0
Gastrointestinal disease (%)	0	0	0	0	3	18
Kidney failure (%)	0	0	0	0	0	7
Hyperplasia/hypertrophy (%)	0	3	29	0	0	4
Anemia (%)	0	0	0	0	0	7
Viral infection (%)	0	0	0	0	0	4
Rheumatoid arthritis (%)	0	0	0	0	3	4
Arthrosis (%)	0	0	14	0	0	0
Depression/anxiety (%)	0	0	0	0	9	18
Number of comorbidities	0	0	2	0	1	2

Mean (range)	(0–1)	(0–1)	(1–4)	(0–1)	(0–3)	(0–5)
Number of medications	0	1	3	0	1	5
Mean (range)	(0–1)	(0–4)	(0–6)	(0–2)	(0–4)	(0–11)
Physical activity						
None (%)	55	35 [4]	86	53	55 [5]	89
Mild (%)	27	19 [4]	14	27	15 [5]	4
Moderate (%)	9	43 [4]	0	20	15 [5]	7
Intense (%)	9	3 [4]	0	0	15 [5]	0
Months after vaccination	6	5	5	5	6	6
Mean (range)	(5–9)	(4–7)	(5–6)	(4–7)	(4–8)	(5–8)

Donor numbers are indicated in parentheses: Y, young (18–40 years); M, middle-aged (41–65 years); O, old (>65 years). [1]Data from 31 donors. [2]Data from 6 donors. [3]Data from 27 donors. [4]Data from 37 donors. [5]Data from 32 donors. [6]Comorbidities not detected were cancer, chronic obstructive pulmonary disease (COPD), hyperthyroidism, hypoglycemia, Parkinson's disease, and polycystic ovary.

3.2.2 Validation cohort

Elderly donors (>75 years) living independently with or without comorbidities were recruited after primary vaccination with either BNT162b2 (n = 79) or ChAdOx1-S (n = 33) and subsequent boosting with BNT162b2 or mRNA-1273 (total, n = 112) via local primary care networks over a limited time period from 29th December 2020 to 4th March 2021 [Table 3.2.2.1]. The study was approved by the Northwest Preston Research Ethics Committee (REC 20/NW/0240). All participants provided written informed consent in accordance with the principles of the Declaration of Helsinki. Venous blood samples were collected via home phlebotomy (Birmingham, UK). Evidence of prior infection sufficient for exclusion was based on serum reactivity against the viral nucleocapsid protein detected using an Elecsys Anti-SARS-CoV-2 Immunoassay (Roche).

Table 3.2.2.1: Characteristics of participants in the validation cohort (UK).

	Donors enrolled after two doses of ChAdOx1-S (AstraZeneca) and one booster dose of BNT162b2 (Pfizer/BioNTech) or mRNA-1273 (*Moderna*)	**Donors enrolled after two doses of BNT162b2 (Pfizer/BioNTech) and one booster dose of BNT162b2 (Pfizer/BioNTech) or mRNA-1273 (*Moderna*)**	**Donors enrolled after two doses of BNT162b2 (Pfizer/BioNTech) with extended interval and one booster dose of BNT162b2 (Pfizer/BioNTech) or mRNA-1273 (*Moderna*)**
N	33	37	42
Booster dose			
BNT162b2 (n)	28	37	42
mRNA-1273 (n)	1	0	0
Unknown (n)	4	0	0
Sex			
Male (%)	45	41	43
Female (%)	55	59	57
Age (years)	84	84	85
Mean (range)	(79–92)	(80–91)	(76–97)

3.2.2 Samples

Peripheral blood mononuclear cells (PBMCs) were isolated via standard density gradient centrifugation using Ficoll-Paque (GE Healthcare), suspended in 90% fetal bovine serum (FBS, Euroclone) and 10% dimethyl sulfoxide (DMSO, Sigma-Aldrich), and cryopreserved in liquid nitrogen. Plasma samples were stored at −80°C. All donors were assessed for the expression of the human leukocyte antigen (HLA)-A2, and this chapter reports data only from those who tested positive for (HLA)-A2.

3.2.3 Peptides and tetramers

HLA-A2-restricted peptides representing optimally defined SARS-CoV-2 spike epitopes [Table 3.2.3.1] were used to assess memory $CD8^+$ T cell responses, alongside a pool of commonly recognized HLA-A2-restricted peptides ("Memory") representing optimally defined epitopes from EBV, Flu, and HSV [Table 3.2.3.2]. All peptides were synthesized in solid phase and purified via reverse-phase high-performance liquid chromatography to >97%. SARS-CoV-2 peptides were selected from the wildtype spike protein (strain HKU-001a) based on immunodominance and immunoprevalence [97]. The fluorescent peptide/HLA-A2 tetramer corresponding to the YLQ epitope was generated as described previously [182].

Table 3.2.3.1: SARS-CoV-2 peptides restricted by HLA-A2.

Protein	Peptide ID	Sequence	Residues	Portion	Length
surface glycoprotein	TLD	TLDSKTQSL	109–117	S1	9
	YLQ	YLQPRTFLL	269–277	S1	9
	KIA	KIADYNYKL	417–425	RBD	9
	KLP	KLPDDFTGCV	424–433	RBD	9
	SII	SIIAYTMSL	691–699	S2	9
	ALN	ALNTLVKQL	958–966	S2	9
	VVF	VVFLHVTYV	1060–1068	S2	9
	RLN	RLNEVAKNL	1185–1193	S2	9
	FIA	FIAGLIAIV	1220–1228	S2	9

Table 3.2.3.2: Viral peptides restricted by HLA-A2.

Virus	Peptide ID	Sequence	Length
Herpes simplex virus	ALM	ALMLRLLRI	9
	NLL	NLLTTPKFT	9
	RML	RMLGDVMAV	9
	FLG	FLGAGALAV	9
	ALL	ALLGLTLGV	9
	GIF	GIFEDRAPV	9
Epstein-Barr virus	CLG	CLGGLLTMV	9
	GLC	GLCTLVAML	9
Influenza virus	GIL	GILGFVFLT	9
	AIM	AIMDKNIIL	9
	FMY	FMYSDFHFI	9

	NML	NMLSTVLGV	9

3.2.4 ELISpot assays

$CD8^+$ T cell responses in the main cohort were enumerated directly *ex vivo* using a Human IFNγ ELISpot PLUS (HRP) Kit (Mabtech). PBMCs from HLA-$A2^+$ donors were thawed and seeded in duplicate at 2.5×10^5 cells/well in precoated capture plates and stimulated with individual peptides or the Memory pool for 24 h. Negative control wells lacked peptide, and positive control wells contained anti-CD3 (clone CD3-2, Mabtech). Plates were developed according to the manufacturer's instructions and analyzed using an automated ELISpot Reader (AELVIS). IFNγ-secreting cells were quantified as spot-forming units (SFUs) per 10^6 cells after background subtraction. Results were excluded if the positive control was negative. Responses were considered positive at >10 SFUs/10^6 PBMCs. The positivity threshold was set at three standard deviations above a mean value calculated from identical assays performed using samples acquired before the pandemic from unexposed and unvaccinated donors expressing HLA-A2 and samples acquired after the pandemic from exposed and vaccinated donors lacking HLA-A2. $CD8^+$ T cell responses in the validation cohort were enumerated similarly using a T-SPOT Discovery SARS-CoV-2 Kit (Oxford Immunotec).

3.2.5 Flow cytometry

Immunophenotypic analyses were performed at each time point using whole fresh blood stained with anti-CD4–PE-Cy7 (clone RM4-5, Thermo Fisher Scientific), anti-CD8–FITC (clone MEM-31, ImmunoTools), anti-CD19–VioGreen (clone REA675, Miltenyi Biotec), anti-CD27–APC (clone REA499, Miltenyi Biotec), anti-CD38–VioBlue (clone REA671, Miltenyi Biotec), anti-CD45RA–PerCP-Cy5.5 (clone HI100, Thermo Fisher Scientific), and anti-HLA-A2–PE (clone BB7.2, BioLegend). Red blood cells were lysed using FACS Lysis Solution (BD Biosciences). Absolute cell numbers were calculated using Precision Count Beads (BioLegend). Tetramer staining was also performed after *in vitro* expansion on day 10. Cells were labeled with LIVE/DEAD Fixable Aqua (Thermo Fisher Scientific) and stained with the YLQ tetramer as described previously [182] followed by anti-CD3–PerCP-Cy5.5 (clone OKT3, Thermo Fisher Scientific), anti-CD4–FITC (clone OKT4, BD Biosciences), anti-CD8–APC/Fire 750 (clone SK1, BioLegend), anti-CD14–FITC (clone 18D11, ImmunoTools), and anti-CD19–FITC (clone ID3, ImmunoTools). Viable tetramer-labeled $CD3^+CD8^+$ T cells were identified after excluding $FITC^+$ events (dump channel). Data were acquired using a FACS Canto II (BD Biosciences), compensated using BD CompBeads (BD Biosciences), and analyzed using FlowJo version 10.8 (FlowJo LLC).

3.2.6 *In vitro* expansion of antigen-specific T cells

Spike-specific memory $CD8^+$ T cells were expanded from thawed PBMCs. Briefly, cells from HLA-$A2^+$ donors were cultured with the YLQ peptide (1 μM) in the presence of IL-2 (20 U/ml, Miltenyi Biotec), and cells from all donors were cultured with SARS-CoV-2 spike 15mer overlapping peptides in the presence of IL-2 (20 U/ml, Miltenyi Biotec). Medium was replaced on days 4 and 7 with fresh RMPI 1640 (Euroclone) enriched with 10% FBS (Euroclone), nonessential amino acids (1X, Euroclone), penicillin/streptomycin (1%, Euroclone), sodium pyruvate (1 mM, Sigma-Aldrich), and IL-2 (20 U/ml, Miltenyi Biotec). YLQ-specific $CD8^+$ T cells were analyzed via tetramer staining on day 10. Populations were considered valid at >0.01%.

3.2.7 Cytotoxicity assay

PBMCs from HLA-$A2^+$ donors were thawed and plated at 10^6 cells/well in 48-well tissue culture plates (Thermo Fisher Scientific). Cells were stimulated with the YLQ peptide in the presence of IL-2 (20 U/ml, Miltenyi Biotec) and IL-7 (20 ng/ml, R&D Systems) added on days 1, 8, 15, and 22. Medium was replaced on days 4, 11, and 18 with fresh RMPI 1640 (Euroclone) enriched with 10% FBS (Euroclone), nonessential amino acids (1X, Euroclone), penicillin/streptomycin (1%, Euroclone), sodium pyruvate (1 mM, Sigma-Aldrich), IL-2 (20 U/ml, Miltenyi Biotec), and IL-7 (20 ng/ml, R&D Systems). Epitope-specific $CD8^+$ T cells were analyzed via tetramer staining on day 24. $CD8^+$ T cells were then purified via magnetic separation using MS Columns (Miltenyi Biotec). In parallel, an HLA-$A2^+$ lymphoblastoid *cell* line (LCL) was pulsed with the YLQ peptide (1 μM) for 90 min at 37°C. Pulsed and unpulsed LCLs were then labeled with carboxyfluoroscein succinimidyl ester (CFSE, Thermo Fisher Scientific) and Cell Proliferation Dye eFluor 450 (CPD, Thermo Fisher Scientific), respectively. Assays were set up to contain equal numbers of epitope-specific $CD8^+$ T cells (effectors) and LCLs (unpulsed controls and pulsed targets) and then incubated overnight at 37°C. Negative control wells lacking effectors were used to calculate background death. Specific killing was calculated as a function of percent survival after background subtraction, comparing the ratio of CFSE-labeled versus CPD-labeled LCLs.

3.2.8 Statistical analysis

Data points generated from assay runs with technical failures in the corresponding negative and positive controls were excluded from the downstream analyses. Entire datasets from individual donors were discarded if positivity to the SARS-CoV-2 N protein was detected at any stage. Investigators were blinded with respect to the vaccine received by donors when performing the experiments. No statistical method was used to predetermine sample size. Significance was assessed

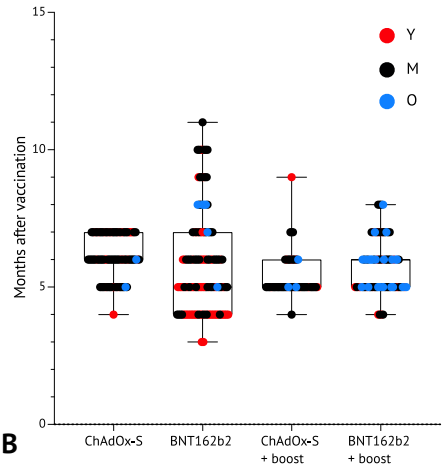
using the Mann–Whitney U-test with or without Bonferroni correction (for comparisons between two or more than two groups, respectively), a one-way analysis of variance with Tukey's test (for comparisons across three different age groups), a chi-squared test (to compare frequencies across more than two groups), Spearman's rank test (to assess correlations) or a Wilcoxon matched-pairs signed-rank test (to compare average values with a given threshold) in Prism 8 (GraphPad Software).

3.3 Results

3.3.1 ChAdOx1-S is less reactogenic than BNT162b2

To delineate the spectrum of vaccine-induced adaptive immunity against SARS-CoV-2, we measured spike-specific cellular responses in young (Y, 18–40 years), middle-aged (M, 41–65 years), and old individuals (O, >65 years) at a median of 6 months (range, 3–11 months) after the second of two doses of BNT162b2 (n = 128) or two doses of ChAdOx1-S (n = 92) and at a median of 5 months (range, 4–9 months) after a booster dose of BNT162b2 or mRNA-1273 following primary immunization with BNT162b2 (n = 76) or ChAdOx1-S (n = 56) [Figure 3.3.1.1 and Figure 3.3.1.2].

A



B

	ChAdOx-S	BNT162b2	ChAdOx-S + boost	BNT162b2 + boost
Minimum	4,000	3,000	4,000	4,000
25% Percentile	6,000	4,000	5,000	5,000
Median	6,000	5,000	5,000	6,000
75% Percentile	7,000	7,000	6,000	6,000
Maximum	7,000	11,00	9,000	8,000
Mean	6,111	5,815	5,357	5,733
Lower 95% CI of mean	5,947	5,492	5,150	5,508
Upper 95% CI of mean	6,276	6,137	5,564	5,958

Figure 3.3.1.1: Distribution of sampling time points after vaccination against SARS-CoV-2. (A) Box and whisker plots showing sampling time points as months after primary vaccination and subsequent boosting for donors represented in Figure 3.3.1.2. Colours indicate age groups (key). Descriptive statistics are reported in (B).

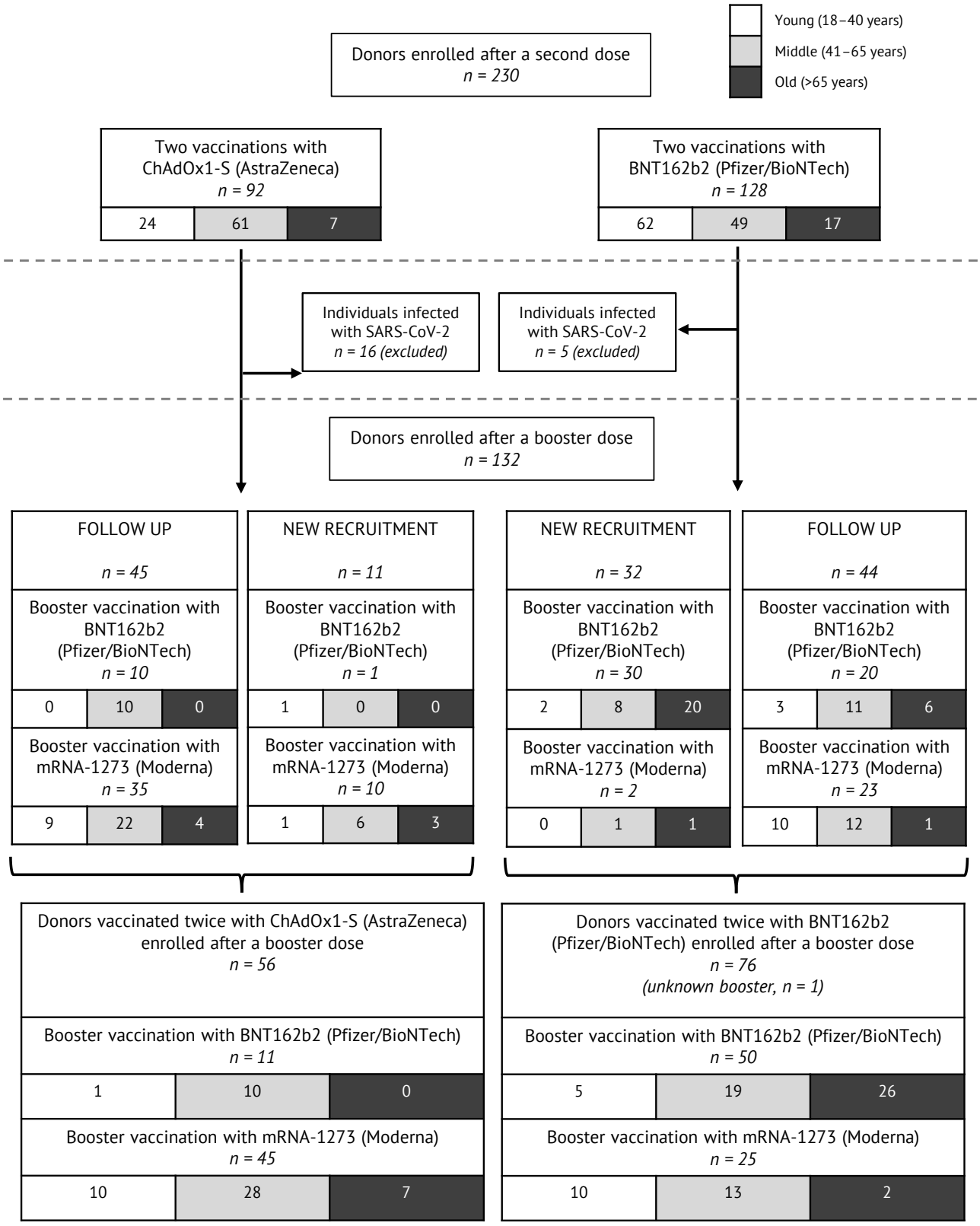


Figure 3.3.1.2: Cohort overview. Participants were enrolled at memory time points after a second (median = 6 months) or third vaccine dose (median = 5 months).

Side effects after vaccination were generally milder in group O compared with groups Y and M [Table 3.3.1.1]. Moreover, the second and third doses were less reactogenic across all age groups vaccinated initially with ChAdOx1-S, and side effects were more protracted among individuals vaccinated initially with BNT162b2, especially in group O**.**

Table 3.3.1.1: Distribution of side effects after vaccination stratified according to age.

Donors vaccinated with two doses of ChAdOx1-S (*AstraZeneca*) and boosted with one dose of BNT162b2 (*Pfizer/BioNTech*) or mRNA-1273 (*Moderna*)									
	I dose			II dose			III dose		
	Y (26)	M (67)	O (10)	Y (26)	M (67)	O (10)	Y (11)	M (38)	O (7)
Side effects									
Pain/swelling (%)	46	43	0	35	34	0	55	37	14
Fatigue (%)	62	63	30	35	31	30	27	26	29
Headache (%)	50	39	10	23	18	10	9	3	0
Fever (%)	65	40	20	19	6	20	18	8	0
Muscle/joint pain (%)	46	34	30	23	7	20	18	8	0
Diarrhea (%)	0	1	0	0	1	0	0	0	0
Nausea (%)	8	3	0	0	0	0	9	0	0
Allergic reaction (%)	0	0	0	0	0	0	9	0	0
Blood clotting (%)	0	1	0	0	0	0	0	0	0
Facial paralysis (%)	0	0	0	0	0	0	0	0	0
Asymptomatic (%)	8	9	40	46	40	50	36	40	57
Duration									
24 h (%)	58	64	30	35	53	50	46	47	29
2–3 days (%)	23	21	20	19	4	0	18	13	0
1 week (%)	11	4	10	0	3	0	0	0	14
>1 week (%)	0	2	0	0	0	0	0	0	0
Donors vaccinated with two doses of BNT162b2 (*Pfizer/BioNTech*) and boosted with one dose of BNT162b2 (*Pfizer/BioNTech*) or mRNA-1273 (*Moderna*)									
	I dose			II dose			III dose		
	Y (64)	M (58)	O (38)	Y (64)	M (58)	O (38)	Y (15)	M (33)	O (28)
Side effects									
Pain/swelling (%)	74[1]	70[2]	68	73[3]	62	71	40	64	71
Fatigue (%)	47[1]	21[2]	13	57[3]	43	13	47	33	11
Headache (%)	18[1]	16[2]	3	29[3]	22	0	13	12	0
Fever (%)	6[1]	2[2]	3	33[3]	21	3	33	15	0
Muscle/joint pain (%)	23[1]	11[2]	5	24[3]	24	0	27	12	4

Diarrhea (%)	0[1]	2[2]	0	0[3]	3	0	0	3	0
Nausea (%)	0[1]	2[2]	0	5[3]	7	0	0	6	0
Allergic reaction (%)	0[1]	4[2]	0	0[3]	2	0	0	0	0
Blood clotting (%)	0[1]	0[2]	0	0[3]	0	0	0	0	0
Facial paralysis (%)	0[1]	0[2]	0	0[3]	0	0	0	0	0
Asymptomatic (%)	13[4]	17[2]	31	9[5]	12	26	13	21	25
Duration									
24 h (%)	56[4]	44[2]	13	63[5]	47	16	80	49	14
2–3 days (%)	29[4]	32[2]	53	26[5]	31	58	7	27	61
1 week (%)	2[4]	2[2]	3	2[5]	7	0	0	3	0
>1 week (%)	0[4]	5[2]	0	0[5]	3	0	0	0	0

Donor numbers are indicated in parentheses: Y, young (18–40 years); M, middle-aged (41–65 years); O, old (>65 years). [1]Data from 62 donors. [2]Data from 57 donors. [3]Data from 63 donors. [4]Data from 61 donors. [5]Data from 62 donors.

3.3.2 Immunization regimen impacts the diversity of $CD8^+$ T cell responses

Italian policies on vaccination changed during the pandemic, and different formulations were offered to the population as a function of age. Therefore, we were unable to recruit equal numbers of BNT162b2-vaccinated and ChAdOx1-S-vaccinated participants in groups Y, M, and O.

To evaluate the impact of age and different immunization regimens on $CD8^+$ T cell specificity, we performed IFNγ ELISpot assays directly *ex vivo* using HLA-A2-restricted peptides representing optimally defined SARS-CoV-2 spike epitopes [Table 3.2.3.1] and, for control purposes to assess broader patterns of immunological memory, a pool (referred to as "Memory") of commonly recognized HLA-A2-restricted peptides representing optimally defined epitopes from Epstein-Barr virus (EBV), influenza virus (Flu), and herpes simplex virus (HSV) [Table 3.2.3.2]. $CD8^+$ T cell responses measured directly *ex vivo* were generally very low and close to the threshold of detection. However, identifiable $CD8^+$ T cell responses were directed against greater numbers of SARS-CoV-2 peptides after primary versus booster vaccination, although there was a potential age bias among donors vaccinated initially with BNT162b2 [Figure 3.3.2.1 (A)]. Cumulative response magnitudes across the SARS-CoV-2 peptides were also higher after primary versus booster vaccination, whereas no such differences were observed for $CD8^+$ T cell responses targeting EBV, Flu, or HSV [Figure 3.3.2.1 (B)]. In addition, epitope-specific response magnitudes were higher and more evenly spread across the SARS-CoV-2 peptides after primary vaccination with ChAdOx1-S versus BNT162b2, subsequently becoming more skewed after the booster dose [Figure 3.3.2.1 (C)].

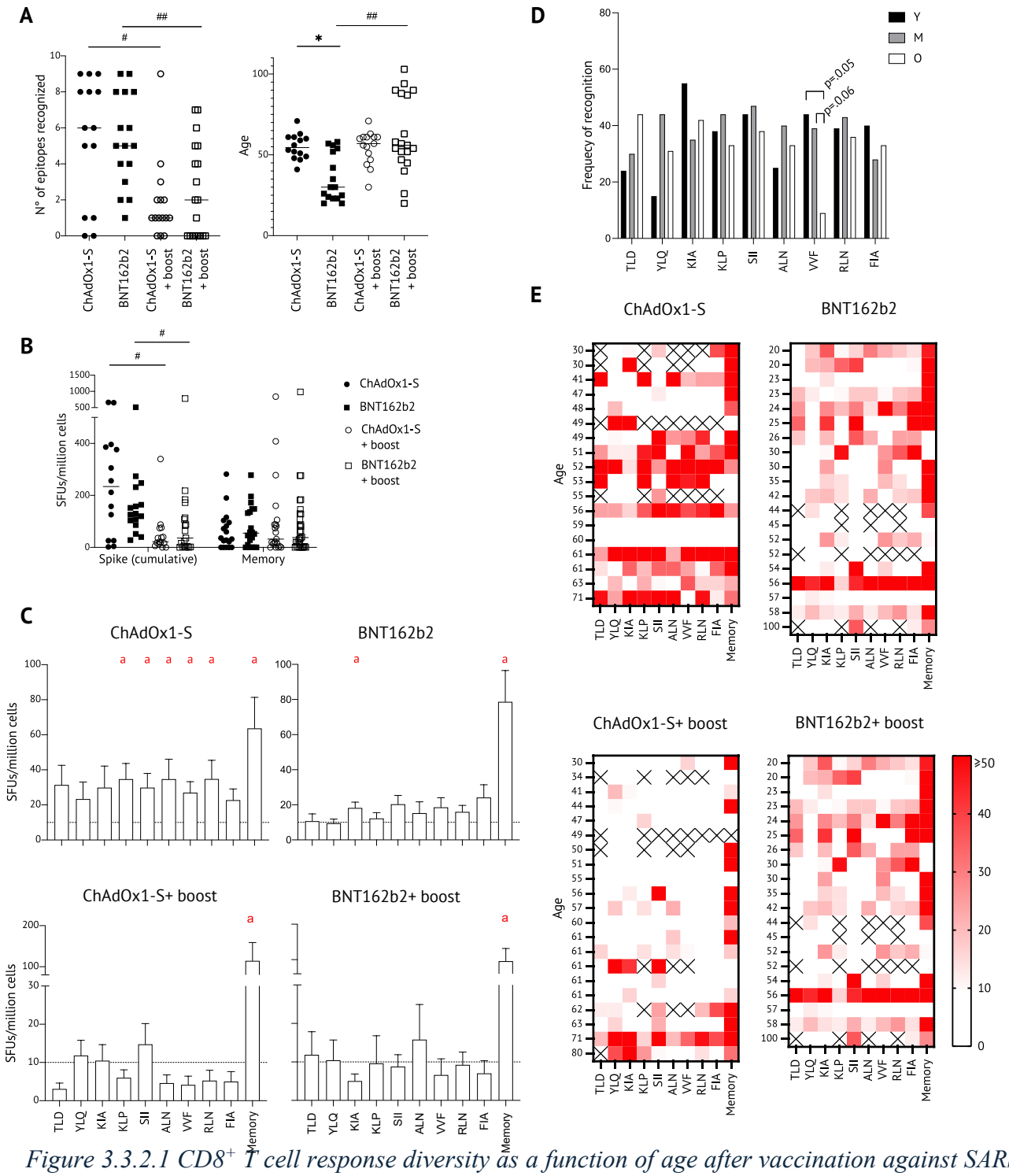


*Figure 3.3.2.1 CD8⁺ T cell response diversity as a function of age after vaccination against SARS-CoV-2. HLA-A2-restricted spike epitope-specific and pooled memory epitope-specific CD8⁺ T cell frequencies were measured using IFNγ ELISpot assays directly ex vivo. (**A**) Left: response diversity stratified by vaccination schedule. Right: donor age distribution (ChAdOx1-S, n = 14; BNT162b2, n = 16; ChAdOx1-S + boost, n = 15; BNT162b2 + boost, n = 19). (**B**) Cumulative response frequencies stratified by vaccination schedule (spike: ChAdOx1-S, n = 14; BNT162b2, n = 16; ChAdOx1-S + boost, n = 15; BNT162b2 + boost, n = 19; memory: ChAdOx1-S, n = 18; BNT162b2, n = 20; ChAdOx1-S + boost, n = 21; BNT162b2 + boost, n = 30). (**C**) Epitope-specific response frequencies stratified by vaccination schedule. Numbers as in (**A**) (continued the other page).*

*(Caption continuation of Figure 3.3.2.1) Dotted lines indicate the threshold of detection. Data are shown as median + SEM. (**d**) Epitope recognition frequencies as a binary function stratified by age (Y, n = 16–20; M, n = 43–54; O, n = 9–13). (**e**) Epitope-specific $CD8^+$ T cell frequencies as a function of age. Data are shown as heatmaps depicting the magnitude of each epitope-specific response in spot-forming units (SFUs) per 10^6 input cells (key). Numbers as in (**D**). X denotes missing values. All data are shown after background subtraction. Horizontal lines represent median values (**A, B**). *p < 0.05 (ChAdOx1-S versus BNT162b2, Mann–Whitney U test with Bonferroni correction). $^{\#}p < 0.05$, $^{\#\#}p < 0.01$ (prime versus boost, Mann–Whitney U test with Bonferroni correction). $^{a}p < 0.05$ (Wilcoxon matched-pairs signed-rank test showing values significantly >10 SFUs/10^6 input cells). Age-associated differences in epitope recognition were assessed using a Chi-square test (**D**). Spike peptides are listed in Table 3.2.3.1, and other viral peptides (memory) are listed in Table 3.2.3.2.*

Comparable immunoprevalence patterns were observed across the SARS-CoV-2 peptides as a function of age, irrespective of the primary vaccine formulation, although the VVF peptide was less commonly recognized by individuals in group O relative to groups Y and M, albeit below the threshold for significance (p = 0.05 for Y versus O, p = 0.06 for M versus O) [Figure 3.3.2.1 (D)].

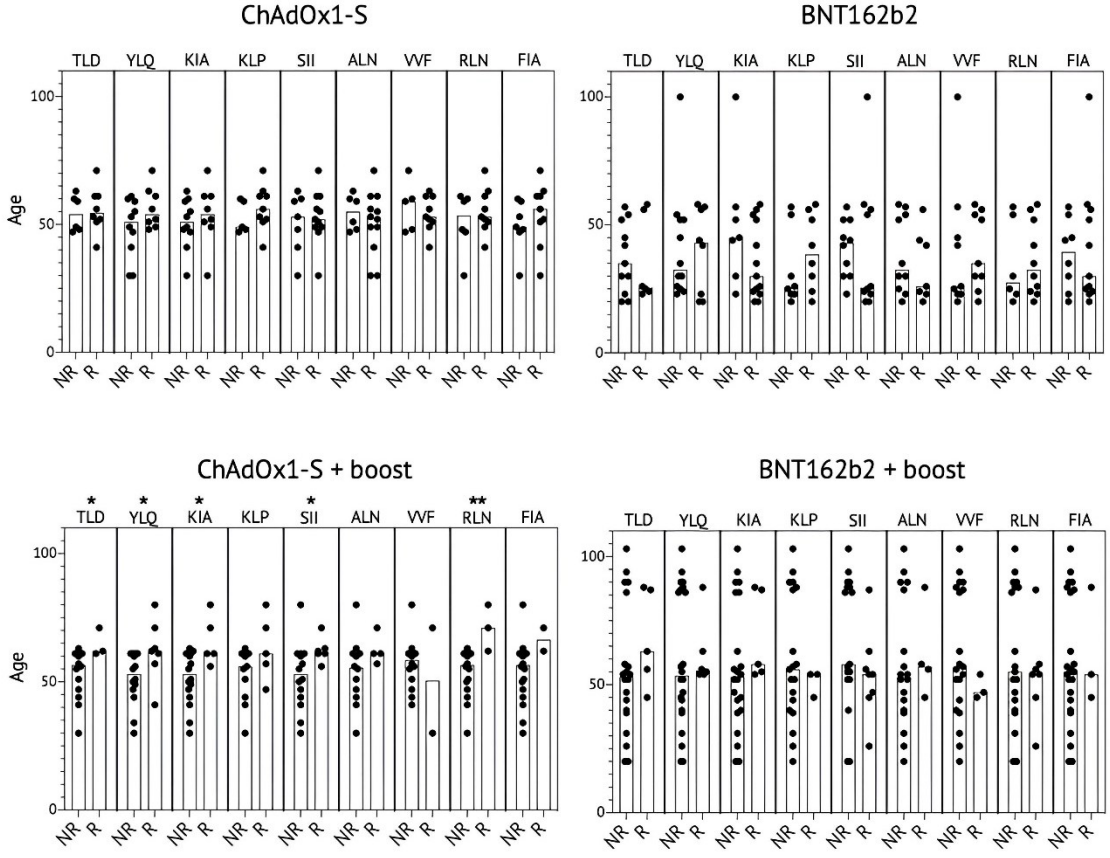


*Figure 3.3.2.2 Epitope-specific $CD8^+$ T cell responses as a function of age after vaccination against SARS-CoV-2. Age distribution for responders (R) and non-responders (NR) against each HLA-A2-restricted spike epitope stratified by vaccination schedule (ChAdOx1-S, n = 14; BNT162b2, n = 16; ChAdOx1-S + boost, n = 15; BNT162b2 + boost, n = 19). The response threshold was set at 10 spot-forming units (SFUs)/million cells after background subtraction. IFNγ ELISpot assays were performed directly ex vivo. Bars represent median values. *P < 0.05, **P < 0.01 (R versus NR, Mann–Whitney U test).*

Similarly, no obvious differences in magnitude as a function of age or immunization regimen were apparent for $CD8^+$ T cell responses directed against the SARS-CoV-2 peptides [Figure 3.3.2.1 (E)], although responders targeting five of these epitopes were slightly older than non-responders after primary vaccination with ChAdOx1-S and subsequent boosting with BNT162b2 or mRNA-1273 [Figure 3.3.2.2].

Collectively, these observations indicated that age minimally impacted vaccine-induced $CD8^+$ T cell responses against SARS-CoV-2, which were generally less diverse and less prominent after primary immunization with BNT162b2 versus ChAdOx1-S.

3.3.3 Age impacts cellular and humoral immune responses elicited by primary vaccination with BNT162b2

In further analyses, we evaluated vaccine-induced immunity as a function of age, in particular we analysed the frequencies of $CD8^+$ T cells specific for the concordantly restricted and typically immundominant spike epitope YLQPRTFLL (YLQ, residues 269–277), as assessed via tetramer staining after transient expansion in the presence of cognate antigen in BNT162b2-vaccinated and ChAdOx1-S-vaccinated $HLA\text{-}A2^+$ individuals.

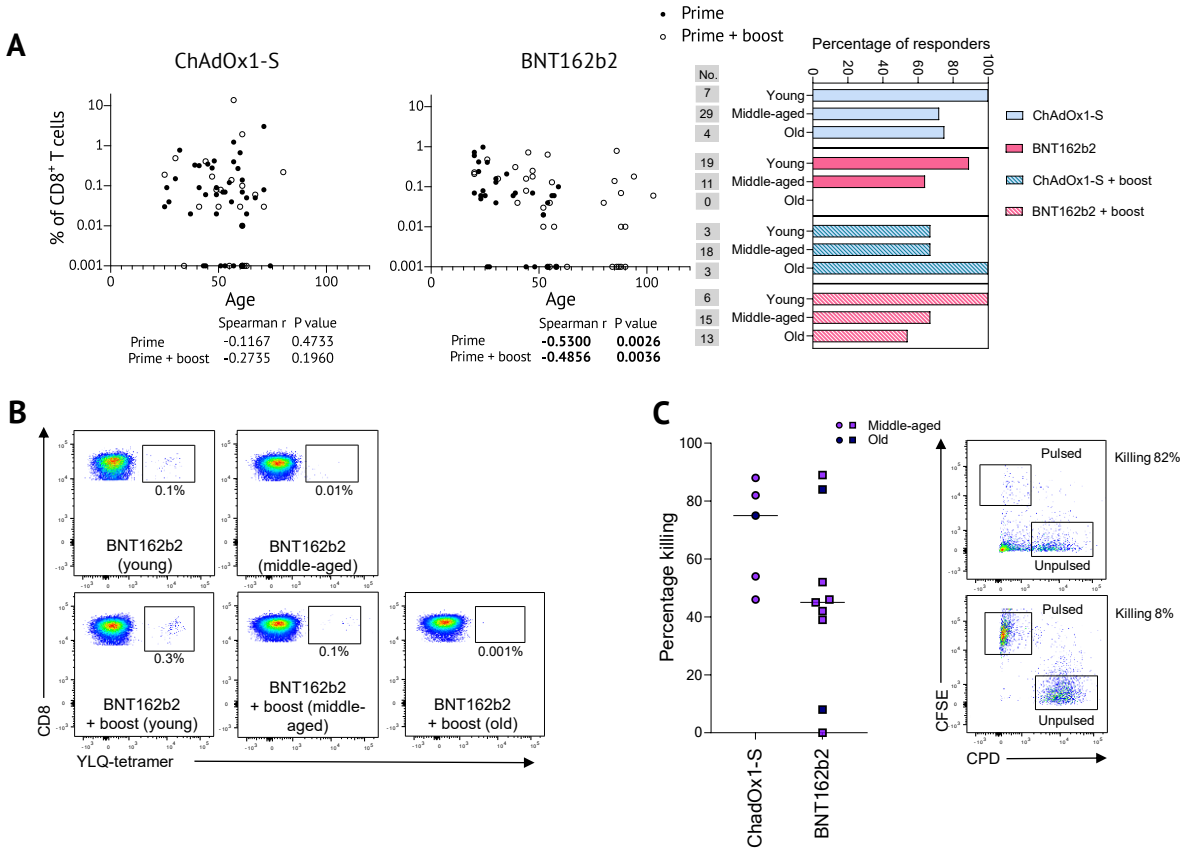


*Figure 3.3.3.1: Cytotoxic immune responses as a function of age after vaccination against SARS-CoV-2. (**A**) Left, Correlations between age and YLQ-specific CD8+ T cell frequencies (ChAdOx1-S, n = 40; BNT162b2, n = 30; ChAdOx1-S + booster dose, n = 24; BNT162b2 + booster dose, n = 34) measured using tetramer staining after transient expansion. Right, Responder frequencies as a function of age (threshold = 0.01% of $CD8^+$ T cells). (**B**) Representative flow cytometry plots showing the enumeration of tetramer-labeled YLQ-specific $CD8^+$ T cells as a function of age. Plots are gated on viable $CD3^+$ events after dump exclusion. (**C**) Cytotoxic activity of YLQ-specific $CD8^+$T cells among donors from the middle-aged (n = 11) and old (n = 3) groups after primary vaccination with BNT162b2 (n = 9) or ChAdOx1-S (n = 5) and subsequent boosting with BNT162b2 or mRNA-1273. Right, Representative flow cytometry plots showing the elimination of $HLA\text{-}A2^+$ target cells pulsed with YLQ. (**C**) The horizontal lines represent the median values. (**A**) Correlations were assessed using a two-sided Spearman's rank test. (**C**) Differences in cytotoxic activity were assessed using a two-sided Mann–Whitney U-test. *P < 0.05, ****P < 0.0001 (two-sided Chi-squared test).*

YLQ-specific $CD8^+$ T cell frequencies decreased as a function of age after primary vaccination with BNT162b2 but not after primary vaccination with ChAdOx1-S [Figure 3.3.3.1 (A, B)]. These cells were nonetheless able to mediate cytotoxic activity after further expansion from individuals in groups M and O, especially after primary vaccination with ChAdOx1-S and subsequent boosting with BNT162b2 or mRNA-1273 [Figure 3.3.3.1 (C)].

As noted above, a major limitation of our cohort was the low number of individuals in group O vaccinated initially with ChAdOx1-S. To exclude the possibility that our observations were biased by the higher median age of participants vaccinated with BNT162b2, we recalculated all correlations after excluding donors aged >70 years [Figure 3.3.3.2], and these analyses confirmed all findings across the entire cohort.

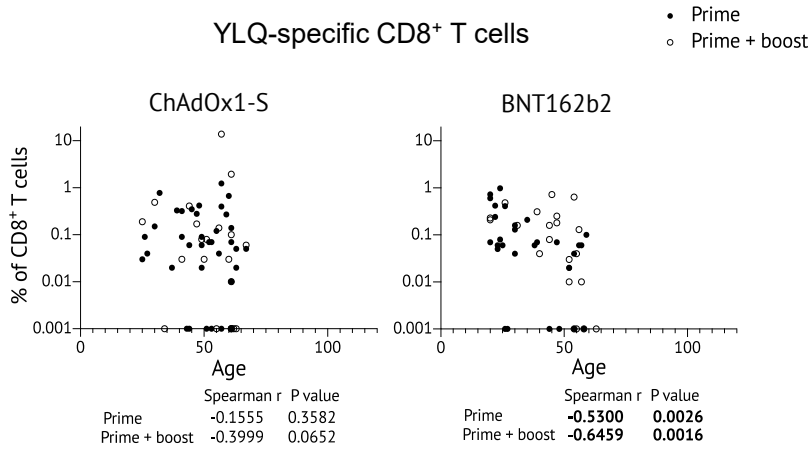


*Figure 3.3.3.2 Cellular immune responses as a function of age in donors aged <70 years after vaccination against SARS-CoV-2. Correlations between age and YLQ-specific CD8+ T cell frequencies measured via tetramer staining after transient expansion (ChAdOx1-S, n = 37; BNT162b2, n = 30; ChAdOx1-S + boost, n = 22; BNT162b2 + boost, n = 21). Correlations were determined using a two-sided Spearman's rank test. ***P < 0.001 the significances were reported in bold.*

3.3.4 Cellular immune responses are optimally maintained in older individuals vaccinated with ChAdOx1-S

On the basis of the findings reported above, we postulated that vaccine-induced immunological memory was best maintained in older individuals after primary immunization with ChAdOx1-S. To investigate this paradigm, we first analyzed S protein-specific cellular immune responses across all donors in the old group, segregated according to immunization regimen [Figure 3.3.4.1]. Although rigorous statistical testing was precluded by the sample size, $CD8^+$ T cell frequencies tended to be higher after primary vaccination with ChAdOx1-S versus BNT162b2 and subsequent boosting with BNT162b2 or mRNA-1273 [Figure 3.3.4.1].

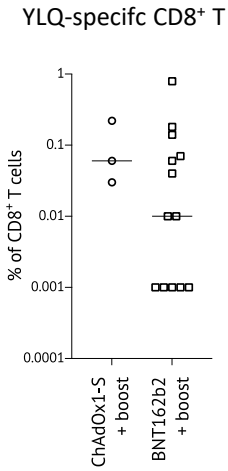


Figure 3.3.4.1: Cellular immune responses in older individuals after boosting with BNT162b2 or mRNA-1273 YLQ-specific $CD8^+$ T cell frequencies measured via tetramer staining after transient expansion (ChAdOx1-S+ boost, n = 3; BNT162b2+ boost, n = 13).

To extend this analysis, which was potentially confounded by demographic and genetic factors as a consequence of the low number of individuals in the old group vaccinated initially with ChAdOx1-S, we assessed S protein-specific cellular responses in a validation cohort of donors aged 75 years and older recruited in the UK [Figure 3.3.4.2 (A)]. Each participant received two doses of BNT162b2, separated by an interval of 3 weeks, as in Italy, or 11 weeks, termed extended interval (EI), or two doses of ChAdOx1-S followed by a booster dose of BNT162b2 or mRNA-1273 (Table 7). Samples were analyzed at a median of 6 months after the booster dose. S protein-specific-$CD8^+$ T cell frequencies, as quantified using an IFNγ ELISpot assay with pooled peptides spanning the S1 and/or S2 domains, were higher after primary vaccination with ChAdOx1-S versus either BNT162b2 or BNT162b2 EI [Figure 3.3.4.2 (B)]. Collectively, these data indicated that S protein-specific cellular

immunological memory, as assessed in different cohorts using different readouts of functionality, was better maintained in older individuals after primary vaccination with ChAdOx1-S versus BNT162b2.

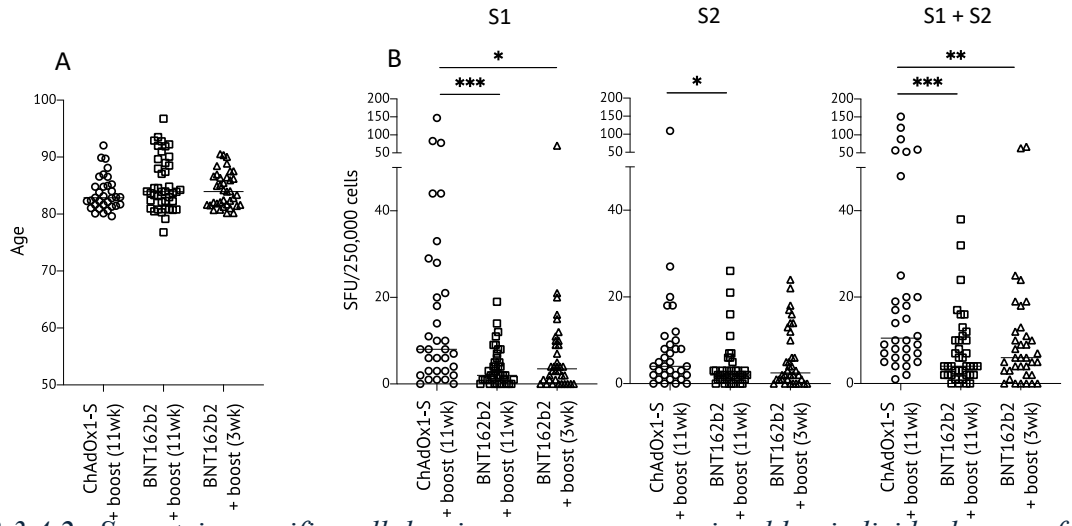


*Figure 3.3.4.2: S protein-specific cellular immune responses in older individuals as a function of primary vaccination schedule after boosting with BNT162b2 or mRNA-1273. Age distribution (A), and S protein-specific cellular immune responses directed against the S1 and/or S2 domains measured in a validation cohort of donors aged 75 years and older using IFNγ ELISpot assays directly ex vivo (B). Each participant received two doses of BNT162b2, separated by a standard interval of 3 weeks (n = 37) or an EI of 11 weeks (n = 42), or two doses of ChAdOx1-S (n = 33) followed by a booster dose of BNT162b2 or mRNA-1273. Samples were analysed at a median of 6 months after the booster dose. The horizontal lines represent the median values. *P < 0.05, **P < 0.01, ***P < 0.001.*

3.3.5 Impact of naïve decrease on cellular responses

Naïve T cells are critical for vaccine responses, but their numbers decline with immunosenescence. In our cohort, we observed, considering all donors stratified by age, a clear shift from naïve T cells to memory subsets in $CD8^+$ T cells [Figure 3.3.5.1].

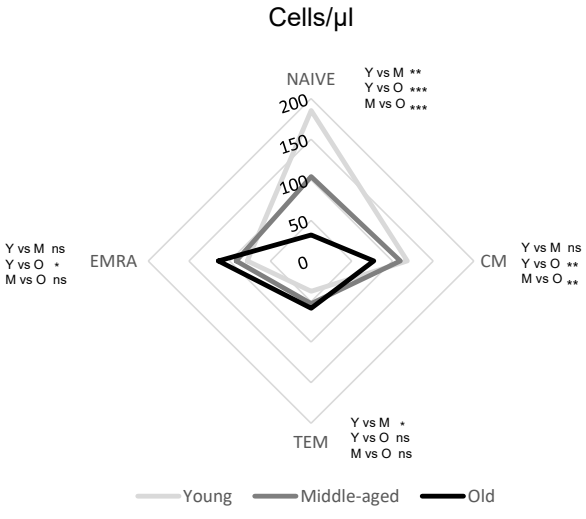


*Figure 3.3.5.1: Immune profiling of donors stratified by age. Absolute numbers of naïve (N, $CD27^+CD45RA^+$), central memory (CM, $CD27^+CD45RA^-$), effector memory (EM, $CD27^-CD45RA^-$), and terminally differentiated effector memory T cells (EMRA, $CD27^-CD45RA^+$), quantified in whole blood directly ex vivo. Data are shown as radar plots representing mean values stratified by age (Y, n = 90; M, n = 125; O, n = 48). *P < 0.05, **P < 0.01, ***P < 0.001 (Y versus M versus O, one-way ANOVA with Tukey's test).*

Given the negative impact of aging on this balance, we aimed to investigate age-associated immune features further and their impact on the frequencies of YLQ-specific $CD8^+$ T cells.

We found no consistent associations linking the absolute numbers of naïve$CD8^+$ T cells with the frequencies of S protein-specific $CD8^+$ T cells across vaccine formulations, considering primary vaccination [Figure 3.3.5.2 (A)]. However, when considering booster dose, the absolute numbers of naïve $CD8^+$ T cells correlated directly with the frequencies of YLQ-specific $CD8^+$ T cells after the booster dose in donors vaccinated initially with BNT162b2 [Figure 3.3.5.2 (B)], underlining the close correlation between the naïve cell pool and maintenance of responses in this type of primary vaccination.

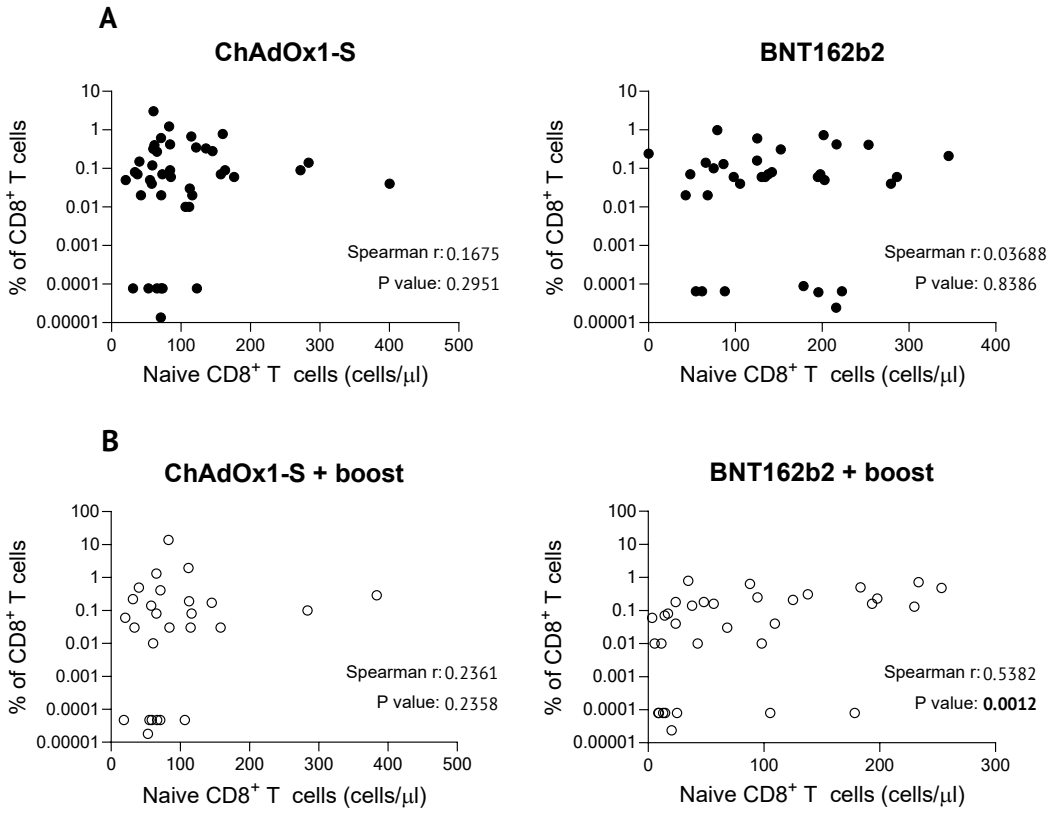


*Figure 3.2.5.2: Role of absolute count of naïve $CD8^+$ T cells and the frequencies of YLQ-specific $CD8^+$ T cells. (**A**) Correlations between absolute number naïve and YLQ-specific $CD8^+$ T cell frequencies measured via tetramer staining after transient expansion after primary (ChAdOx1-S, n = 41; BNT162b2, n = 33), and (**B**) boosting vaccination (ChAdOx1-S + boost, n = 27; BNT162b2 + boost, n = 36). Correlations were determined using a two-sided Spearman's rank test. **P < 0.001 the significances were in bold.*

Collectively, these observations indicated that age-related erosion of the naïve lymphocyte pool, a typical feature of immunosenescence, constrained the induction and/or maintenance of adaptive immune responses to a greater extent after primary vaccination with BNT162b2 versus ChAdOx1-S.

3.4 Discussion

COVID-19 vaccines become less effective over time in terms of preventing infection and symptomatic disease [198], probably as a consequence of waning antibody-mediated neutralization [219], whereas protection against severe disease is maintained more durably [220], probably as a consequence of cell-mediated immunological memory [201], which is generally more stable [221]. It is nonetheless unclear to what extent age-related changes in the immune system impact the efficacy and immunogenicity of vaccines designed to elicit protective immunity against SARS-CoV-2. To address this issue, we performed a comprehensive evaluation of S protein-specific adaptive immune responses as continuous and discrete functions of age after primary vaccination with two doses of BNT162b2 or ChAdOx1-S and subsequent boosting with a single dose of BNT162b2 or mRNA-1273, excluding donors with evidence of previous infection with SARS-CoV-2. We also found that aging negatively impacted S protein-specific cellular responses as a probable function of progressive erosion of the naïve lymphocyte pool in donors vaccinated initially with BNT162b2. These collective findings indicated that adaptive immunological memory was optimally maintained in older individuals after primary vaccination with ChAdOx1-S and subsequent boosting with BNT162b2 or mRNA-1273.

BNT162b2 is known to induce higher humoral responses than ChAdOx1-S [215,218,222,223]. S protein-specific $CD4^+$ and $CD8^+$ T cells are also typically more frequent in the circulation a few weeks after vaccination with BNT162b2 versus ChAdOx1-S [202,222,223]. In contrast, we found that S protein-specific $CD8^+$ T cell responses were generally less prominent after primary vaccination with BNT162b2 versus ChAdOx1-S, as indicated by the lower number of responses above threshold detected by ELISpot [Figure 3.3.2.1 C]. These observations could be explained by a more rapid loss of S protein-specific $CD8^+$ T cells after vaccination with BNT162b2 versus Ad26.COV2.S or ChAdOx1-S [221,224,225]. In line with this possibility, BNT162b2 commonly induces highly differentiated effector-like $CD8^+$ T cells [226], which are prone to contraction in the absence of persistent antigen. Vaccine efficacy can nonetheless be enhanced and prolonged by booster doses, which have been delivered primarily in the form of mRNA [200,227]. This advantage was maintained at memory time points in our study, as reported for other vectored vaccines previously [202], albeit with an attendant reduction in the diversity of $CD8^+$ T cell responses directed against S epitopes restricted by HLA-A2. This latter phenomenon probably occurred as a consequence of variable expansion after repetitive antigen stimulation, which has also been described in the context of breakthrough infection with SARS-CoV-2 [228].

Age has been shown to impair S protein-specific cellular immune responses after primary vaccination with BNT162b2 but not after primary vaccination with ChAdOx1-S2 [200,211,225,229–232]. Accordingly, cellular immune responses elicited by mRNA vaccines may be uniquely vulnerable to the ravages of age, whereas cellular immune responses elicited by vectored vaccines may be more robust as a consequence of molecular mechanisms that somehow circumvent the limitations of immunosenescence and warrant further investigation. Our study was potentially limited by the fact that we used an expansion protocol to amplify memory $CD8^+$ T cells as a prelude to subsequent evaluations of response magnitude and functionality, the accuracy of which could be confounded by differences in proliferation and secretory capacity after recall stimulation. Our main findings were nonetheless largely recapitulated directly *ex vivo* using a validation cohort from the UK, because another potential limitation of our study was the low number of older donors [233]. Our cohorts also lacked ethnic and racial diversity, potentially leading to bias and confounding broader interpretation.

These observations could provide a mechanistic explanation for epidemiological associations showing that BNT162b2 protects against infection but not against severe disease more effectively than ChAdOx1-S2.

CHAPTER 4:

Study of T lymphocyte metabolism as a function of the degree of response to antipneumococcal vaccination

4.1 Introduction

Streptococcus pneumoniae is an important global pathogen that causes a wide range of clinical disease in children and adults. Its most common manifestation is pneumococcal pneumonia, but it can also occur with non-invasive (e.g. otitis media, sinusitis, conjunctivitis, pneumonia) and invasive (e.g. bacteremic pneumonia, meningitis, sepsis) events; it disproportionately affects the young, the elderly, and the immunocompromised [234] and bacterial co- or secondary infections are frequently observed in influenza patients [126].

Vaccination is crucial against morbidity and mortality caused by this pathogen, and it represents the only way to prevent the invasive pneumococcal disease or co-infection, or to mitigate the effects caused by *Streptococcus pneumoniae.* Two types of vaccines are available against *S. pneumoniae*: polysaccharide vaccines (PPV), which contain the purified bacterial capsule polysaccharides, and conjugated vaccines (PCV), for which the polysaccharides are conjugated to carrier proteins, such as CRM197, non-toxic variant of diphtheria toxin [107].

In 2023, 1783 cases of invasive pneumococcal disease were reported in Italy, and the age groups with the highest incidence were children <1 year and adults >64 years. Specifically, the incidence of the disease in children <1 year old was 10.41 cases per 100,000 inhabitants; in adults >64 years old, it was 7.45 cases per 100,000 inhabitants. This represents a notable increase compared to previous years (0.84 cases per 100,000 inhabitants in 2021 and 1.79 cases per 100,000 inhabitants in 2022) [235].

Vaccination with PCV13 (13-valent pneumococcal conjugate vaccine) has been shown to significantly reduce morbidity and mortality from pneumococcal diseases in older adults. In fact, in the CAPITA trial, a large randomized controlled study, demonstrated that PCV13 reduces the incidence of vaccine-type invasive-pneumococcal diseases by 75% in adults aged 65 and older [236,237]. However, current vaccination strategies do not provide adequate protection for all older adults, leading to high medical costs and a great societal impact in an increasingly aging population [238].

Low response to vaccines in the elderly is influenced by aging, in specifically through “immunosenescence”, a gradual decline of immune system functions with age, which determinates increased susceptibility to infections and reduced vaccination responses. Vaccination is a reliable way

to protect the aging population from infections [239]. However, vaccine effectiveness can differ greatly among individuals, especially in older adults. It is crucial to identify those who have a poor response to vaccines and understand the reasons behind it, to develop alternative vaccination strategies [240] or implement immunomodulatory interventions [72] that can enhance protection for these individuals.

Immunosenescence causes both a rearrangement of cellular subsets and alterations at the levels of cellular function and metabolism. In fact, alterations in immune cell metabolism, especially at the lymphocyte level, adversely affect the ability these cells to get activated and proliferate, thus influencing antigen-specific responses in the elderly (including those elicited by vaccination).

It has been observed that mitochondrial dysfunction leads to a lower production of ATP, and to reactive oxygen species (ROS) accumulation [241], which contribute to the low-grade inflammation typical of the older individuals, a phenomenon known as inflammaging [242,243]. The metabolic switch from oxidative to glycolytic metabolism, is essential for the activation and proliferation of T and B lymphocytes, after presentation of antigens. In the elderly, this metabolic switching is reduced, limiting the effective activation of immune cells. Cells tend to rely more on oxidative metabolism, which is less efficient during rapid immune responses [244]. The accumulation of lipids in older individuals, driven by disruptions in fatty acid oxidation (FAO) despite energy predominantly coming from oxidative pathways, alters immune signalling processes [245,246]. Considering the functional changes in the immune system of older adults and their resulting low response to vaccine a key challenge today is enhancing the efficacy of vaccines to better protect the growing aging population from infectious diseases (ID). The VITAL project (*Vaccines and Infectious Diseases in the Aging Population*), funded by the Innovative Medicines Initiative 2 Joint Undertaking (JU) under grant agreement No. 806776, aims to address this issue. It focuses on evaluating the burden of ID and the mechanisms of immunosenescence, ultimately providing evidence-based insights into vaccination strategies to promote healthy aging (https://vital-imi.eu/about-page/).

This project involves partners from 17 academic and research groups, public institutes and 7 companies, and seeks to improve the efficacy of vaccines to protect the growing elderly population from infectious diseases by developing effective vaccination strategies aimed at establishing healthy aging. However, some of the currently licensed vaccines against major communicable diseases, such as pneumococcal disease, show a diminishing protective effect in the elderly, a phenomenon that could be explained by the deterioration of immunity. Understanding why older adults often exhibit poor or limited responses to vaccines and finding ways to improve these responses. Identifying biological markers that can predict or explain vaccination outcomes is crucial for developing

personalized vaccination strategies, particularly for vulnerable populations like the elderly. This approach can enhance vaccine efficacy and provide tailored protection to those most at risk

4.2 Materials and Methods

4.2.1 Main Cohort

The Vaccines and InfecTious diseases in the Aging popuLation (VITAL) cohort started in 2019 in the Netherlands (September 2019- October 2022) [247]. The purpose of the study was to investigate age-associated changes in immune functioning. At the Department of Chemical, Pharmaceutical and Agricultural Sciences (DOCPAS), the study of immunometaboism was conducted on 43 individuals (median age 68 (25- 98), M= 20, F= 23), who were recruited in the Netherlands and categorized into three age groups: young (25–49 years), middle-aged (50-65 years) and older adults (65–92 years).
Whole blood samples were collected from participants at four time points: at baseline before vaccination (day 0) and 1–2 days, 7 days, and approximately 1 year after receiving the 2019–2021 seasonal quadrivalent inactivated influenza (autumn 2019) vaccine or PCV-13 vaccination (summer/ autumn 2020) or SARS-COV-2 mRNA-1273 vaccine (spring 2021). Samples were collected in EDTA-coated tubes. The metabolic profile of vaccinees was performed at the baseline in respect to PCV13 vaccination, with the aim of identifying factors that could predict/explain the subsequent response pattern.
Participants were excluded if they were using or had used immunomodulatory drugs, or if they had conditions causing immunosuppression, such as organ or bone marrow transplants, high-dose daily corticosteroid use, or chemotherapy within the past 3 years. Additional exclusion criteria included a history of allergic reactions to vaccine components, conditions affecting blood collection (e.g., known anaemia with levels <8.5 mmol/L for men and <7.5 mmol/L for women), known or suspected coagulation disorders, or any factors that could interfere with immunological analyses.
The study was approved by the Medical Research Ethics Committee Utrecht (EudraCT Number: 2019–000836–24) and registered in the Clinical Trials database (Anon Clinical Trials register n.d.). The study followed Good Clinical Practice guidelines and the Declaration of Helsinki, with written informed consent obtained from all participants.

4.2.2 Basal metabolic profiling by Flow Cytometry

To determinate glucose and fatty acids uptake and neutral lipid, PBMCs were incubated in PBS with 2′-(N-(7-nitrobenz-2-oxa-1,3-diazol-4-yl)amino)-2-deoxyglucose (2-NBDG, conc. 50 μM, catalogue no. N13195, Thermo Fisher Scientific), 4,4-difluoro-5,7-dimethyl-4-bora-3a,4a-diaza-*s*-indacene-3-hexadecanoic acid (BODIPY FL C16, conc. 1 μM, catalogue no. D3821, Thermo Fisher Scientific),

4,4-Difluoro-1,3,5,7,8-Pentamethyl-4-Bora-3a,4a-Diaza-s-Indacene (BODIPY™ 493/503, conc. 10 μM, catalogue no. D3922, Thermo Fisher Scientific), respectively, for 20 min at 37°C.

To determinate the mitochondrial mass, cells were incubated with MitoTracker™ Green FM Dye (conc. 50 μM, catalogue no. M46750, Thermo Fisher Scientific), for 30 min at 37°C, while, to determinate the mitochondrial membrane potential (ΔΨM), PBMCs were incubate with tetramethylrhodamine, Methyl Ester- Perchlorate (TMRM (ΔΨM), conc. 25 nM, catalogue no. T668, Thermo Fisher Scientific, non-quenching mode) for 30 min at 37°C. Finally, to quantify the total intracellular ROS study, as a surrogate marker of oxidative stress, cells were incubated for 30 min at 37°C with CellROX^{TM} Green Reagent (conc. 5 μM, catalogue no. C10444, Thermo Fisher Scientific).

4.2.3 SCENITH assay

The SCENITH (Single Cell ENergetIc metabolism by profilIng Translation inHibition) assay was used to analyse the energy metabolism of cells using flow cytometry. Its primary focus is to evaluate how cells generate energy by measuring protein synthesis; this technique relies on using specific inhibitors of metabolic pathways, such as glycolysis and oxidative phosphorylation (OXPHOS), to assess cellular dependencies on these pathways.

PBMCs were plated in a 96-well round bottom plate at 37°C, 5% CO_2 and the assays was performed without or with stimulation with anti-CD3/-CD28 (1ug/ml: 0.5ug/ml) for 24h. The condition in absence of stimulation represented the basal metabolism [248,249]

After 24h, cells were untreated or treated for 15 min at 37°C with only medium (control, CRT), 2-deoxy-glucose (2DG, 100 mM, catalogue no. D6134, Sigma–Aldrich, an inhibitor of glycolysis), oligomycin (O, 1μM, catalogue no. 75351, Sigma–Aldrich, an inhibitor of ATP synthase), CB-839 (AAO, 3μM, catalogue no. 5337170001, Sigma–Aldrich, an inhibitor of amino acids oxidation), Etomoxir (FAO, 4μM, catalogue no. 236020, Sigma–Aldrich, an inhibitor of FAO), and a combination of 2DG and Oligomycin (2-DGO). Following incubation with metabolic inhibitors, cells were treated with Puromycin (final concentration 10ug/ml, catalogue no. P7255, Sigma–Aldrich) for 30 min at 37°C. After puromycin treatment, cells were washed with PBS, labeled with LIVE/DEAD Fixable Aqua (catalogue no. L34966A, Thermo Fisher Scientific) and stained with anti-CD4 phycoerythrin (PE)-Cyanine7 (Cy7) (clone RM4-5, 1:50 dilution, catalogue no. 25-0049-42, Thermo Fisher Scientific), anti-CD8 APC/Fire 750 (clone SK1, 1:50 dilution, catalogue no. 300932, BioLegend), anti-CD27 fluorescein isothiocyanate (FITC) (clone LG.7F9, 1:50 dilution, catalogue no. 11-0271-85, Thermo Fisher Scientific), anti-CD45RA peridinin-chlorophyll-protein (PerCP)-Cyanine5.5 (Cy5.5) (clone HI100, 3:50 dilution, catalogue no. 45-0458-42, Thermo Fisher Scientific), anti-CD154 phycoerythrin (PE) (clone 24-31, 2:50 dilution, catalogue no. 568007, BD

Biosciences), and anti- CXCR5 BV421 (clone RF8B2, 2:50 dilution, catalogue no. 562747, BD Biosciences) antibodies at room temperature for 15 min. After incubation with antibodies, the cells were fixed and permeabilized with Foxp3 intracellular staining kit (catalogue no. 00-5523-00, ThermoFisher Scientific) for 40 min at 4°C. Intracellular staining of puromycin was performed by using 1:100 dilution of anti-puromycin Alexa-Fluor647 antibody (Clone 12D10, catalogue no. MABE343-AF647, Sigma-Aldrich) in kit supplied perm/wash buffer and incubated for 45 min at 4°C. After incubation, the cells were washed and resuspended in PBS. Data were acquired using a FACS Canto II (BD Biosciences), compensated using BD CompBeads (catalog no. 656047, BD Biosciences), and analyzed using FlowJo v.10.8 (FlowJo LLC).

Calculation used to derive SCENITH parameters [250], the geometric mean fluorescent intensity (GeoMFI) of the anti-puromycin Alexa-Fluor647 antibody was measured in each condition, and the following formula were applied:

CRT= GeoMFI of anti-Puro- Alexa-Fluor647 upon Control treatment

2DG = GeoMFI of anti-Puro- Alexa-Fluor647 upon 2DG treatment

O = GeoMFI of anti-Puro- Alexa-Fluor647 upon Oligomycin treatment

AAO= GeoMFI of anti-Puro- Alexa-Fluor647 upon CB-839 treatment

FAO= GeoMFI of anti-Puro- Alexa-Fluor647 upon Etomoxir treatment

2-DGO= GeoMFI of anti-Puro- Alexa-Fluor647 upon 2DG + Oligomycin (DGO) treatment

To calculate the metabolic dependence:

Glucose dependence = 100(CRT – 2-DG)/(CRT– 2-DGO)

Mitochondrial dependence = 100(CRT – O)/(CRT– 2-DGO)

Glutaminolysis dependence = 100(CRT – AAO)/(CRT– 2-DGO)

FAO dependence = 100(CRT – FAO)/ (CRT– 2-DGO)

Glycolytic Capacity = 100 − Mitochondrial dependence

FAAO = 100 − Glucose dependence

Fold induction of protein synthesis = activated control/ basal control

4.2.4 Flow cytometry

For the basal metabolic profiling the PBMCs were stained with anti-CD4 PE-Cy7, anti-CD8 APC/Fire 750, anti-CD19 VioGreen (clone REA675, 1.5:50 dilution, catalogue no. 130-113-649, Miltenyi Biotec), anti-CD27 allophycocyanin (APC) (clone M-T271, 1.5:50 dilution, catalogue no. 130-113-626), anti-CD38 VioBlue (clone REA671, 1.5:50 dilution, catalogue no. 130-123-898, Miltenyi Biotec), and anti-CD45RA peridinin-chlorophyll-protein (PerCP)-Cyanine5.5 (Cy5.5)

(clone HI100, 3:50 dilution, catalogue no. 45-0458-42, ThermoFisher Scientific) at room temperature for 15 min (NL, ROS, and MitoTracker) or at 4°C for 30 min (2-NBDG, FA, and TMRM).

Cells stained with NL and FA probes were fixed with BD Fix Buffer (catalogue no. 554655, BD Biosciences), and then stained with anti-CD45RAPerCP-Cyanine5.5 only. After washing, the PBMCs were resuspended in PBS.

The analysis of the nutrient biomarker expression was performed in a 96-well round bottom plate. For the basal condition, the PBMCs were incubated only with medium: RPMI1640 + 10% fetal calf serum (FBS, EuroClone) + penicillin and streptomycin (1X, EuroClone). For the activated condition, 96-well round bottom was coated with anti-CD3 (1ug/ml) for 5h at 37°C, 5% CO_2; then, PBMCs were stimulated with anti-CD28 (0.5ug/ml) in RPMI1640 + 10% fetal calf serum (FBS, EuroClone) + penicillin and streptomycin (1X, EuroClone). Finally, the PBMCs were incubated for 24h at 37°C, 5% CO2.

Cells were washed and stained with anti-CD4 PE (clone EDU-2, 5:50 dilution, catalogue no. 21278044, ImmunoTools), anti-CD4 PE-Cy7, anti-CD8 APC/Fire 750, anti-CD19, anti-CD27 FITC, anti-CD36 PeCy7 (clone 5-271, 2:50 dilution, catalogue no. 336222, Biolegend), anti-CD38 VioBlue, anti-CD45RA PerCP-Cyanine5.5, anti-CD98 PE (clone, 2:50 dilution, catalogue no. 130-120-137, Miltenyi Biotec), anti-LDL receptor APC (clone 301; 2:50 dilution, catalogue no. ab275614, Abcam), anti-GLUT-1 receptor Alexa Fluor647 (clone 202915, 2:50 dilution, catalogue no. 566580, BD Biosciences) for 15 min at room temperature. Then, cells were washed and resuspended in PBS. Data were acquired using a FACS Canto II (BD Biosciences), compensated using BD CompBeads (catalog no. 656047, BD Biosciences), and analyzed using FlowJo v.10.8 (FlowJo LLC).

4.2.5 Statistical analysis

For the statistical analysis we used the same approaches used in the previous chapters (1, 2.1 and 3). In order to find the optimal cut-off values that would best differentiate between responder and non-responder participants, the receiver operating characteristics (ROC) analyses were carried out. The accuracy was assessed using the values for the sensitivity and specificity [251]. A sensitivity rate of 100% would mean that all patients response to the vaccine would be correctly classified as "responders". A specificity rate of 100% would mean that all non-responder persons would be classified by the test as non-responders [252]. The AUC values were calculated for LDL-r or LDL-r^+CD98^+ in total $CD4^+$ T cells (basal) or naïve $CD4^+$ T cells (basal and post-activation).

4.3 Results

4.3.1 Characterization of basal metabolism and expression of nutrient markers in T cells from subjects of different age groups

To predict the responsiveness to PCV13 vaccination and to discover possible differences between young and older adults, we studied the basal metabolism of PBMCs collected pre-vaccination in respect to anti-pneumococcal vaccine (day 0), and we focused on cellular metabolism of naïve $CD4^+$ and $CD8^+$ T cells as this vaccine was administered to study subjects for the first time, thus most likely inducing response from naïve precursors.

Participants were stratified by age in two groups: young (YA, median= 36 years old, range 25-39) and old (OA, median= 79 years old, range 70- 90) participants.

We first analysed the mitochondrial profile, measuring the mitochondrial mass, mitochondrial membrane potential (MMP, $\Delta\Psi m$) and the production of ROS. The two groups (YA versus OA) show similar levels of ROS and mitochondrial mass, but significantly differed for the $\Delta\Psi m$, which was higher in older adults [Figure 4.3.1.1 (A)]. This characteristic is a classical manifestation of immunosenescence, that reflect compensatory mechanisms rather than a baseline increase in MMP across aging population [253]. No differences were found in respect to nutrient uptake, such as FA and glucose, or neutral lipid content, between the two groups.

Simultaneously, we analysed the expression of some nutrient markers, like LDL-receptor, amino acid receptor (CD98), CD36 (important for the oxidation of long-chain fatty acid), and GLUT-1 (glucose receptors), in basal and post-activation (coated anti-CD3) conditions [Figure 4.3.1.1 (B)]. We observed a lower expression of amino acid receptor, post-activation, in naïve $CD4^+$ and $CD8^+$ T cells in older adults, and this aspect was observed also for the expression of GLUT-1, post-activation. Consistently, $\Delta\Psi m$ of both naïve $CD4^+$ and $CD8^+$ T cells was significantly directly corelated with age, while CD98 showed an inverse correlation [Figure 4.3.1.1 (B)]. Moreover, GLUT-1 also displayed a tendency toward negative correlation with age in naïve $CD4^+$ T cells.

In summary, we observed different changes with aging in older adults of VITAL cohort. Firstly, there was a difference in MMP, which was higher in older individuals, suggesting an altered mitochondrial bioenergetic metabolism. In addition, a decrease in CD98 and GLUT-1 (only on naïve $CD4^+$ T cells) expression was observed in activated metabolism in elderly group. These metabolic differences suggest a shift towards altered mitochondrial bioenergetics and metabolic reprogramming, often linked with immunosenescence [254].

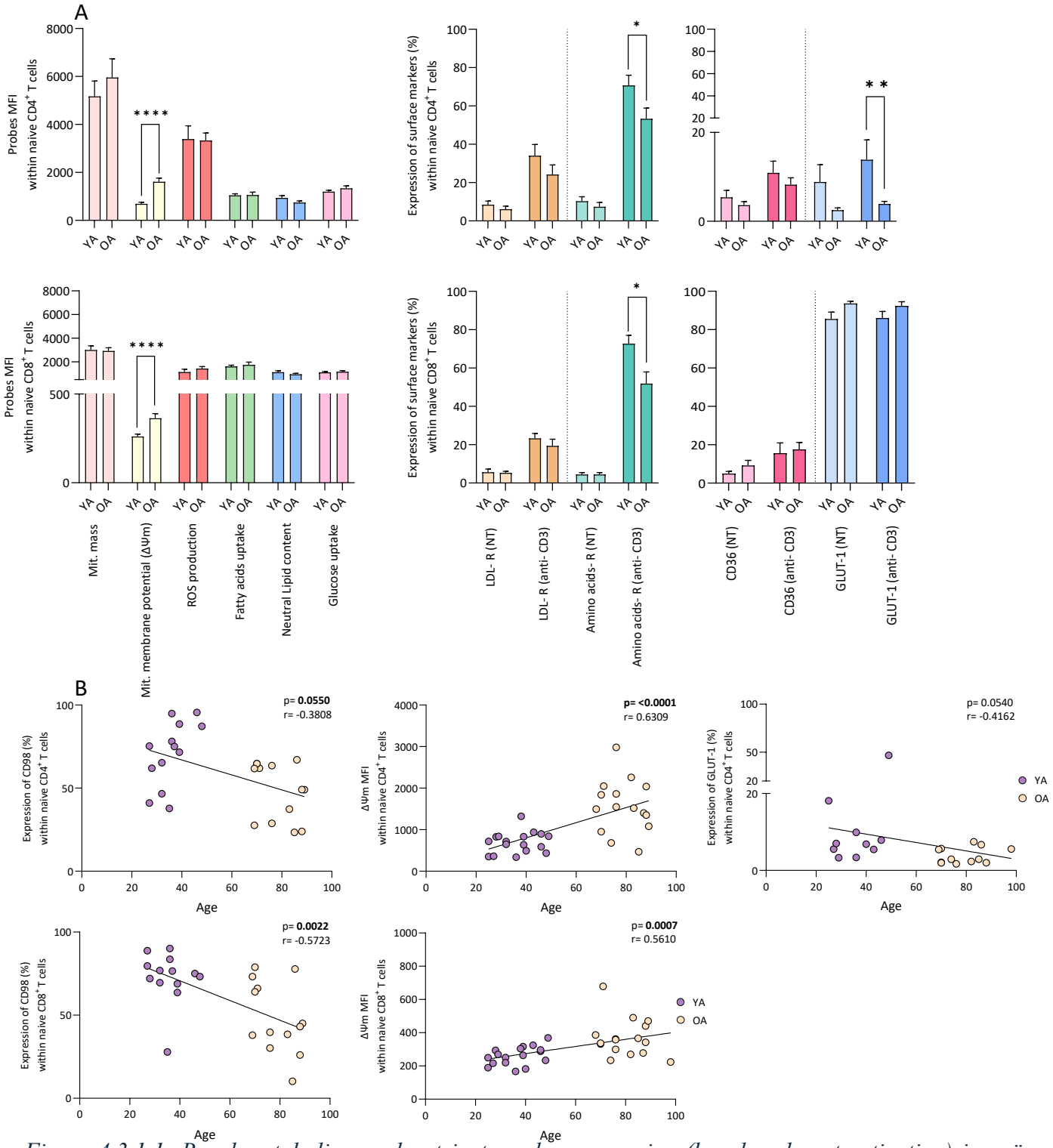


*Figure 4.3.1.1: Basal metabolism and nutrient marker expression (basal and post-activation) in naïve CD4$^+$ and CD8$^+$ T cells as a function of age. (**A**) Mitochondrial status (mitochondrial mass (YA= 13; OA= 14), ΔΨm (YA= 17; OA= 17), and ROS production (YA= 11; OA= 11)), nutrient uptake (fatty acids (YA= 10; OA= 12) and glucose (YA= 10; OA= 12)), neutral lipid content, expression of LDL-r (YA= 13; OA= 15), amino acid receptors (YA= 13, OA= 15), CD36 (YA= 11; OA= 12) and GLUT-1 (YA=11; OA= 12) basal and post-activation with coated anti-CD3 for 24h were measured by flow cytometry and reported as MFI (for probe staining) or as % or marker expression in naïve CD4$^+$ (top) and CD8$^+$ (bottom) T cells. (**B**) Correlation between the indicated measures and age in naïve CD4$^+$ (top) and CD8$^+$ (bottom) T cells. Data are shown as median + SEM and statistical significance was determined by Mann-Whitney test (**A**). To determine correlations, Spearman's rank test was used (**B**). Spearman's R and p values are shown for each panel. *P<0.05, **P < 0.01, ***P < 0.001, ****P< 0.0001.*

4.3.2 Young and old adults vaccinated with PCV13 vaccine show similar cellular responses

Vaccine-specific cellular responses were longitudinally monitored in study subjects at day 0, 7, 28 and at 6 months after PCV13 vaccination via ELISpot[1], assessing the reactivity against the vaccine carrier (CRM197, mutated diphtheria toxin), and results were shown after stratification by age group. A similar magnitude of response between YA and OA for the 4 timepoints was observed [Figure 4.3.2.1 (A)]. The participants were thus stratified as responders (>20 SFC/4x10^5 cells) and non-responders (<10 SFC/4x10^5 cells), based on data collected at day 7, corresponding to the response peak. However, mean response intensity was comparable between YA and OA among the responder groups, and the same was observed in non-responders, suggesting the age was not implicate in the responsiveness of PCV13 vaccine [Figure 4.3.2.1 (B)].

As we previously identified some age-specific metabolic pattern (see paragraph 4.3.1), we wanted to investigate whether the same difference previously observed between YA and OA highlighted in the whole cohort were still evident after segregation between responders and non-responders. In fact, $\Delta\Psi m$ was consistently higher in naïve $CD4^+$ and $CD8^+$ T cells of OA in both responders and non-responders [Figure 4.3.2.1 (C)]. CD98 and GLUT-1 were generally higher in naïve T cells from YA in both responder and non-responder subgroups, although not always reaching the threshold for statistical significance [Figure 4.3.2.1 (D, E)].

These data suggest that, despite the age-related differences observed at metabolic levels, the magnitude of the PCV13 vaccine cellular response is not affected by age.

[1] Experiments performed in collaboration with the research group of Prof. Birgit Weinberger, University of Innsbruck, Institute for Biomedical Aging Research, Innsbruck, Austria.

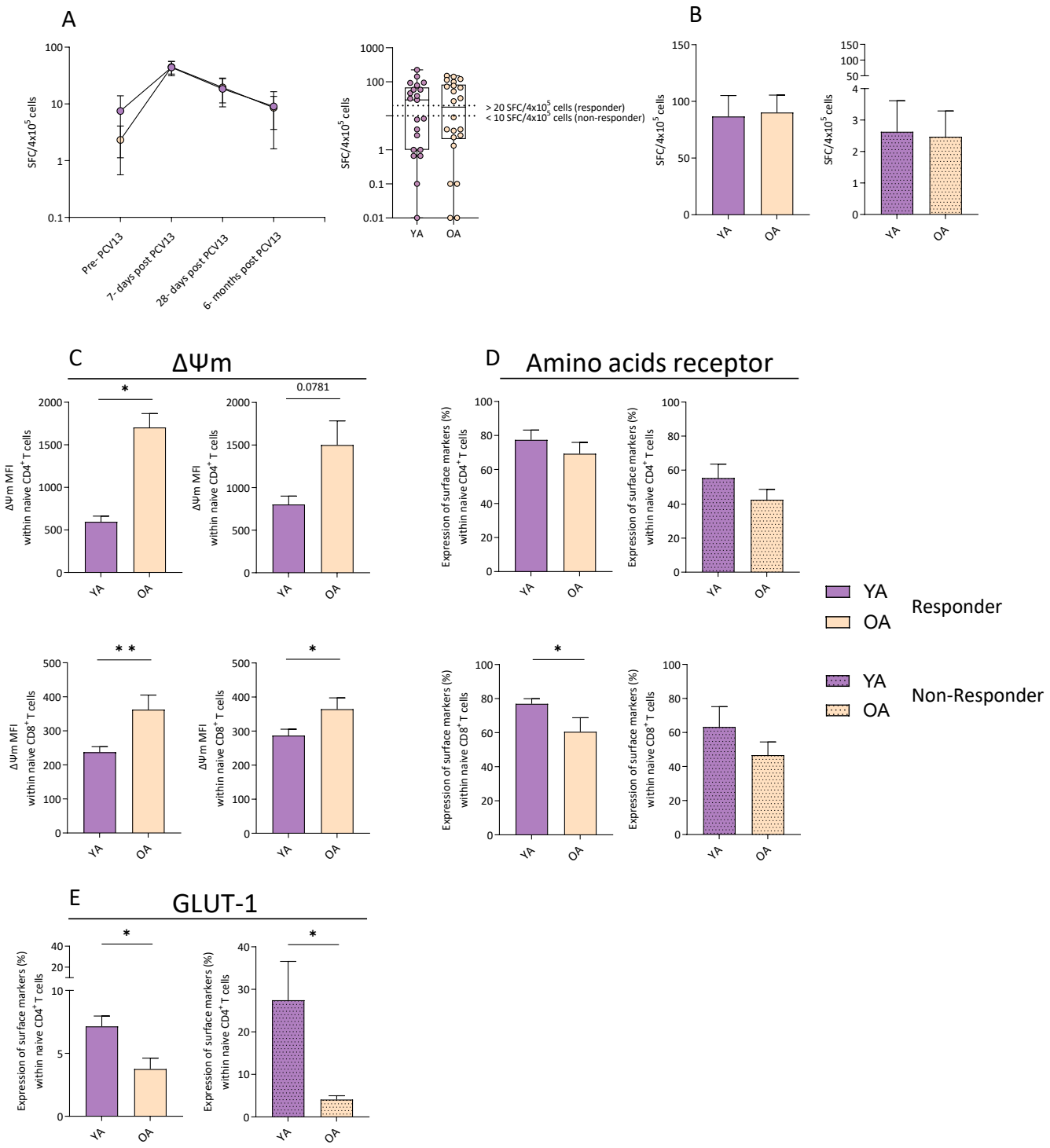


*Figure 4.3.2.1: Longitudinal study of cellular response to PCV13 vaccination. (**A**) PBMCs of participants were tested in ELISpot against the CRM197, mutated diphtheria toxin, at d0, d7, d28, and 6 months post-vaccination, and the spot-forming-cells (SFC) was reported in the panel. (**B**) The young (n= 21) and older (n= 22) participants were stratified in responder (R) and non-responder (NR) adults, considering the responses to CRM197 at day 7 post-vaccination. (**C, D, E**) The stratification YA- OA responder (R) and non- responder (NR) was performed to observe difference in MMP (ΔΨm, YA-R= 9, OA-R= 9; YA-NR= 8, OA-NR= 8), in expression of amino acid (YA-R= 9, OA-R= 6; YA-NR= 4, OA-NR= 9, and GLUT-1 receptors (YA-R= 5, OA-R= 7; YA-NR= 4, OA-NR= 5) in naïve $CD4^+$ (top) and $CD8^+$ (bottom) T cells. Data are shown as median + SEM. The dotted line represented the response threshold in ELISpot (>20 SFC/ 4 X 10^5 cells or <10 SFC/ 4 X 10^5 cells) and statistical significance was determined by Mann-Whitney test (**A, B, C, D, E**). *P<0.05, **P < 0.01.*

4.3.3 Basal metabolic properties of naïve T cells from responder and non-responder groups

To understand whether baseline metabolic features of naïve T cells can biologically explain the segregation of donors into responders (R, ELISpot responses > 20 SFC/4 X 10^5 cells at day 7) and non-responders (NR, ELISpot responses <10 SFC/4 X 10^5 cells at day 7), the bioenergetic profile of both naïve $CD4^+$ and $CD8^+$ T cells from study subjects was assessed at baseline (irrespective to the donor age). Overall, naïve T cells from the two study groups showed similar mitochondrial status, uptake of fatty acids and glucose, and neutral lipid content [Figure 4.3.3.1 (A)], further to comparable levels of both CD36 and GLUT-1 expression both at rest and upon activation with anti-CD3 [Figure 4.3.3.1 (B)]. Conversely, the expression of LDL-r and amino acid receptors (either basal and post-activation) was significantly in R participants [Figure 4.3.3.1 (C)]. The same was confirmed when looking at LDL-r^+CD98^+ double positive naïve $CD4^+$ and $CD8^+$ T cells [Figure 4.3.3.1 (C)]. Consistently, the expression of these two receptors was positively correlated with ELISpot responses [Table 4.3.3.1]. These data suggest that the expression of LDL-r and CD98 prior to vaccination could confer biological advantages to mount higher vaccine-specific cellular responses.

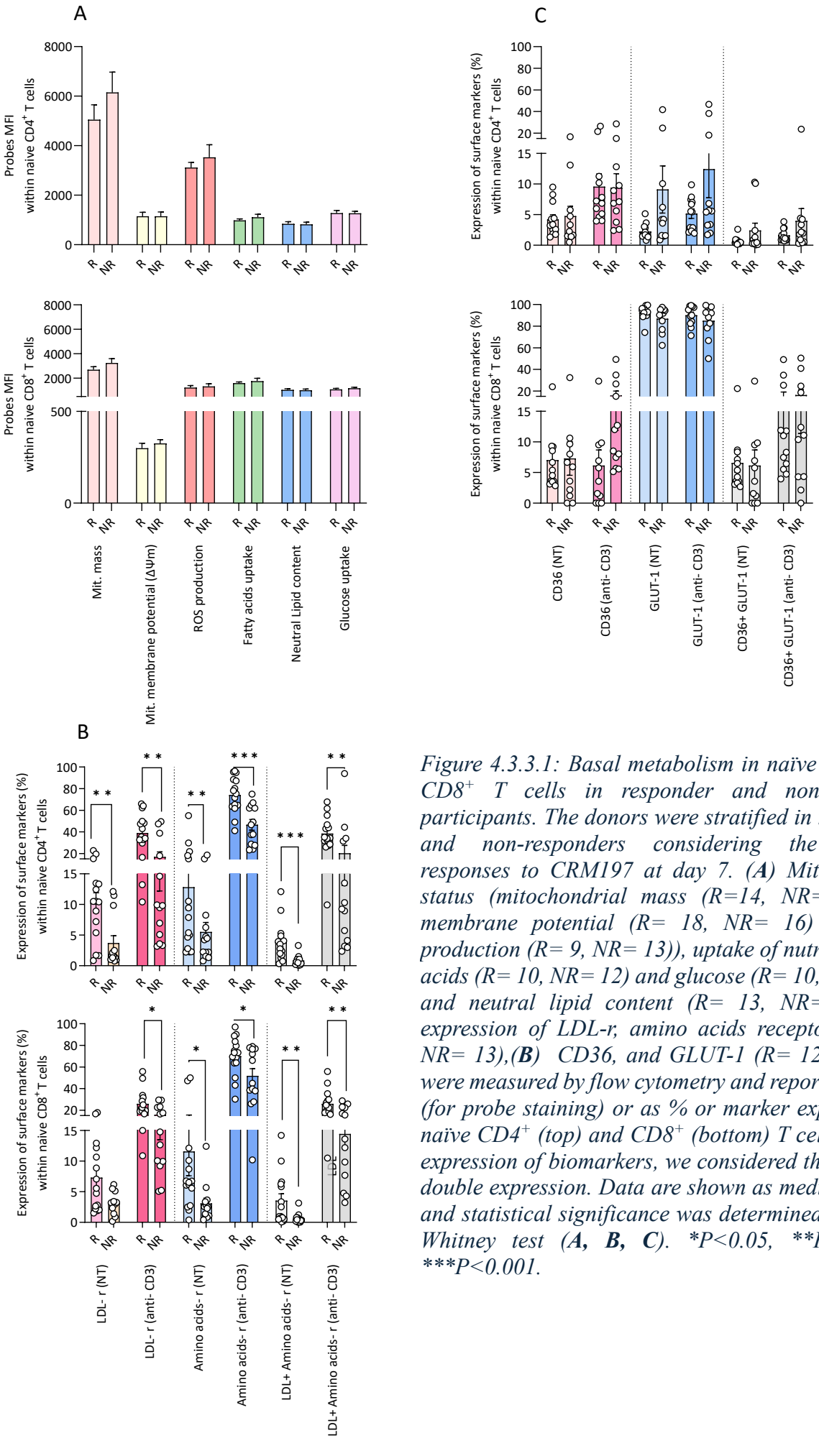


*Figure 4.3.3.1: Basal metabolism in naïve CD4⁺ and CD8⁺ T cells in responder and non-responder participants. The donors were stratified in responders and non-responders considering the ELISpot responses to CRM197 at day 7. (**A**) Mitochondrial status (mitochondrial mass (R=14, NR= 13) and membrane potential (R= 18, NR= 16) and ROS production (R= 9, NR= 13)), uptake of nutrients (fatty acids (R= 10, NR= 12) and glucose (R= 10, NR= 12)), and neutral lipid content (R= 13, NR= 13), (**C**) expression of LDL-r, amino acids receptors (R=15, NR= 13),(**B**) CD36, and GLUT-1 (R= 12, NR= 12) were measured by flow cytometry and reported as MFI (for probe staining) or as % or marker expression in naïve CD4⁺ (top) and CD8⁺ (bottom) T cells. For the expression of biomarkers, we considered the single or double expression. Data are shown as median + SEM and statistical significance was determined by Mann-Whitney test (**A, B, C**). *P<0.05, **P < 0.01, ***P<0.001.*

*Table 4.3.3.1: Correlation between ELISpot responses to CRM197 at day 7, basal metabolism (mitochondrial status, uptake of nutrients, and neutral lipids content), nutrient surface markers (basal or post-activation). For the correlation, Spearman's rank correlation was used, and the significatively was reported in bold. *P<0.05, **P < 0.01, ***P < 0.001.*

		CD4 N	CD8 N
BASAL METABOLISM	Mitochondrial mass	**-0.4301***	**-0.5016****
	Mitochondrial membrane potential	-0.05819	-0.1367
	ROS	-0.3009	-0.1001
	FA uptake	0.1317	0.2809
	Lipids store	-0.03139	0.01579
	Glucose uptake	0.01781	-0.234
NUTRIENT SURFECE MARKERS	LDL-r (NT)	0.3508	**0.4636***
	AA- r (NT)	**0.503****	**0.5412****
	LDL-r+ AA- r (NT)	**0.5011****	**0.6188*****
	CD36 (NT)	0.1419	0.1231
	GLUT-1 (NT)	-0.3396	0.2318
	CD36+ GLUT-1 (NT)	-0.07763	0.2622
	LDL-r (anti-CD3)	**0.4914****	0.2203
	AA- r (anti- CD3)	**0.4037***	0.3249
	LDL-r+ AA- r (anti- CD3)	0.3551	**0.3837***
	CD36 (anti- CD3)	-0.1315	-0.01384
	GLUT-1 (anti- CD3)	-0.3356	0.2496
	CD36+ GLUT-1 (anti- CD3)	-0.3038	0.009392

4.3.4 Increased protein synthesis and metabolic shift characterizes naïve T cells from responders

To better characterize the metabolic profile of naïve $CD4^+$ and $CD8^+$ T cells prior to vaccination, we measured the metabolic shift (i.e. the change in metabolic properties occurring after T cell activation), including protein synthesis, glycolytic and oxidative capacity, as well as basal and post-activation dependencies on glucose, mitochondrial activity, amino acids oxidation, and fatty acids oxidation, in R and NR participants. These studies were performed through the Single-cell Energetic Metabolism by Profiling Translation Inhibition (SCENITH) [248]. The SCENITH assay is a method used to analyse the metabolic activity of individual cells by assessing their protein synthesis rates under various metabolic conditions; the assay measures protein synthesis using a puromycin-based approach and inhibitors, which affect different metabolic pathways. Naïve $CD4^+$ T cells from subjects of the two study groups showed no differences at the level of basal protein synthesis, while R presented with significantly higher protein synthesis upon activation [Figure 4.3.4.1 (A)]. A similar trend was observed for naïve $CD8^+$ T cells [Figure 4.3.4.1 (B)]. Consistently, the fold protein synthesis (i.e. the increase of metabolic rate upon activation) was significantly higher in responder-participants for both naïve $CD4^+$ and $CD8^+$ T cells [Figure 4.3.4.1 (C)].

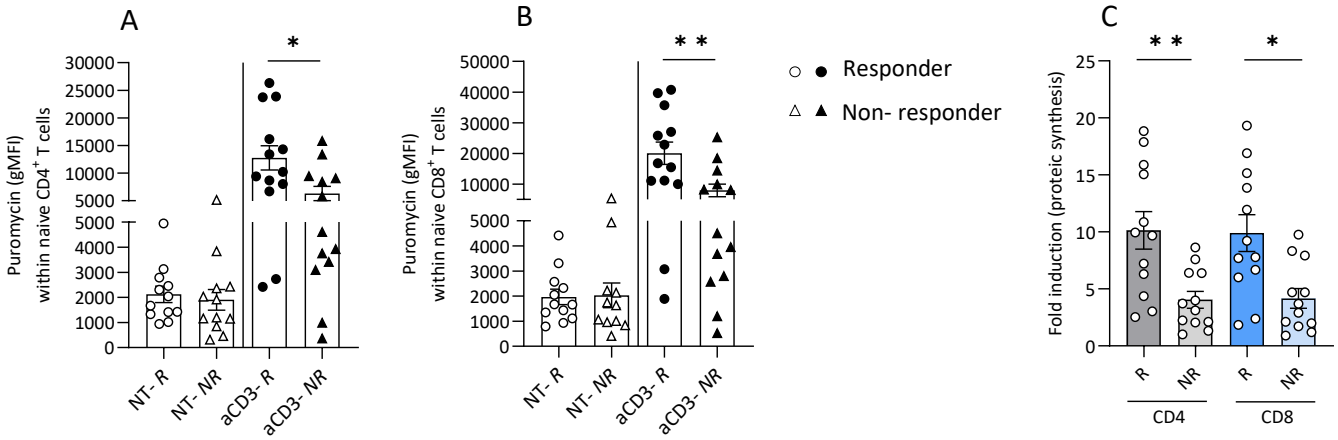


*Figure 4.3.4.1: Protein synthesis in naïve $CD4^+$ and $CD8^+$ T cells via SCENITH. (**A, B**) The pre-vaccination PBMCs were cultured with only medium or with coated anti-CD3 and soluble anti-CD28 for 24h, to study the basal (R= 12, NR= 12) and activated (R= 13, NR= 13) protein synthesis in naïve $CD4^+$ and $CD8^+$ T cells. (**C**) The fold induction of protein synthesis was calculated considering basal and post-activated protein synthesis. Data are shown as median + SEM and statistical significance was determined by Mann-Whitney test (**A, B, C**). *P<0.05, **P < 0.01.*

The four metabolic dependencies (glucose, mitochondrial, amino acids (AAO) and fatty acids oxidation (FAO)) were similar between responders and non-responders in resting naïve $CD4^+$ T cells [Figure 4.3.4.2 (A)]. However, upon activation, glucose dependence was higher in the responder group compared to the non-responder group, highlighting a noticeable metabolic shift between glucose dependence and mitochondrial dependence. In non-responder participants, this metabolic

shift between glycolytic and oxidative metabolism was absent; instead, their metabolic dependencies on the two pathways remained unchanged. This observation was further confirmed by analysing glycolytic and fatty acid-amino acids oxidation (FAAO). In responders, the metabolic capacity shift was evident, with a post-activation drop in oxidative capacity that approached statistical significance ($p = 0.0770$) [Figure 4.3.4.2 (B)]

For naïve $CD8^+$ T cells, glucose and mitochondrial basal dependencies were similar between groups, and this was also observed upon activation. However, no conclusions could be drawn for the other two dependencies (amino acids oxidation (AAO) and fatty acids oxidation (FAO)) due to the low sample size [Figure 4.3.4.3 (A)]. Interestingly, R exhibited higher glucose basal capacity, but this difference disappeared when considering the metabolic shift (from basal to activated metabolism), where the two groups showed a similar behaviour [Figure 4.3.4.3 (B)].

Together these data indicate a superior metabolic shift upon activation in naïve T cells from responders, and in particularly in the $CD4^+$ compartment which seemed mor efficient in using glycolysis to fuel the energetic requirements dictated by TCR-mediated activation.

These findings also suggest that the differences observed in activated metabolism between R and NR—particularly in dependence and metabolic shifts—are more pronounced in naïve $CD4^+$ lymphocytes than in naïve $CD8^+$ lymphocytes. This aligns with the idea that the response observed in ELISpot was likely CD4-dependent, as the response to an internal protein like CRM197 typically generates CD4-driven responses [255,256].

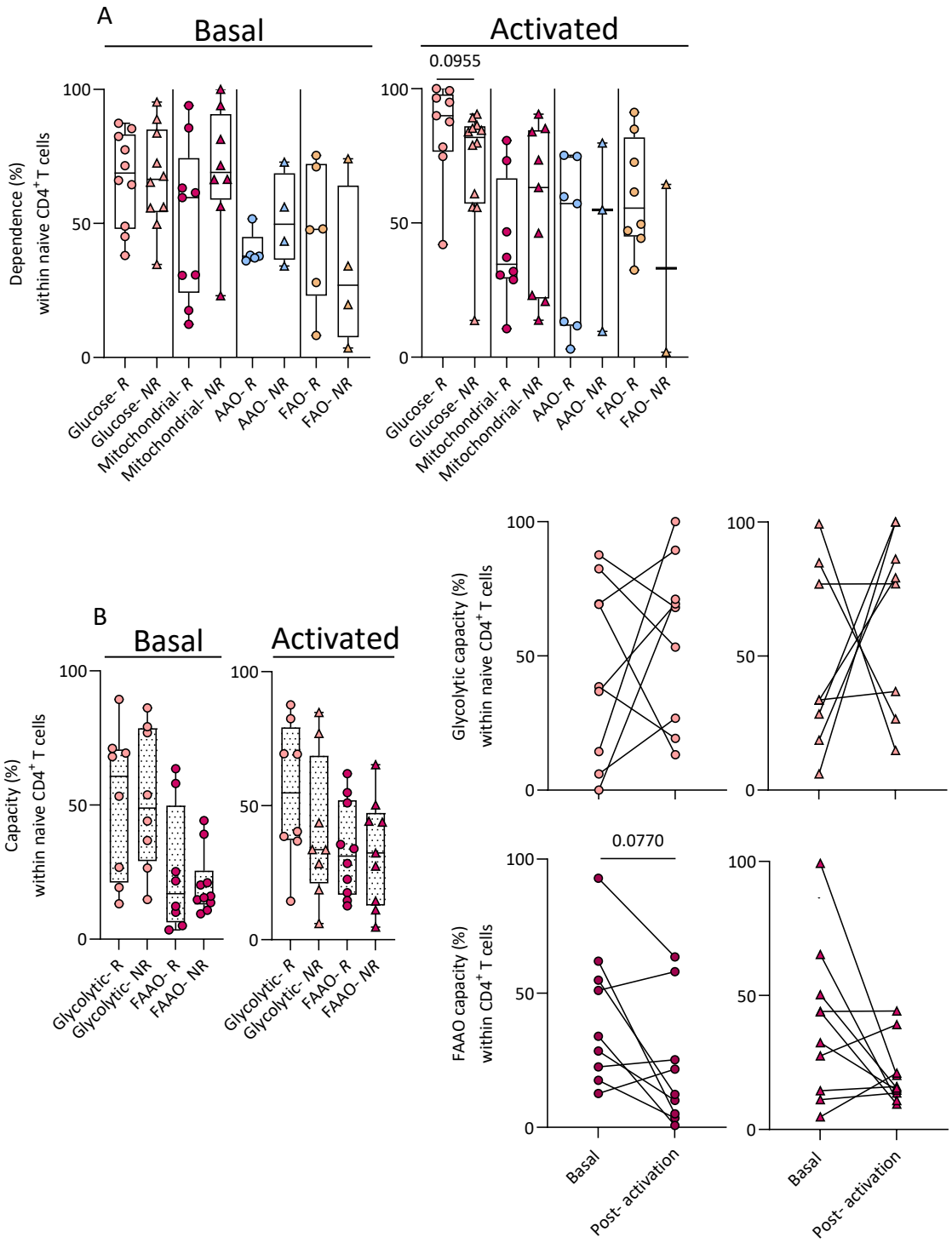


*Figure 4.3.4.2: Metabolic dependences and capacity in naïve CD4⁺ T cells. The PBMCs were cultured in presence or absence of inhibitors molecules (2-DG, Oligomycin, CB839, and Etomoxir), for 24h, to obtain (**A**) metabolic dependences (glucose, mitochondrial, amino acids and fatty acids oxidation) and (**B**) capacity (glycolytic and fatty acids- amino acids oxidation) in naïve CD4⁺ T cells in basal and post-activation, with coated anti-CD3 and anti-CD28. Data are shown as median and statistical significance was determined by Mann-Whitney test and Wilcoxon signed rank test (**A, B**).*

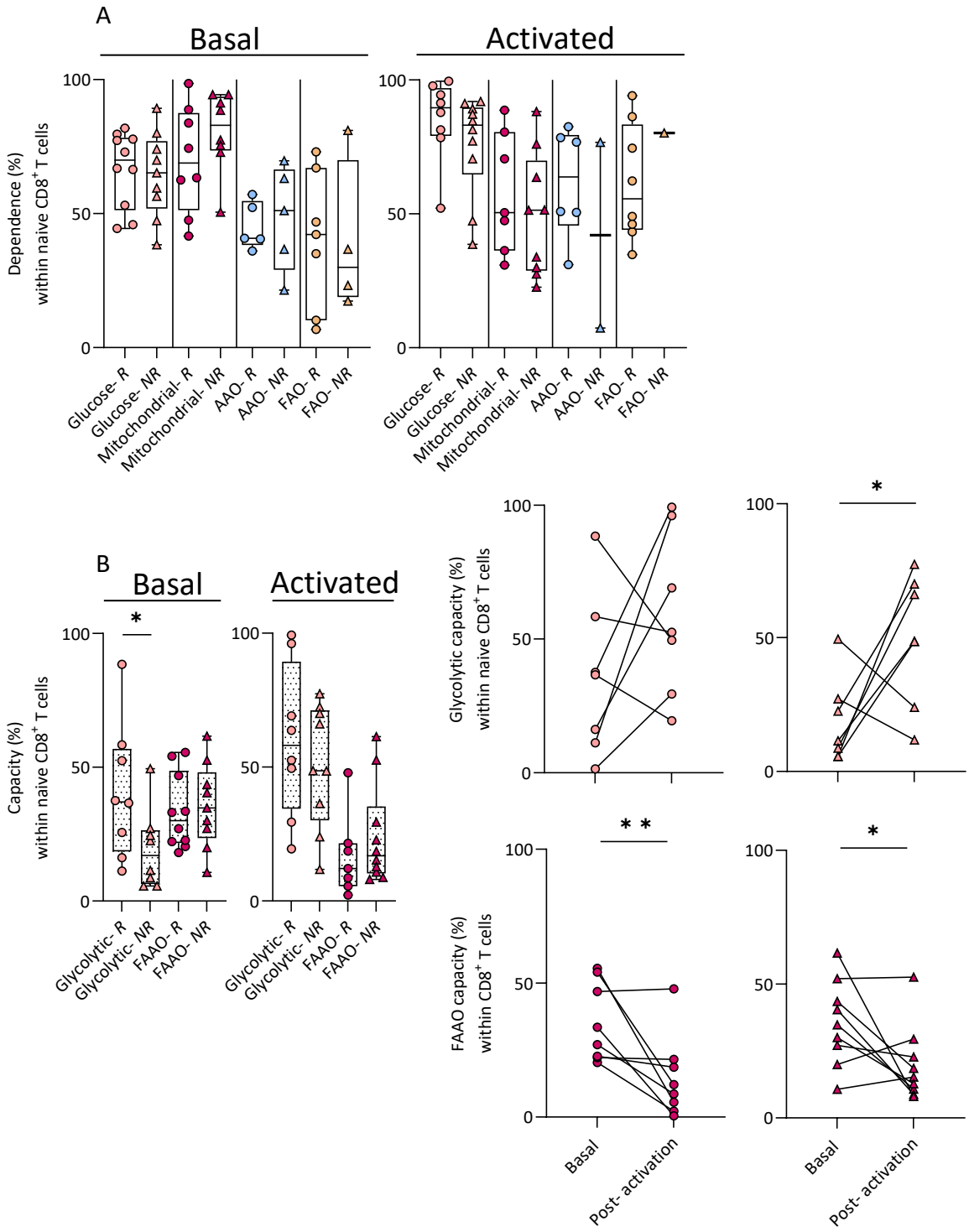


*Figure 4.3.4.3: Metabolic dependences and capacity in naïve CD8⁺ T cells. The PBMCs were cultured in presence or absence of inhibitors molecules (2-DG, Oligomycin, CB839, and Etomoxir), for 24h, to obtain (**A**) metabolic dependences (glucose, mitochondrial, amino acids and fatty acids oxidation) and (**B**) capacity (glycolytic and fatty acids- amino acids oxidation) in naïve CD8⁺ T cells in basal and post-activation with anti-CD3 and anti-CD28. Data are shown as median and statistical significance was determined by Mann-Whitney test and Wilcoxon signed rank test (**A, B**). *P<0.05, **P < 0.01.*

4.3.5 The expression of nutrient receptors confers metabolic advantages to naïve T cells of responder donors

We next evaluated potential correlations between the T cell metabolic fitness, measured through SCENITH, with basal metabolic properties such as nutrient uptake and storage, mitochondrial functionality and receptor expression [Table 4.3.5.1]. Interestingly, we observed a positive correlation between basal and post-activation metabolic activity and the expression of nutrient markers, such as LDL-r (both basal and activated) and LDL-r combined with amino acid receptors (both basal and activated), highlighting a strong interconnection between these parameters. Specifically, as protein synthesis increases, so does the expression of these receptors. As previously noted, both LDL-r and CD98 expression in $CD4^+$ naïve cells, as well as protein synthesis (post-activation and fold induction), are overexpressed in the responder group. This underscores that, in the activated state, $CD4^+$ naïve cells exhibit greater metabolic activity, supporting critical processes such as activation, proliferation, and clonal expansion. The behaviour of $CD8^+$ naïve lymphocytes, while similar in some respects, shows a distinct pattern. In this case, basal and post-activation metabolic activity does not significantly correlate with LDL-r and CD98 expression but instead correlate with CD36 and GLUT-1 expression. Although no differences in CD36 and GLUT-1 expression were observed between responders and non-responders, these two receptors were found to correlate with metabolic activity specifically in $CD8^+$ naïve individuals.

*Table 4.3.5.1: Correlation between SCENITH data (basal metabolic activity, metabolic activity upon activation, and fold induction of protein synthesis), basal metabolism and expression of nutrient surface markers (basal (NT) and post-activation (anti-CD3)). For the correlation, Spearman's rank correlation was used, and the significatively was reported in bold. *P<0.05, **P < 0.01.*

		Basal metabolic activity		Metabolic activity upon activation		Fold induction (protein synthesis)	
		CD4 N	**CD8 N**	**CD4 N**	**CD8 N**	**CD4 N**	**CD8 N**
BASAL METABOLISM	Mitochondrial mass	-0.03316	-0.1316	-0.1744	-0.1654	-0.107	-0.1333
	ΔΨm	-0.1649	-0.02079	-0.09994	-0.1389	0.07662	-0.1065
	ROS	-0.1	-03286	-0.06765	-0.2676	-0.01786	-0.06786
	FA uptake	0.1868	0.2879	-0.1286	-0.03929	-0.3714	-0.3714
	Lipids store	-0.3432	-0.1232	-0.2464	-0.1232	-0.2244	-0.2024
	Glucose uptake	-0.2	-0.2118	-0.04537	-0.1152	-0.01471	-0.1912
NUTRIENT SURFECE MARKERS	LDL-r (NT)	0.2264	-0.02747	**0.2735***	0.2879	0.3821	0.478
	AA- r (NT)	0.389	-0.2357	0.5706*	0.04118	**0.5536***	0.2393
	LDL-r+ AA- r (NT)	0.367	-0.08929	**0.5206***	0.1029	**0.6607****	0.3179
	CD36 (NT)	0.2967	0.4272	0.3588	**0.652****	0.3214	**0.7328****
	GLUT-1 (NT)	0.1385	0.1679	-0.1265	0.02941	-0.2857	-0.03214
	CD36+ GLUT-1 (NT)	0.3187	0.4	0.2147	**0.6265***	0.1214	**0.7071****
	LDL-r (anti-CD3)	0.367	0.2071	0.3618	0.3353	**0.5607***	0.3571
	AA- r (anti- CD3)	0.1648	-0.03571	0.4091	0.2412	0.4111	0.2679
	LDL-r+ AA- r (anti- CD3)	0.3495	0.2198	**0.5029***	0.4827	**0.6***	0.4897
	CD36 (anti- CD3)	0.09011	0.4679	0.2206	**0.5853***	0.1607	0.4821
	GLUT-1 (anti- CD3)	0.1692	0	0.02353	0.2588	-0.125	0.35
	CD36+ GLUT-1 (anti-CD3)	-0.06813	0.4179	0.03824	**0.5088***	0.003571	0.4357

4.3.6 Naïve T cell metabolic properties are associated with systemic immune system, age-related, features

We next wondered whether T cell specific metabolic features were linked by association with systemic immune system parameters. We first focused on immune entropy[2], defined as a measure to quantify cumulative perturbations (e.g. CMV infection and numbers of reactivation and comorbidities) in the immune cell subset network [Table 4.3.6.1 (a, b)]. Correlations between immune entropy and metabolic data were generally sparse and statistically significant in few cases.

[2] Analysis performed in collaboration with the research group of Prof. Debbie van Baarle, University of Groningen, Faculty of Medicine, Transitional Immunology, Groningen, The Netherlands.

However, we observed few correlations in respect to some measures distinguishing responders and non-responders (such as metabolic activity in activated T cells). Therefore, although immune entropy levels are significantly higher in NR, we could not find direct associations between this measure and metabolic perturbations predicting low vaccine responsiveness [Figure 4.3.6.1 (A)].

*Table 4.3.6.1: Correlation between immune entropy, (**a**) basal metabolism (mitochondrial status, uptake of nutrients, and neutral lipids content), nutrient surface markers (basal (NT) and post-activation (anti-CD3)), (**b**) protein synthesis, dependences and capacities, and fold induction of protein synthesis (basal and post-activation) (**b**). For the correlation, Spearman's rank correlation was used. Spearman's R and p values are shown in the panel. *P<0.05, **P < 0.01 and the significatively was reported in bold.*

a		CD4 N	CD8 N
BASAL METABOLISM	Mitochondrial mass	-0.08692	-0.04
	ΔΨm	**0.3526***	**0.4445***
	ROS	0.08571	-0.00752
	FA uptake	-0.2466	-0.2481
	Lipids store	-0.2035	-0.08771
	Glucose uptake	-0.1684	0.07669
NUTRIENT SURFECE MARKERS	LDL-r (NT)	0.04884	0.1231
	AA- r (NT)	-0.09646	**-0.3767 (0.0528)**
	LDL-r+ AA- r (NT)	-0.00366	-0.2308
	CD36 (NT)	0.1247	0.1819
	GLUT-1 (NT)	0.187	-0.387
	CD36+ GLUT-1 (NT)	**0.4424***	0.2118
	LDL-r (anti-CD3)	-0.1502	-0.2308
	AA- r (anti- CD3)	-0.1994	-0.2781
	LDL-r+ AA- r (anti- CD3)	-0.03236	-0.2082
	CD36 (anti- CD3)	0.2688	0.2584
	GLUT-1 (anti- CD3)	0.1519	-0.1299
	CD36+ GLUT-1 (anti- CD3)	0.3469	0.213

b		CD4 N	CD8 N
BASAL METABOLIC ACTIVITY	Control	0.07556	0.0359
	Glucose dependence	-0.413 (0.06)	-0.03377
	MithocondriaL dependence	-0.3439	-0.08772
	AAO dependence	0.1868	-0.04176
	FAAO dependence	-0.08392	-0.04196
	Glycolytic capacity	0.3439	0.08772
	FAAO capacity	0.413 (0.06)	0.02208
	Fold of protein synthesis	0**.4862***	0.1468
METABOLIC ACTIVITY UPON ACTIVATION	Control	**0.4496***	**0.4414***
	Glucose dependence	0.05237	-0.09881
	Mithocondrial dependence	-0.1675	-0.1857
	AAO dependence	-0.03736	-0.1385
	FAAO dependence	0.4126	0.5035
	Glycolytic capacity	0.1675	0.05714
	FAAO capacity	-0.05237	0.09881

Instead, age-associated metabolic perturbations such as ΔΨm in both naïve $CD8^+$ and $CD4^+$ T cells were significantly positively correlated with entropy. Most likely, this phenomenon is influenced by age as can be appreciated from the Figure 4.3.6.1 (B); in fact, as age increases, the cumulative perturbations in the immune cell subset network increases.

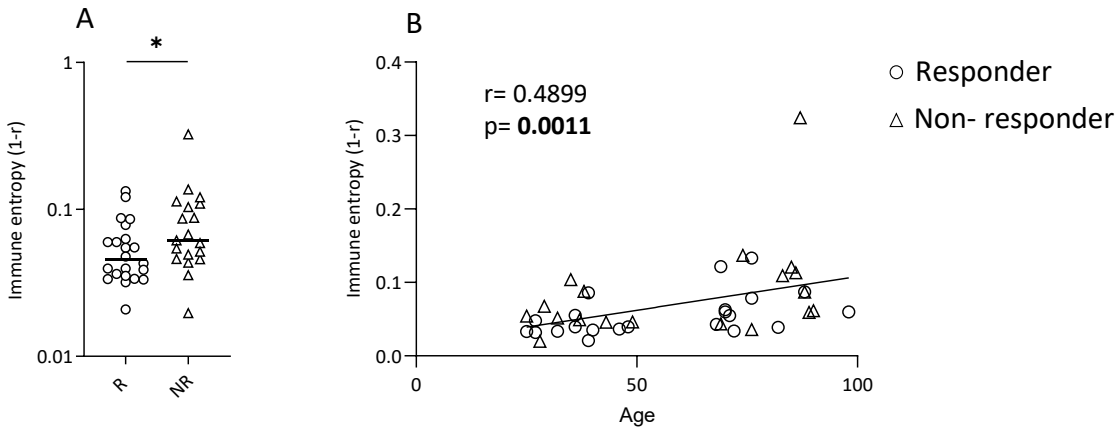


*Figure 4.3.6.1: Immune entropy in responders and non-responders' participants. (**A**) The responders (n= 22) and non-responders (n= 19) participants were stratified by entropy: cumulative perturbations in the immune cell subset network. (**B**) The entropy of two groups was correlated with age. The horizontal lines represent the median values (**A**). The statistical analyses between R and NR were determined by Mann-Whitney test (**A**) and the correlation was assessed using a two-sided Spearman's rank test and was reported in the panel (**B**). *P < 0.05.*

A further aspect related to imunosenescence, is the frailty index[3] [Figure 4.3.6.2 (A, B)], which is a widely used tool in geriatrics to measure frailty [257,258]. Frailty is a state of increased vulnerability to stressors due to a decline in physiological reserves and functions. The index helps predict adverse health outcomes such as falls, hospitalizations, disability and mortality in older adults.

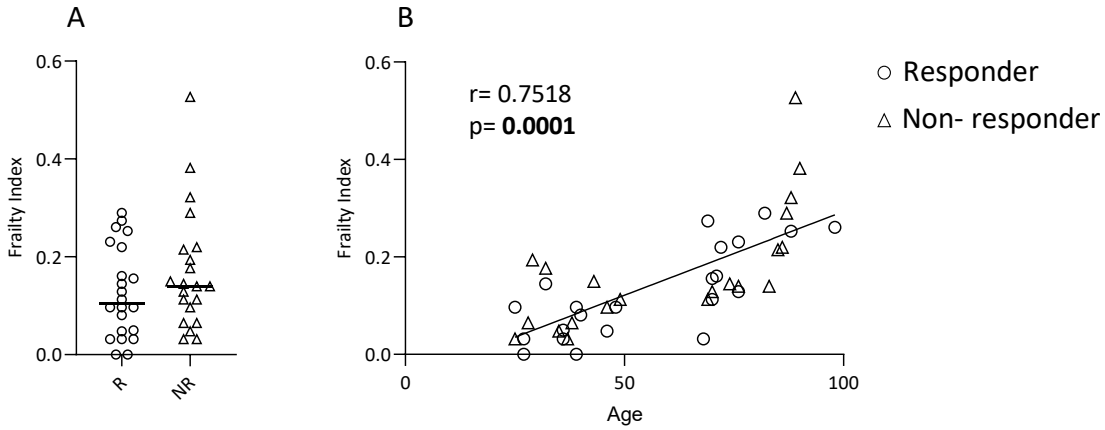


*Figure 4.3.6.2: Frailty Index in responders and non-responders' participants. (**A**) The responders (n= 22) and non-responders (n= 11) participants were stratified by frailty index, a composite score based on deficit accumulation. (**B**) The frailty index of two groups was correlated with age. The horizontal lines represent the median values (**A**) and the o. The statistical analyses between R and NR were determined by Mann-Whitney test (**A**) and the correlation was assessed using a two-sided Spearman's rank test and was reported in the panel (**B**).*

[3] Analysis performed in collaboration with the research group of Prof. Debbie van Baarle, University of Groningen, Faculty of Medicine, Transitional Immunology, Groningen, The Netherlands.

A significant and positive correlation with the ΔΨm is observed [Table 4.3.6.2 (a, b)]. Moreover, we also observed significant negative correlations with the expression of some surface markers associated with both aging (e.g. GLUT-1 in activated cells) and non-responsiveness (CD98 and LDL-r), despite the frailty index was not significantly different between R and NR index [Figure 4.3.6.2 (A)]. Instead, consistently with the positive association with ΔΨm and negative association with GLUT-1 (that display higher and lower levels in the elderly respectively), the frailty index increasing getting older [Figure 4.3.6.2 (B)].

*Table 4.3.6.2: Correlation between frailty index, (**a**) basal metabolism (mitochondrial status, uptake of nutrients, and neutral lipids content), nutrient surface markers (basal (NT) and post-activation (anti-CD3)), (**b**) protein synthesis, dependences and capacities, and fold induction of protein synthesis (basal and post-activation) (**b**). For the correlation, Spearman's rank correlation was used. Spearman's R and p values are shown in the panel. *P<0.05, **P < 0.01 and the significatively was reported in bold.*

a		CD4 N	CD8 N
BASAL METABOLISM	Mitochondrial mass	0.1294	-0.1251
	ΔΨm	**0.5054****	**0.3287***
	ROS	0.09564	0.1726
	FA uptake	-0.1302	-0.1596
	Lipids store	-0.2945	-0.2714
	Glucose uptake	0.1924	0.0742
NUTRIENT SURFECE MARKERS	LDL-r (NT)	-0.28	0.02397
	AA- r (NT)	0.3077	-0.08029
	LDL-r+ AA- r (NT)	**-0.4195***	-0.06795
	CD36 (NT)	-0.292	0.2112
	GLUT-1 (NT)	-0.1529	0.2039
	CD36+ GLUT-1 (NT)	-0.1911	0.3413
	LDL-r (anti-CD3)	-0.2992	-0.2992
	AA- r (anti- CD3)	**-0.4203***	**-0.4498***
	LDL-r+ AA- r (anti- CD3)	**-0.5812****	-0.2529
	CD36 (anti- CD3)	-0.1282	0.3445
	GLUT-1 (anti- CD3)	**-0.4667***	0.2757
	CD36+ GLUT-1 (anti- CD3)	-0.1413	0.4123

b		CD4 N	CD8 N
BASAL METABOLIC ACTIVITY	Control	-0.1709	-0.0746
	Glucose dependence	-0.4558*	-0.3524
	MithocondriaL dependence	-0.03513	0.1862
	AAO dependence	-0.07261	-0.275
	FAAO dependence	0.3783	0.2452
	Glycolytic capacity	0.03513	-0.1862
	FAAO capacity	0.4558*	0.3336
	Fold of protein synthesis	0.08012	-0.00305
METABOLIC ACTIVITY UPON ACTIVATION	Control	0.03234	0.03399
	Glucose dependence	-0.1433	-0.1986
	Mithocondrial dependence	-0.215	-0.1595
	AAO dependence	-0.2218	-0.3453
	FAAO dependence	0.1653	0.1818
	Glycolytic capacity	0.215	0.09567
	FAAO capacity	0.1433	0.1986

Together, these data suggest that immunosenescence features are marginally related to cell responsiveness to the PCV13 vaccine and to metabolic perturbations which are instead strongly associated with the lack of T cell immunity.

4.3.7 LDL-r expression can predict the responsiveness to PCV13 vaccination

Our results suggest that immunosenescence does not strongly impact on cellular response of antipneumococcal vaccination (PCV13 vaccine); in fact, we observed elderly subjects with good responses and young subjects who poorly responded. The identification of predictive markers that could segregate, at baseline, those who will develop strong T cell immunity versus those who will not mount such responses is certainly a major public health goal to provide informed decisions in personalized vaccination approaches. Therefore, we hypothesized to use those metabolic features that, in out cohort, clearly differentiated responders versus non-responders. In particular studies conducted on the expression of nutritional biomarkers identified the increased basal and post-activation expression of LDL-r and CD98, (single or double, i.e. LDL-$r^{+}CD98^{+}$) in naïve $CD4^{+}$ T cells assessed at pre-vaccination time points as the metabolic parameters most strongly associated with responsiveness [Figure 4.3.7.1].

With the idea of making of these parameters future biomarkers to predict vaccine responses, we plotted expression of LDL-r and CD98, both expressed as single or double (LDL-$r^{+}CD98^{+}$) positivity, either on total or naïve $CD4^{+}$ T cells, at rest (basal) and upon activation. For almost all the combinations considered, we could observe a clear and statistically significant differences between the R and NR.

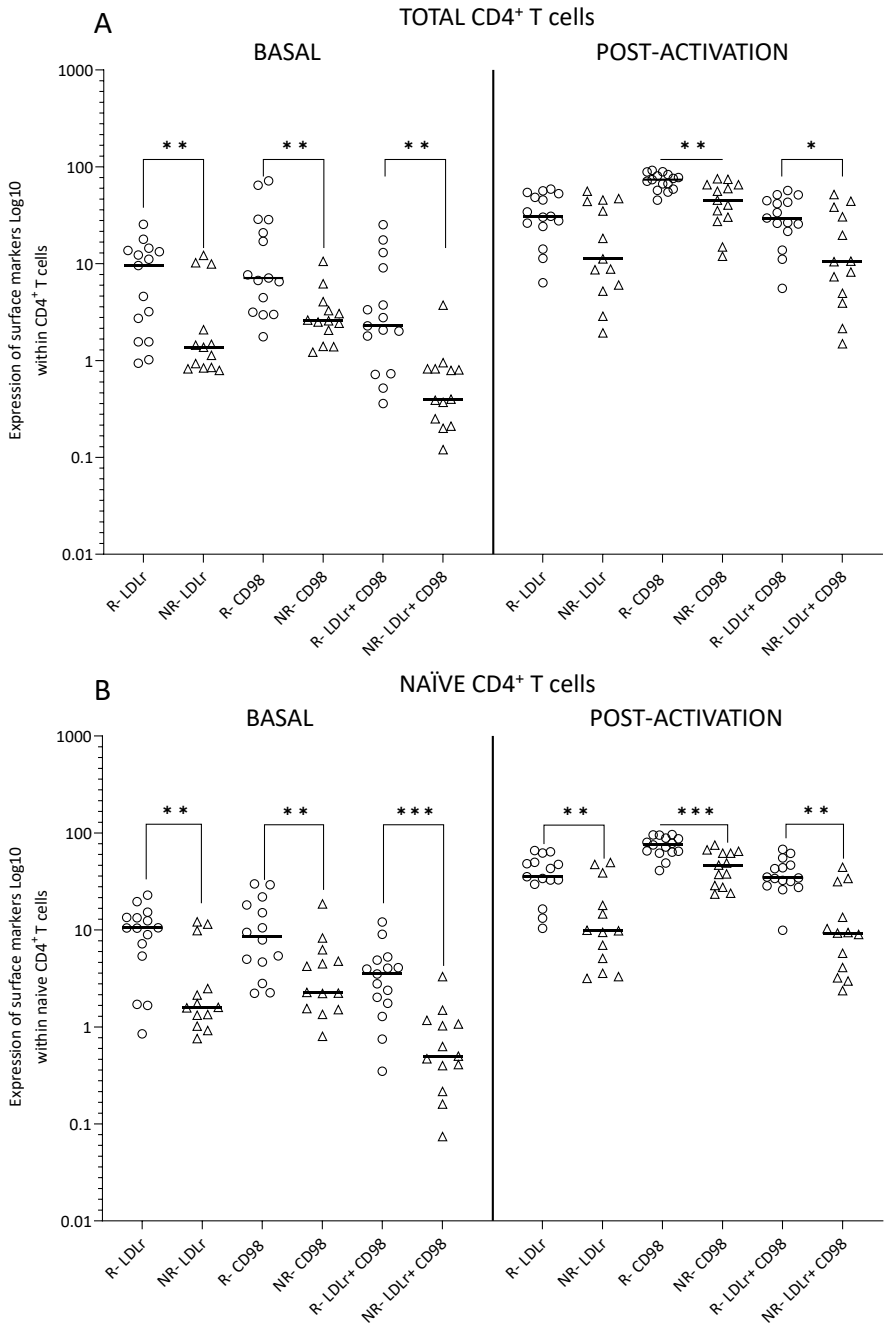


*Figure 4.3.7.1: Expression of nutritional surface biomarkers in total and naïve CD4 T cells. Expression of LDL-r (R= 13; NR= 15), amino acid receptors (CD98, R= 13, NR= 15) basal and post-activation with coated anti-CD3 for 24h were measured by flow cytometry and reported as Log10 in naïve (**A**) and total (**B**) CD4$^+$ T cells. The line represents the median and the statistical analyses between R and NR were determined by Mann-Whitney test (**A, B**). *P<0.05, **P < 0.01, ***P<0.001.*

We thus chose the receptor combinations that were more strongly differentiating R from NR and conducted a ROC (Receiver Operating Characteristic) analysis [251], a statistical technique commonly used to evaluate the performance of a binary classification model. Thus, by comparing the expression of LDL-r in total (basal) and naïve CD4$^+$ T cells (basal and upon anti-CD3 activation) or

the concomitant expression of LDL-r and CD98 in naïve $CD4^+$ cells (basal and upon aCD3 activation) between responders and non-responders, ROC analysis shows a high sensitivity and specificity of the system for all conditions assessed [Figure 4.3.7.2]. This is also confirmed by the AUC (Area Under the Curve) which was close to 1 and always ≥ 0.9 in all five cases considered, underlining the accuracy of the test. These results suggest that the baseline analysis of LDL-r and CD98 markers, especially after stimulation with anti-CD3, could be used as a diagnostic tool to predict response in clinical settings or in experimental studies.

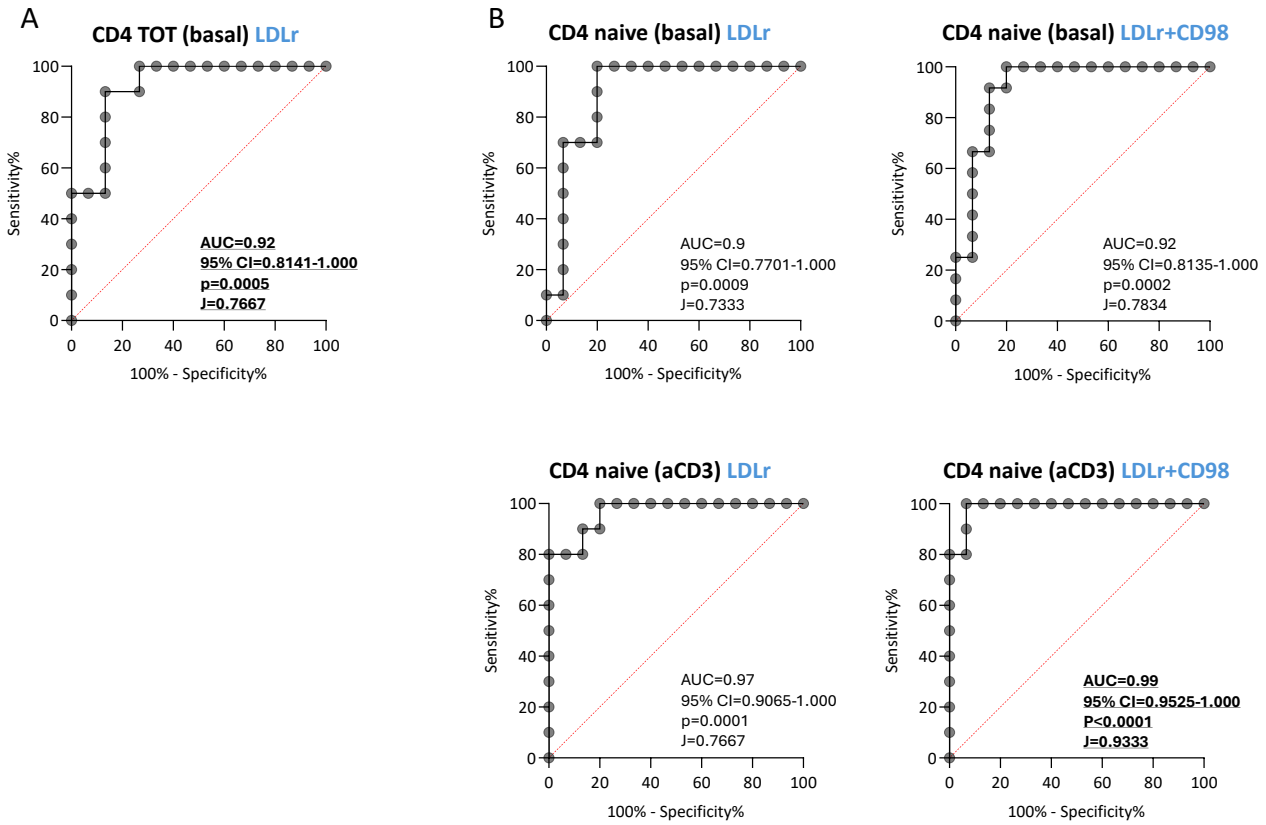


*Figure 4.3.7.2: Expression of LDL-r and CD98 surface biomarkers in total and naïve $CD4^+$ T cells to predict the responsiveness to vaccination. We analysed the expression of LDL-r and amino acid receptors (CD98) in total (**A**) and naïve (**B**) $CD4^+$ T cells, in basal and post-activation (for 24h) in responders (n= 15) and non-responders (n= 13) participants (pre-vaccination). We conducted an ROC analysis to find out whether the expression of LDL-r or LDL-r+CD98 in total (basal only) or naïve (basal and post-activated) $CD4^+$ T cells. In the panels were reported: AUC (Area Under the Curve), CI (Confidence Interval), p value, and Youden's J statistic (for the discrimination between the two groups).*

4.4 Discussion

Immunosenescence refers to the decline of the immune system associated with aging [259,260]. As mentioned earlier, immunosenescence has a broad impact, affecting both innate and adaptive immunity. For instance, it leads to a decline in naïve cells with age and a reduction in antigen presentation by antigen-presenting cells (APCs) [133].

The elderly are particularly affected by immunosenescence, as the deterioration of their immune system results in a diminished response to pathogens (e.g., SARS-CoV-2 and influenza virus) and reduced vaccine effectiveness, both therapeutic and preventive [261–263].
Thus, a robust vaccination strategy and the development of new vaccines are essential to counteract pathogens and their consequences. It is crucial that vaccines are designed to stimulate both humoral and cellular ($CD4^+$ and $CD8^+$ T cells) immunity, as these cells provide immunological memory and are vital for preventing or resolving infections.

The PCV13 vaccine is an anti-pneumococcal vaccine, which protects against 13 types of *Streptococcus pneumoniae* bacteria; it is a conjugate vaccine as the polysaccharides of the bacterial capsule are bound to a carrier protein (CRM197, a mutated diphtheria toxin protein) to stimulate a more robust and long-lasting immune response; this allows the stimulation of both B cells, caused by the polysaccharides, and T cells, caused by a protein antigen.
The study of determinants of vaccine responsiveness/non-responsiveness is crucial to both understand the biological mechanisms that explain poor vaccine-induced immunity (in order to plan corrective strategies and improve protection), as well as to develop predictive biomarkers that will, a priori, identify those subjects that will mount poor responses after immunization. Considering the pivotal role of metabolism in dictating lymphocyte reactions, the characterization of immunometabolism of immune cells at baseline (pre-vaccination) constitutes a promising field to investigate in this sense. By examining the basal metabolism of T lymphocytes specifically mitochondrial status, nutrient uptake, and neutral lipid content- we observed that naïve T cells from elderly subjects exhibit a high mitochondrial membrane potential, a measure which however is not associated with the degree to vaccine responsiveness. Similarly, the expression of some nutrient markers, and in particular the co-expression of the receptors for LDL-r and amino acids following stimulation, particularly in naïve $CD4^+$ and $CD8^+$ T lymphocytes, was differentially expressed in individuals of different age groups, with lower values in the elderly. This reduction was correlated with the changes in mitochondrial membrane potential.
The assessment of the cellular response patterns obtained via ELISpot following 24-hours stimulation with the vaccine carrier protein CRM197 (performed by the University of Innsbruck) indicated no

differences between young and elderly participants across different time points (days 0, 7, and 28-, and 6-months post-vaccination). Specifically, the magnitude of the response was consistent between the two groups. Furthermore, age-related metabolic differences did not appear to influence this response.

However, given that the magnitude of the response was comparable between younger and older adults, we explored why some older individuals demonstrated better responses than some younger ones. Participants were categorized as responders (>20 SFC/4x10^5 cells) or non-responders (<10 SFC/4x10^5 cells) based on their peak cellular response in the ELISpot assay (day 7) and irrespectively of age. Interestingly, while both groups shared similar basal metabolic profiles, the expression of specific surface markers stood out. Specifically, responders exhibited higher basal and activated levels of LDL receptors, amino acid receptors, and LDL-r^+CD98^+ expression in $CD4^+$ naïve T cells.

To investigate a potential metabolic mechanism underlying this elevated receptor expression, we employed SCENITH, a technique that allows the study of protein synthesis, metabolic dependencies, and capacities in $CD4^+$ and $CD8^+$ naïve cells (pre-vaccination), under both resting and activated conditions. SCENITH revealed markedly increased protein synthesis and a dependence on glucose metabolism in responders during activation with anti-CD3 and anti-CD28 [264,265]. This was accompanied by a pronounced metabolic shift from oxidative phosphorylation to glycolysis. Notably, the fold increase in protein synthesis was particularly significant in naïve $CD4^+$ T cells among responders.

This heightened metabolic activity and the shift from oxidative to glycolytic metabolism in $CD4^+$ naïve cells suggest greater metabolic readiness for activation. This readiness likely underpins the enhanced expression of receptors such as that for LDL-r, critical for cell division and membrane production, and CD98, which facilitates amino acid uptake required for the synthesis of effector proteins [266–268].

The distinct expression of LDL-r and CD98 receptors in total and naïve $CD4^+$ T cells, as confirmed by ROC analysis, and their correlation with activated metabolic states, points to the potential of these receptors as immunological markers for vaccine responsiveness. This is particularly relevant for PCV vaccines, offering an opportunity to enhance vaccination efficacy by tailoring vaccination protocols and ensuring optimal protection against infectious diseases. The assessment of the same markers as predictive tools in other vaccination contexts is required and in plan.

While immunosenescence is a known factor that negatively impacts infection resistance and vaccine efficacy, it is not equally observed among subjects of the same age group [269]. Inter-individual differences, such as immunological stability or a history of recurrent infections, likely influence

vaccine outcomes. It is, therefore, critical to identify and address these individual variations, leveraging potential biomarkers like LDL-r and CD98 to predict vaccination success.

4. CONCLUSIONS

Immunosenescence refers to the gradual and irreversible decline in immune system function that occurs as a natural consequence of aging, a process that is fundamentally intricate, encompassing both biological and social-psychological dimensions [133,270,271]. This decline affects the immune system both qualitatively and quantitatively, leading to a reduction in adaptive immunity and an increase in the non-specific production of pro-inflammatory cytokines [272,273]. This chronic inflammation, known as inflammaging, contributes to heightened susceptibility to infections and diminished vaccine responses [76,274,275].

As immunity weakens progressively, older adults face a range of health challenges. The aging immune system is less effective at combating infections, resulting in more severe and frequent illnesses with advancing age. The elderly are also more prone to cancers, autoimmune diseases, and chronic inflammatory disorders[276]. Moreover, the reduced capacity to mount effective responses to pathogens and the lower efficacy of preventive vaccinations further exacerbate their vulnerability [277].

A key contributor to immune aging is thymic involution, a process where the thymus shrinks and loses functionality, resulting in fewer thymocytes and their replacement by fat cells (adipocytes). This shift results in a diminished pool of naïve T cells and a predominance of memory T cell populations, including terminally differentiated T cells (T_{EMRA}), which are often dysfunctional or exhausted [82,83]. These changes destabilize immune system homeostasis and increase entropy, reflecting a loss of immune stability.

Studies across different cohorts (PIpELINe, blood donors, RIV and VITAL) have consistently shown that elderly individuals have a lower number of naïve T cells compared to younger subjects, alongside higher expression of activation markers such as HLA-DR and CD38.

HLA-DR plays a central role in immune cell communication, essential for the body's defence mechanisms but also implicated in various pathological conditions. Elevated HLA-DR expression indicates immune system overactivation, often accompanied by increased pro-inflammatory cytokine production, driving chronic low-grade inflammation[278,279]. For instance, during myocardial infarction, there is a surge in HLA-DR expression, signalling a state of immune stress. While HLA-DR levels decrease after the acute event resolves, the persistent inflammaging fuelled by T_{EMRA} cells remains a challenge to immune stability.

These changes limit the ability of elderly individuals to mount *de novo* cellular immune responses against previously unencountered pathogens in the context of natural infection and/or vaccination

[179,187]. T cells are particularly susceptible to the ravages of age, potentially explaining the vulnerability of elderly individuals to emerging viral infections, such as SARS-CoV-2 [280].

To see how aging, that results in declining naïve T cells and functionality, affected the response to new viral antigens and what role it played during vaccination, targeted studies were conducted. To characterize the responses to new antigens, we used an *in vitro* approach to prime epitope-specific $CD8^+$ T cells from healthy donors stratified by age, ensuring a complete absence of prior exposure to antigens derived from SARS-CoV-2. We found that age was associated with reductions in the diversity and magnitude of functional $CD8^+$ T cell responses elicited against SARS-CoV-2, measured via the recall induction of IFNγ and there was a reduction in the diversity of functional $CD8^+$ T cell responses elicited *in vitro* against a panel of typically immunodominant epitopes derived from SARS-CoV-2. We noticed that the age-related loss of naïve T cells was strictly dictating this overall poorer immunocompetence.

We next assessed how this event may have affected anti-SARS-CoV-2 vaccinations, focusing particularly on BNT162b2 (mRNA) and ChAdOx1-S (adenoviral vector) vaccines and how the response to these, varies with immunosenescence.

Age-related immune decline negatively affects S protein-specific immune responses, especially with mRNA vaccines like BNT162b2. This type of vaccine has been shown to generate very high initial humoral and cellular responses but exhibit a rapid contraction of effector-like $CD8^+$ T cells. This decline is exacerbated in older individuals, even after booster doses, and functional $CD8^+$ T cell responses get compromised [203].

Conversely, ChAdOx1-S induces more durable cellular immune responses, particularly $CD8^+$ T cells, which are less affected by aging [211,229–232]. This durability may stem from mechanisms that counteract immunosenescence, although further investigation is required. Booster doses with mRNA vaccines enhance immune responses across both platforms but are most effective in those initially vaccinated with ChAdOx1-S.

Therefore, it remains increasingly important to investigate and find the right vaccine strategy that considers the inter-individual differences, because advancing age is not always associated with a ‘non-response’ to vaccines [213]

In fact, cellular responses to the anti-*Streptococcus pneumoniae* PCV13 vaccine measured by ELISpot against the CRM197 carrier protein were minimally affected by age in our cohort, although naïve $CD4^+$ and $CD8^+$ T cells from elderly individuals were characterized by a specific metabolic profile at the level of mitochondria and expression of nutrient markers. Therefore, we observed that

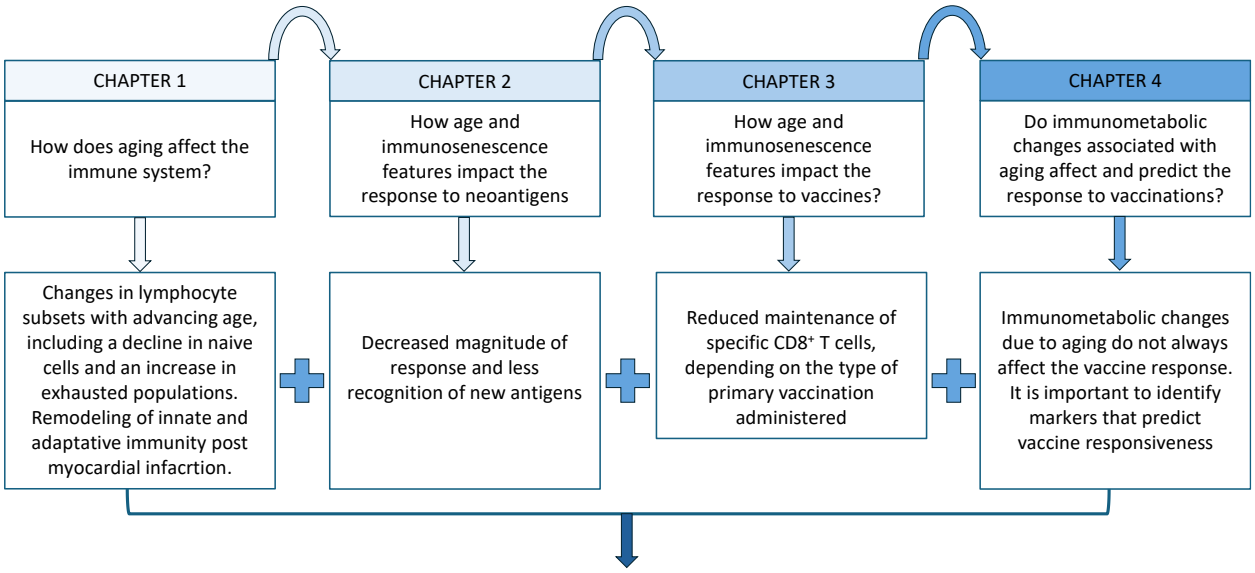
while elderly may display weak responses, also younger adults do not consistently exhibit optimal immunity.

We then decided to focus on baseline differences (i.e. prior to PCV13 immunization) that could discriminate and predict individuals who will develop poor versus good cellular responses to the vaccine, regardless of their age. These analyses revealed that naïve $CD4^+$ and $CD8^+$ T cells from vaccine responders (both young and elderly) displayed higher expression of LDL-r and CD98 receptors both at rest and upon activation. Moreover, responders had enhanced protein synthesis and a metabolic shift from oxidative phosphorylation to glycolysis during T cell activation, demonstrating greater metabolic readiness.

The high baseline expression of LDL receptor (LDL-r) in responders appears to facilitate the uptake of extracellular cholesterol, supporting mTORC1 activation, which is critical for metabolic reprogramming during lymphocyte activation, enhancing effector function [281,282]. Even after activation, LDL-r expression remains elevated, sustaining the mTORC1 activity which, in turn promotes protein synthesis as observed via SCENITH. This aligns with the metabolic demands of activated lymphocytes, thus enabling $CD4^+$ and $CD8^+$ T cells to carry out their functions more effectively.

The robust metabolic performance and reprogramming regulated by mTORC1 further lead to increased expression of amino acids receptors (CD98), which are essential for protein synthesis. Conversely, low LDL-r expression is associated with reduced activation of the mTOR pathway, leading to diminished lymphocyte proliferation and reduced functionality [268].

The identification of strategies to predict and improve future vaccinations is a key priority for the control of infectious diseases, especially in geriatric populations. Our findings suggest that markers like LDL-r and CD98 could predict vaccine responsiveness, particularly in the context of PCV13. The assessment of their predictive value in other vaccination context is now undergoing. Developing tailored vaccination strategies that enhance immune responses in older adults represents a critical step in addressing the challenges posed by immunosenescence. While aging broadly impacts immune function, our findings highlight significant individual variability in immune stability and metabolic readiness. These insights underscore the need for personalized approaches to optimize vaccine efficacy [283,284], particularly by leveraging predictive markers such as LDL-r and CD98. Such strategies hold the potential to mitigate age-related vulnerabilities and improve health outcomes in aging populations.



While aging leads to immunosenescence and decreased vaccine responsiveness, individual variability in immune function and metabolic readiness highlights the importance of identifying predictive markers, such as LDLr and CD98, to tailor vaccination strategies and optimize immune responses in older adults

5. BIBLIOGRAPHY

1. Roth, G.A.; Picece, V.C.T.M.; Ou, B.S.; Luo, W.; Pulendran, B.; Appel, E.A. Designing Spatial and Temporal Control of Vaccine Responses. *Nat Rev Mater* **2021**, *7*, 174–195, doi:10.1038/s41578-021-00372-2.
2. Gordon, S. Phagocytosis: An Immunobiologic Process. *Immunity* 2016, *44*, 463–475.
3. Rosales, C.; Uribe-Querol, E. Phagocytosis: A Fundamental Process in Immunity. *Biomed Res Int* 2017, *2017*.
4. Wang, N.S.; McHeyzer-Williams, L.J.; Okitsu, S.L.; Burris, T.P.; Reiner, S.L.; McHeyzer-Williams, M.G. Divergent Transcriptional Programming of Class-Specific B Cell Memory by T-Bet and RORα. *Nat Immunol* **2012**, *13*, 604–611, doi:10.1038/ni.2294.
5. Knox, J.J.; Myles, A.; Cancro, M.P. T-bet $^{+}$ Memory B Cells: Generation, Function, and Fate. *Immunol Rev* **2019**, *288*, 149–160, doi:10.1111/imr.12736.
6. Munang'andu, H.M.; Evensen, Ø. A Review of Intra- and Extracellular Antigen Delivery Systems for Virus Vaccines of Finfish. *J Immunol Res* **2015**, *2015*, 1–19, doi:10.1155/2015/960859.
7. Myers, D.R.; Wheeler, B.; Roose, J.P. MTOR and Other Effector Kinase Signals That Impact T Cell Function and Activity. *Immunol Rev* **2019**, *291*, 134–153, doi:10.1111/imr.12796.
8. Zou, Z.; Tao, T.; Li, H.; Zhu, X. MTOR Signaling Pathway and MTOR Inhibitors in Cancer: Progress and Challenges. *Cell Biosci* 2020, *10*.
9. Sun, L.; Su, Y.; Jiao, A.; Wang, X.; Zhang, B. T Cells in Health and Disease. *Signal Transduct Target Ther* 2023, *8*.
10. Kaech, S.M.; Wherry, E.J.; Ahmed, R. Effector and Memory T-Cell Differentiation: Implications for Vaccine Development. *Nat Rev Immunol* 2002, *2*, 251–262.
11. Pennock, N.D.; White, J.T.; Cross, E.W.; Cheney, E.E.; Tamburini, B.A.; Kedl, R.M. T Cell Responses: Naïve to Memory and Everything in Between. *American Journal of Physiology - Advances in Physiology Education* **2013**, *37*, 273–283, doi:10.1152/advan.00066.2013.
12. Mailliard, R.B.; Egawa, S.; Cai, Q.; Kalinska, A.; Bykovskaya, S.N.; Lotze, M.T.; Kapsenberg, M.L.; Storkus, W.J.; Kalinski, P. *Complementary Dendritic Cell-Activating Function of CD8 and CD4 T Cells: Helper Role of CD8 T Cells in the Development of T Helper Type 1 Responses*; 2002; Vol. 195;.
13. Chowdhury, F.Z.; Ramos, H.J.; Davis, L.S.; Forman, J.; Farrar, J.D. IL-12 Selectively Programs Effector Pathways That Are Stably Expressed in Human CD8+ Effector Memory T Cells in Vivo. *Blood* **2011**, *118*, 3890–3900, doi:10.1182/blood-2011-05-357111.
14. Ylikoski, E.; Lund, R.; Kyläniemi, M.; Filén, S.; Kilpeläinen, M.; Savolainen, J.; Lahesmaa, R. IL-12 up-Regulates T-Bet Independently of IFN-γ in Human CD4+ T Cells. *Eur J Immunol* **2005**, *35*, 3297–3306, doi:10.1002/eji.200526101.
15. Le Gallo, M.; Poissonnier, A.; Blanco, P.; Legembre, P. CD95/Fas, Non-Apoptotic Signaling Pathways, and Kinases. *Front Immunol* 2017, *8*.
16. Buchbinder, E.I.; Desai, A. CTLA-4 and PD-1 Pathways Similarities, Differences, and Implications of Their Inhibition. *American Journal of Clinical Oncology: Cancer Clinical Trials* 2016, *39*, 98–106.
17. Almeida, L.; Lochner, M.; Berod, L.; Sparwasser, T. Metabolic Pathways in T Cell Activation and Lineage Differentiation. *Semin Immunol* 2016, *28*, 514–524.
18. Farber, D.L.; Yudanin, N.A.; Restifo, N.P. Human Memory T Cells: Generation, Compartmentalization and Homeostasis. *Nat Rev Immunol* **2014**, *14*, 24–35, doi:10.1038/nri3567.
19. Corrado, M.; Pearce, E.L. Targeting Memory T Cell Metabolism to Improve Immunity. *Journal of Clinical Investigation* **2022**, *132*, doi:10.1172/JCI148546.

20. O'Sullivan, D. The Metabolic Spectrum of Memory T Cells. *Immunol Cell Biol* **2019**, *97*, 636–646, doi:10.1111/imcb.12274.
21. Winer, H.; Rodrigues, G.O.L.; Hixon, J.A.; Aiello, F.B.; Hsu, T.C.; Wachter, B.T.; Li, W.; Durum, S.K. IL-7: Comprehensive Review. *Cytokine* **2022**, *160*, 156049, doi:10.1016/j.cyto.2022.156049.
22. Qian, S.; Wei, Z.; Yang, W.; Huang, J.; Yang, Y.; Wang, J. The Role of BCL-2 Family Proteins in Regulating Apoptosis and Cancer Therapy. *Front Oncol* 2022, *12*.
23. Iijima, N. The Emerging Role of Effector Functions Exerted by Tissue-Resident Memory T Cells. *Oxf Open Immunol* **2024**, *5*, doi:10.1093/oxfimm/iqae006.
24. Unsoeld, H.; Pircher, H. Complex Memory T-Cell Phenotypes Revealed by Coexpression of CD62L and CCR7. *J Virol* **2005**, *79*, 4510–4513, doi:10.1128/jvi.79.7.4510-4513.2005.
25. Gattinoni, L.; Speiser, D.E.; Lichterfeld, M.; Bonini, C. T Memory Stem Cells in Health and Disease. *Nat Med* 2017, *23*, 18–27.
26. Gebhardt, T.; Park, S.L.; Parish, I.A. Stem-like Exhausted and Memory CD8+ T Cells in Cancer. *Nat Rev Cancer* **2023**, *23*, 780–798, doi:10.1038/s41568-023-00615-0.
27. Sallusto, F.; Lenig, D.; Förster, R.; Lipp, M.; Lanzavecchia, A. Two Subsets of Memory T Lymphocytes with Distinct Homing Potentials and Effector Functions. *Nature* **1999**, *401*, 708–712, doi:10.1038/44385.
28. Bevilacqua, A.; Ho, P.-C.; Franco, F. Metabolic Reprogramming in Inflammaging and Aging in T Cells. *Life Metabolism* **2023**, *2*, doi:10.1093/lifemeta/load028.
29. Han, S.; Georgiev, P.; Ringel, A.E.; Sharpe, A.H.; Haigis, M.C. Age-Associated Remodeling of T Cell Immunity and Metabolism. *Cell Metab* **2023**, *35*, 36–55, doi:10.1016/j.cmet.2022.11.005.
30. Martin, D.E.; Torrance, B.L.; Haynes, L.; Bartley, J.M. Targeting Aging: Lessons Learned From Immunometabolism and Cellular Senescence. *Front Immunol* **2021**, *12*, 714742, doi:10.3389/fimmu.2021.714742.
31. Slack, M.; Wang, T.; Wang, R. T Cell Metabolic Reprogramming and Plasticity. *Mol Immunol* **2015**, *68*, 507–512, doi:10.1016/j.molimm.2015.07.036.
32. Møller, S.H.; Hsueh, P.C.; Yu, Y.R.; Zhang, L.; Ho, P.C. Metabolic Programs Tailor T Cell Immunity in Viral Infection, Cancer, and Aging. *Cell Metab* 2022, *34*, 378–395.
33. Wik, J.A.; Skålhegg, B.S. T Cell Metabolism in Infection. *Front Immunol* 2022, *13*.
34. Green, W.D.; Beck, M.A. Obesity Altered T Cell Metabolism and the Response to Infection. *Curr Opin Immunol* 2017, *46*, 1–7.
35. Pearce, E.L. Metabolism in T Cell Activation and Differentiation. *Curr Opin Immunol* 2010, *22*, 314–320.
36. Chan, D.C. Mitochondrial Dynamics and Its Involvement in Disease. *Annual Review of Pathology: Mechanisms of Disease* **2020**, *15*, 235–259, doi:10.1146/annurev-pathmechdis-012419-032711.
37. O'Neill, L.A.J.; Kishton, R.J.; Rathmell, J. A Guide to Immunometabolism for Immunologists. *Nat Rev Immunol* **2016**, *16*, 553–565, doi:10.1038/nri.2016.70.
38. Cao, J.; Liao, S.; Zeng, F.; Liao, Q.; Luo, G.; Zhou, Y. Effects of Altered Glycolysis Levels on CD8+ T Cell Activation and Function. *Cell Death Dis* **2023**, *14*, 407, doi:10.1038/s41419-023-05937-3.
39. Donnelly, R.P.; Finlay, D.K. Glucose, Glycolysis and Lymphocyte Responses. *Mol Immunol* **2015**, *68*, 513–519, doi:10.1016/j.molimm.2015.07.034.
40. Stark, H.; Fichtner, M.; König, R.; Lorkowski, S.; Schuster, S. Causes of Upregulation of Glycolysis in Lymphocytes upon Stimulation. A Comparison with Other Cell Types. *Biochimie* **2015**, *118*, 185–194, doi:10.1016/j.biochi.2015.09.017.
41. De Carvalho, C.C.C.R.; Caramujo, M.J. The Various Roles of Fatty Acids. *Molecules* 2018, *23*.

42. Lee, J.; Walsh, M.C.; Hoehn, K.L.; James, D.E.; Wherry, E.J.; Choi, Y. Regulator of Fatty Acid Metabolism, Acetyl Coenzyme A Carboxylase 1, Controls T Cell Immunity. *The Journal of Immunology* **2014**, *192*, 3190–3199, doi:10.4049/jimmunol.1302985.
43. Kemp, F.; Braverman, E.L.; Byersdorfer, C.A. Fatty Acid Oxidation in Immune Function. *Front Immunol* **2024**, *15*, doi:10.3389/fimmu.2024.1420336.
44. Raud, B.; McGuire, P.J.; Jones, R.G.; Sparwasser, T.; Berod, L. Fatty Acid Metabolism in <scp>CD</Scp> 8 $^{+}$ T Cell Memory: Challenging Current Concepts. *Immunol Rev* **2018**, *283*, 213–231, doi:10.1111/imr.12655.
45. Newsholme, P. Why Is L-Glutamine Metabolism Important to Cells of the Immune System in Health, Postinjury, Surgery or Infection? *J Nutr* **2001**, *131*, 2515S-2522S, doi:10.1093/jn/131.9.2515S.
46. Yoo, H.C.; Yu, Y.C.; Sung, Y.; Han, J.M. Glutamine Reliance in Cell Metabolism. *Exp Mol Med* 2020, *52*, 1496–1516.
47. Yang, L.; Venneti, S.; Nagrath, D. Glutaminolysis: A Hallmark of Cancer Metabolism. **2024**, *21*, 14, doi:10.1146/annurev-bioeng-071516.
48. Nicoli, F.; Papagno, L.; Frere, J.J.; Cabral-Piccin, M.P.; Clave, E.; Gostick, E.; Toubert, A.; Price, D.A.; Caputo, A.; Appay, V. Naïve CD8+ T-Cells Engage a Versatile Metabolic Program upon Activation in Humans and Differ Energetically from Memory CD8+ T-Cells. *Front Immunol* **2018**, *9*, 1–12, doi:10.3389/fimmu.2018.02736.
49. Rangel Rivera, G.O.; Knochelmann, H.M.; Dwyer, C.J.; Smith, A.S.; Wyatt, M.M.; Rivera-Reyes, A.M.; Thaxton, J.E.; Paulos, C.M. Fundamentals of T Cell Metabolism and Strategies to Enhance Cancer Immunotherapy. *Front Immunol* 2021, *12*.
50. Bental, M.; Deutsch, C. Metabolic Changes in Activated T Cells: An NMR Study of Human Peripheral Blood Lymphocytes. *Magn Reson Med* **1993**, *29*, 317–326, doi:10.1002/mrm.1910290307.
51. Chang, C.H.; Curtis, J.D.; Maggi, L.B.; Faubert, B.; Villarino, A. V.; O'Sullivan, D.; Huang, S.C.C.; Van Der Windt, G.J.W.; Blagih, J.; Qiu, J.; et al. XPosttranscriptional Control of T Cell Effector Function by Aerobic Glycolysis. *Cell* **2013**, *153*, 1239, doi:10.1016/j.cell.2013.05.016.
52. Pearce, E.L.; Pearce, E.J. Metabolic Pathways in Immune Cell Activation and Quiescence. *Immunity* 2013, *38*, 633–643.
53. Almeida, L.; Lochner, M.; Berod, L.; Sparwasser, T. Metabolic Pathways in T Cell Activation and Lineage Differentiation. *Semin Immunol* 2016, *28*, 514–524.
54. Wu, S.; Zou, M.H. AMPK, Mitochondrial Function, and Cardiovascular Disease. *Int J Mol Sci* 2020, *21*, 1–34.
55. Ma, E.H.; Poffenberger, M.C.; Wong, A.H.T.; Jones, R.G. The Role of AMPK in T Cell Metabolism and Function. *Curr Opin Immunol* 2017, *46*, 45–52.
56. Panwar, V.; Singh, A.; Bhatt, M.; Tonk, R.K.; Azizov, S.; Raza, A.S.; Sengupta, S.; Kumar, D.; Garg, M. Multifaceted Role of MTOR (Mammalian Target of Rapamycin) Signaling Pathway in Human Health and Disease. *Signal Transduct Target Ther* 2023, *8*.
57. Palmer, C.S.; Ostrowski, M.; Balderson, B.; Christian, N.; Crowe, S.M. Glucose Metabolism Regulates T Cell Activation, Differentiation, and Functions. *Front Immunol* 2015, *6*.
58. Chen, Z.; Han, F.; Du, Y.; Shi, H.; Zhou, W. Hypoxic Microenvironment in Cancer: Molecular Mechanisms and Therapeutic Interventions. *Signal Transduct Target Ther* 2023, *8*.
59. Taylor, C.T.; Scholz, C.C. The Effect of HIF on Metabolism and Immunity. *Nat Rev Nephrol* 2022, *18*, 573–587.
60. Carreira, A.S.A.; Ravera, S.; Zucal, C.; Thongon, N.; Irene, C.; Astigiano, C.; Bertola, N.; Buongiorno, A.; Roccuzzo, M.; Bisio, A.; et al. Mitochondrial Rewiring Drives Metabolic Adaptation to NAD(H) Shortage in Triple Negative Breast Cancer Cells. *Neoplasia* **2023**, *41*, 100903, doi:10.1016/j.neo.2023.100903.

61. Buck, M.D.D.; O'Sullivan, D.; Klein Geltink, R.I.I.; Curtis, J.D.D.; Chang, C.H.; Sanin, D.E.E.; Qiu, J.; Kretz, O.; Braas, D.; van der Windt, G.J.J.W.; et al. Mitochondrial Dynamics Controls T Cell Fate through Metabolic Programming. *Cell* **2016**, *166*, 63–76, doi:10.1016/j.cell.2016.05.035.
62. O'Sullivan, D.; vanderWindt, G.W.J.; Huang, S.C.C.; Curtis, J.D.; Chang, C.H.; Buck, M.D.L.; Qiu, J.; Smith, A.M.; Lam, W.Y.; DiPlato, L.M.; et al. Memory CD8+ T Cells Use Cell-Intrinsic Lipolysis to Support the Metabolic Programming Necessary for Development. *Immunity* **2014**, *41*, 75–88, doi:10.1016/j.immuni.2014.06.005.
63. Ragupathi, A.; Kim, C.; Jacinto, E. The MTORC2 Signaling Network: Targets and Cross-Talks. *Biochemical Journal* **2024**, *481*, 45–91, doi:10.1042/BCJ20220325.
64. Wang, Y.; Zhou, Y.; Graves, D.T. FOXO Transcription Factors: Their Clinical Significance and Regulation. *Biomed Res Int* 2014, *2014*.
65. Ma, S.; Ming, Y.; Wu, J.; Cui, G. Cellular Metabolism Regulates the Differentiation and Function of T-Cell Subsets. *Cell Mol Immunol* 2024, *21*, 419–435.
66. Kim, H.-R.; Hwang, K.-A.; Park, S.-H.; Kang, I. IL-7 and IL-15: Biology and Roles in T-Cell Immunity in Health and Disease. *Crit Rev Immunol* **2008**, *28*, 325–339, doi:10.1615/CritRevImmunol.v28.i4.40.
67. van der Windt, G.J.W.; Everts, B.; Chang, C.H.; Curtis, J.D.; Freitas, T.C.; Amiel, E.; Pearce, E.J.; Pearce, E.L. Mitochondrial Respiratory Capacity Is a Critical Regulator of CD8 + T Cell Memory Development. *Immunity* **2012**, *36*, 68–78, doi:10.1016/j.immuni.2011.12.007.
68. Chang, J.T.; Palanivel, V.R.; Kinjyo, I.; Schambach, F.; Intlekofer, A.M.; Banerjee, A.; Longworth, S.A.; Vinup, K.E.; Mrass, P.; Oliaro, J.; et al. Asymmetric T Lymphocyte Division in the Initiation of Adaptive Immune Responses. *Science (1979)* **2007**, *315*, 1687–1691, doi:10.1126/science.1139393.
69. Ajoolabady, A.; Pratico, D.; Tang, D.; Zhou, S.; Franceschi, C.; Ren, J. Immunosenescence and Inflammaging: Mechanisms and Role in Diseases. *Ageing Res Rev* 2024, *101*.
70. Santoro, A.; Bientinesi, E.; Monti, D. Immunosenescence and Inflammaging in the Aging Process: Age-Related Diseases or Longevity? *Ageing Res Rev* 2021, *71*.
71. Xu, W.; Wong, G.; Hwang, Y.Y.; Larbi, A. The Untwining of Immunosenescence and Aging., doi:10.1007/s00281-020-00824-x/Published.
72. Aiello, A.; Farzaneh, F.; Candore, G.; Caruso, C.; Davinelli, S.; Gambino, C.M.; Ligotti, M.E.; Zareian, N.; Accardi, G. Immunosenescence and Its Hallmarks: How to Oppose Aging Strategically? A Review of Potential Options for Therapeutic Intervention. *Front Immunol* 2019, *10*.
73. Pereira, B.I.; De Maeyer, R.P.H.; Covre, L.P.; Nehar-Belaid, D.; Lanna, A.; Ward, S.; Marches, R.; Chambers, E.S.; Gomes, D.C.O.; Riddell, N.E.; et al. Sestrins Induce Natural Killer Function in Senescent-like CD8+ T Cells. *Nat Immunol* **2020**, *21*, 684–694, doi:10.1038/s41590-020-0643-3.
74. Quinn, K.M.; Palchaudhuri, R.; Palmer, C.S.; La Gruta, N.L. The Clock Is Ticking: The Impact of Ageing on T Cell Metabolism. *Clin Transl Immunology* 2019, *8*.
75. Goronzy, J.J.; Weyand, C.M. Mechanisms Underlying T Cell Ageing. *Nat Rev Immunol* **2019**, *19*, 573–583, doi:10.1038/s41577-019-0180-1.
76. Oh, S.J.; Lee, J.K.; Shin, O.S. Aging and the Immune System: The Impact of Immunosenescence on Viral Infection, Immunity and Vaccine Immunogenicity. *Immune Netw* **2019**, *19*, doi:10.4110/in.2019.19.e37.
77. Agrawal, A.; Agrawal, S.; Gupta, S. Role of Dendritic Cells in Inflammation and Loss of Tolerance in the Elderly. *Front Immunol* 2017, *8*.
78. Liu, Z.; Liang, Q.; Ren, Y.; Guo, C.; Ge, X.; Wang, L.; Cheng, Q.; Luo, P.; Zhang, Y.; Han, X. Immunosenescence: Molecular Mechanisms and Diseases. *Signal Transduct Target Ther* **2023**, *8*, 200, doi:10.1038/s41392-023-01451-2.

79. Lu, R.J.; Wang, E.K.; Benayoun, B.A. Functional Genomics of Inflamm-Aging and Immunosenescence. *Brief Funct Genomics* **2022**, *21*, 43–55, doi:10.1093/bfgp/elab009.
80. Cunha, L.L.; Valsecchi, V.A. dos S.; Ward, L.S. Investigating Population-Level Immunosenescence: From Bench to Bedside. *Front Immunol* 2022, *13*.
81. Rodrigues, L.P.; Teixeira, V.R.; Alencar-Silva, T.; Simonassi-Paiva, B.; Pereira, R.W.; Pogue, R.; Carvalho, J.L. Hallmarks of Aging and Immunosenescence: Connecting the Dots. *Cytokine Growth Factor Rev* 2021, *59*, 9–21.
82. Liang, Z.; Dong, X.; Zhang, Z.; Zhang, Q.; Zhao, Y. Age-Related Thymic Involution: Mechanisms and Functional Impact. *Aging Cell* 2022, *21*.
83. Rodriguez, I.J.; Lalinde Ruiz, N.; Llano León, M.; Martínez Enríquez, L.; Montilla Velásquez, M. del P.; Ortiz Aguirre, J.P.; Rodríguez Bohórquez, O.M.; Velandia Vargas, E.A.; Hernández, E.D.; Parra López, C.A. Immunosenescence Study of T Cells: A Systematic Review. *Front Immunol* **2021**, *11*, doi:10.3389/fimmu.2020.604591.
84. Ackermann, J.; Arndt, L.; Fröba, J.; Lindhorst, A.; Glaß, M.; Kirstein, M.; Hobusch, C.; Wunderlich, F.T.; Braune, J.; Gericke, M. IL-6 Signaling Drives Self-Renewal and Alternative Activation of Adipose Tissue Macrophages. *Front Immunol* **2024**, *15*, doi:10.3389/fimmu.2024.1201439.
85. Belarif, L.; Mary, C.; Jacquemont, L.; Mai, H. Le; Danger, R.; Hervouet, J.; Minault, D.; Thepenier, V.; Nerrière-Daguin, V.; Nguyen, E.; et al. IL-7 Receptor Blockade Blunts Antigen-Specific Memory T Cell Responses and Chronic Inflammation in Primates. *Nat Commun* **2018**, *9*, 4483, doi:10.1038/s41467-018-06804-y.
86. Appay, V.; Sauce, D. Naive T Cells: The Crux of Cellular Immune Aging? *Exp Gerontol* 2014, *54*, 90–93.
87. Moro-García, M.A. When Aging Reaches CD4+ T-Cells: Phenotypic and Functional Changes. *Front Immunol* **2013**, *4*, doi:10.3389/fimmu.2013.00107.
88. Zhang, J.; He, T.; Xue, L.; Guo, H. Senescent T Cells: A Potential Biomarker and Target for Cancer Therapy. *EBioMedicine* **2021**, *68*, 103409, doi:10.1016/j.ebiom.2021.103409.
89. Goronzy, J.J.; Fang, F.; Cavanagh, M.M.; Qi, Q.; Weyand, C.M. Naive T Cell Maintenance and Function in Human Aging. *The Journal of Immunology* **2015**, *194*, 4073–4080, doi:10.4049/jimmunol.1500046.
90. Shirakawa, K.; Sano, M. T Cell Immunosenescence in Aging, Obesity, and Cardiovascular Disease. *Cells* 2021, *10*.
91. Pinti, M.; Appay, V.; Campisi, J.; Frasca, D.; Fülöp, T.; Sauce, D.; Larbi, A.; Weinberger, B.; Cossarizza, A. Aging of the Immune System: Focus on Inflammation and Vaccination. *Eur J Immunol* 2016, *46*, 2286–2301.
92. Briceño, O.; Lissina, A.; Wanke, K.; Afonso, G.; von Braun, A.; Ragon, K.; Miquel, T.; Gostick, E.; Papagno, L.; Stiasny, K.; et al. Reduced Naïve CD8+ T-Cell Priming Efficacy in Elderly Adults. *Aging Cell* **2016**, *15*, 14–21, doi:10.1111/acel.12384.
93. GUPTA, S.; GOLLAPUDI, S. TNF-α-Induced Apoptosis in Human Naïve and Memory CD8+ T Cells in Aged Humans. *Exp Gerontol* **2006**, *41*, 69–77, doi:10.1016/j.exger.2005.10.001.
94. Lee, K. a.; Robbins, P.D.; Camell, C.D. Intersection of Immunometabolism and Immunosenescence during Aging. *Curr Opin Pharmacol* 2021, *57*, 107–116.
95. Dock, J.N.; Effros, R.B. Role of CD8 T Cell Replicative Senescence in Human Aging and in HIV-Mediated Immunosenescence. *Aging Dis* **2011**, *2*, 382–397.
96. Bartleson, J.M.; Radenkovic, D.; Covarrubias, A.J.; Furman, D.; Winer, D.A.; Verdin, E. SARS-CoV-2, COVID-19 and the Aging Immune System. *Nat Aging* 2021, *1*, 769–782.
97. Gallerani, E.; Proietto, D.; Dallan, B.; Campagnaro, M.; Pacifico, S.; Albanese, V.; Marzola, E.; Marconi, P.; Caputo, A.; Appay, V.; et al. Impaired Priming of SARS-CoV-2-Specific Naive CD8+ T Cells in Older Subjects. *Front Immunol* **2021**, *12*, doi:10.3389/fimmu.2021.693054.

98. Wang, Y.; Dong, C.; Han, Y.; Gu, Z.; Sun, C. Immunosenescence, Aging and Successful Aging. *Front Immunol* 2022, *13*.
99. Frasca, D.; Diaz, A.; Romero, M.; Landin, A.M.; Blomberg, B.B. Age Effects on B Cells and Humoral Immunity in Humans. *Ageing Res Rev* 2011, *10*, 330–335.
100. Pioli, P.D.; Casero, D.; Montecino-Rodriguez, E.; Morrison, S.L.; Dorshkind, K. Plasma Cells Are Obligate Effectors of Enhanced Myelopoiesis in Aging Bone Marrow. *Immunity* **2019**, *51*, 351-366.e6, doi:10.1016/j.immuni.2019.06.006.
101. Roth-Walter, F.; Adcock, I.M.; Benito-Villalvilla, C.; Bianchini, R.; Bjermer, L.; Caramori, G.; Cari, L.; Chung, K.F.; Diamant, Z.; Eguiluz-Gracia, I.; et al. Metabolic Pathways in Immune Senescence and Inflammaging: Novel Therapeutic Strategy for Chronic Inflammatory Lung Diseases. An EAACI Position Paper from the Task Force for Immunopharmacology. *Allergy: European Journal of Allergy and Clinical Immunology* **2024**, *79*, 1089–1122, doi:10.1111/all.15977.
102. Mehdizadeh, M.; Aguilar, M.; Thorin, E.; Ferbeyre, G.; Nattel, S. The Role of Cellular Senescence in Cardiac Disease: Basic Biology and Clinical Relevance. *Nat Rev Cardiol* **2022**, *19*, 250–264, doi:10.1038/s41569-021-00624-2.
103. Chini, C.; Hogan, K.A.; Warner, G.M.; Tarragó, M.G.; Peclat, T.R.; Tchkonia, T.; Kirkland, J.L.; Chini, E. The NADase CD38 Is Induced by Factors Secreted from Senescent Cells Providing a Potential Link between Senescence and Age-Related Cellular NAD+ Decline. *Biochem Biophys Res Commun* **2019**, *513*, 486–493, doi:10.1016/j.bbrc.2019.03.199.
104. Kurupati, R.K.; Haut, L.H.; Schmader, K.E.; Ertl, H.CJ. Age-Related Changes in B Cell Metabolism. *Aging* **2019**, *11*, 4367–4381, doi:10.18632/aging.102058.
105. Nicoli, F.; Cabral-Piccin, M.P.; Papagno, L.; Gallerani, E.; Fusaro, M.; Folcher, V.; Dubois, M.; Clave, E.; Vallet, H.; Frere, J.J.; et al. Altered Basal Lipid Metabolism Underlies the Functional Impairment of Naive CD8+ T Cells in Elderly Humans. *The Journal of Immunology* **2022**, *208*, 562–570, doi:10.4049/jimmunol.2100194.
106. Pera, A.; Campos, C.; López, N.; Hassouneh, F.; Alonso, C.; Tarazona, R.; Solana, R. Immunosenescence: Implications for Response to Infection and Vaccination in Older People. *Maturitas* **2015**, *82*, 50–55, doi:10.1016/j.maturitas.2015.05.004.
107. Weinberger, B. Vaccination of Older Adults: Influenza, Pneumococcal Disease, Herpes Zoster, COVID-19 and Beyond. *Immunity and Ageing* 2021, *18*.
108. Addario, A.; Célarier, T.; Bongue, B.; Barth, N.; Gavazzi, G.; Botelho-Nevers, E. Impact of Influenza, Herpes Zoster, and Pneumococcal Vaccinations on the Incidence of Cardiovascular Events in Subjects Aged over 65 Years: A Systematic Review. *Geroscience* 2023, *45*, 3419–3447.
109. Cunningham, A.L.; McIntyre, P.; Subbarao, K.; Booy, R.; Levin, M.J. Vaccines for Older Adults. *BMJ* **2021**, n188, doi:10.1136/bmj.n188.
110. Hou, Y.; Chen, M.; Bian, Y.; Hu, Y.; Chuan, J.; Zhong, L.; Zhu, Y.; Tong, R. Insights into Vaccines for Elderly Individuals: From the Impacts of Immunosenescence to Delivery Strategies. *NPJ Vaccines* **2024**, *9*, 77, doi:10.1038/s41541-024-00874-4.
111. Ma, S.; Wang, C.; Mao, X.; Hao, Y. R Cells Dysfunction Associated with Aging and Autoimmune Disease. *Front Immunol* 2019, *10*.
112. Lee, B.; Bae, G.E.; Jeong, I.H.; Kim, J.-H.; Kwon, M.-J.; Kim, J.; Kim, B.; Lee, J.-W.; Nam, J.-H.; Huh, H.J.; et al. Age-Related Differences in Neutralizing Antibody Responses against SARS-CoV-2 Delta and Omicron Variants in 151 SARS-CoV-2-Naïve Metropolitan Residents Boosted with BNT162b2. *J Appl Lab Med* **2024**, *9*, 741–751, doi:10.1093/jalm/jfae014.
113. Decman, V.; Laidlaw, B.J.; Doering, T.A.; Leng, J.; Ertl, H.C.J.; Goldstein, D.R.; Wherry, E.J. Defective CD8 T Cell Responses in Aged Mice Are Due to Quantitative and Qualitative Changes in Virus-Specific Precursors. *The Journal of Immunology* **2012**, *188*, 1933–1941, doi:10.4049/jimmunol.1101098.

114. Lages, C.S.; Lewkowich, I.; Sproles, A.; Wills-Karp, M.; Chougnet, C. Partial Restoration of T-Cell Function in Aged Mice by in Vitro Blockade of the PD-1/PD-L1 Pathway. *Aging Cell* **2010**, *9*, 785–798, doi:10.1111/j.1474-9726.2010.00611.x.
115. Lee, K.A.; Shin, K.S.; Kim, G.Y.; Song, Y.C.; Bae, E.A.; Kim, I.K.; Koh, C.H.; Kang, C.Y. Characterization of Age-Associated Exhausted CD8+ T Cells Defined by Increased Expression of Tim-3 and PD-1. *Aging Cell* **2016**, *15*, 291–300, doi:10.1111/acel.12435.
116. Grifoni, A.; Alonzi, T.; Alter, G.; Noonan, D.M.C.; Landay, A.L.; Albini, A.; Goletti, D. Impact of Aging on Immunity in the Context of COVID-19, HIV, and Tuberculosis. *Front Immunol* 2023, *14*.
117. Booth, A.; Reed, A.B.; Ponzo, S.; Yassaee, A.; Aral, M.; Plans, D.; Labrique, A.; Mohan, D. Population Risk Factors for Severe Disease and Mortality in COVID-19: A Global Systematic Review and Meta-Analysis. *PLoS One* 2021, *16*.
118. Nalbandian, A.; Sehgal, K.; Gupta, A.; Madhavan, M. V.; McGroder, C.; Stevens, J.S.; Cook, J.R.; Nordvig, A.S.; Shalev, D.; Sehrawat, T.S.; et al. Post-Acute COVID-19 Syndrome. *Nat Med* 2021, *27*, 601–615.
119. Song, J.Y.; Nahm, M.H.; Moseley, M.A. Clinical Implications of Pneumococcal Serotypes: Invasive Disease Potential, Clinical Presentations, and Antibiotic Resistance. *J Korean Med Sci* 2013, *28*, 4–15.
120. Klein, E.Y.; Monteforte, B.; Gupta, A.; Jiang, W.; May, L.; Hsieh, Y.H.; Dugas, A. The Frequency of Influenza and Bacterial Coinfection: A Systematic Review and Meta-Analysis. *Influenza Other Respir Viruses* 2016, *10*, 394–403.
121. Kelly, D.F.; Snape, M.D.; Cutterbuck, E.A.; Green, S.; Snowden, C.; Diggle, L.; Yu, L.M.; Borkowski, A.; Moxon, E.R.; Pollard, A.J. CRM197-Conjugated Serogroup C Meningococcal Capsular Polysaccharide, but Not the Native Polysaccharide, Induces Persistent Antigen-Specific Memory B Cells. *Blood* **2006**, *108*, 2642–2647, doi:10.1182/blood-2006-01-009282.
122. Pilishvili, T.; Lexau, C.; Farley, M.M.; Hadler, J.; Harrison, L.H.; Bennett, N.M.; Reingold, A.; Thomas, A.; Schaffner, W.; Craig, A.S.; et al. Sustained Reductions in Invasive Pneumococcal Disease in the Era of Conjugate Vaccine. *J Infect Dis* **2010**, *201*, 32–41, doi:10.1086/648593.
123. Wrona, M. V.; Ghosh, R.; Coll, K.; Chun, C.; Yousefzadeh, M.J. The 3 I's of Immunity and Aging: Immunosenescence, Inflammaging, and Immune Resilience. *Frontiers in Aging* **2024**, *5*, doi:10.3389/fragi.2024.1490302.
124. Kline, K.A.; Bowdish, D.M. Infection in an Aging Population. *Curr Opin Microbiol* **2016**, *29*, 63–67, doi:10.1016/j.mib.2015.11.003.
125. Kim, D.; Quinn, J.; Pinsky, B.; Shah, N.H.; Brown, I. Rates of Co-Infection Between SARS-CoV-2 and Other Respiratory Pathogens. *JAMA* **2020**, *323*, 2085, doi:10.1001/jama.2020.6266.
126. Morris, D.E.; Cleary, D.W.; Clarke, S.C. Secondary Bacterial Infections Associated with Influenza Pandemics. *Front Microbiol* **2017**, *8*, doi:10.3389/fmicb.2017.01041.
127. Chertow, D.S.; Memoli, M.J. Bacterial Coinfection in Influenza. *JAMA* **2013**, *309*, 275, doi:10.1001/jama.2012.194139.
128. Gustafson, C.E.; Kim, C.; Weyand, C.M.; Goronzy, J.J. Influence of Immune Aging on Vaccine Responses. *J Allergy Clin Immunol* **2020**, *145*, 1309–1321, doi:10.1016/j.jaci.2020.03.017.
129. Bredholt, G.; Sævik, M.; Søyland, H.; Ueland, T.; Zhou, F.; Pathirana, R.; Madsen, A.; Vahokoski, J.; Lartey, S.; Halvorsen, B.E.; et al. Three Doses of Sars-CoV-2 MRNA Vaccine in Older Adults Result in Similar Antibody Responses but Reduced Cellular Cytokine Responses Relative to Younger Adults. *Vaccine X* **2024**, *20*, 100564, doi:10.1016/j.jvacx.2024.100564.
130. Kawasuji, H.; Morinaga, Y.; Tani, H.; Saga, Y.; Kaneda, M.; Murai, Y.; Ueno, A.; Miyajima, Y.; Fukui, Y.; Nagaoka, K.; et al. Age-Dependent Reduction in Neutralization against Alpha

and Beta Variants of BNT162b2 SARS-CoV-2 Vaccine-Induced Immunity. *Microbiol Spectr* **2021**, *9*, doi:10.1128/Spectrum.00561-21.
131. Hou, Y.; Chen, M.; Bian, Y.; Hu, Y.; Chuan, J.; Zhong, L.; Zhu, Y.; Tong, R. Insights into Vaccines for Elderly Individuals: From the Impacts of Immunosenescence to Delivery Strategies. *NPJ Vaccines* **2024**, *9*, 77, doi:10.1038/s41541-024-00874-4.
132. Edelman, R.; Deming, M.E.; Toapanta, F.R.; Heuser, M.D.; Chrisley, L.; Barnes, R.S.; Wasserman, S.S.; Blackwelder, W.C.; Handwerger, B.S.; Pasetti, M.; et al. The SENIEUR Protocol and the Efficacy of Hepatitis B Vaccination in Healthy Elderly Persons by Age, Gender, and Vaccine Route. *Immunity & Ageing* **2020**, *17*, 9, doi:10.1186/s12979-020-00179-9.
133. Fulop, T.; Larbi, A.; Pawelec, G.; Khalil, A.; Cohen, A.A.; Hirokawa, K.; Witkowski, J.M.; Franceschi, C. Immunology of Aging: The Birth of Inflammaging. *Clin Rev Allergy Immunol* 2023, *64*, 109–122.
134. Lee, K.A.; Flores, R.R.; Jang, I.H.; Saathoff, A.; Robbins, P.D. Immune Senescence, Immunosenescence and Aging. *Frontiers in Aging* 2022, *3*.
135. Witkowski, J.M.; Fulop, T.; Bryl, E. Immunosenescence and COVID-19. *Mech Ageing Dev* **2022**, *204*, doi:10.1016/j.mad.2022.111672.
136. Timóteo, A.T.; Ramos, R.; Toste, A.; Lousinha, A.; Oliveira, J.A.; Ferreira, M.L.; Ferreira, R.C. Impacto Da Idade No Tratamento e Resultados Após Enfarte Agudo Do Miocárdio Em Particular Nos Muito Idosos. *Revista Portuguesa de Cardiologia* **2011**, *30*, 897–903, doi:10.1016/j.repc.2011.09.013.
137. McMechan, S.R.; Adgey, A.A.J. Age Related Outcome in Acute Myocardial Infarction. *BMJ* **1998**, *317*, 1334–1335, doi:10.1136/bmj.317.7169.1334.
138. Sagris, M.; Antonopoulos, A.S.; Theofilis, P.; Oikonomou, E.; Siasos, G.; Tsalamandris, S.; Antoniades, C.; Brilakis, E.S.; Kaski, J.C.; Tousoulis, D. Risk Factors Profile of Young and Older Patients with Myocardial Infarction. *Cardiovasc Res* 2022, *118*, 2281–2292.
139. Xia, T.; Zhou, Y.; An, J.; Cui, Z.; Zhong, X.; Cui, T.; Lv, B.; Zhao, X.; Gao, X. Benefit Delayed Immunosenescence by Regulating CD4+T Cells: A Promising Therapeutic Target for Aging-Related Diseases. *Aging Cell* 2024.
140. Ross, M.D.; Malone, E.M.; Simpson, R.; Cranston, I.; Ingram, L.; Wright, G.P.; Chambers, G.; Florida-James, G. Lower Resting and Exercise-Induced Circulating Angiogenic Progenitors and Angiogenic T Cells in Older Men. *Am J Physiol Heart Circ Physiol* **2018**, *314*, H392–H402, doi:10.1152/ajpheart.00592.2017.
141. Gaddis, D.E.; Padgett, L.E.; Wu, R.; Nguyen, A.; McSkimming, C.; Dinh, H.Q.; Araujo, D.J.; Taylor, A.M.; McNamara, C.A.; Hedrick, C.C. Atherosclerosis Impairs Naive CD4 T-Cell Responses via Disruption of Glycolysis. *Arterioscler Thromb Vasc Biol* **2021**, *41*, 2387–2398, doi:10.1161/ATVBAHA.120.314189.
142. He, C.; Kim, H.I.; Park, J.; Guo, J.; Huang, W. The Role of Immune Cells in Different Stages of Atherosclerosis. *Int J Med Sci* **2024**, *21*, 1129–1143, doi:10.7150/ijms.94570.
143. Guan, Y.; Cao, M.; Wu, X.; Yan, J.; Hao, Y.; Zhang, C. CD28null T Cells in Aging and Diseases: From Biology to Assessment and Intervention. *Int Immunopharmacol* 2024, *131*.
144. Kong, P.; Cui, Z.Y.; Huang, X.F.; Zhang, D.D.; Guo, R.J.; Han, M. Inflammation and Atherosclerosis: Signaling Pathways and Therapeutic Intervention. *Signal Transduct Target Ther* 2022, *7*.
145. Palatella, M.; Guillaume, S.M.; Linterman, M.A.; Huehn, J. The Dark Side of Tregs during Aging. *Front Immunol* 2022, *13*.
146. Jagger, A.; Shimojima, Y.; Goronzy, J.J.; Weyand, C.M. Regulatory T Cells and the Immune Aging Process: A Mini-Review. *Gerontology* 2014, *60*, 130–137.
147. Malaikah, S.; Willis, S.A.; Henson, J.; Sargeant, J.A.; Yates, T.; Thackray, A.E.; Goltz, F.R.; Roberts, M.J.; Bodicoat, D.H.; Aithal, G.P.; et al. Associations of Objectively Measured Physical Activity, Sedentary Time and Cardiorespiratory Fitness with Adipose Tissue Insulin

Resistance and Ectopic Fat. *Int J Obes* **2023**, *47*, 1000–1007, doi:10.1038/s41366-023-01350-0.
148. Salvestrini, V.; Sell, C.; Lorenzini, A. Obesity May Accelerate the Aging Process. *Front Endocrinol (Lausanne)* 2019, *10*.
149. Jura, M.; Kozak, L.P. Obesity and Related Consequences to Ageing. *Age (Omaha)* **2016**, *38*, doi:10.1007/s11357-016-9884-3.
150. Zhang, Y.; Wen, W.; Liu, H. *The Role of Immune Cells in Cardiac Remodeling After Myocardial Infarction*; 2020;
151. Pangrazzi, L.; Naismith, E.; Miggitsch, C.; Carmona Arana, J.A.; Keller, M.; Grubeck-Loebenstein, B.; Weinberger, B. The Impact of Body Mass Index on Adaptive Immune Cells in the Human Bone Marrow. *Immunity and Ageing* **2020**, *17*, doi:10.1186/s12979-020-00186-w.
152. Joisten, N.; Wences Chirino, T.Y.; Boßlau, T.K.; Wasserfurth, P.; Hahn, A.; Krüger, K.; Zimmer, P. Older Adults with Cytomegalovirus Reveal Increased CD8+/CD4+ EMRA T Cells and Elevated Systemic Levels of Kynurenic Acid. *Immunology* 2023, *169*, 113–116.
153. Ghattas, A.; Griffiths, H.R.; Devitt, A.; Lip, G.Y.H.; Shantsila, E. Monocytes in Coronary Artery Disease and Atherosclerosis: Where Are We Now? *J Am Coll Cardiol* 2013, *62*, 1541–1551.
154. Feng, Q.; Li, Q.; Zhou, H.; Sun, L.; Lin, C.; Jin, Y.; Wang, D.; Guo, G. The Role of Major Immune Cells in Myocardial Infarction. *Front Immunol* **2023**, *13*, doi:10.3389/fimmu.2022.1084460.
155. Kino, T.; Khan, M.; Mohsin, S. The Regulatory Role of T Cell Responses in Cardiac Remodeling Following Myocardial Infarction. *Int J Mol Sci* **2020**, *21*, 5013, doi:10.3390/ijms21145013.
156. García-Rivas, G.; Castillo, E.C.; Gonzalez-Gil, A.M.; Maravillas-Montero, J.L.; Brunck, M.; Torres-Quintanilla, A.; Elizondo-Montemayor, L.; Torre-Amione, G. The Role of B Cells in Heart Failure and Implications for Future Immunomodulatory Treatment Strategies. *ESC Heart Fail* **2020**, *7*, 1387–1399, doi:10.1002/ehf2.12744.
157. Tonet, E.; Raisi, A.; Zagnoni, S.; Chiaranda, G.; Pavasini, R.; Vitali, F.; Gibiino, F.; Campana, R.; Boccadoro, A.; Scala, A.; et al. Multi-Domain Lifestyle Intervention in Older Adults after Myocardial Infarction: Rationale and Design of the PIpELINe Randomized Clinical Trial. *Aging Clin Exp Res* **2023**, *35*, 1107–1115, doi:10.1007/s40520-023-02389-9.
158. Raisi, A.; Piva, T.; Myers, J.; Zerbini, V.; Mandini, S.; Zappaterra, T.; Mazzoni, G.; Tonet, E.; Pavasini, R.; Campo, G.; et al. Experience and Perceptions among Older Outpatients after Myocardial Infarction Following an Exercise Intervention: A Qualitative Analysis from the PIpELINe Trial. *Int J Environ Res Public Health* **2023**, *20*, doi:10.3390/ijerph20032196.
159. Fermont, J.M.; Mohan, D.; Fisk, M.; Bolton, C.E.; Macnee, W.; Cockcroft, J.R.; McEniery, C.; Fuld, J.; Cheriyan, J.; Tal-Singer, R.; et al. Short Physical Performance Battery as a Practical Tool to Assess Mortality Risk in Chronic Obstructive Pulmonary Disease. *Age Ageing* **2021**, *50*, 795–801, doi:10.1093/ageing/afaa138.
160. Kologrivova, I.; Shtatolkina, M.; Suslova, T.; Ryabov, V. Cells of the Immune System in Cardiac Remodeling: Main Players in Resolution of Inflammation and Repair After Myocardial Infarction. *Front Immunol* 2021, *12*.
161. Tsujioka, H.; Imanishi, T.; Ikejima, H.; Kuroi, A.; Takarada, S.; Tanimoto, T.; Kitabata, H.; Okochi, K.; Arita, Y.; Ishibashi, K.; et al. Impact of Heterogeneity of Human Peripheral Blood Monocyte Subsets on Myocardial Salvage in Patients With Primary Acute Myocardial Infarction. *J Am Coll Cardiol* **2009**, *54*, 130–138, doi:10.1016/j.jacc.2009.04.021.
162. Kapellos, T.S.; Bonaguro, L.; Gemünd, I.; Reusch, N.; Saglam, A.; Hinkley, E.R.; Schultze, J.L. Human Monocyte Subsets and Phenotypes in Major Chronic Inflammatory Diseases. *Front Immunol* 2019, *10*.

163. Le Page, A.; Dupuis, G.; Larbi, A.; Witkowski, J.M.; Fülöp, T. Signal Transduction Changes in CD4 + and CD8 + T Cell Subpopulations with Aging. *Exp Gerontol* **2018**, *105*, 128–139, doi:10.1016/j.exger.2018.01.005.
164. Ventura, M.T.; Casciaro, M.; Gangemi, S.; Buquicchio, R. Immunosenescence in Aging: Between Immune Cells Depletion and Cytokines up-Regulation. *Clinical and Molecular Allergy* 2017, *15*.
165. Piao, L.; Zhao, G.; Zhu, E.; Inoue, A.; Shibata, R.; Lei, Y.; Hu, L.; Yu, C.; Yang, G.; Wu, H.; et al. Chronic Psychological Stress Accelerates Vascular Senescence and Impairs Ischemia-Induced Neovascularization: The Role of Dipeptidyl Peptidase-4/Glucagon-Like Peptide-1-Adiponectin Axis. *J Am Heart Assoc* **2017**, *6*, doi:10.1161/JAHA.117.006421.
166. Quiros-Roldan, E.; Sottini, A.; Natali, P.G.; Imberti, L. The Impact of Immune System Aging on Infectious Diseases. *Microorganisms* 2024, *12*.
167. Zhang, R.Y.K.; Cochran, B.J.; Thomas, S.R.; Rye, K.A. Impact of Reperfusion on Temporal Immune Cell Dynamics After Myocardial Infarction. *J Am Heart Assoc* 2023, *12*.
168. Lazuardi, L.; Jenewein, B.; Wolf, A.M.; Pfister, G.; Tzankov, A.; Grubeck-Loebenstein, B. Age-Related Loss of Naïve T Cells and Dysregulation of T-Cell/B-Cell Interactions in Human Lymph Nodes. *Immunology* **2005**, *114*, 37–43, doi:10.1111/j.1365-2567.2004.02006.x.
169. Xing, Y.F.; Cai, J.R.; Qin, J.J.; Zhou, W.Y.; Li, C.M.; Li, X. Expansion of Monocytic Myeloid-Derived Suppressor Cells in Patients Under Hemodialysis Might Lead to Cardiovascular and Cerebrovascular Events. *Front Immunol* **2021**, *11*, doi:10.3389/fimmu.2020.577253.
170. Callender, L.A.; Carroll, E.C.; Beal, R.W.J.; Chambers, E.S.; Nourshargh, S.; Akbar, A.N.; Henson, S.M. Human CD8+ EMRA T Cells Display a Senescence-Associated Secretory Phenotype Regulated by P38 MAPK. *Aging Cell* **2018**, *17*, doi:10.1111/acel.12675.
171. Tobin, S.W.; Alibhai, F.J.; Weisel, R.D.; Li, R.K. Considering Cause and Effect of Immune Cell Aging on Cardiac Repair after Myocardial Infarction. *Cells* 2020, *9*.
172. Cao, W.; Wang, K.; Wang, J.; Chen, Y.; Gong, H.; Xiao, L.; Pan, W. Causal Relationship between Immune Cells and Risk of Myocardial Infarction: Evidence from a Mendelian Randomization Study. *Front Cardiovasc Med* **2024**, *11*, doi:10.3389/fcvm.2024.1416112.
173. Nicoli, F.; Solis-Soto, M.T.; Paudel, D.; Marconi, P.; Gavioli, R.; Appay, V.; Caputo, A. Age-Related Decline of de Novo T Cell Responsiveness as a Cause of COVID-19 Severity. *Geroscience* 2020, *42*, 1015–1019.
174. Nicoli, F.; Paudel, D.; Solis-Soto, M.T. Old and New Coronaviruses in the Elderly. *Aging* **2021**, *13*, 12295–12296, doi:10.18632/aging.203065.
175. Arregocés-Castillo, L.; Fernández-Niño, J.; Rojas-Botero, M.; Palacios-Clavijo, A.; Galvis-Pedraza, M.; Rincón-Medrano, L.; Pinto-Álvarez, M.; Ruiz-Gómez, F.; Trejo-Valdivia, B. Effectiveness of COVID-19 Vaccines in Older Adults in Colombia: A Retrospective, Population-Based Study of the ESPERANZA Cohort. *Lancet Healthy Longev* **2022**, *3*, e242–e252, doi:10.1016/S2666-7568(22)00035-6.
176. Verity, R.; Okell, L.C.; Dorigatti, I.; Winskill, P.; Whittaker, C.; Imai, N.; Cuomo-Dannenburg, G.; Thompson, H.; Walker, P.G.T.; Fu, H.; et al. Estimates of the Severity of Coronavirus Disease 2019: A Model-Based Analysis. *Lancet Infect Dis* **2020**, *20*, 669–677, doi:10.1016/S1473-3099(20)30243-7.
177. Hazeldine, J.; Lord, J.M. Innate Immunesenescence: Underlying Mechanisms and Clinical Relevance. *Biogerontology* **2015**, *16*, 187–201, doi:10.1007/s10522-014-9514-3.
178. Rydyznski Moderbacher, C.; Ramirez, S.I.; Dan, J.M.; Grifoni, A.; Hastie, K.M.; Weiskopf, D.; Belanger, S.; Abbott, R.K.; Kim, C.; Choi, J.; et al. Antigen-Specific Adaptive Immunity to SARS-CoV-2 in Acute COVID-19 and Associations with Age and Disease Severity. *Cell* **2020**, *183*, 996-1012.e19, doi:10.1016/j.cell.2020.09.038.
179. Nicoli, F.; Clave, E.; Wanke, K.; von Braun, A.; Bondet, V.; Alanio, C.; Douay, C.; Baque, M.; Lependu, C.; Marconi, P.; et al. Primary Immune Responses Are Negatively Impacted by Persistent Herpesvirus Infections in Older People: Results from an Observational Study on

Healthy Subjects and a Vaccination Trial on Subjects Aged More than 70 Years Old. *EBioMedicine* **2022**, *76*, 103852, doi:10.1016/j.ebiom.2022.103852.
180. Westmeier, J.; Paniskaki, K.; Karaköse, Z.; Werner, T.; Sutter, K.; Dolff, S.; Overbeck, M.; Limmer, A.; Liu, J.; Zheng, X.; et al. Erratum for Westmeier et al., "Impaired Cytotoxic CD8 $^{+}$ T Cell Response in Elderly COVID-19 Patients." *mBio* **2020**, *11*, doi:10.1128/mBio.02805-20.
181. Pittet, M.J.; Valmori, D.; Dunbar, P.R.; Speiser, D.E.; Liénard, D.; Lejeune, F.; Fleischhauer, K.; Cerundolo, V.; Cerottini, J.-C.; Romero, P. *High Frequencies of Naive Melan-A/MART-1-Specific CD8 T Cells in a Large Proportion of Human Histocompatibility Leukocyte Antigen (HLA)-A2 Individuals*; 1999; Vol. 190;.
182. Price, D.A.; Brenchley, J.M.; Ruff, L.E.; Betts, M.R.; Hill, B.J.; Roederer, M.; Koup, R.A.; Migueles, S.A.; Gostick, E.; Wooldridge, L.; et al. Avidity for Antigen Shapes Clonal Dominance in CD8+ T Cell Populations Specific for Persistent DNA Viruses. *Journal of Experimental Medicine* **2005**, *202*, 1349–1361, doi:10.1084/jem.20051357.
183. Prakash, S.; Srivastava, R.; Coulon, P.-G.; Dhanushkodi, N.R.; Chentoufi, A.A.; Tifrea, D.F.; Edwards, R.A.; Figueroa, C.J.; Schubl, S.D.; Hsieh, L.; et al. Genome-Wide Asymptomatic B-Cell, CD4 $^{+}$ and CD8 $^{+}$ T-Cell Epitopes, That Are Highly Conserved Between Human and Animal Coronaviruses, Identified from SARS-CoV-2 as Immune Targets for Pre-Emptive Pan-Coronavirus Vaccines 2020.
184. Lee, E.; Sandgren, K.; Duette, G.; Stylianou, V. V.; Khanna, R.; Eden, J.-S.; Blyth, E.; Gottlieb, D.; Cunningham, A.L.; Palmer, S. Identification of SARS-CoV-2 Nucleocapsid and Spike T-Cell Epitopes for Assessing T-Cell Immunity. *J Virol* **2021**, *95*, doi:10.1128/JVI.02002-20.
185. Gutjahr, A.; Papagno, L.; Nicoli, F.; Lamoureux, A.; Vernejoul, F.; Lioux, T.; Gostick, E.; Price, D.A.; Tiraby, G.; Perouzel, E.; et al. Cutting Edge: A Dual TLR2 and TLR7 Ligand Induces Highly Potent Humoral and Cell-Mediated Immune Responses. *The Journal of Immunology* **2017**, *198*, 4205–4209, doi:10.4049/jimmunol.1602131.
186. Fali, T.; Fabre-Mersseman, V.; Yamamoto, T.; Bayard, C.; Papagno, L.; Fastenackels, S.; Zoorab, R.; Koup, R.A.; Boddaert, J.; Sauce, D.; et al. Elderly Human Hematopoietic Progenitor Cells Express Cellular Senescence Markers and Are More Susceptible to Pyroptosis. *JCI Insight* **2018**, *3*, doi:10.1172/jci.insight.95319.
187. Zhang, H.; Weyand, C.M.; Goronzy, J.J.; Gustafson, C.E. Understanding T Cell Aging to Improve Anti-Viral Immunity. *Curr Opin Virol* 2021, *51*, 127–133.
188. Mathew, D.; Giles, J.R.; Baxter, A.E.; Oldridge, D.A.; Greenplate, A.R.; Wu, J.E.; Alanio, C.; Kuri-Cervantes, L.; Pampena, M.B.; D'Andrea, K.; et al. Deep Immune Profiling of COVID-19 Patients Reveals Distinct Immunotypes with Therapeutic Implications. *Science (1979)* **2020**, *369*, doi:10.1126/science.abc8511.
189. Witkowski, J.M. Immune System Aging and the Aging-Related Diseases in the COVID-19 Era. *Immunol Lett* **2022**, *243*, 19–27, doi:10.1016/j.imlet.2022.01.005.
190. Szeto, C.; Nguyen, A.T.; Lobos, C.A.; Chatzileontiadou, D.S.M.; Jayasinghe, D.; Grant, E.J.; Riboldi-Tunnicliffe, A.; Smith, C.; Gras, S. Molecular Basis of a Dominant SARS-CoV-2 Spike-Derived Epitope Presented by HLA-A*02:01 Recognised by a Public TCR. *Cells* **2021**, *10*, 2646, doi:10.3390/cells10102646.
191. Chaurasia, P.; Nguyen, T.H.O.; Rowntree, L.C.; Juno, J.A.; Wheatley, A.K.; Kent, S.J.; Kedzierska, K.; Rossjohn, J.; Petersen, J. Structural Basis of Biased T Cell Receptor Recognition of an Immunodominant HLA-A2 Epitope of the SARS-CoV-2 Spike Protein. *Journal of Biological Chemistry* **2021**, *297*, 101065, doi:10.1016/j.jbc.2021.101065.
192. Qiu, C.; Xiao, C.; Wang, Z.; Zhu, G.; Mao, L.; Chen, X.; Gao, L.; Deng, J.; Su, J.; Su, H.; et al. CD8+ T-Cell Epitope Variations Suggest a Potential Antigen HLA-A2 Binding Deficiency for Spike Protein of SARS-CoV-2. *Front Immunol* **2022**, *12*, doi:10.3389/fimmu.2021.764949.

193. Rowntree, L.C.; Petersen, J.; Juno, J.A.; Chaurasia, P.; Wragg, K.; Koutsakos, M.; Hensen, L.; Wheatley, A.K.; Kent, S.J.; Rossjohn, J.; et al. SARS-CoV-2-specific CD8 $^{+}$ T-cell Responses and TCR Signatures in the Context of a Prominent HLA-A*24:02 Allomorph. *Immunol Cell Biol* **2021**, *99*, 990–1000, doi:10.1111/imcb.12482.
194. Habel, J.R.; Nguyen, T.H.O.; van de Sandt, C.E.; Juno, J.A.; Chaurasia, P.; Wragg, K.; Koutsakos, M.; Hensen, L.; Jia, X.; Chua, B.; et al. Suboptimal SARS-CoV-2−specific CD8 $^{+}$ T Cell Response Associated with the Prominent HLA-A*02:01 Phenotype. *Proceedings of the National Academy of Sciences* **2020**, *117*, 24384–24391, doi:10.1073/pnas.2015486117.
195. Ranieri, E.; Popescu, I.; Gigante, M. CTL ELISPOT Assay. In; 2014; pp. 75–86.
196. Chen, Y.; Klein, S.L.; Garibaldi, B.T.; Li, H.; Wu, C.; Osevala, N.M.; Li, T.; Margolick, J.B.; Pawelec, G.; Leng, S.X. Aging in COVID-19: Vulnerability, Immunity and Intervention. *Ageing Res Rev* **2021**, *65*, 101205, doi:10.1016/j.arr.2020.101205.
197. Levin, E.G.; Lustig, Y.; Cohen, C.; Fluss, R.; Indenbaum, V.; Amit, S.; Doolman, R.; Asraf, K.; Mendelson, E.; Ziv, A.; et al. Waning Immune Humoral Response to BNT162b2 Covid-19 Vaccine over 6 Months. *New England Journal of Medicine* **2021**, *385*, doi:10.1056/nejmoa2114583.
198. Feikin, D.R.; Higdon, M.M.; Abu-Raddad, L.J.; Andrews, N.; Araos, R.; Goldberg, Y.; Groome, M.J.; Huppert, A.; O'Brien, K.L.; Smith, P.G.; et al. Duration of Effectiveness of Vaccines against SARS-CoV-2 Infection and COVID-19 Disease: Results of a Systematic Review and Meta-Regression. *Lancet* **2022**, *399*, 924–944, doi:10.1016/S0140-6736(22)00152-0.
199. Andeweg, S.P.; Vennema, H.; Veldhuijzen, I.; Smorenburg, N.; Schmitz, D.; Zwagemaker, F.; van Gageldonk-Lafeber, A.B.; Hahné, S.J.M.; Reusken, C.; Knol, M.J.; et al. Elevated Risk of Infection with SARS-CoV-2 Beta, Gamma, and Delta Variants Compared with Alpha Variant in Vaccinated Individuals. *Sci Transl Med* **2023**, *15*, doi:10.1126/scitranslmed.abn4338.
200. Bar-On, Y.M.; Goldberg, Y.; Mandel, M.; Bodenheimer, O.; Freedman, L.; Kalkstein, N.; Mizrahi, B.; Alroy-Preis, S.; Ash, N.; Milo, R.; et al. Protection of BNT162b2 Vaccine Booster against Covid-19 in Israel. *New England Journal of Medicine* **2021**, *385*, 1393–1400, doi:10.1056/nejmoa2114255.
201. Tan, S.T.; Kwan, A.T.; Rodríguez-Barraquer, I.; Singer, B.J.; Park, H.J.; Lewnard, J.A.; Sears, D.; Lo, N.C. Infectiousness of SARS-CoV-2 Breakthrough Infections and Reinfections during the Omicron Wave. *Nat Med* **2023**, *29*, 358–365, doi:10.1038/s41591-022-02138-x.
202. Maringer, Y.; Nelde, A.; Schroeder, S.M.; Schuhmacher, J.; Hörber, S.; Peter, A.; Karbach, J.; Jäger, E.; Walz, J.S. Durable Spike-Specific T Cell Responses after Different COVID-19 Vaccination Regimens Are Not Further Enhanced by Booster Vaccination. *Sci Immunol* **2022**, *7*, doi:10.1126/sciimmunol.add3899.
203. Nanishi, E.; Levy, O.; Ozonoff, A. Waning Effectiveness of SARS-CoV-2 MRNA Vaccines in Older Adults: A Rapid Review. *Hum Vaccin Immunother* 2022, *18*.
204. van Ewijk, C.E.; Hazelhorst, E.I.; Hahné, S.J.M.; Knol, M.J. COVID-19 Outbreak in an Elderly Care Home: Very Low Vaccine Effectiveness and Late Impact of Booster Vaccination Campaign. *Vaccine* **2022**, *40*, 6664–6669, doi:10.1016/j.vaccine.2022.09.080.
205. Bajči, M.P.; Lendak, D.F.; Ristić, M.; Drljača, M.M.; Brkić, S.; Turkulov, V.; Petrović, V. COVID-19 Breakthrough Infections among Patients Aged ≥65 Years in Serbia: Morbidity and Mortality Overview. *Vaccines (Basel)* **2022**, *10*, doi:10.3390/vaccines10111818.
206. Ventura, M.I.; Azizian, A.; Evans, S.E.; Velasquez, S.; Arguello, J.C.; Warburton, K. Vaccine Breakthrough Infections with SARS-CoV-2: Why Older Adults Need Booster Vaccinations. *Public Health in Practice* **2022**, *4*, doi:10.1016/j.puhip.2022.100307.
207. Cunha, L.L.; Perazzio, S.F.; Azzi, J.; Cravedi, P.; Riella, L.V. Remodeling of the Immune Response With Aging: Immunosenescence and Its Potential Impact on COVID-19 Immune Response. *Front Immunol* **2020**, *11*, doi:10.3389/fimmu.2020.01748.

208. Proietto, D.; Dallan, B.; Gallerani, E.; Albanese, V.; Llewellyn-Lacey, S.; Price, D.A.; Appay, V.; Pacifico, S.; Caputo, A.; Nicoli, F.; et al. Ageing Curtails the Diversity and Functionality of Nascent CD8+ T Cell Responses against SARS-CoV-2. *Vaccines (Basel)* **2023**, *11*, doi:10.3390/vaccines11010154.
209. Xiao, C.; Ren, Z.; Zhang, B.; Mao, L.; Zhu, G.; Gao, L.; Su, J.; Ye, J.; Long, Z.; Zhu, Y.; et al. Insufficient Epitope-Specific T Cell Clones Are Responsible for Impaired Cellular Immunity to Inactivated SARS-CoV-2 Vaccine in Older Adults. *Nat Aging* **2023**, *3*, 418–435, doi:10.1038/s43587-023-00379-0.
210. Wei, J.; Pouwels, K.B.; Stoesser, N.; Matthews, P.C.; Diamond, I.; Studley, R.; Rourke, E.; Cook, D.; Bell, J.I.; Newton, J.N.; et al. Antibody Responses and Correlates of Protection in the General Population after Two Doses of the ChAdOx1 or BNT162b2 Vaccines. *Nat Med* **2022**, *28*, 1072–1082, doi:10.1038/s41591-022-01721-6.
211. Tut, G.; Lancaster, T.; Krutikov, M.; Sylla, P.; Bone, D.; Spalkova, E.; Bentley, C.; Amin, U.; Jadir, A.; Hulme, S.; et al. Strong Peak Immunogenicity but Rapid Antibody Waning Following Third Vaccine Dose in Older Residents of Care Homes. *Nat Aging* **2023**, *3*, 93–104, doi:10.1038/s43587-022-00328-3.
212. Roukens, A.H.; Soonawala, D.; Joosten, S.A.; de Visser, A.W.; Jiang, X.; Dirksen, K.; de Gruijter, M.; van Dissel, J.T.; Bredenbeek, P.J.; Visser, L.G. Elderly Subjects Have a Delayed Antibody Response and Prolonged Viraemia Following Yellow Fever Vaccination: A Prospective Controlled Cohort Study. *PLoS One* **2011**, *6*, e27753, doi:10.1371/journal.pone.0027753.
213. Weinberger, B. Vaccines for the Elderly: Current Use and Future Challenges. *Immunity and Ageing* 2018, *15*.
214. Kim, D.K.; Riley, L.E.; Hunter, P. Recommended Immunization Schedule for Adults Aged 19 Years or Older, United States, 2018*. *Ann Intern Med* **2018**, *168*, 210, doi:10.7326/M17-3439.
215. Chivu-Economescu, M.; Bleotu, C.; Grancea, C.; Chiriac, D.; Botezatu, A.; Iancu, I. V.; Pitica, I.; Necula, L.G.; Neagu, A.; Matei, L.; et al. Kinetics and Persistence of Cellular and Humoral Immune Responses to SARS-CoV-2 Vaccine in Healthcare Workers with or without Prior COVID-19. *J Cell Mol Med* **2022**, *26*, 1293–1305, doi:10.1111/jcmm.17186.
216. Newman, J.; Thakur, N.; Peacock, T.P.; Bialy, D.; Elrefaey, A.M.E.; Bogaardt, C.; Horton, D.L.; Ho, S.; Kankeyan, T.; Carr, C.; et al. Neutralizing Antibody Activity against 21 SARS-CoV-2 Variants in Older Adults Vaccinated with BNT162b2. *Nat Microbiol* **2022**, *7*, 1180–1188, doi:10.1038/s41564-022-01163-3.
217. Brasu, N.; Elia, I.; Russo, V.; Montacchiesi, G.; Stabile, S.A.; De Intinis, C.; Fesi, F.; Gizzi, K.; Macagno, M.; Montone, M.; et al. Memory CD8+ T Cell Diversity and B Cell Responses Correlate with Protection against SARS-CoV-2 Following MRNA Vaccination. *Nat Immunol* **2022**, *23*, 1445–1456, doi:10.1038/s41590-022-01313-z.
218. Agallou, M.; Koutsoni, O.S.; Michail, M.; Zisimopoulou, P.; Tsitsilonis, O.E.; Karagouni, E. Antibody and T-Cell Subsets Analysis Unveils an Immune Profile Heterogeneity Mediating Long-Term Responses in Individuals Vaccinated Against SARS-CoV-2. *J Infect Dis* **2023**, *227*, 353–363, doi:10.1093/infdis/jiac421.
219. Khoury, D.S.; Cromer, D.; Reynaldi, A.; Schlub, T.E.; Wheatley, A.K.; Juno, J.A.; Subbarao, K.; Kent, S.J.; Triccas, J.A.; Davenport, M.P. Neutralizing Antibody Levels Are Highly Predictive of Immune Protection from Symptomatic SARS-CoV-2 Infection. *Nat Med* **2021**, *27*, 1205–1211, doi:10.1038/s41591-021-01377-8.
220. Tartof, S.Y.; Slezak, J.M.; Fischer, H.; Hong, V.; Ackerson, B.K.; Ranasinghe, O.N.; Frankland, T.B.; Ogun, O.A.; Zamparo, J.M.; Gray, S.; et al. Effectiveness of MRNA BNT162b2 COVID-19 Vaccine up to 6 Months in a Large Integrated Health System in the USA: A Retrospective Cohort Study. *The Lancet* **2021**, *398*, 1407–1416, doi:10.1016/S0140-6736(21)02183-8.

221. Zhang, Z.; Mateus, J.; Coelho, C.H.; Dan, J.M.; Moderbacher, C.R.; Gálvez, R.I.; Cortes, F.H.; Grifoni, A.; Tarke, A.; Chang, J.; et al. Humoral and Cellular Immune Memory to Four COVID-19 Vaccines. *Cell* **2022**, *185*, 2434-2451.e17, doi:10.1016/j.cell.2022.05.022.
222. Schmidt, T.; Klemis, V.; Schub, D.; Mihm, J.; Hielscher, F.; Marx, S.; Abu-Omar, A.; Ziegler, L.; Guckelmus, C.; Urschel, R.; et al. Immunogenicity and Reactogenicity of Heterologous ChAdOx1 NCoV-19/MRNA Vaccination. *Nat Med* **2021**, *27*, 1530–1535, doi:10.1038/s41591-021-01464-w.
223. Hillus, D.; Schwarz, T.; Tober-Lau, P.; Vanshylla, K.; Hastor, H.; Thibeault, C.; Jentzsch, S.; Helbig, E.T.; Lippert, L.J.; Tscheak, P.; et al. Safety, Reactogenicity, and Immunogenicity of Homologous and Heterologous Prime-Boost Immunisation with ChAdOx1 NCoV-19 and BNT162b2: A Prospective Cohort Study. *Lancet Respir Med* **2021**, *9*, 1255–1265, doi:10.1016/S2213-2600(21)00357-X.
224. Collier, D.A.; Ferreira, I.A.T.M.; Kotagiri, P.; Datir, R.P.; Lim, E.Y.; Touizer, E.; Meng, B.; Abdullahi, A.; Baker, S.; Dougan, G.; et al. Age-Related Immune Response Heterogeneity to SARS-CoV-2 Vaccine BNT162b2. *Nature* **2021**, *596*, 417–422, doi:10.1038/s41586-021-03739-1.
225. Munro, A.P.S.; Janani, L.; Cornelius, V.; Aley, P.K.; Babbage, G.; Baxter, D.; Bula, M.; Cathie, K.; Chatterjee, K.; Dodd, K.; et al. Safety and Immunogenicity of Seven COVID-19 Vaccines as a Third Dose (Booster) Following Two Doses of ChAdOx1 NCov-19 or BNT162b2 in the UK (COV-BOOST): A Blinded, Multicentre, Randomised, Controlled, Phase 2 Trial. *The Lancet* **2021**, *398*, 2258–2276, doi:10.1016/S0140-6736(21)02717-3.
226. Guerrera, G.; Picozza, M.; Placido, R.; Pirronello, M.; Verdiani, A.; Termine, A.; Fabrizio, C.; Giannessi, F.; Sambucci, M.; Pia Balice, M.; et al. *BNT162b2 Vaccination Induces Durable SARS-CoV-2-Specific T Cells with a Stem Cell Memory Phenotype*; 2021; Vol. 6;.
227. Lau, J.J.; Cheng, S.M.S.; Leung, K.; Lee, C.K.; Hachim, A.; Tsang, L.C.H.; Yam, K.W.H.; Chaothai, S.; Kwan, K.K.H.; Chai, Z.Y.H.; et al. Author Correction: Real-World COVID-19 Vaccine Effectiveness against the Omicron BA.2 Variant in a SARS-CoV-2 Infection-Naive Population. *Nat Med* **2024**, *30*, 305–305, doi:10.1038/s41591-023-02648-2.
228. Koutsakos, M.; Reynaldi, A.; Lee, W.S.; Nguyen, J.; Amarasena, T.; Taiaroa, G.; Kinsella, P.; Liew, K.C.; Tran, T.; Kent, H.E.; et al. SARS-CoV-2 Breakthrough Infection Induces Rapid Memory and de Novo T Cell Responses. *Immunity* **2023**, *56*, 879-892.e4, doi:10.1016/j.immuni.2023.02.017.
229. Palacios-Pedrero, M.Á.; Jansen, J.M.; Blume, C.; Stanislawski, N.; Jonczyk, R.; Molle, A.; Hernandez, M.G.; Kaiser, F.K.; Jung, K.; Osterhaus, A.D.M.E.; et al. Signs of Immunosenescence Correlate with Poor Outcome of MRNA COVID-19 Vaccination in Older Adults. *Nat Aging* **2022**, *2*, 896–905, doi:10.1038/s43587-022-00292-y.
230. Tut, G.; Lancaster, T.; Sylla, P.; Butler, M.S.; Kaur, N.; Spalkova, E.; Bentley, C.; Amin, U.; Jadir, A.; Hulme, S.; et al. Antibody and Cellular Immune Responses Following Dual COVID-19 Vaccination within Infection-Naive Residents of Long-Term Care Facilities: An Observational Cohort Study. *Lancet Healthy Longev* **2022**, *3*, e461–e469, doi:10.1016/S2666-7568(22)00118-0.
231. Parry, H.; Bruton, R.; Ayodele, R.; Sylla, P.; McIlroy, G.; Logan, N.; Scott, S.; Nicol, S.; Verma, K.; Stephens, C.; et al. Vaccine Subtype and Dose Interval Determine Immunogenicity of Primary Series COVID-19 Vaccines in Older People. *Cell Rep Med* **2022**, *3*, doi:10.1016/j.xcrm.2022.100739.
232. Wang, Z.; Muecksch, F.; Raspe, R.; Johannsen, F.; Turroja, M.; Canis, M.; ElTanbouly, M.A.; Santos, G.S.S.; Johnson, B.; Baharani, V.A.; et al. Memory B Cell Development Elicited by MRNA Booster Vaccinations in the Elderly. *J Exp Med* **2023**, *220*, doi:10.1084/jem.20230668.
233. Jo, N.; Hidaka, Y.; Kikuchi, O.; Fukahori, M.; Sawada, T.; Aoki, M.; Yamamoto, M.; Nagao, M.; Morita, S.; Nakajima, T.E.; et al. Author Correction: Impaired CD4+ T Cell Response in

Older Adults Is Associated with Reduced Immunogenicity and Reactogenicity of MRNA COVID-19 Vaccination. *Nat Aging* **2023**, *3*, 751–751, doi:10.1038/s43587-023-00426-w.
234. Berical, A.C.; Harris, D.; Dela Cruz, C.S.; Possick, J.D. Pneumococcal Vaccination Strategies: An Update and Perspective. *Ann Am Thorac Soc* 2016, *13*, 933–944.
235. Monali, R.; De Vita, E.; Mariottini, F.; Privitera, G.; Lopalco, P.L.; Tavoschi, L. Impact of Vaccination on Invasive Pneumococcal Disease in Italy 2007–2017: Surveillance Challenges and Epidemiological Changes. *Epidemiol Infect* **2020**, *148*, e187, doi:10.1017/S0950268820001077.
236. Ravichandran, S.; Erra-Diaz, F.; Karakaslar, O.E.; Marches, R.; Kenyon-Pesce, L.; Rossi, R.; Chaussabel, D.; Nehar-Belaid, D.; LaFon, D.C.; Pascual, V.; et al. Distinct Baseline Immune Characteristics Associated with Responses to Conjugated and Unconjugated Pneumococcal Polysaccharide Vaccines in Older Adults. *Nat Immunol* **2024**, *25*, 316–329, doi:10.1038/s41590-023-01717-5.
237. Rokney, A.; Ben-Shimol, S.; Korenman, Z.; Porat, N.; Gorodnitzky, Z.; Givon-Lavi, N.; Ron, M.; Agmon, V.; Dagan, R.; Valinsky, L. Emergence of *Streptococcus Pneumoniae* Serotype 12F after Sequential Introduction of 7- and 13-Valent Vaccines, Israel. *Emerg Infect Dis* **2018**, *24*, 453–461, doi:10.3201/eid2403.170769.
238. van der Heiden, M.; Shetty, S.; Bijvank, E.; Beckers, L.; Cevirgel, A.; van Sleen, Y.; Tcherniaeva, I.; Ollinger, T.; Burny, W.; van Binnendijk, R.S.; et al. Multiple Vaccine Comparison in the Same Adults Reveals Vaccine-Specific and Age-Related Humoral Response Patterns: An Open Phase IV Trial. *Nat Commun* **2024**, *15*, 6603, doi:10.1038/s41467-024-50760-9.
239. Andre, F.; Booy, R.; Bock, H.; Clemens, J.; Datta, S.; John, T.; Lee, B.; Lolekha, S.; Peltola, H.; Ruff, T.; et al. Vaccination Greatly Reduces Disease, Disability, Death and Inequity Worldwide. *Bull World Health Organ* **2008**, *86*, 140–146, doi:10.2471/BLT.07.040089.
240. Lang, P.O.; Mendes, A.; Socquet, J.; Assir, N.; Govind, S.; Aspinall, R. Effectiveness of Influenza Vaccine in Aging and Older Adults: Comprehensive Analysis of the Evidence. *Clin Interv Aging* 2012, *7*, 55–64.
241. Giorgi, C.; Marchi, S.; Simoes, I.C.M.; Ren, Z.; Morciano, G.; Perrone, M.; Patalas-Krawczyk, P.; Borchard, S.; Jędrak, P.; Pierzynowska, K.; et al. Mitochondria and Reactive Oxygen Species in Aging and Age-Related Diseases. *Int Rev Cell Mol Biol* **2018**, *340*, 209–344, doi:10.1016/bs.ircmb.2018.05.006.
242. Fang, E.F.; Lautrup, S.; Hou, Y.; Demarest, T.G.; Croteau, D.L.; Mattson, M.P.; Bohr, V.A. NAD+ in Aging: Molecular Mechanisms and Translational Implications. *Trends Mol Med* 2017, *23*, 899–916.
243. Somasundaram, I.; Jain, S.M.; Blot-Chabaud, M.; Pathak, S.; Banerjee, A.; Rawat, S.; Sharma, N.R.; Duttaroy, A.K. Mitochondrial Dysfunction and Its Association with Age-Related Disorders. *Front Physiol* **2024**, *15*, doi:10.3389/fphys.2024.1384966.
244. Saleh, Z.; Mirzazadeh, S.; Mirzaei, F.; Heidarnejad, K.; Meri, S.; Kalantar, K. Alterations in Metabolic Pathways: A Bridge between Aging and Weaker Innate Immune Response. *Frontiers in Aging* 2024, *5*.
245. Kuhla, A.; Blei, T.; Jaster, R.; Vollmar, B. Aging Is Associated with a Shift of Fatty Metabolism toward Lipogenesis. *Journals of Gerontology - Series A Biological Sciences and Medical Sciences* **2011**, *66 A*, 1192–1200, doi:10.1093/gerona/glr124.
246. Chung, K.W. Advances in Understanding of the Role of Lipid Metabolism in Aging. *Cells* 2021, *10*.
247. Van Baarle, D.; Bollaerts, K.; Del Giudice, G.; Lockhart, S.; Luxemburger, C.; Postma, M.J.; Timen, A.; Standaert, B. Preventing Infectious Diseases for Healthy Ageing: The VITAL Public-Private Partnership Project. *Vaccine* **2020**, *38*, 5896–5904, doi:10.1016/j.vaccine.2020.07.005.

248. Argüello, R.J.; Combes, A.J.; Char, R.; Gigan, J.P.; Baaziz, A.I.; Bousiquot, E.; Camosseto, V.; Samad, B.; Tsui, J.; Yan, P.; et al. SCENITH: A Flow Cytometry-Based Method to Functionally Profile Energy Metabolism with Single-Cell Resolution. *Cell Metab* **2020**, *32*, 1063-1075.e7, doi:10.1016/j.cmet.2020.11.007.
249. Rose, J.R.; Akdogan-Ozdilek, B.; Rahmberg, A.R.; Powell, M.D.; Hicks, S.L.; Scharer, C.D.; Boss, J.M. Distinct Transcriptomic and Epigenomic Modalities Underpin Human Memory T Cell Subsets and Their Activation Potential. *Commun Biol* **2023**, *6*, doi:10.1038/s42003-023-04747-9.
250. Adamik, J.; Munson, P. V.; Maurer, D.M.; Hartmann, F.J.; Bendall, S.C.; Argüello, R.J.; Butterfield, L.H. Immuno-Metabolic Dendritic Cell Vaccine Signatures Associate with Overall Survival in Vaccinated Melanoma Patients. *Nat Commun* **2023**, *14*, doi:10.1038/s41467-023-42881-4.
251. Hassanzad, M.; Hajian-Tilaki, K. Methods of Determining Optimal Cut-Point of Diagnostic Biomarkers with Application of Clinical Data in ROC Analysis: An Update Review. *BMC Med Res Methodol* **2024**, *24*, doi:10.1186/s12874-024-02198-2.
252. Akobeng, A.K. Understanding Diagnostic Tests 1: Sensitivity, Specificity and Predictive Values. *Acta Paediatrica, International Journal of Paediatrics* 2007, *96*, 338–341.
253. Gonzalez-Freire, M.; De Cabo, R.; Bernier, M.; Sollott, S.J.; Fabbri, E.; Navas, P.; Ferrucci, L. Reconsidering the Role of Mitochondria in Aging. *Journals of Gerontology - Series A Biological Sciences and Medical Sciences* 2015, *70*, 1334–1342.
254. Barbato, A.; Scandura, G.; Puglisi, F.; Cambria, D.; La Spina, E.; Palumbo, G.A.; Lazzarino, G.; Tibullo, D.; Di Raimondo, F.; Giallongo, C.; et al. Mitochondrial Bioenergetics at the Onset of Drug Resistance in Hematological Malignancies: An Overview. *Front Oncol* 2020, *10*.
255. Scales, H.E.; Meehan, G.R.; Hayes, A.J.; Benson, R.A.; Watson, E.; Walters, A.; Tomura, M.; Maraskovsky, E.; Garside, P.; Morelli, A.B.; et al. A Novel Cellular Pathway of Antigen Presentation and CD4 T Cell Activation in Vivo. *Front Immunol* **2018**, *9*, doi:10.3389/fimmu.2018.02684.
256. Dolina, J.S.; Lee, J.; Brightman, S.E.; McArdle, S.; Hall, S.M.; Thota, R.R.; Lanka, M.; Premlal, A.L.R.; Greenbaum, J.A.; Cohen, E.E.W.; et al. Linked CD4 $^{+}$ /CD8 $^{+}$ T Cell Neoantigen Vaccination Overcomes Immune Checkpoint Blockade Resistance and Enables Tumor Regression 2023.
257. Cesari, M.; Calvani, R.; Marzetti, E. Frailty in Older Persons. *Clin Geriatr Med* **2017**, *33*, 293–303, doi:10.1016/j.cger.2017.02.002.
258. Fried, L.P.; Tangen, C.M.; Walston, J.; Newman, A.B.; Hirsch, C.; Gottdiener, J.; Seeman, T.; Tracy, R.; Kop, W.J.; Burke, G.; et al. *Frailty in Older Adults: Evidence for a Phenotype*; 2001; Vol. 56;.
259. Pollard, A.J.; Bijker, E.M. A Guide to Vaccinology: From Basic Principles to New Developments. *Nat Rev Immunol* 2021, *21*, 83–100.
260. Rappuoli, R.; Mandl, C.W.; Black, S.; De Gregorio, E. Vaccines for the Twenty-First Century Society. *Nat Rev Immunol* 2011, *11*, 865–872.
261. McElhaney, J.E.; Verschoor, C.P.; Andrew, M.K.; Haynes, L.; Kuchel, G.A.; Pawelec, G. The Immune Response to Influenza in Older Humans: Beyond Immune Senescence. *Immunity & Ageing* **2020**, *17*, 10, doi:10.1186/s12979-020-00181-1.
262. van den Hoogen, L.L.; Boer, M.; Postema, A.; de Rond, L.; de Zeeuw-Brouwer, M.; Pronk, I.; Wijmenga-Monsuur, A.J.; Bijvank, E.; Kruiper, C.; Beckers, L.; et al. Reduced Antibody Acquisition with Increasing Age Following Vaccination with BNT162b2: Results from Two Longitudinal Cohort Studies in The Netherlands. *Vaccines (Basel)* **2022**, *10*, 1480, doi:10.3390/vaccines10091480.
263. Niederman, M.S.; Folaranmi, T.; Buchwald, U.K.; Musey, L.; Cripps, A.W.; Johnson, K.D. Efficacy and Effectiveness of a 23-Valent Polysaccharide Vaccine against Invasive and

Noninvasive Pneumococcal Disease and Related Outcomes: A Review of Available Evidence. *Expert Rev Vaccines* **2021**, *20*, 243–256, doi:10.1080/14760584.2021.1880328.
264. Ron-Harel, N.; Ghergurovich, J.M.; Notarangelo, G.; LaFleur, M.W.; Tsubosaka, Y.; Sharpe, A.H.; Rabinowitz, J.D.; Haigis, M.C. T Cell Activation Depends on Extracellular Alanine. *Cell Rep* **2019**, *28*, 3011-3021.e4, doi:10.1016/j.celrep.2019.08.034.
265. Marchingo, J.M.; Cantrell, D.A. Protein Synthesis, Degradation, and Energy Metabolism in T Cell Immunity. *Cell Mol Immunol* 2022, *19*, 303–315.
266. Kurihara, T.; Arimochi, H.; Bhuyan, Z.A.; Ishifune, C.; Tsumura, H.; Ito, M.; Ito, Y.; Kitamura, A.; Maekawa, Y.; Yasutomo, K. CD98 Heavy Chain Is a Potent Positive Regulator of CD4+ T Cell Proliferation and Interferon-γ Production In Vivo. *PLoS One* **2015**, *10*, e0139692, doi:10.1371/journal.pone.0139692.
267. Hess, K.; Yang, Y.; Golech, S.; Sharov, A.; Becker, K.G.; Weng, N. Kinetic Assessment of General Gene Expression Changes during Human Naive CD4+ T Cell Activation. *Int Immunol* **2004**, *16*, 1711–1721, doi:10.1093/intimm/dxh172.
268. Bonacina, F.; Moregola, A.; Svecla, M.; Coe, D.; Uboldi, P.; Fraire, S.; Beretta, S.; Beretta, G.; Pellegatta, F.; Catapano, A.L.; et al. The Low-Density Lipoprotein Receptor–MTORC1 Axis Coordinates CD8+ T Cell Activation. *Journal of Cell Biology* **2022**, *221*, doi:10.1083/jcb.202202011.
269. Rubino, G.; Bulati, M.; Aiello, A.; Aprile, S.; Gambino, C.M.; Gervasi, F.; Caruso, C.; Accardi, G. Sicilian Centenarian Offspring Are More Resistant to Immune Ageing. *Aging Clin Exp Res* **2019**, *31*, 125–133, doi:10.1007/s40520-018-0936-7.
270. Fülöp, T.; Dupuis, G.; Witkowski, J.M.; Larbi, A. The Role of Immunosenescence in the Development of Age-Related Diseases. *Rev Invest Clin* **2016**, *68*, 84–91.
271. Feehan, J.; Tripodi, N.; Apostolopoulos, V. The Twilight of the Immune System: The Impact of Immunosenescence in Aging. *Maturitas* **2021**, *147*, 7–13, doi:10.1016/j.maturitas.2021.02.006.
272. Rea, I.M.; Gibson, D.S.; McGilligan, V.; McNerlan, S.E.; Alexander, H.D.; Ross, O.A. Age and Age-Related Diseases: Role of Inflammation Triggers and Cytokines. *Front Immunol* **2018**, *9*, 586, doi:10.3389/fimmu.2018.00586.
273. Crooke, S.N.; Ovsyannikova, I.G.; Poland, G.A.; Kennedy, R.B. Immunosenescence: A Systems-Level Overview of Immune Cell Biology and Strategies for Improving Vaccine Responses. *Exp Gerontol* **2019**, *124*, 110632, doi:10.1016/j.exger.2019.110632.
274. Mancinetti, F.; Marinelli, A.; Boccardi, V.; Mecocci, P. Challenges of Infectious Diseases in Older Adults: From Immunosenescence and Inflammaging through Antibiotic Resistance to Management Strategies. *Mech Ageing Dev* **2024**, *222*, 111998, doi:10.1016/j.mad.2024.111998.
275. Coperchini, F.; Greco, A.; Teliti, M.; Croce, L.; Chytiris, S.; Magri, F.; Gaetano, C.; Rotondi, M. Inflamm-Ageing: How Cytokines and Nutrition Shape the Trajectory of Ageing. *Cytokine Growth Factor Rev* **2024**, doi:10.1016/j.cytogfr.2024.08.004.
276. Laconi, E.; Marongiu, F.; DeGregori, J. Cancer as a Disease of Old Age: Changing Mutational and Microenvironmental Landscapes. *Br J Cancer* **2020**, *122*, 943–952, doi:10.1038/s41416-019-0721-1.
277. Soegiarto, G.; Purnomosari, D. Challenges in the Vaccination of the Elderly and Strategies for Improvement. *Pathophysiology* **2023**, *30*, 155–173, doi:10.3390/pathophysiology30020014.
278. Rea, I.M.; McNerlan, S.E.; Alexander, H.D. CD69, CD25, and HLA-DR Activation Antigen Expression on CD3+ Lymphocytes and Relationship to Serum TNF-α, IFN-γ, and SIL-2R Levels in Aging. *Exp Gerontol* **1999**, *34*, 79–93, doi:10.1016/S0531-5565(98)00058-8.
279. Wu, J.; Liu, Z.; Zhang, Y.; Wang, L.; Feng, D.; Liu, L.; Peng, Y.; Dai, B.; Li, W. Age-Dependent Alterations of HLA-DR Expression and Effect of Lipopolysaccharide on Cytokine Secretion of Peripheral Blood Mononuclear Cells in the Elderly Population. *Scand J Immunol* **2011**, *74*, 603–608, doi:10.1111/j.1365-3083.2011.02612.x.

280. Bajaj, V.; Gadi, N.; Spihlman, A.P.; Wu, S.C.; Choi, C.H.; Moulton, V.R. Aging, Immunity, and COVID-19: How Age Influences the Host Immune Response to Coronavirus Infections? *Front Physiol* **2021**, *11*, doi:10.3389/fphys.2020.571416.
281. Fessler, M.B. The Intracellular Cholesterol Landscape: Dynamic Integrator of the Immune Response. *Trends Immunol* **2016**, *37*, 819–830, doi:10.1016/j.it.2016.09.001.
282. Castellano, B.M.; Thelen, A.M.; Moldavski, O.; Feltes, M.; van der Welle, R.E.N.; Mydock-McGrane, L.; Jiang, X.; van Eijkeren, R.J.; Davis, O.B.; Louie, S.M.; et al. Lysosomal Cholesterol Activates MTORC1 via an SLC38A9–Niemann-Pick C1 Signaling Complex. *Science (1979)* **2017**, *355*, 1306–1311, doi:10.1126/science.aag1417.
283. Olawade, D.B.; Teke, J.; Fapohunda, O.; Weerasinghe, K.; Usman, S.O.; Ige, A.O.; Clement David-Olawade, A. Leveraging Artificial Intelligence in Vaccine Development: A Narrative Review. *J Microbiol Methods* **2024**, *224*, 106998, doi:10.1016/j.mimet.2024.106998.
284. Spehner, L.; Orillard, E.; Falcoz, A.; Lepiller, Q.; Bouard, A.; Almotlak, H.; Kim, S.; Curtit, E.; Meynard, G.; Jary, M.; et al. Predictive Biomarkers and Specific Immune Responses of COVID-19 MRNA Vaccine in Patients with Cancer: Prospective Results from the CACOV-VAC Trial. *BMJ Oncology* **2023**, *2*, e000054, doi:10.1136/bmjonc-2023-000054.